A NEW DISSECTION METHODOLOGY AND INVESTIGATION INTO COAL PROPERTY TRANSFORMATIONAL BEHAVIOUR IMPACTING ON A COMMERCIAL-SCALE SASOL-LURGI MK IV FIXED-BED GASIFIER

J R BUNT

May 2006

DECLARATION

I, the undersigned, declare that the work contained in this thesis is my own original study and has not previously been submitted at any university for a degree.

J R BUNT **Date**

A NEW DISSECTION METHODOLOGY AND INVESTIGATION INTO COAL PROPERTY TRANSFORMATIONAL BEHAVIOUR IMPACTING ON A COMMERCIAL-SCALE SASOL-LURGI MK IV FIXED-BED GASIFIER

A thesis submitted to the NORTH-WEST UNIVERSITY, Potchefstroom,
In fulfillment of the requirements for the degree PhD (Chemical Engineering)

By
John Reginald Bunt
NHD (Extractive Metallurgy)(WITS TECHNIKON)(1986)
GDE (Coal Technology))(WITS)(1997)
M.Sc. (Applied Science)(UCT)(1997)

Promoter: Prof F. B. Waanders
School of Chemical and Mineral Engineering
North-West University
Potchefstroom
South Africa

May 2006

ACKNOWLEDGEMENTS

The author would like to extend his thanks and appreciation to the following people and organizations for their help and assistance throughout this study:

Firstly, Prof Frans Waanders (Academic Study Supervisor) and Dr Tjaart van der Walt (Internal Sasol Supervisor) for their outstanding assistance and guidance throughout the course of the study. Secondly, Mr Johan van Dyk for his extremely valuable insight and advice at crucial times.

Dr Johannes van Heerden and the Sasol Technology (Syngas and Coal Technology R+D team) for their financial, as well as technical and moral support.

Messrs Jozef Venter and Anton van Zyl (Sasol Synfuels Gas Production Department in Secunda), for allowing Mr Henry Matjie and myself to sample the GG41 gasifier, as well as for providing logistical assistance throughout the sampling campaign.

Colleagues Ben Ashton and Sarel du Plessis for their practical help in preparing the samples for the various analyses conducted. Special thanks to Ben who also conducted the AFT and true density analyses of the GG41 samples and to Vanessa Claasens who co-ordinated the fragmentation, tar and caking analysis runs.

A special thanks to colleagues Dr Nikki Wagner and Mr Johan Joubert (Sasol Technology R+D) for the highly specialized petrographic analysis (morphology and vitrinite reflectance) conducted on the samples. Thanks also to Johan for characterising the coal char CO_2 reactivity of selected samples, using the in-house TGA equipment.

C.M.T. laboratories for conducting the particle size distribution, proximate and ultimate analysis on the GG41 gasifier samples obtained.

Mrs René van der Westhuizen for proof-reading and grammar checking of the thesis.

My wife, Erna and sons, Byron and Lance for their encouragement, interest and support during the write-up phase of this project.

Finally, to my Creator who deserves all honour, for blessing me with the intellect and perseverance to successfully reach this goal in my life.

SYNOPSIS

Gasification behaviour is particle dependent, whilst gasifier (reactor) behaviour is an averaging process of individual responses of each particle [Glover, 1991]. It was hypothesized in the case of the present study that if it were possible to extract and analyse particles from different reaction zones within a gasifier, it may be likely to enhance the understanding as to the contribution that these particles make towards gasification. This better understanding of the particle-type compositional responses could act as an enabler to further influence gasifier performance.

The primary focus of this study was to develop a "new-to-Sasol" sequential (axial) sampling methodology of the entire GG41 commercial-scale Sasol-Lurgi FBDB MK IV gasifier (isolated after running on medium load), having a Bosman skirt feeder configuration and standard ash grate. Detailed characterisation profiles of the ***chemical, physical, and petrographical properties*** in the sample increments were expected to deliver distinct profiles of the drying, pyrolysis, reduction, and combustion (ash-bed) zones. The input value of this experimental data, in the form of a "pan-cake" model to the existing one-dimensional kinetic models at Sasol Technology R+D were expected to advance the prediction capability significantly. The Sasol Gasification Operations could then possibly benefit in terms of an improved control philosophy of their process, yielding better gasification stability, improved efficiency and availability. The kinetic model development was not considered to be part of this particular study.

The "controlled" GG41 gasifier turn-out and sampling methodology employed, provided excellent residual internal profile results, clearly showing the complexity and heterogeneity of the coal properties studied with respect to transformational behaviour during gasification. By keeping the turn-out sample increment size constant ($3m^3$), whilst maintaining a constant ash-grate discharge speed (3rph) to assimilate plug-flow conditions; 32 fractional "slices" of the entire gasifier contents (100t) were successfully extracted. Truck "sub-sampling" of the increments taken, was also found to be successful. The entire sampling methodology is considered to be plausible when observing the "pan-cake" model derived for the GG41 gasifier, in that minimal scatter in the data trends are evident.

The GG41 drying zone was found to be prevalent in the Bosman skirt feeder region in the uppermost part of the fixed bed gasifier. Volatile matter recondensation and some evidence of particle size segregation and primary fragmentation was observed as the

charge descended within this reaction zone. The pyrolysis zone was found to be the largest reaction zone, followed by the reduction zone and the combustion (ash-bed) zones. Whilst the boundary of the pyrolysis zone was very clearly defined by the residual volatile matter distribution profile, distinctive regional overlap characterised by a "fast devolatilisation" region and a "slow pyrolysis with gasification" region, observed in the bottom half of the pyrolysis zone, were evident.

A gasification region was observed to occur at the end of the pyrolysis zone, where the coal char CO_2 reactivity was found to reach a maximum, midway into the reduction zone, characterising the onset of an oxidation front occurring above the combustion zone position, where 65 % carbon conversion had occurred and the char was subsequently rapidly consumed. Melting of the ash-forming minerals tended to act as a "glue", agglomerating particles together and thereby increasing the amount of the coarse +25mm fraction in the bottom half of the gasifier. Rapid carbon consumption occurred in the low ash-bed, but 8% fixed carbon was still evident in the ash at the grate position at the base of the reactor. The char types responsible for the carbon losses have however been quantified in this study.

From the unique petrographic char morphology results obtained, it was found that the maceral type appears to play a pivotal role in the changes experienced by carbon particles when exposed to increasing temperature. Whole vitrinite particles and vitrinite bands within particles devolatilised first, followed at higher temperatures by reactive inertinite types. The porous chars remained predominantly isotropic, while the mixed and dense chars showed varying degrees of anisotropy, which is related to the aromaticity of the carbon. At the end of pyrolysis, all the coal was found to be essentially converted to char, but chars continued to increase as the charge further descended within the gasifier, becoming consumed in the oxidation / combustion zone.

Comparison of the GG41 gasifier (4 m diameter) internal profile, on a factorised basis with a quarter-scale Lurgi gasifier (1.13 m diameter) operating on Indian coal, provided an excellent basis for comparison. The good agreement obtained, substantiates credibility of the current findings with respect to repeatability, albeit that different coal types and reactor geometries were being compared. This also has implications regarding scale-ability to smaller gasifier sizes, should the need arise to conduct small scale gasification experiments, which can be scaled up to a commercial sized 4m diameter reactor.

The positive "bench-mark" findings indicate that considerable benefit could be obtained by carrying out more extensive and detailed studies on other Sasol-Lurgi MK IV gasifier operating systems, i.e. low load and high load conditions; as well as internal mechanical influences on performance, such as the rubble finger positioned on the ash grate, and "Unifeeder" compared with the Bosman skirt feeder configuration.

The findings of this study also clearly indicate where optimisation opportunities exist for the MK IV gasifier, i.e. the char type responsible for carbon-loss, the oxygen scavenging effect of minerals, volatile matter recondensation in the cooler zone of the gasifier, localised oxygen sparging that causes hot-spots just above the ash grate and reduction of the top size of the feed coal to a "thermally stable" size, which could result in a more stable gasifier operation with possible process efficiency benefits.

It is likely that this thesis will ultimately have a major impact on the profitability of many existing and new Sasol-Lurgi gasification plants. It also represents a contribution towards a better understanding of the key phenomena involved in the fixed-bed gasification process.

OORSIG

Die bedryfbaarheid van 'n vergassingstegnologie, meer spesifiek vaste-bed vergassing, is grootliks afhanklik van die gedrag van die individuele partikels (fisies en chemies) binne-in die reactor [Glover, 1991]. Die hipotese bestaan dat, indien partikels in verskillende sones binne-in die vergassingsreaktor gemonster en ontleed kan word, die bydrae van partikels in spesifieke sones beter verstaan en beskryf kan word. Hierdie kennis kan dan moontlik bydra tot die verdere optimisering van die vergassingsbedryf.

Die hoofdoel van hierdie studie was om 'n sekwensiële monsternemingsmetodologie vir 'n MK IV Sasol-Lurgi Vaste-Bed vergasser (met Bosman romp en standaard rooster) te ontwikkel. Breedvoerige ***chemiese, fisiese en petrografiese*** analises is op elke monster uitgevoer om gedetailleerde profiele in die droging-, pirolise, vergassing- en verbranding- (as-bed) sones te ontwikkel. Die waardetoevoeging wat verwag is van die eksperimentele data, in die vorm van 'n "pannekoek" model, in vergelyking met die huidige 1-dimensionele kinetiese model wat tans bestaan by Sasol Tegnologie N&O, was om die voorspelbaarheid betekenisvol te verbeter in terme van die beheerfilosofie van die proses, verhoogde suiwergasproduksie, beter doeltreffendheid en stabiliteit. Die evaluering en verdere ontwikkeling van die kinetiese model was nie deel van hierdie studie nie.

Uitstekende interne profiel resultate is met die die nuutontwikkelde vergasser monsternemingsmetodologie wat toegepas is, verkry. Die komplekse en heterogene aard van die steenkooleienskappe kon duidelik waargeneem word. Die vergasserbed is suksesvol onttrek deur middel van 'n monsternemingsmetodologie (prop-vloei), waar die monstergrootte konstant gehou is op $3m^3$ met 'n konstante roosterspoed van 3rph. 32 monsters van ongeveer 100t, is in lae onttrek. Die totale monsternemingsmetodologie kan as suksesvol en aanvaarbaar beskou word, as dit in ag geneem word dat daar minimum variasie in die profiele waargeneem is.

Die drogingsone is in die boonste gedeelte van die vergasser in die Bosman romp waargeneem. Vlugstof herkondensasie, partikelsegregasie en primêre verbrokkeling is verder af in die reaksiesone waargeneem. Daar is bevind dat die pirolisesone die grootste is, gevolg deur die reduksiesone en die verbrandingsone. Alhoewel die grense van die pirolisesone duidelik deur die vlugstofresiduprofiel geïndentifiseer is, was daar wel oorvleueling van 'n vinnige ontvlugtingsone en 'n stadige pirolisesone wat geïdentifiseer kon word.

'n Vergassingsone is net na die pirolisesone geïdentifiseer, waar die steenkool CO_2 reaktiwiteit in die middel van die reduksiesone 'n maksimum bereik het. Dit beklemtoon die begin van die oksidasiesone bo die verbrandingsone, waar 65% koolstofomsetting reeds plaasgevind het. Smelting van die minerale wat as "gom" opgetree het om partikels aan mekaar te bind het begin plaasvind, wat gelei het tot 'n vermeerdering in die +25mm partikels in die onderste helfte van die vergasser. Koolstofomsetting het baie vinnig plaasgevind in die lae verbrandingsone, maar 8% vaste koolstof was steeds teenwoordig in die as op die rooster posisie.

Vanuit die resultate van 'n unieke petrografiese morfologiese analise is bevind dat die maseraaltipe 'n beduidende rol gespeel het in die verandering wat die koolstofdeeltjies met temperatuurtoename ondergaan het. Vitrinietpartikels en -bande in steenkoolpartikels het eerste ontvlug, gevolg deur inertiniet by hoër temperature. Die poreuse struktuur het grootliks isotropies gebly, terwyl die gemengde en digte ontvlugte-steenkool variasie tussen isotropies en an-isotropies getoon het, hoofsaaklik as gevolg van die aromatiese eienskappe van die ontvlugte steenkool. Al die steenkool was hoofsaaklik aan die einde van die pirolisesone omgeskakel in ontvlugte steenkool, maar dit het verder af in die vergasser steeds toegeneem, en is in die oksidasie- of verbrandingsone opgebruik.

Die interne profiel van die GG41 vergasser is vergelyk met 'n kwartskaal Lurgi vergasser wat met Indiese steenkool bedryf is. Baie goeie vergelykbare profiele is waargeneem, ten spyte daarvan dat verskillende grootte vergassers en steenkoolbronne gebruik is. Die vergelykbare resultate het ook positiewe waarde indien kleiner-skaal toetse gedoen word, en vergoting volgens die uitslae dan toegepas word.

Die positiewe vergelykbare data dui aan dat meer navorsing en uitgebreide studies (verskillende gasvragte, vergasser bedryfskondisies, roosterkonfigurasies, ens.) beslis van waarde kan wees om die Sasol-Lurgi Vaste Bed vergassingsproses verder te kan optimiseer. Die resultate het ook aangedui waar verdere optimiseringsmoontlikhede vir die MK IV vergasser bestaan, byvoorbeeld: koolstof in die as, vlugstof herkondensasie in die kouer sones, suurstof-in-as toename, afname in top-grootte van die steenkool na 'n termies stabiele grootte.

Hierdie tesis het nie net 'n bydrae gelewer tot 'n beter begrip van die vergasser bedryf nie, maar sal waarskynlik ook 'n positiewe uitwerking op die winsgewendheid van bestaande, sowel as nuwe aanlegte hê.

INDEX

LIST OF ABBREVIATIONS		*I*
LIST OF FIGURES		*III*
LIST OF TABLES		*VI*
LIST OF APPENDICES		*VII*
CHAPTER 1: BACKGROUND AND LITERATURE REVIEW		*1*
1	*OBJECTIVES OF THIS STUDY*	*6*
2	*GASIFICATION*	*8*
2.1	*Sasol-Lurgi Fixed-Bed Dry Bottom (FBDB) gasification*	*8*
2.1.1	*Basic reactions occurring in a coal gasifier*	*11*
3	*COAL*	*14*
3.1	*Definition of coal*	*14*
3.2	*Coal formation*	*15*
3.3	*Coal composition (types) of coal macerals*	*16*
3.3.1	*Vitrinite*	*17*
3.3.2	*Inertinite*	*17*
3.3.3	*Liptinite*	*17*
3.3.4	*Reactive semi-fusinite*	*18*
3.4	*Minerals present in coal*	*18*
3.5	*Microlithotypes*	*19*
4	*THE MOST IMPORTANT COAL PROPERTIES WHICH IMPACT ON GASIFICATION PERFORMANCE*	*19*
4.1	*Coal char reactivity*	*20*
4.2	*Feed coal particle size*	*21*
4.3	*Thermal fragmentation*	*22*
4.4	*Ash, fixed carbon, volatile matter and moisture content*	*23*
4.5	*Ash fusion temperature*	*26*

4.6 Mechanical fragmentation 27
4.7 Caking properties 27
4.8 Petrographic coal char morphology 29

5 SAMPLING 31
5.1 Gasifier sampling methodologies 33
5.1.1 Turn-out sampling methodology 33
5.1.2 Dissection (dig-out) sampling methodology 34
5.1.3 Drill core sampling methodology 34

6 REVIEW OF PREVIOUS RESEARCH DONE ON EXPERIMENTAL AND COMMERCIAL-SCALE FIXED-BED GASIFICATION REACTORS 35
6.1 The pilot-scale moving bed pressure gasification plant in India 35
6.2 Sasol-Lurgi commercial-scale fixed-bed gasification studies 39
6.2.1 Sasolburg dissection (gasifier 15 – water quenched) 40
6.2.2 Sasolburg run-out (gasifier 16 – not quenched) 42
6.2.3 Secunda dissection (gasifiers 14 [water cooled] & 17 [N_2 and water cooled]) 45
6.2.4 Secunda run-out (gasifier 16 – N_2 cooled for 16 hours) 45
6.2.5 Specific findings and conclusions [Glover, 1988, 1991] 45

***CHAPTER 2: EXPERIMENTAL PROCEDURES** 48*

1 INTRODUCTION 48

2 GG41 GASIFIER SAMPLING METHODOLOGY 48
2.1 Process conditions at the time of quenching for GG41 and the Indian pilot plant 53
2.2 Factor used to compare GG41 results with the Indian pilot plant data 54

3 COAL AND COAL ASH CHARACTERISATION TECHNIQUES CONDUCTED AND UTILISED IN THIS STUDY 57
3.1 Chemical properties 59
3.1.1 Proximate analysis 59
3.1.2 Fischer tar analysis 59
3.1.3 Ash fusion temperature 60
3.1.4 Ultimate analysis 60
3.1.5 Coal char reactivity 60

3.2 Physical properties 61
3.2.1 Bulk density 61
3.2.2 True density 61
3.2.3 Particle size distribution 61
3.2.4 Ergun Index 61
3.2.5 Thermal fragmentation 62
3.2.6 Mechanical fragmentation 62
3.2.7 Caking propensity 62

3.3 Petrographic properties 62
3.3.1 Petrographic analysis 63
3.3.2 Char morphology analysis 63
3.3.3 Temperature estimation using optical reflectance 64
3.3.3.1 Preparation of reflectance / temperature calibration curve 64
3.3.3.2 Vitrinite reflectance on the GG41 gasifier turn-out samples 65

4 FACT-SAGE MODELLING 66

CHAPTER 3: RESULTS AND DISCUSSION 68

1 INTRODUCTION 68

2 RESULTS 69

3 CHEMICAL PROPERTY PROFILES 98
3.1 Proximate analysis results 98
3.1.1 Volatile matter distribution profile 98
3.1.2 Fixed carbon distribution profile 101
3.1.3 Ash distribution profile 106
3.2 Ultimate analysis results 110
3.2.1 GG41 Carbon (C) distribution profile 110
3.2.2 GG41 Hydrogen (H) distribution profile 111
3.2.3 GG41 Nitrogen (N) distribution profile 113
3.2.4 GG41 Sulphur (S) distribution profile 114
3.2.5 GG41 Oxygen (O) distribution profile 115

3.3 GG41 Coal char reactivity results 117

4 PHYSICAL PROPERTY PROFILES 120
4.1 Density profiles 120
4.1.1 The bulk density profile 120
4.1.2 The true density profile 122
4.2 Particle size distribution results 124
4.2.1 The +25mm size distribution profile 125
4.2.2 The -25mm +6.3mm size distribution profile 126
4.2.3 The -6.3mm size distribution profile 127
4.2.4 The Ergun Index profile 128
4.2.5 The thermal fragmentation profile 131
4.2.6 The mechanical fragmentation profile 132
4.2.7 The caking propensity profile 133

5 PETROGRAPHIC PROPERTY PROFILES 134

5.1 GG41 feed coal maceral group analysis results 135
5.2 GG41 Petrograhic morphology results 135
5.2.1 The GG41 devolatilised coal profile 137
5.2.2 The GG41 total char profile 140
5.2.3 The GG41 consumed char profile 141
5.2.4 The GG41 char type results 141
5.2.5 The GG41 heat affected mineral profile 144
5.3 Temperature profile results 144
5.3.1 The GG41 temperature profile results 145
5.3.2 The temperature profiles of the Indian pilot plant [Krishnudu, et. al. 1989a] and work conducted by [Glover, 1988] on the #15 Sasolburg gasifier 148
5.3.3 Temperature correlation with petrographic char morphology 150
5.3.4 Temperature correlation with chemical properties 151
5.3.5 Temperature correlation with physical properties 152

6 THE GG41 GASIFIER "PAN-CAKE" MODEL 153

CONCLUSIONS AND RECOMMENDATIONS 156

APPENDIX A *GG41 gasifier detail results* *i*

APPENDIX B *Indian pilot plant data [Krishnudu, et. al., 1989a,b] and Glover [1988] detail results* *viii*

APPENDIX C *FACT-SAGE modelling detail results* *xi*

REFERENCES *xvii*

LIST OF ABBREVIATIONS

AFT	ash fusion temperature
ASTM	American Society for Testing and Materials
C	carbon
C:H	carbon to hydrogen ratio
CBMN	carbominerite
CCSEM	computer- controlled scanning electron microscopy
CMT	Coal and Mineral Technologies
CTL	coal to liquids technology
daf	dry ash free
DRIFT	diffuse-reflectance infrared Fourier transform
DT	deformation temperature
EI	Ergun Index
FBDB	fixed-bed dry bottom
FC	fixed carbon
FBG	fixed-bed gasification
FT	flow temperature
Fus/scl	fusinite and sclerotinte
GG41	Gasifier number 41
HP	high pressure
HPBF	high pressure boiler feed
HT	hemispherical temperature
HT-XRD	high temperature X-ray diffraction
H	hydrogen
IDT	initial deformation temperature
IGCC	integrated gasification combined cycle
I	inertinite
I.int	inert inertodetrinite
IPP	Indian pilot plant
IR	infra-red
ISF	inert semi-fusinite
ISO	International Organization for Standardization
L	liptinite
Mic	micrinite
MK III	Mark three (ID 3.66m diameter gasifier)
MK IV	Mark four (ID 3.848m diameter gasifier)
MK V	Mark five (ID 4.659m diameter gasifier)

Mmf	mineral matter free
N	nitrogen
N+O	Navorsing en Ontwikkeling
O	oxygen
P	pressure
ROM	run of mine
PSD	particle size distribution
R&D	research and development
R.int	reactive inertodetrinite
RoV	reflectance of vitrinite
RSF	reactive semi-fusinite
S	sulphur
SABS	South African Bureau of Standards
SCS	Sasol Coal Supply
SCT	Syngas and Coal Technology R+D Group
SEM	scanning electron microscopy
SI	Sasol Infrachem
SL	Sasol Lurgi
SSF	Sasol Synfuels
ST	softening temperature
T	temperature
TGA	thermogravimetric analyzer
V	vitrinite
Vol.	volume
VM	volatile matter
XRD	X-ray diffractometry
#15	Gasifier number 15 (Sasolburg)
#16	Gasifier number 16 (Sasolburg)

LIST OF FIGURES

CHAPTER 1: BACKGROUND AND LITERATURE REVIEW

FIGURE	TITLE	PAGE
1.1	SCHEMATIC REPRESENTATION OF A FIXED BED GASIFIER SHOWING THE FOUR ZONES OF REACTIVITY (AFTER HEBDEN AND STROUD, 1981)	9
1.2	SCHEMATIC REPRESENTATION OF A FIXED OR MOVING-BED GASIFIER SHOWING SOLID AND GAS TEMPERATURE PROFILES OCCURING WITHIN THE REACTOR [NOWACKI, 1981]	10
1.3	SCHEMATIC REPRESENTATION OF THE SASOL-LURGI MK III, MK IV, AND MK V GASIFIER DIMENSIONS WITH RESPECT TO HOURLY FEED COAL RATE AND RAW GAS PRODUCTION RATE [SASOL-LURGI, 2005]	10
1.4	BAR CHART DEPICTING THE THERMAL FRAGMENTATION BEHAVIOUR OF A NUMBER OF DIFFERENT COAL SOURCES SHOWING THE EFFECT OF MOISTURE AND WEATHERING ON BREAKAGE [VAN DYK, 2001b, 2002b]	23
1.5	BAR CHART SHOWING THE VARIATION IN FEED ASH CONTENT (AIR DRIED BASIS) FOR VARIOUS LOCAL AND FOREIGN COAL SOURCES AS WELL AS FOR BIOMASS [VAN DYK, 2001b, 2002b]	24
1.6	BAR CHART SHOWING THE CAKING PROPENSITY AND ASSOCIATED RISK WITH RESPECT TO FIXED-BED GASIFICATION OF A NUMBER OF LOCAL AND FOREIGN COAL SOURCES [VAN DYK, 2001b, 2002b]	27
1.7	GRAPH SHOWING THE RECOMMENDED MINIMUM INCREMENT SIZE AND WIDTH OF OPENING IN SAMPLING DEVICE, REQUIRED IN RELATION TO NOMINAL TOP SIZE OF COAL WHEN SAMPLING [COAL PREPARATION IN SOUTH AFRICA HANDBOOK, 2002]	31
1.8	GRAPH SHOWING THE VOLATILE MATTER AND FIXED CARBON DISTRIBUTION PROFILES (NORMALISED TO A CONSTANT ASH CONTENT) FOR THE GODAVARI KHANI-RAMAGUNDAM COAL [KRISHNUDU, *et. al.*, 1989a]	35
1.9	GRAPH SHOWING THE EFFECT OF SIZE DEGRADATION IN RELATION TO GASIFIER HEIGHT FOR THE INDIAN PILOT SCALE GASIFIER OPERATING ON GODVARI KHANI-RAMAGUNDAM COAL [KRISHNUDU, *et. al.*, 1989a]	36
1.10	FIGURE SHOWING THE BULK DENSITY AND TRUE DENSITY PROFILES RELATIVE TO SAMPLE POSITION HEIGHT FOR THE INDIAN PILOT PLANT GASIFIER OPERATING ON GODVARI KHANI-RAMAGUNDAM COAL [KRISHNUDU, *et. al.*, 1989a]	37
1.11	GRAPH SHOWING THE PREDICTED TEMPERATURE PROFILE OF THE INDIAN PILOT SCALE GASIFIER [KRISHNUDU, *et. al.*, 1989a]	37
1.12	GRAPH SHOWING THE TEMPERATURE PROFILE IN THE SASOL ONE #15 GASIFIER. TEMPERATURES ARE INDICATED IN KELVIN. THE POSITION OF THE ASH BED IS SHOWN BY-------. (a) SECTION 3-9; (b) SECTION 12-6 [GLOVER, 1988]	40
1.13	GRAPH SHOWING THE VOLATILE MATTER PROFILE FOR DIFFERENT SIZED COAL IN THE SASOL ONE #16 GASIFIER. RECONDENSATION IS APPARENT TOWARDS THE TOP OF THE BED. VOLATILE MATTER EXPRESSED IN UNITS PER 100g OF ASH (EFFECTIVELY VOLATILE CONTENT PER UNIT VOLUME OF BED). [GLOVER, 1991]	42
1.14	GRAPH DEPICTING THE RELATIVE VOLATILE MATTER CONTENT OF THE DIFFERENT CHAR TYPES IDENTIFIED IN THE SASOL ONE #16 GASIFIER [GLOVER, 1991]	42
1.15	GRAPH SHOWING VOLATILE MATTER CONTENT AS A FUNCTION OF PARTICLE SIZE, AT DIFFERENT BED POSITIONS IN THE SASOL ONE #16 GASIFIER [GLOVER, 1991]	43

CHAPTER 2: EXPERIMENTAL PROCEDURES

FIGURE	TITLE	PAGE
2.1	24-HOURLY TREND FLOW RATE DATA FOR STEAM, OXYGEN, HIGH PRESSURE BOILER FEED WATER AND CO_2 FOR THE GG41 GASIFIER BEFORE DECOMMISSIONING	49
2.2	GG41 GASIFIER TREND DATA REFLECTING CONDITIONS USED IN THE DE-COMMISSIONING PROCESS ONCE THE OXYGEN SUPPLY WAS CUT	50
2.3	PHOTOGRAPH SHOWING A SAMPLE INCREMENT BEING TURNED-OUT OF THE	51

	GG41 GASIFIER	
2.4	PHOTOGRAPH SHOWING THE FRONT-END LOADER 3m^3 SHOVEL CONTAINING THE GG41 GASIFIER SAMPLE INCREMENT SIZE	51
2.5	PHOTOGRPH SHOWING THE SUB-SAMPLING PROCEDURE OF THE GG41 GASIFIER SAMPLE INCREMENT	52
2.6	PHOTOGRAPHIC IMAGES SHOWING A MACROSCOPIC VIEW OF THE GG41 GASIFIER TURN-OUT SAMPLES (1 TO 32)	57

CHAPTER 3: RESULTS AND DISCUSSION

FIGURE	TITLE	PAGE
3.1	GRAPH DEPICTING THE PERCENTAGE VOLATILE MATTER, FIXED CARBON AND ASH DISTRIBUTION PROFILES (DRY-BASIS) HIGHLIGHTING THE GG41 GASIFIER REACTION ZONES	68
3.2	GRAPH SHOWING THE NORMALISED VOLATILE MATTER DISTRIBUTION AT CONSTANT ASH CONTENT FOR THE GG41 GASIFIER AS WELL AS FOR THE FACTORISED INDIAN PILOT PLANT DATA	69
3.3	GRAPH DEPICTING THE RESIDUAL FISCHER TAR DISTRIBUTION PROFILE FOR THE GG41 GASIFIER, HIGHLIGHTING THE OCCURENCE OF VOLATILE MATTER RECONDENSATION	69
3.4	LINE GRAPH DEPICTING THE NORMALISED FIXED CARBON DISTRIBUTION AT CONSTANT ASH CONTENT FOR THE GG41 GASIFIER AND THE FACTORISED INDIAN PILOT PLANT DATA	70
3.5	GRAPH SHOWING THE NORMALISED PERCENTAGE CARBON CONVERSION FOR THE GG41 GASIFIER, FACTORISED INDIAN PILOT PLANT DATA AND THE #15 SASOLBURG MK 111 GASIFIER [GLOVER, 1988].	70
3.6	LINE GRAPH DEPICTING THE ASH PERCENTAGE CONTENT PROFILES FOR THE GG41 GASIFIER AND FACTORISED INDIAN PILOT PLANT DATA	71
3.7	GRAPH SHOWING THE ASH FUSION TEMPERATURE DISTRIBUTION PROFILES OBTAINED FOR THE GG41 GASIFIER	71
3.8	CHART DEPICTING THE PERCENTAGE HYDROGEN, NITROGEN, SULPHUR AND OXYGEN DISTRIBUTION PROFILES ON A NORMALISED kg / 100kg ASH BASIS FOR THE GG41 GASIFIER	72
3.9	CHART SHOWING THE EQUILIBRIUM COMPOSITION PROFILE CALCULATED FOR CARBON IN THE DRYING AND PYROLYSIS ZONES	72
3.10	CHART SHOWING THE EQUILIBRIUM COMPOSITION PROFILE CALCULATED FOR CARBON IN THE REDUCTION ZONE	73
3.11	CHART SHOWING THE CARBON : HYDROGEN RATIO DISTRIBUTION PROFILE FOR THE GG41 GASIFIER	73
3.12	CHART DEPICTING THE EQUILIBRIUM COMPOSITION PROFILE CALCULATED FOR HYDROGEN IN THE DRYING AND PYROLYSIS ZONES	74
3.13	CHART SHOWING THE EQUILIBRIUM COMPOSITION PROFILE CALCULATED FOR HYDROGEN IN THE REDUCTION ZONE	74
3.14	CHART SHOWING THE EQUILIBRIUM COMPOSITION PROFILE CALCULATED FOR NITROGEN IN THE DRYING AND PYROLYSIS ZONES	75
3.15	CHART DEPICTING THE EQUILIBRIUM COMPOSITION PROFILE CALCULATED FOR NITROGEN IN THE REDUCTION ZONE	75
3.16	CHART SHOWING THE EQUILIBRIUM COMPOSITION PROFILE CALCULATED FOR SULPHUR IN THE DRYING AND PYROLYSIS ZONES	76
3.17	CHART SHOWING THE EQUILIBRIUM COMPOSITION PROFILE CALCULATED FOR SULPHUR IN THE REDUCTION ZONE	76
3.18	CHART DEPICTING THE EQUILIBRIUM COMPOSITION PROFILE CALCULATED FOR OXYGEN IN THE DRYING AND PYROLYSIS ZONES	77
3.19	CHART SHOWING THE EQUILIBRIUM COMPOSITION PROFILE CALCULATED FOR OXYGEN IN THE REDUCTION ZONE	77
3.20	AN EXPANDED VIEW OF THE EQUILIBRIUM COMPOSITION PROFILE, CALCULATED FOR OXYGEN IN THE REDUCTION ZONE, HIGHLIGHTING THE OXYGEN SCAVENGING EFFECT OF MINERALS	78
3.21	LINE GRAPH SHOWING THE COAL CHAR CO_2 REACTIVITY PROFILE (50% BURN-OFF AT 1000 °C) FOR THE GG41 GASIFIER (h^{-1})]	78
3.22	*GRAPH SHOWING THE RELATIONSHIP BETWEEN HYDROGEN CONTENT (%daf)* AND CO_2 REACTIVITY (50% BURN-OFF AT 1000 °C) FOR THE GG41 GASIFIER	79

3.23	FIGURE DEPICTING THE BULK DENSITY PROFILE OF THE GG41 GASIFIER	79
3.24	GRAPH SHOWING THE BULK DENSITY PROFILE COMPARISON OF THE GG41 GASIFIER DATA AND THE FACTORISED INDIAN PILOT PLANT DATA	80
3.25	FIGURE DEPICTING THE TRUE DENSITY PROFILES OBTAINED FOR THE GG41 GASIFIER AND THE FACTORISED INDIAN PILOT PLANT DATA	80
3.26	CHART SHOWING THE RELATIONSHIP BETWEEN ASH CONTENT (%) AND TRUE DENSITY (kg/m^3) PROFILES FOR THE GG41 GASIFIER AND THE FACTORISED INDIAN PILOT PLANT DATA	81
3.27	GRAPHIC REPRESENTATION OF THE COAL PARTICLE SIZE DISTRIBUTION TRENDS FOR THE GG41 GASIFIER	81
3.28	GRAPHICAL REPRESENTATION OF THE +25mm SIZE FRACTION DISTRIBUTION PROFILE FOR THE GG41 GASIFIER SHOWING THE SEVERE EFFECT OF FRAGMENTATION LEADING TO GASIFIER INSTABILITY	82
3.29	LINE GRAPH SHOWING THE -25mm + 6.3mm SIZE FRACTION DISTRIBUTION PROFILE OBTAINED FOR THE GG41 GASIFIER	82
3.30	LINEAR PLOT SHOWING THE RELATIONSHIP BETWEEN BULK DENSITY (kg/m^3) AND PERCENTAGE -25mm +6.3mm RETAINED FRACTION OBTAINED FOR THE GG41 GASIFIER	83
3.31	CHART SHOWING THE -6.3mm SIZE FRACTION DISTRIBUTION PROFILE FOR THE GG41 GASIFIER	83
3.32	PLOT OF THE ERGUN INDEX PROFILE HIGHLIGHTING THE ZONES OF PRIMARY, SECONDARY AND TERTIARY FRAGMENTATION OBTAINED FOR THE GG41 GASIFIER	84
3.33	LINEAR PLOT SHOWING THE RELATIONSHIP BETWEEN THE ERGUN INDEX DISTRIBUTION PROFILE AND THE PERCENTAGE -6.3mm SIZE FRACTION OBTAINED FOR THE GG41 GASIFIER	84
3.34	CHART SHOWING THE ERGUN INDEX PROFILE COMPARISON OF THE GG41 GASIFIER AND THE FACTORISED INDIAN PILOT PLANT DATA.	85
3.35	LINE GRAPH DEPICTING THE GG41 GASIFIER THERMAL FRAGMENTATION PROFILE	85
3.36	LINE GRAPH SHOWING THE GG41 GASIFIER PERCENTAGE MECHANICAL FRAGMENTATION PROFILE	86
3.37	CHART SHOWING THE CAKING PROPENSITY PROFILE OF THE GG41 GASIFIER.	86
3.38	BAR CHART SHOWING THE COAL AND CHAR MORPHOLOGY CLASSIFICATION PROFILE OF THE GG41 GASIFIER TURN-OUT SAMPLES	87
3.39	LINE GRAPH SHOWING THE COAL MICROLYTHOTYPE BEHAVIOUR OCCURING IN THE GG41 GASIFIER	87
3.40	GRAPH SHOWING THE RELATIONSHIP BETWEEN THE GG41 GASIFIER DEVOLATILISED COAL CONTENT (vol. %) VERSUS THE COAL CHAR CO_2 REACTIVITY PROFILE (50% CARBON BURN-OFF AT 1000°C)	88
3.41	GRAPH SHOWING THE TOTAL CHAR (vol. %) PROFILE OBTAINED FOR THE GG41 GASIFIER	88
3.42	GRAPH SHOWING THE CONSUMED CHAR (vol. %) PROFILE OBTAINED FOR THE GG41 GASIFIER	89
3.43	FIGURE SHOWING THE CHAR PARTICLE TYPE ANALYSIS (vol. %) AS A FUNCTION OF BED DEPTH FOR THE GG41 GASIFIER TURN-OUT SAMPLES	89
3.44	FIGURE DEPICTING THE HEAT AFFECTED MINERAL (vol. %) AND ASH (%) PROFILES FOR THE GG41 GASIFIER	90
3.45	CHART SHOWING THE MEAN OPTICAL REFLECTANCE AND TEMPERATURE CALIBRATION CURVE FOR THE GG41 GASIFIER FEED COAL SAMPLE 32	90
3.46	GRAPH DEPICTING THE SOLIDS TEMPERATURE PROFILES OBTAINED FOR THE GG41 GASIFIER SHOWING AVERAGE, SURFACE AND PEAK TEMPERATURES (°C), COMPARED TO THE FACTORISED INDIAN PILOT PLANT DATA AND THE #15. SASOLBURG MK 111 GASIFIER	91
3.47	SCHEMATIC DIAGRAM DEPICTING A "PAN-CAKE" MODEL OF THE SASOL-LURGI MK IV GG41 GASIFIER SHOWING REACTION ZONES WITH RESPECT TO CHEMICAL AND PETROGRAPHICAL PROPERTY PROFILES	91
3.48	PHOTOGRAPHS (1 a-f) SHOWING THE TRANSFORMATION OF COAL TO CHAR FOR THE GG41 GASIFIER TURN-OUT SAMPLES (MAGNIFICATION X500, OIL IMMERSION, REFLECTED LIGHT)[WAGNER, 2005b]	136
3.49	PHOTOGRAPHS (2 a-f) SHOWING THE MINERALS OBSERVED IN THE GG41 GASIFIER TURN-OUT SAMPLES (MAGNIFICATION X500, OIL IMMERSION, REFLECTED LIGHT) [WAGNER, 2005b].	137

LIST OF TABLES

CHAPTER 1: BACKGROUND AND LITERATURE REVIEW

TABLE	TITLE	PAGE
1.1	TABLE SHOWING THE SASOL MINING (PTY) LTD. COAL PRODUCTION FIGURES PER COLLIERY [SASOL ANNUAL REPORT, 2003]	13
1.2	TABLE SHOWING THE EFFECT OF CHANGE IN PARTICLE SIZE ON SAUTER DIAMETER.	21
1.3	TABLE SHOWING THE PROXIMATE ANALYSIS (AIR DRIED BASIS) FOR TYPICAL SCS WEST BLEND. [SASOL GASIFICATION HANDBOOK, 2005].	23
1.4	TABLE SHOWING THE PROXIMATE ANALYSIS RESULTS (DRY BASIS) FOR TYPICAL SCS WEST BLEND. [SASOL GASIFICATION HANDBOOK, 2005].	23
1.5	TABLE SHOWING THE ELEMENTAL ASH ANALYSIS (MASS %) FOR THE TYPICAL SCS WEST BLEND. [SASOL GASIFICATION HANDBOOK, 2005].	24
1.6	TABLE SHOWING THE ASH MELTING PROPERTIES (OXIDIZNG) FOR THE TYPICAL SCS WEST BLEND. [SASOL GASIFICATION HANDBOOK, 2005].	25
1.7	TABLE SHOWING THE PROCESS CONDITIONS AT THE TIME OF QUENCHING FOR THE GODVARI KHANI-RAMAGUNDAM COAL. [KRISHNUDU et al., 1989]	34

CHAPTER 2: EXPERIMENTAL PROCEDURES

TABLE	TITLE	PAGE
2.1	TABLE SHOWING THE GG41 GASIFIER SAMPLE NUMBER RELATIONSHIP WITH GG41 GASIFIER HEIGHT (m)	48
2.2	PROCESS CONDITIONS AT THE TIME OF QUENCHING FOR THE INDIAN PILOT PLANT AND THE SASOL-LURGI GG41 COMMERCIAL SCALE MKIV GASIFIER.	52
2.3	TABLE SHOWING THE FACTORISED SAMPLE NUMBER CORRELATION FOR THE INDIAN PILOT PLANT DATA WITH THE GG41 GASIFIER.	53
2.4	PROPERTIES THAT WILL BE COMPARED WITH THE GG41 GASIFIER DATA.	55

CHAPTER 3: RESULTS AND DISCUSSION

TABLE	TITLE	PAGE
3.1	TABLE SHOWING THE STATISTICAL AVERAGE CHEMICAL PROPERTY RANGE CALCULATED FOR THE GG41 GASIFIER IN RELATION TO THE FOUR REACTION ZONES IDENTIFIED.	90
3.2	TABLE SHOWING THE STATISTICAL AVERAGE CHEMICAL PROPERTY RANGE CALCULATED FOR THE FACTORISED INDIAN PILOT PLANT DATA AND [GLOVER, 1989] IN RELATION TO THE FOUR REACTION ZONES IDENTIFIED.	90
3.3	TABLE SHOWING THE STATISTICAL AVERAGE PHYSICAL PROPERTY RANGE CALCULATED FOR THE GG41 GASIFIER IN RELATION TO THE FOUR REACTION ZONES.	91
3.4	TABLE SHOWING THE STATISTICAL AVERAGE PETROGRAPHIC PROPERTY RANGE CALCULATED FOR THE GG41 GASIFIER, FACTORISED INDIAN PILOT PLANT DATA AND [GLOVER, 1989] IN RELATION TO THE FOUR REACTION ZONES IDENTIFIED.	91
3.5	THE GG41 GASIFIER FEED COAL MACERAL GROUP ANALYSIS CONDUCTED ON COAL SAMPLE 32 (vol. %l)	92
3.6	RELATIONSHIP BETWEEN THE GG41 REFLECTANCE OF VITRINITE (ROV %) AND CHAR MORPHOLOGY MEASUREMENTS TO DETERMINE SIGNIFICANT ZONAL LEVELS.	92
3.7	RELATIONSHIP BETWEEN THE GG41 REFLECTANCE OF VITRINITE (ROV %) AND CHEMICAL PROPERTY MEASUREMENTS TO DETERMINE SIGNIFICANT ZONAL LEVELS.	93
3.8	RELATIONSHIP BETWEEN THE GG41 REFLECTANCE OF VITRINITE ROV %) AND PHYSICAL PROPERTY MEASUREMENTS TO DETERMINE SIGNIFICANT ZONAL LEVELS.	94

LIST OF APPENDICES

APPENDIX A: GG41 GASIFIER DETAIL RESULTS

TABLE	TITLE	PAGE
A1	THE GG41 GASIFIER PROXIMATE ANALYSIS RESULTS REPORTED ON AN AS RECEIVED (%) BASIS AS WELL AS DRY	i
A2	THE GG41 NORMALISED VOLATILE MATTER, NORMALISED FIXED CARBON, CARBON CONVERSION AND ASH FUSION TEMPERATURE RESULTS	ii
A3	THE GG41 ULTIMATE ANALYSIS, FISCHER TAR AND CO_2 REACTIVITY RESULTS	iii
A4	THE GG41 GASIFIER BULK DENSITY, TRUE DENSITY, ERGUN INDEX, THERMAL FRAGMENTATION, MECHANICAL FRAGMENTATION AND CAKING PROPENSITY RESULTS	iv
A5	LINEAR CORRELATION DATA ANALYSIS RESULTS (ANALYSIS TOOLPACK PACKAGE) FOR THE GG41 GASIFIER VARIABLES: AVERAGE TEMPERATURE, ERGUN INDEX, THERMAL FRAGMENTAION, MECHANICAL FRAGMENTATION, CAKING AND MOISTURE	iv
A6	THE GG41 GASIFIER FRACTIONAL PARTICLE SIZE DISTRIBUTION RESULTS REPORTED ON A PERCENTAGE RETAINED BASIS	v
A7	GASIFIER GG41 TURN-OUT INVESTIGATION – PETROGRAPHIC RESULTS	vi
A8	VITRINITE REFLECTANCE ANALYSIS ON TGA TREATED GG41 - #32 (FEED SAMPLE) FOR TEMPERATURE CALIBRATION	vii
A9	VITRINITE REFLECTANCE ANALYSIS ON THE GG41 GASIFIER TURN-OUT SAMPLES SHOWING AVERAGE, SURFACE AND PEAK TEMPERATURE RESULTS	vii

APPENDIX B: FACTORISED INDIAN PILOT PLANT DATA [KRISHNUDU, et al., 1989]; AND GLOVER [1988] DETAIL RESULTS)

TABLE	TITLE	PAGE
B1	NORMALISED VOLATILE MATTER, NORMALISED FIXED CARBON, CARBON CONVERSION AND ASH DISTRIBUTION RESULTS FOR THE FACTORISED INDIAN PILOT PLANT DATA	viii
B2	BULK DENSITY, TRUE DENSITY, ERGUN INDEX AND SOLIDS TEMPERATURE RESULTS FOR THE FACTORISED INDIAN PILOT PLANT DATA	viii
B3	INDIAN PILOT PLANT FRACTIONAL PARTICLE SIZE DISTRIBUTION RESULTS REPORTED ON A PERCENTAGE RETAINED BASIS	ix
B4	ANALYSES OF SEQUENTIAL LAYER SAMPLES FROM QUENCHING EXPERIMENTS (GODVARI KHANI-RAMAGUNDAM COAL)	ix
B5	CARBON CONVERSION AND SOLIDS TEMPERATURE RESULTS AFTER GLOVER [1988] FOR THE #15 MK III GASIFIER IN SASOLBURG	x

APPENDIX C: FACT-SAGE MODELLING RESULTS

TABLE	TITLE	PAGE
C1	SUMMARY OF INPUT REACTANTS INTO FACTSAGE DEVOLATILISATION ZONE	xi
C2	GAS FLOW FROM REDUCTION ZONE	xi
C3	CARBON SPECIATION WITHIN THE DRYING AND PYROLYSIS ZONES	xiii
C4	CARBON SPECIATION WITHIN THE REDUCTION ZONE	xiii
C5	HYDROGEN SPECIATION WITHIN THE DRYING AND PYROLYSIS ZONES	xiii
C6	HYDROGEN SPECIATION WITHIN THE REDUCTION ZONE	xiv
C7	NITROGEN SPECIATION WITHIN THE DRYING AND PYROLYSIS ZONES	xiv
C8	NITROGEN SPECIATION WITHIN THE REDUCTION ZONE	xiv
C9	SULPHUR SPECIATION WITHIN THE DRYING AND PYROLYSIS ZONES	xiv
C10	SULPHUR SPECIATION WITHIN THE REDUCTION ZONE	xv
C11	OXYGEN SPECIATION WITHIN THE DRYING AND PYROLYSIS ZONES	xv
C12	OXYGEN SPECIATION WITHIN THE REDUCTION ZONE	xvi

CHAPTER 1
BACKGROUND AND LITERATURE REVIEW

Optimisation of the Sasol-Lurgi Fixed Bed Dry Bottom (FBDB) gasification process is strategically necessary if anticipated demands for increased gas loads are to be met in the medium and long term, both in Secunda and globally, with the drive to globalize Sasol's coal to liquids technology (CTL). Over the years incremental improvements in gasification efficiencies have resulted from enhanced engineering design and maintenance procedures. Yet surprisingly, the gasification process remains obscure, hindering attempts to optimise around the physical phenomena and chemical reactions occurring within the reactor. The optimisation of the fixed-bed gasification process with respect to the consumption of oxygen, steam and carbon efficiency, as well as reactor stability remain the major challenges in advancing the understanding applicable to this technological field [Van de Venter, 2004; Van Heerden, 2005]. Further optimisation of the gasification plant control philosophy by means of accurate kinetic reaction models has also been proposed by Van der Walt [1994].

Much fundamental and empirical work has been conducted over the years in the field of power generation [Hartman, *et. al.*, 1978; Blazek, *et. al.*, 1979; Jaeger and Mayer, 2000; Shadle and Swanson, 2001], i.e. optimising entrained flow and fluidized bed reactors. In parallel, but on a much smaller scale, fixed-bed gasification has also been researched. Early work involved experimentation on a pilot-scale fixed-bed pressure gasifier (internal diameter 0.6m) which was used by Hebden, *et. al.* [1954 – 55] to map the temperature and gas concentration profiles along the vertical axis. This reactor was oxygen-steam-blown and operated up to 4MPa and ash was removed dry. The reactor differed from commercial gasifiers in that the water jacket was replaced with refractory material to limit heat losses through the sides. Temperature data was collected from thermocouples and gas sampling tubes, which ran parallel to the vertical axis through the centreline of the fuel bed. It should be noted that such probes may perturb the local flow of char and gas [Johnson and Thomas, 1987].

Krishnudu, *et. al.* [1989a,b] studied a larger-diameter (1.13m) fixed-bed reactor, quenched by cutting off the supply of oxygen and steam. Sequential samples were collected by running-out the fuel bed through the ash discharge grate and a significant change in average particle size and voidage along the reactor axis was recorded. The extent of the different reaction zones in the gasifier was also revealed. The use of residual volatiles yield as a temperature indicator for the char samples is questionable

[Johnson and Thomas, 1987]. Nevertheless, a one-dimensional model of the gasifier was put forward [Prasad and Reddy, 1989] based on the observed axial particle size distribution and voidage profiles. A similar one-dimensional model was proposed by Radulovic and Smoot [1992], which is already an improvement on older gasifier models [Yoon and Denn, 1978] that assumed a homogeneous voidage distribution throughout the fuel bed, as well as plug-flow of the solid and gaseous phases.

The extension of one-dimensional mathematical models of gasifiers to two-dimensional models [Denn, *et. al.*, 1982] lacks experimental evidence on the radial distribution of bed voidage and on the gaseous flow patterns in large-scale gasifiers [Madhusudhan *et. al.*, 1989]. This experimental evidence can be obtained only through indirect methods of characterising the gas flow patterns through gasifier beds. One such method is to characterise the char samples from digging out the bed of a quenched gasifier, i.e. a "post mortem" examination. This technique provides information on gasifier behaviour at shutdown. Its disadvantage is that there may be cool-down and bed collapse effects.

In an attempt to better understand the gasification reactor within the context of the internal processes, and thereby determine an optimisation path of commercial-scale Sasol-Lurgi FBDB gasifiers [Glover, 1988, 1991] conducted several gasifier dissection sampling campaigns. Glover's work [1988, 1991] focused predominantly on quantifying the carbon behaviour during gasification, but did not investigate the mineral matter transformation and interactions occurring during the gasification process within the fire-bed and ash zone regions. However, with relevance to this zone he postulated that where thermal-channeling was observed, local steam : oxygen ratio variations may occur; possibly allowing for higher temperatures to be reached above ash melting, giving rise to clinker formation in certain areas of the gasifier.

To put the gasification of coal into perspective, Glover [1991] found that there are only a limited number of coal properties that may significantly affect reactor behaviour. These are in no specific order of importance:

- The reactivity of the coal
- The feed coal particle size distribution (PSD)
- The ash content and ash melting properties of the coal
- The fixed carbon content of the coal
- The de-volatilisation behaviour of the coal

Glover's [1988, 1991] findings were highly significant and will be discussed in more detail in Section 6.2 of this review. A major conclusion from this work was that particle size measurements clearly showed a radial pattern, i.e. a lower fines content in the centre and at the edge of the vessel. This strongly suggested a radial distribution of permeability, and hence a radial distribution of flow; the higher flows being at the centre and near the wall. DRIFT (diffuse-reflectance infrared Fourier transform) spectra revealed that a temperature profile, consistent with the highest flows in the centre and wall regions of the vessel existed; therefore greater reaction occurred in these regions [Glover *et al.,* 1995].

Glover's [1988, 1991, 1995] work added value to the Sasol operations in elucidating coal segregation effects which resulted in gasifier operating instabilities. This led to the development of a new gasifier coal feeding design, viz. "Unifeeder", which has been implemented. The output from this work was also used as input in the development of kinetic models of the fixed-bed gasifier. Two kinetic models are currently being used by Sasol Technology R+D [Keyser, 1997], these being:

- The one-dimensional pseudo-homogeneous model in which plug flow of the gas and solid phase are assumed. Pseudo-homogeneous means that it is assumed that the gasifier bed is homogeneous in the sense that no distinction is made between the solid and gas phases with regards to heat transfer. It is thus assumed that the gas and solid phases are at the same temperature. The model was developed using data from the sequential sampling campaign of the Indian pilot-plant as discussed by Krishnudu *et. al.* [1989a,b] in a PhD study by Van der Walt [1994].

- The one-dimensional heterogeneous model was developed after certain shortcomings of the pseudo-homogeneous model became apparent when the effect of increased ash content was modelled. In the heterogeneous model, the gas and solid phases are still assumed to be plug flow, but it is not assumed that the gas and solid phases are at the same temperature. The temperature difference between the gas and solid phases is determined by heat and mass transfer rates and the values assumed for the transport coefficients also impact on the reliability and accuracy of the model predictions. All the other assumptions for the pseudo-homogeneous model apply to the heterogeneous model as well [Botes, 1996].

Unfortunately the value of these models has not been fully realized, mainly due to a lack of complete input data and assumptions made, i.e. only fixed carbon and ash content were used as input in these kinetic models [Van der Walt, 2005].

Glover [1988, 1991] also observed in his work that ash was found with relatively unconverted char, as well as the large range of optical reflectance of individual samples taken, suggesting that there is not only a large variation of average properties radially, but also a wide range of actual properties locally. This is not surprising, since coal itself is very heterogeneous. The more reactive particles reacted at a higher rate, hence tending to be burnt out when the less reactive ones were still quite far from complete conversion. These in-homogeneities are likely to have implications for gasifier operation. The large radial distribution of permeability and hence flow, probably limits the maximum throughput of the bed. It is vital to avoid oxygen breakthrough into the raw gas stream leaving the gasifier, especially in flows following the most permeable pathways through the fuel bed. This implies that the maximum throughput of the gasifier is effectively limited by the worst-case properties, rather than the average properties of the bed.

Local variations of properties may also have consequences for gasifier operation, since the ash from the more reactive particles may impede the access of fresh gas to areas where there may still be un-reacted char. This again may tend to limit the capacity of the gasifier. In such a case, the solids flow rate needs to be adjusted so that even in the parts of the bed with least reaction, effectively no un-burnt carbon is removed (with the ash) from the bed [Glover, 1988].

The ash from the Secunda gasification process typically contains 4% to 7% carbon in ash, and discrete carbon particles in a range of sizes can readily be observed in the ash. Slaghuis [2004] discussed possible reasons for the occurrence of discrete remnant carbon in the ash. A probable theory is that the steam added towards the bottom of the gasifier to control ash melting temperatures and provide hydrogen for the production of syngas, has a "quenching" effect on the exothermic char reactions in this region. The reason for chars not being fully consumed in the combustion zone in the gasifier could also be due to lack of opportunity caused by channeling and uneven reaction zones, diffusion limitations (heat and mass transfer effects) leading to incomplete reaction [Keyser, 2006].

Sintering of ash particles is considered desirable in Sasol-Lurgi FBDB gasification, since it promotes easy gas flow, whereas clinkering creates channeling and localised "hot spots", leading to unstable gasifier operation. Encapsulation of carbon has been observed in clinkers using computer-controlled scanning electron microscopy (CCSEM), giving rise to a lower carbon efficiency during gasification [Van Alphen, 2003]. The sintering and encapsulation processes are still poorly understood; these phenomena are being investigated in a study by Matjie [2005].

From an ash melting characteristic perspective, a major optimisation constraint is that the Sasol-Lurgi FBDB gasification process is essentially operated under thermodynamically controlled conditions. It is governed to a large extent by operating the reactor temperature below the ash fusion characteristics of the feed coal. This temperature control is via excess steam addition, which negatively impacts on the water gas shift reaction, producing carbon dioxide and hydrogen.

A study is currently being conducted by Van Dyk [2006], which aims at increasing the ash fusion temperature during gasification with the use of additives. By increasing the ash fusion temperature, the direct effect will be that steam consumption can be decreased, which in turn will improve carbon utilisation. This study [Van Dyk, 2006] focuses on additive effects on mineral transformation, culminating in mechanism elucidation using high temperature XRD, together with viscosity modelling. Fact-Sage thermodynamic equilibrium modelling as well as gasifier dissection data, which forms a part of this study, will be used to confirm the findings. The mineralogical and trace element compositional profiles from the envisaged Sasol-Lurgi FBDB excavation, together with the thermodynamic modelling, is not reported on in this study; but has to be done.

Very accurate statistical models were developed by Keyser and Coetzer [1999, 2000] using the data obtained from a fully instrumented MK IV test gasifier GG09, situated within the Secunda gasification plant. Although it is an empirical fit to the data, much more value has been obtained with this approach, when compared to the reaction kinetic models. The effect of the particle size distribution (PSD) could be quantified very accurately, which is something that none of the existing Sasol gasification models can do, because they do not accommodate PSD [Keyser, 1997].

From numerous test gasifier runs, [Van Dyk 2002a,b; Keyser and Coetzer, 1999, 2000], an understanding of the oxygen consumption on the basis of ash content has not been clearly explained. Even when using statistically designed experimental runs, the lack in closures with respect to oxygen balance could not always be clarified [Coetzer, 2005].

In summary, Glover's [1988, 1991] pioneering gasifier excavation work essentially showed detailed evidence of the complex localised behaviour occurring within the Sasol-Lurgi FBDB gasifier, i.e. variation in the radial position. The gasification community within Sasol has since believed for numerous years that a simplified "pan-cake" model showing the reaction zones within this commercial-scale gasifier was not

possible. This is in contrast to the earlier work done by Krishnudu *et. al.*, [1989a,b], but could possibly be explained by the fact that the sequential sampling technique applied by Krishnudu *et. al.*,[1989a,b], examined 0.25m slices of the pilot plant gasifier; this size of sample could possibly average much of the localised properties sufficiently to provide a clear axially–derived picture of the reaction zones occurring within the reactor.

Gasification behaviour is particle dependent, whilst gasifier (reactor) behaviour is an averaging process of individual responses of each particle [Glover, 1991]. It is hypothesized, in the case of this study, that if it were possible to extract and analyze particles from different reaction zones within a gasifier, it may be likely to enhance the understanding as to the contribution that these particles make towards gasification. This better understanding of the particle-type compositional responses could act as an enabler to further influence gasifier performance. The proposed gasifier "turn-out" sampling methodology, in the case of this study could therefore possibly provide accurate information regarding the chemical, physical and petrographical property behaviour occurring within a Sasol-Lurgi FBDB MK IV gasifier.

From the foregoing, it is clear that a simplified "pan-cake" model showing the reaction zones within the Sasol-Lurgi FBDB gasifier is much needed and is expected to provide essential data to advance this reactor's kinetic modelling capability. A well planned reactor excavation is necessary to obtain the required data, as well as simultaneously addressing the challenges of better understanding carbon loss and oxygen scavenging behaviour during mineral transformation, as well as identifying regions of instability occurring within the gasification reactor.

1 OBJECTIVES OF THIS STUDY

The primary focus of this study was to evaluate the proposed sequential (axial) sampling "turn-out" methodology of the entire Sasol Lurgi FBDB MK IV gasifier, in order to present samples to accurately describe operational aspects occurring in the reaction zones within the reactor. Characterisation of the chemical, physical and petrographical properties of the sample increments are expected to deliver distinct profiles of the drying, pyrolysis, reduction and combustion (ash bed) zones. In order to interpret the coal property transformational behaviour occurring within the commercial-scale gasifier, the following analysis will be undertaken:

- Proximate and ultimate analysis
- Coal reactivity analysis
- Ash melting characteristics
- Density characteristics
- Particle size distribution
- Thermal and mechanical fragmentation
- Caking propensity
- Petrographic coal and char morphology characterisation
- Temperature profile using optical reflectance

The experimental results obtained from this study can possibly be used to validate the existing one-dimensional kinetic models at Sasol Technology R+D in terms of fixed carbon and ash content, but an understanding of the chemical, physical and petrographic behaviour within the reactor could advance the model prediction capability significantly. The Sasol Gasification Operations can then also possibly benefit in terms of an improved control philosophy of their process, yielding better gasification stability, improved efficiency and availability. The kinetic model development is not considered to be part of this particular study.

Secondary objectives include:

- Obtaining a better understanding of the loss of carbon to the discarded ash,
- Ascertaining whether oxygen scavenging during mineral transformation occurs in the gasification process, and
- Developing an understanding of the zones of instability occurring within the gasifier.

The literature survey describes the Sasol-Lurgi FBDB gasification process, coal origin and composition, as well as coal characteristics with specific emphasis on the coal properties that affect gasification performance. The sampling of the commercial-scale MK IV FBDB gasifier forms an integral part of this study. The available literature is next reviewed in terms of obtaining an understanding of the principles of good sampling as well as methodologies used for gasifier sampling. Two case studies [Krishnudu *et. al.* 1989a,b] and [Glover, 1988, 1991] are presented, which describe previously-conducted fixed-bed gasifier dissections, with the emphasis on understanding the chemical, physical and petrographic phenomena which affect gasification performance.

2 GASIFICATION

SASOL was established on 26 September 1950, with the prime objective of converting low grade coal into petroleum products and chemical feedstocks [Financial Mail, 2000]. Sasol One was built in Sasolburg and produced its first liquid product in 1955. In 1969 the Natref crude oil refinery was commissioned and in 1980 and 1982 Sasol Two and Sasol Three respectively began production in Secunda [Bulletin 113, 2000]. Today, more than 50 years after the initial start-up, Sasol gasifies more than 30 million tons of coal per annum to produce the equivalent of 150 000 barrels per day of fuels and petrochemicals via its indirect liquefaction process [Sasol Annual Report, 2003]. The process produces in excess of 40% of South Africa's liquid fuels requirements. Sasol manufactures more than 200 fuel and chemical products in Sasolburg and Secunda in South Africa, as well as at several other overseas locations. The products are exported to more than 70 countries around the world [Financial Mail, 2000].

The history of Sasol revolves around the Group's impressive track record in innovating new or improved products and processes. Notable breakthroughs have been achieved in the fields of geology, mining production systems, coal preparation and gasification systems, mining explosives, fertilizers, biotechnology, environmental engineering and gas to liquids technology [Van Dyk, *et. al.*, 2001c; Sasol Annual Report, 2003].

2.1 Sasol-Lurgi Fixed-Bed Dry Bottom (FBDB) gasification

Lump sized coal is used by Sasol as a feedstock to produce synthesis gas via the Sasol-Lurgi FBDB gasification process. Once the coal is mined, it is crushed down to less than 100 mm (typical top-size of about 65mm) and screened to a bottom size of 5mm to 8mm. The coal enters the top of the gasifier through a lock-hopper system, while reactant gases (steam and oxygen) are introduced at the bottom of the gasifier. The reactant gases flow at a relatively low velocity upwards through the spaces between the coal lumps. The counter-current operation results in a temperature profile in the reactor, with the result that four characteristic zones (Figure 1.1) can be identified in a fixed-bed gasifier [Berkowitz, 1979; Hebden and Stroud, 1981; Slaghuis, 1989].

It should be noted however, that the characteristic reaction zones shown in Figure 1.1 have to date not been quantified in the Sasol-Lurgi FBDB gasifier. It is the primary focus of this study to elucidate on this information in order to advance the reactor kinetic modelling capability.

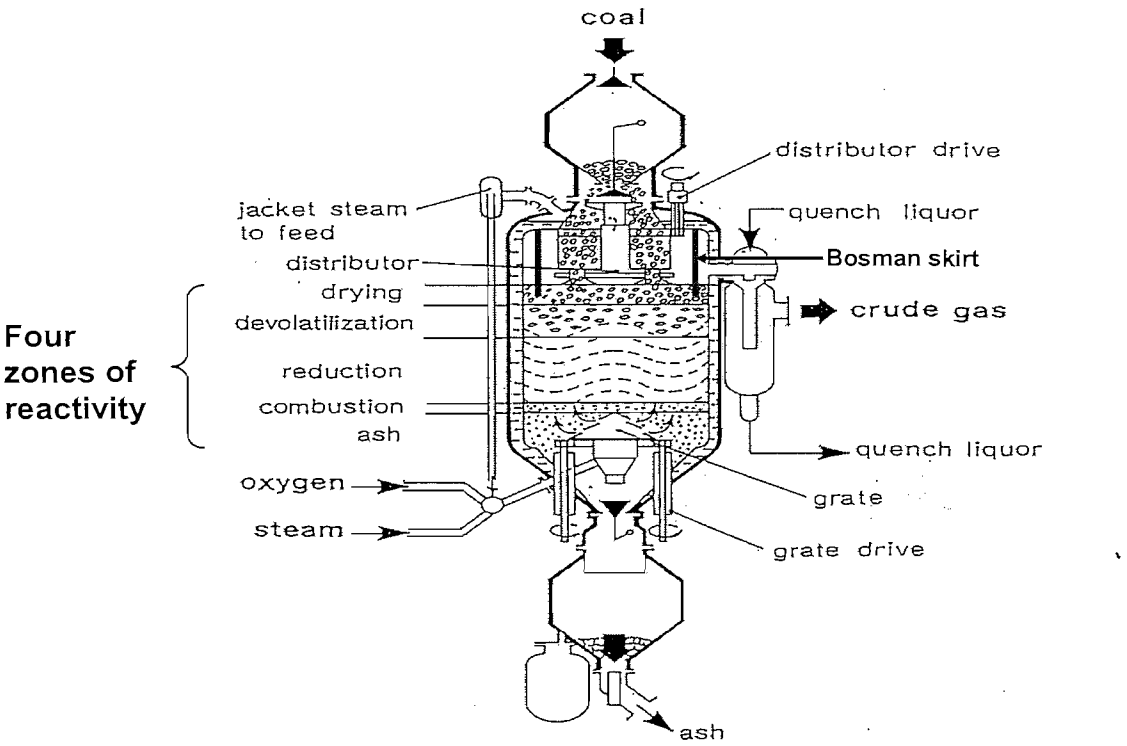

FIGURE 1.1: SCHEMATIC REPRESENTATION OF A FIXED-BED GASIFIER SHOWING THE FOUR ZONES OF REACTIVITY (AFTER HEBDEN AND STROUD, 1981)

As the coal descends, it is first dried and devolatilised by the heat of the rising gas. The devolatilised coal, better known as char, then enters a gasification zone and residual char is finally burnt to ash. Ash is removed at the bottom of the gasifier by a rotating grate and lock-hopper (Figure 1.1). It should be noted from Figure 1.1 that the coal distributor which is shown is not used today in the Sasol-Lurgi MK IV gasifier, but is incorporated here merely showing the original schematic design after [Hebden and Stroud, 1981] ; the Figure was modified to also show the Bosman skirt design which is the coal feeder arrangement used by Sasol today. Generally, either a coal distributor or a Bosman skirt feeder arrangement can be used.

During gasification, the mineral matter in coal undergoes various transformations as the temperature increases. The final product of these transformations is ash or agglomerates of ash particles. The size of the ash particle agglomerates (clinker) can vary from tiny particles to lumps larger than 100mm. Ash clinkering inside the gasifier can lead to channel-burning, pressure drop problems and unstable gasifier operation [Keyser, *et. al.*, 2005].

The Sasol-Lurgi FBDB gasifier technology requires that the temperature of the ash must not exceed the ash fusion temperature (flow) in the above-lying combustion zone. When the temperature in the combustion zone exceeds the melting point of the ash-forming minerals, the minerals will melt / flow and agglomerate. Due to the

counter-current mode of operation, hot ash exchanges heat with the cold incoming agent (steam and oxygen or air), while at the same time hot raw gas exchanges heat with cold incoming coal. This results in the ash and raw gas leaving the gasifier at relatively low temperatures compared to other types of gasifiers, which improves the thermal efficiency and lowers the steam consumption. A schematic representation of the solid and gas temperature profiles of a fixed-bed gasifier is given in Figure 1.2 [Schilling, *et. al.*, 1979; and Nowacki, 1981]. It will be attempted in this study to measure the solid temperature profile occurring within the Sasol-Lurgi FBDB gasifier.

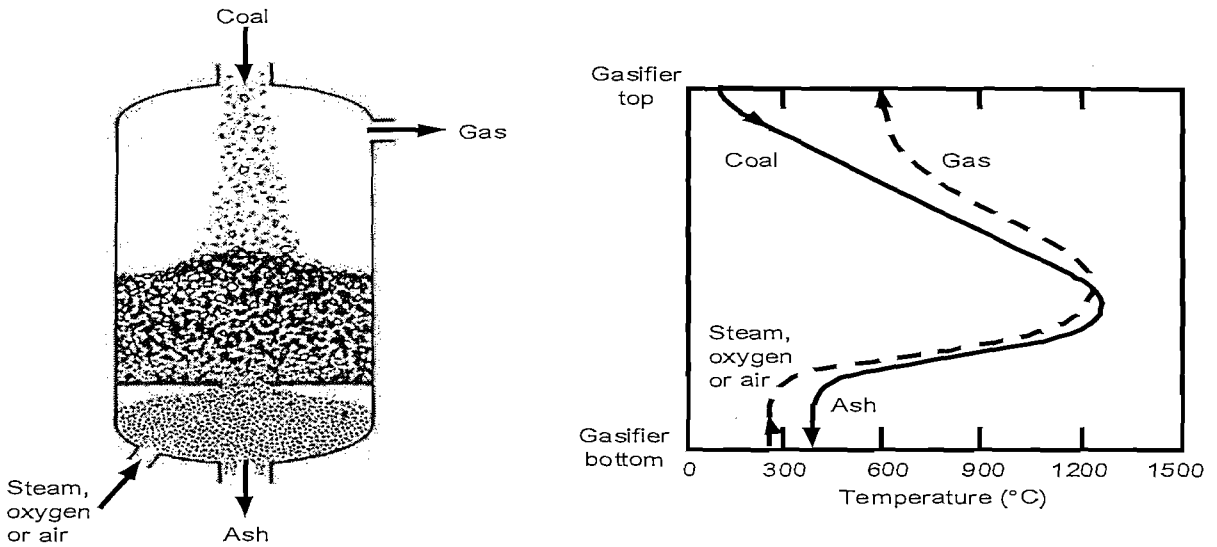

FIGURE 1.2: SCHEMATIC REPRESENTATION OF A FIXED OR MOVING-BED GASIFIER SHOWING SOLID AND GAS TEMPERATURE PROFILES OCCURING WITHIN THE REACTOR [NOWACKI, 1981]

Sasol One was originally equipped with ten Mark III gasifiers, having an internal diameter of 3,66m. Three gasifiers of similar design were added in 1966. In 1978 three Mark IV gasifiers, scaled up to 55% above original design, were installed; and a Mark V (scaled up by 114% above original design) was commissioned in 1980. Figure 1.3 [Sasol-Lurgi, 2005] shows a schematic representation of the Sasol-Lurgi MK III, MK IV and MK V gasifier dimensions, with respect to hourly feed coal rate and raw gas production rate.

Sasol currently operates 80 Mark IV gasifiers, of which Sasol Two and Three each have 40 units. These units can truly be seen as the "work-horses" of syngas production from coal. The demand for synthesis gas at Sasol has increased steadily over the years, resulting in continuous pressure to increase production rates of individual units [Sasol Annual Report, 2003].

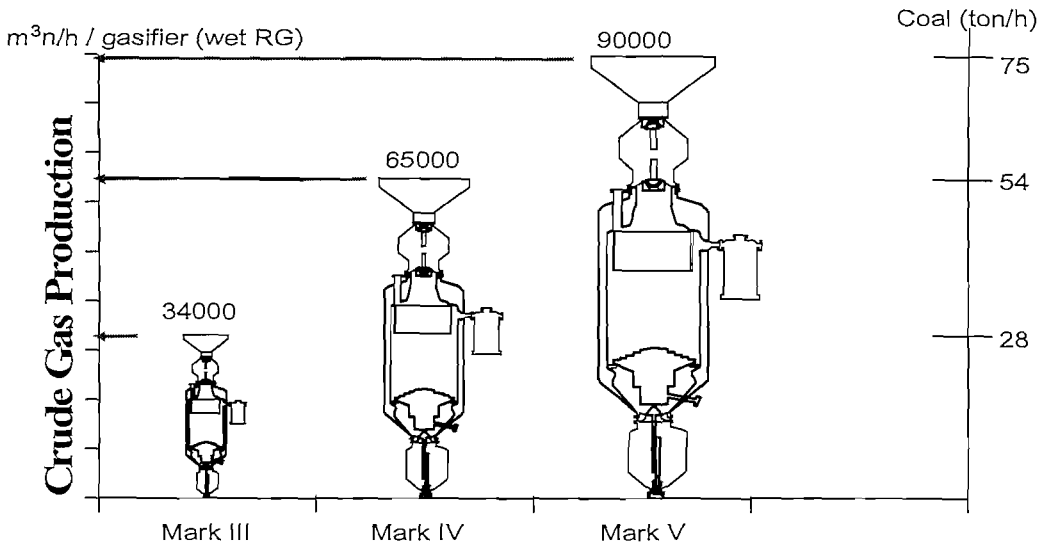

FIGURE 1.3: SCHEMATIC REPRESENTATION OF THE SASOL-LURGI MK III, MK IV, AND MK V GASIFIER DIMENSIONS SHOWING HOURLY FEED COAL RATE AND RAW GAS (WET) PRODUCTION RATE [SASOL-LURGI, 2005]

The chemistry of gasification is extremely complex. The topic is widely covered in the open literature [Schilling, *et. al.*, 1979; Howard, *et. al.*, 1981; Nowacki, 1981; Slaghuis, 1993a,b], and the basic reactions occurring within a coal gasifier will be discussed in section 2.1.1.

2.1.1 Basic reactions occurring in a coal gasifier

Kinetic studies on the gasification of coal have to do with the rate at which a specific coal can be gasified to desired gaseous products and the factors by which the rate is controlled. The most important reactions relevant to the gasification process are similar to those of gas reforming; the processes of gasification and reforming therefore have a lot in common. Both take place at a relatively high temperature (approximately 1000°C or more), which is as a result of the exothermic combustion (oxidation) reactions which are required to drive the endothermic reduction reactions. In the drying zone, the coal loses all of its moisture and this drying process results in an endothermic reaction. The temperature of the exit gas will be highly affected by the moisture content present in the feed coal. When the dried coal reaches a temperature of about 350-400°C, it starts to devolatilise with the production of gases, oils and tars [Nowacki, 1981; Slaghuis, 1989,1993a,b]. In the pyrolysis zone the coal is heated in an inert atmosphere, to a temperature of 700°C. The coal undergoes pyrolysis or destructive distillation, due to the action of heat and the decomposition could be described as follows:

Pyrolysis or char formation:

$C_mH_n \rightarrow (n/4)\ CH_4 + [(m-n)/4]\ C$ (1)

"True" gasification reactions

Gasification with carbon dioxide (Boudouard reaction)

$C + CO_2 \rightarrow 2CO$ ΔH = 159.7 kJ/mol (2)

Gasification with steam (water gas reaction)

$C + H_2O \rightarrow CO + H_2$ ΔH = 118.9 kJ/mol (3)

Gasification with hydrogen (hydro-gasification):

$C + 2H_2 \rightarrow CH_4$ ΔH = -87.4 kJ/mol (4)

Combustion reaction

Gasification with oxygen (partial combustion):

$C + 0.5\ O_2 \rightarrow CO$ ΔH = -123.1 kJ/mol (5)

$C + O_2 \rightarrow CO_2$ ΔH = -405.9 kJ/mol (6)

Gas phase reactions

Water gas shift reaction:

$CO + H_2O \rightarrow CO_2 + H_2$ ΔH = -40.9 kJ/mol (7)

Methanation:

$CO + 3H_2 \rightarrow CH_4 + H_2O$ ΔH = -206.3 kJ/mol (8)

In reactions 1 – 8, char is depicted as C, which is of course not strictly true. The enthalpies have been given for standard conditions (298 K, and 1, 013 bar) with the standard enthalpy of formation of carbon taken as ΔH^o = 12.5 kJ/mol, which makes allowance for the fact that the carbon in char differs from graphitic carbon [Slaghuis, 1993a].

Active sites in char are per definition those points on the surface of the coal where reactions 2 – 6 can occur [Morgan, 1991]. Reactants such as oxygen, carbon dioxide and water (steam) do not readily react with carbon, unless they are able to dissociate in order to chemisorb on the carbon surface. This dissociation occurs primarily on the edges of the

aromatic layers of the char, or otherwise at any point where the chemical structure shows a defect [Slaghuis, 1993a]. These reactions may be visualised as follows:

$$C_{(char)} + CO_2 \rightarrow C(O) + CO \quad (9)$$

$$C(O) \rightarrow CO + C_{(char)} \quad (10)$$

or

$$C_{(char)} + H_2O \rightarrow C(O) + H_2 \quad (11)$$

$$C(O) \rightarrow CO + C_{(char)} \quad (12)$$

In both cases the reactant dissociates with the adsorption of an oxygen atom on the carbon active sites. In the second step, the carbon-oxygen complex is desorbed from the bulk of the char structure, creating a new active site.

The reactivity of a given char is a measure of the rate at which the specific char will react with a given reactant, under well defined conditions of temperature and pressure. The rate of the Boudouard reaction (equation 2 above) can be described as follows:

$$R_{(CO2)} = (dX / dt) . [1 / (1-X)] \quad (13)$$

$R_{(CO2)}$ = Carbon gasification rate (or reactivity)
X = Carbon conversion factor
t = Time

Closer inspection of the formula will reveal that the unit by which reactivity is expressed, is inverse time (s^{-1} or h^{-1}), where R is sometimes referred to as the "specific" or "intrinsic" gasification rate. The formula implies that the moles of carbon gasified per unit time (under conditions of constant temperature, pressure and gas flow) is directly proportional to the amount of carbon present at any point in time. This means that R should remain constant with increasing conversion [Slaghuis, 1993a].

With the basic principles of fixed bed gasification explained, it is necessary to understand coal and coal properties in more detail and to elucidate on the role of these coal properties during gasification. Much has been written [Stopes, 1919; Brown, 1962; Snyman, *et. al.*, 1984; Falcon and Falcon, 1987] about the origin of coal and its various maceral and mineral constituents; therefore only a short summary is given in Section 3. In Section 4 a discussion of the most important coal properties with respect to gasification performance is given; while in Section 6, two case studies that consider the gasification relevance of coal property transformational behaviour from an in-field plant measurement perspective are presented.

3 COAL

Sasol Mining (Pty) Ltd. is responsible for coal mining in the Sasolburg and Secunda regions supplying coal to Sasol's synthetic fuels and chemical plants. The division controls regional operations comprising the Sigma Colliery and Wonderwater strip mining operations in Sasolburg; as well as the Secunda Collieries, which consist of six underground operations. The combined run-of-mine output from the Sasolburg and Secunda operations increased from a total production of ≈20 million tons in the ten year period 1954 – 1964 to 51.6 million tons per annum in 2002 [Sasol Annual Report, 2003].

During the 2003 financial year, the company supplied 46 million tons of saleable coal from the 51.3 million tons of coal extracted to the operations of Sasol Synfuels (SSF) in Secunda and Sasol Infrachem (SCI) in Sasolburg. The company commenced its coal export operations in Secunda during the 1997 financial year, producing 3.6 million tons of thermal grade export quality coal, which was exported mainly to Europe during the 2003 financial year (Table 1.1) [Sasol Annual Report, 2003].

TABLE 1.1 TABLE SHOWING THE SASOL MINING (PTY) LTD COAL PRODUCTION FIGURES PER COLLIERY [SASOL ANNUAL REPORT, 2003]

Production (millions of tons)	2001	2002	2003
	51.3	51.6	51.3
Total production	5.4	5.9	5.9
Sigma Colliery including Wonderwater			
Secunda Collieries:	7.3	7.3	7.8
Bosjesspruit Colliery	8.5	8.3	8.4
Brandspruit Colliery	8.2	8.1	7.7
Middelbult Colliery	5.5	5.2	5.9
Twistdraai Colliery	7.4	8.1	7.8
Twistdraai Export Colliery	9.0	8.7	7.8
Saleable production from all mines	49.5	49.5	49.6

3.1 Definition of coal

Coal is a generic term referring to a family of solid fossil fuels with a wide range of physical and chemical compositions. Coal is actually a heterogeneous rock composed of different kinds of organic matter, which vary in their proportions in different coals, with no two coals being absolutely identical in nature, composition or origin [Sanders, 1996]. Petrography allows for the optical consideration of the changes occurring in the carbon particles and associated minerals through the gasifier, which can be related to temperature and morphological changes [Wagner, 2005b].

Coal is fundamentally composed of the fossilised remains of plant debris, which have undergone progressive physical and chemical alteration through geological time [Stopes, 1919; Falcon and Snyman, 1986]. Sanders [1996] proposed that "coal is a compact stratified mass of metamorphosed plants which have, in part, suffered arrested decay to varying degrees of completeness". South African coals and Indian coals are both of Gondwanaland origin, having similar characteristics [Falcon and Snyman, 1986].

3.2 Coal formation

Coalification is the process of metamorphism which takes place over time, under conditions of higher temperature and pressure, resulting in the transformation of the original peat swamp through the progressive stages of lignite, sub-bituminous, bituminous coals, anthracite and graphite [Grainger and Gibson, 1981; Falcon and Snyman, 1986]. This process may be distinguished into a biochemical stage, which includes the whole of the peat-forming process and a geochemical stage, during which metamorphosis takes place.

(i) Biochemical stage

The principal initiating requirements for coal formation are a swampy or marshy environment, climatic conditions favourable for rapid plant growth and enough depth of water to restrict oxygen supply during the breakdown of the original plant material when it dies and falls into the water [Grainger and Gibson, 1981]. During this stage the GRADE of the coal is determined, being dependent on the amount of inorganic mineral material washed into the system [Falcon and Snyman, 1986].

Micro-organisms in the presence of water induce a chemical change in the plant material, resulting in the formation of peat. Continued subsidence of the swamp allows further growth and accumulation of plant material [Grainger and Gibson, 1981].

The proportions and chemical composition of the organic constituents formed during the peatification stage are the precursors of the macerals, which impart to the fossilised plant material its characteristic organic composition (TYPE) [Falcon and Snyman, 1986].

(ii) Geochemical stage

The differing degrees of pressure and heat over different periods of time in the geochemical stage, which act on the peat-like deposits, are responsible for the difference in coalification, referred to as the RANK of the coal [Grainger and Gibson, 1981]. The most reliable parameter used in South Africa to define rank is the reflectance of vitrinite, which is measured petrographically under oil immersion [Falcon and Falcon, 1987; Wagner and Joubert, 2005a].

The proportions of organic constituents (type) and the process of maturation (rank) are independent of one another. Grade refers to both the mineral matter composition and the amount of mineral mater present in the coal [Falcon and Snyman, 1986].

3.3 Coal composition (types) of coal macerals

Coal consists of a number of microscopic organic constituents (macerals) and inorganic constituents (minerals) that occur together in different ratios or associations, forming microscopic bands (microlithotypes). A succession of these bands forms the macroscopic bands, known as lithotypes [Falcon, 1978, 1991].

The physical and chemical properties of coal macerals vary widely, due to the variety of the original plant materials, depositional environment and the extent of metamorphism. Macerals are divided into three main groups, namely vitrinite (v), liptinite (l) and inertinite (i). Due to the chemical differences between macerals, behavioural differences in various chemical processes and utilisation may occur.

The term "maceral" is used to represent the different organic plant tissue from which the coal was originally formed. Vitrinite is relatively oxygen-rich and is derived from cell walls and cell contents of precipitated gels preserved under water. Liptinite, is the hydrogen-rich maceral type formed from algae, spores and waxy leaves. Carbon-rich inertinite originated from plant tissue that had oxidised, altered, degraded or burnt in the peat stage of coal formation [Falcon and Falcon, 1987].

When coal samples are microscopically examined, the macerals are distinguished on the basis of their reflectivity, colour, shape, relief and hardness. Each plant remain forms a specific maceral. Coal petrology is the study of the microscopic organic and inorganic constituents in coal [Falcon and Snyman, 1986]. It is possible to predict the technological behaviour of a coal from its petrographic composition [Falcon and

Snyman, 1986]. Since understanding carbon loss during fixed-bed gasification is an integral part of this study, char morphology [Wagner, 2004a; Wagner and Joubert, 2005a] will be discussed in detail in Section 4.8. The following typical properties of the different macerals are summarized as one needs to refer to these during gasification:

3.3.1 Vitrinite:

The oxygen content of vitrinite decreases with an increase in rank and vitrinite tends to show fissures and cracks upon heating. The density of vitrinite ranges between 1,27 g/cm^3 and 1,8 g/cm^3 and reflectivity varies with rank [Borrego *et. al.*, 1997].

3.3.2 Inertinite

Inertinite is the highest reflecting group maceral found in bituminous coals. It generally has a low volatile matter content, is not readily oxidized and is more aromatic than vitrinite or liptinite in low rank coals. Due to low hydrogen content, hydrogenation is not possible [Borrego, *et. al.*, 1997]. Schobert [2006] questions whether hydrogenation of inertinite is truly impossible; firstly it should be recalled that this maceral name derives from its behaviour during coking, and does not necessarily imply chemical inertness in other reactions. Secondly, even if it were found to be inert to hydrogenation, the reason is not the "low hydrogen content". Large multi-ring aromatic compounds have low hydrogen contents, but can be readily hydrogenated. Except for fusinite, which is relatively friable, the inertinite maceral group strengthens the coal band in which it occurs [Falcon, 1978; Falcon and Snyman, 1986; Stach *et. al,* 1982]. The density of inertinite varies between 1.35 g/cm^3 and 1.70 g/cm^3 [Borrego, *et. al.*, 1997].

3.3.3 Liptinite

Liptinite has a high volatile matter content and produces high yields of tar and gas during carbonisation. It has an aliphatic-aromatic skeleton and oxidizes more rapidly than inertinite and vitrinite. Due to its high hydrogen content, liptinite is very suitable for hydrogenation. The density of liptinite varies between 1.18 g/cm^3 and 1.25 g/cm^3 [Grainger and Gibson, 1981; Stach, *et. al.*, 1982; Borrego *et. al.*, 1997].

3.3.4 Reactive semifusinite

As the name states, it is a reactive maceral having properties which range between vitrinite and inertinite [Falcon and Falcon, 1983]. The structure of reactive semifusinite ranges between unstructured to slightly structured [Smith *et al.*, 1983]. The reflectance of reactive semifusinite is always higher than that of the vitrinite in which it occurs [Smith *et. al.*,1983].

3.4 Minerals present in coal

In addition to the organic constituents mentioned above, coal also contains varying amounts of inorganic components (mineral matter). Minerals are naturally-occurring homogeneous solids with a definite chemical composition and an ordered atomic structure [Falcon and Snyman, 1986]. The mineral matter present in coal can be divided into two categories, namely intrinsic and extrinsic mineral matter [Grainger and Gibson, 1981]. The intrinsic mineral matter is inorganic material that was present in the original plants as well as the inorganic-organic complexes and minerals that formed during the first stage of coalification. The extrinsic mineral matter can be divided into two groups on the basis of their origin:

(i) Syngenetic (primary) mineral matter was formed or accumulated, up to the time of peatification. The material was transported to the coal swamps by wind and water. These minerals are intimately inter-grown with the coal and are thus difficult to remove from the coal [Falcon and Falcon, 1983].

(ii) Epigenetic (secondary) mineral matter was formed by material that was deposited into fractures, cavities and cleats after the solidification (gelification). These minerals are easier to liberate by comminution compared to syngenetic minerals.

Major minerals include kaolinite, quartz, pyrite, calcite and dolomite [Alpern, *et. al.*, 1984]. Clay is the mineral that occurs most commonly in coal (60-70% of all mineral matter intergrowths). Carbonates usually occur as nodules of siderite (1-2mm) or as veins and cell fillings of calcite, dolomite and ankerite. Quartz generally occurs in small quantities as small isolated grains (5 - 20µm diameter). Iron sulphides occur as pyrite, marcasite or melinkovite. Epigentic pyrite and replacement pyrite occur more abundantly than syngenetic iron sulphide [Falcon and Snyman, 1986; Deer *et. al.*, 1966].

Ash is the product of inorganic dehydration, decomposition and oxidation reactions which occur when the coal mass is combusted. The chemical composition and properties of mineral matter and ash are quite different. The mass of mineral matter may be related to the ash content by using Parr's formula [Tsai, 1982].

3.5 Microlithotypes

The organic and inorganic constituents of coal combine in various associations to form microscopic layers, termed microlithotypes which are greater than 50μm in width [Falcon and Snyman, 1986]. The chief microlithotypes are vitrite, inertite and durite. Vitrite (composed of vitrinite, V>95%) and inertite (composition of inertinite, I>95%) are mono-maceral types. Clarite is composed of vitrinite and liptinite (V+I>95%), while durite is a mixture of liptinite and inertinite (I+L>95%). Both clarite and durite are examples of bi-maceral types. Trimacerite is a tri-maceral microlithotype and is a combination of clarite and durite. In South African coals, trimacerite and pure forms of inertinite are dominant [Falcon and Snyman, 1986]. Carbominerite refers to the associations of organic and inorganic microlithotypes. Mineral rich particles (>60 vol% minerals) are refered to as minerite [Wagner, 1998].

The term "mineral matter" usually applies to all the inorganic non-coal material occurring in coal and includes those inorganic elements which may occur in organic combination [Bryers and Taylor, 1976]. According to Ward [2002], the term mineral matter in coal includes the dissolved salts in the pore water, inorganic elements associated with the organic compounds and discrete crystalline and non-crystalline mineral particles.

A succession of microlithotypes form macroscopically identifiable layers of 5mm or more called lithotypes. There are four main classifications of lithotypes, viz. vitrain, clarain, durain and fusain [Falcon and Falcon, 1987].

4 THE MOST IMPORTANT COAL PROPERTIES WHICH IMPACT ON GASIFICATION PERFORMANCE

To put the gasification of coal into perspective, Glover [1991], Van Dyk *et. al.* [2001c]; and Wagner [2004a] found that there are only a limited number of coal properties that may significantly affect reactor behaviour, given in no specific order of importance:

- The coal char reactivity
- The petrographic morphology of the coal type
- The feed coal particle size distribution (PSD)
- The ash content and ash melting characteristics of the coal
- The fixed carbon content and devolatilisation behaviour of the coal
- The thermal and mechanical properties of the coal
- The caking propensity of the coal

4.1 Coal char reactivity

There is no internationally accepted standard method of determining the reactivity of a given coal char. The method employed by the Syngas and Coal Technologies R+D Group at Sasol measures the rate of mass loss, using a thermogravimetric analyzer (TGA). The temperature is maintained until the mass is stable (complete carbon burn–off) and the reactivity is then calculated at 50% carbon burn-off [Slaghuis, 1993b]. The CO_2 reactivity provides an indication of the expected rate of gasification reactions. Reactivity is expressed as a mass loss per unit time at 50% burn-off under a CO_2 atmosphere [Slaghuis, 2003b; Van Dyk and Keyser, 2005]. The reactivity of a given coal char is often measured with the sole purpose of comparing the results to that of another coal or similar product. Important factors which affect char reactivity are: char preparation conditions, particle size, sample size, temperature, reacting gas and gas flow [Slaghuis, 1993b; Morgan, 1991].

The reactivities of coal from the various sources used by Sasol in Secunda vary between $2hr^{-1}$ and $5hr^{-1}$. Although the reactivities of Sasol coals vary between $2hr^{-1}$ and $5hr^{-1}$, coal sources with lower and higher reactivities have been gasified in the past. Some of the non-South African coal sources tested for gasification purposes have shown reactivities as low as $0.5hr^{-1}$ and as high as $9hr^{-1}$. However, it is uncertain what the lower limit for reactivity is, below which the gasification reactions will become too slow for complete conversion [Van Dyk *et. al,* 2001c].

Various other parameters have been correlated with coal char reactivity. Fatemi-Badi, *et. al.* [1988] found a direct correlation between char reactivity and the hydrogen content of the coal during lab-scale pyrolysis experiments. The higher the hydrogen content, the higher was the reactivity.

Solomon, *et. al.* [1988] used the dry ash-free hydrogen content as a measure of the

extent of pyrolysis, i.e. the hydrogen content was found to decrease with an increase in temperature. It was found, for a range of coal types, that there was a trend of decreasing reactivity in air with decreasing hydrogen content (increase in temperature). It was found that most of the change occurred below 2% hydrogen, i.e. after the evolution of aliphatic hydrogen was complete. The lignite, however, increased in reactivity until between 3.5% and 4% hydrogen and then decreased in reactivity. They also concluded that the variation in reactivity with extent of pyrolysis did not depend strongly on the char surface area measured by N_2 or CO_2.

4.2 Feed coal particle size distribution

The particle size distribution (PSD) is determined in order to estimate or predict which size distributions are more likely to cause unstable gasifier operation due to pressure drop effects [Van Dyk *et. al*; 2001c, Van Dyk, 2002a]. Pressure drop problems include grate traction loss (due to bed fluidization), channel-burning leading to unacceptable gas outlet temperature, and solids carry-over [Keyser *et. al.*, 2005]. Probably the best known estimation method for pressure drop is the Ergun equation [Leva, 1959], which gives pressure drop as a function of bed voidage ε, viscosity μ, fluid density ρ, superficial velocity U_s and particle diameter d_p :

$$\frac{\Delta P}{L} = 150\,\frac{(1-\varepsilon)^2\,\mu U_s}{\varepsilon^3 d_p^2} + 1.75\,\frac{(1-\varepsilon)pU_s^2}{\varepsilon^3 d_p} \qquad (14)$$

When dealing with particle size distributions instead of uniformly sized particles, the particle size d_p has to be replaced by $\phi\overline{d_p}$, where ϕ is the particle sphericity and $\overline{d_p}$ the average particle size reflecting the mean surface area (also referred to as the Sauter mean diameter). The Sauter diameter of a coal sample with a specific particle size distribution is calculated as follows [Leva, 1959; Bennet and Myers, 1982]:

$$\overline{d}_p = \frac{1}{\sum_i \left(\frac{x_i}{d_{p,i}}\right)} \qquad (15)$$

where i = screen number, x_i = fraction (mass %) on screen I; and $d_{p,i}$ = diameter (mm) of screen i.

The Sasol Coal Supply (SCS) West benchmark Ergun Index value is 11.6, and the higher this value the more stable the gasifier is considered to be during operation [Van Dyk, *et. al.*, 2001c].

Experience has shown that $\overline{d_p}$ is a useful parameter for predicting which PSD' s are more likely to result in gasifier instability. The value of $\overline{d_p}$ is extremely sensitive to the smaller particle sizes or the so-called "tail" of the PSD. As illustrated in Table 1.2, a 10% change to the coarser side resulted in a change of only 3% in the Sauter diameter, while a 10% change in particle size to the finer fraction resulted in a 7% change [Van Dyk, *et. al.,* 2001c].

Extensive operating experience has shown that size distributions with a Sauter diameter below about 7.5 can result in unstable gasifier operation. Inefficient screening due to screen overload causes misplacement of fine coal, which can easily reduce the Sauter diameter to unacceptably low values resulting in unstable gasifier operation [Van Dyk, *et. al.,* 2001c].

TABLE 1.2 : TABLE SHOWING THE EFFECT OF CHANGE IN PARTICLE SIZE ON SAUTER DIAMETER

Fraction (mm)	Standard composition	Coarser fraction	Finer fraction
-5.8	42.1	52.1	42.1
-3.7	33.3	23.3	23.3
-2.8	24.6	24.6	34.6
% Change in Sauter diameter	-	3	7

4.3 Thermal fragmentation

When lump coal from certain origins is exposed to high temperatures, it will tend to undergo fragmentation, thus changing the particle size distribution of the coal. This may lead to a change in permeability of the coal bed resulting in non-ideal reaction conditions where unstable gasifier conditions arise. Fragmentation is the breaking of a single particle into two or more pieces [Stubington and Linjewile, 1989]. One type of fragmentation occurs during devolatilisation (primary fragmentation); while secondary fragmentation occurs during combustion of the char by burn-out of carbon bridges connecting part of the particle [Stubington and Linjewile, 1989; Dakic, *et. al.*, 1989].

The percentage thermal fragmentation of coal is given as a percentage decrease in Sauter diameter. Thermal fragmentation is defined as [Van Dyk, 2001a] :

$$\%\,Thermal\ fragmentation = \frac{\overline{d}_{p\ before\ test} - \overline{d}_{p\ after\ test}}{\overline{d}_{p\ before\ test}} x100 \qquad (16)$$

The smaller the percentage decrease in Sauter diameter, the better the thermal stability is. As illustrated in Figure 1.4, weathering / oxidation and moisture content affect the thermal fragmentation of coal sources. An extensive study [Van Dyk, 2001a] revealed that the presence of moisture contributes to ±75% of the thermal fragmentation of coal. This is not only surface moisture, but a combination of surface moisture and inherent moisture captured within the pores of the coal structure. Although moisture contributes significantly towards fragmentation, it is also affected by a complex interaction with other factors [Van Dyk, 2001a].

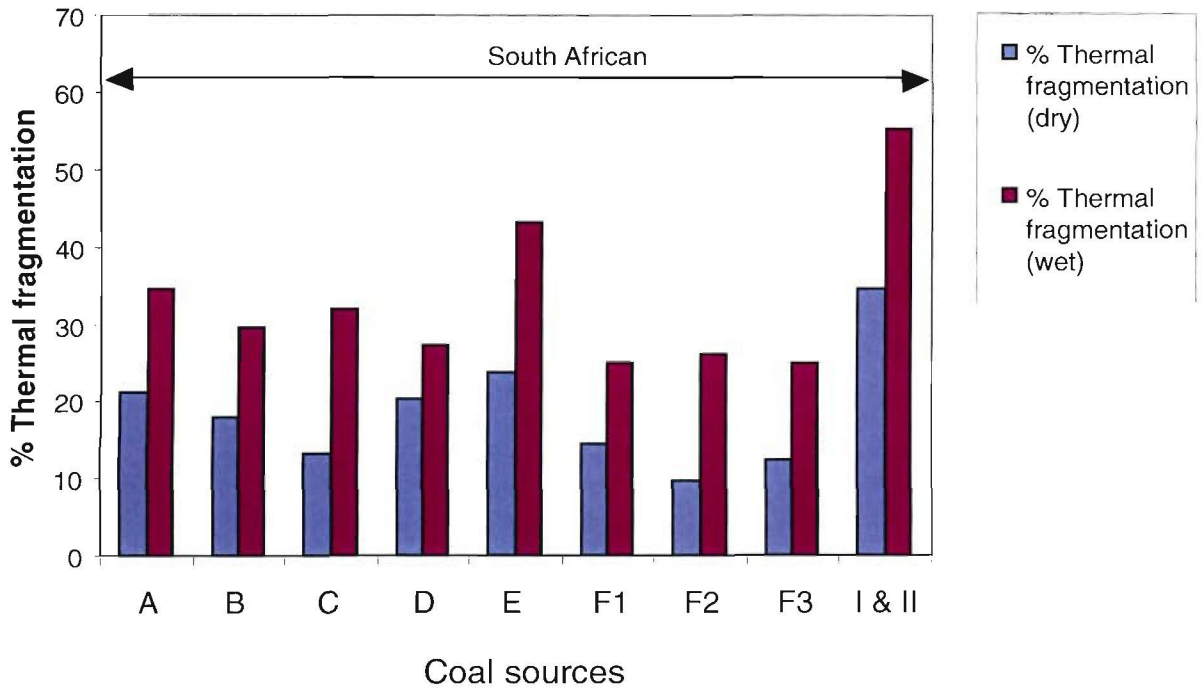

FIGURE 1.4: **BAR CHART DEPICTING THE THERMAL FRAGMENTATION BEHAVIOUR OF A NUMBER OF DIFFERENT COAL SOURCES SHOWING THE EFFECT OF MOISTURE AND WEATHERING ON BREAKAGE**

The Sasol SCS West thermal fragmentation value of the run-of-mine (R.O.M.) coal on an as-received basis typically ranges between 15% and 25% [Van Dyk, 2001a].

4.4 Ash, fixed carbon, volatile matter and moisture content

The proximate analysis of a coal describes its composition in terms of the relative amounts of moisture, volatile matter and ash content, while the fixed carbon in the

coal is calculated by difference. The determination of the moisture content of the laboratory-conditioned sample provides for the calculation of the results of general analyses (also determined on the laboratory-conditioned sample) to other bases, e.g. dry basis, dry ash-free basis, etc. The volatile matter provides an indication of the reactivity of a coal, as well as of the amount of tar and oil that might be produced during gasification. The ash content gives an indication of the amount of inorganic material in the coal and includes mineral matter inherent in the coal structure, as well as out-of-seam inorganic contamination [Slaghuis, 2003a,b].

In the determination of the proximate analysis of coal, standard methods to measure the percentage of moisture (SABS 924, ISO 589), ash content (ISO 1171) and volatile matter (ISO 562) are used. The difference between these three percentages and the mass of the original sample (100%) is referred to as fixed carbon. Another method used to determine the proximate analysis of coal by thermogravimetry has also been developed by Slaghuis, [1993], and is frequently used by the Syngas and Coal Technologies R+D Group at Sasol.

The Sasol proximate analysis bench-mark for typical SCS coal blends [Van Dyk, *et. al.*, 2001c] is given in Tables 1.3 and 1.4 (air-dried and dry basis respectively).

TABLE 1.3: TABLE SHOWING THE PROXIMATE ANALYSIS (AIR DRIED BASIS) FOR TYPICAL SCS WEST BLEND

Sample	% Moisture	% Volatile matter	% Fixed carbon	% Ash
Typical SCS West blend	3.5-5.5	21.4-25.7	42.6-51.6	22.2-30.5

TABLE 1.4: TABLE SHOWING THE PROXIMATE ANALYSIS (DRY BASIS) FOR TYPICAL SCS WEST BLEND

Sample	% Volatile matter	% Fixed carbon	% Ash
Typical SCS West blend	24.9-27.2	44.1-54.6	23.0-32.3

The variation in ash content between the different coal sources currently used for gasification in Secunda and Sasolburg, as well as non-South African coal sources tested, are illustrated in Figure 1.5. The non-South African sources were investigated for potential use by Sasol [Van Dyk, 2001b, 2002b].

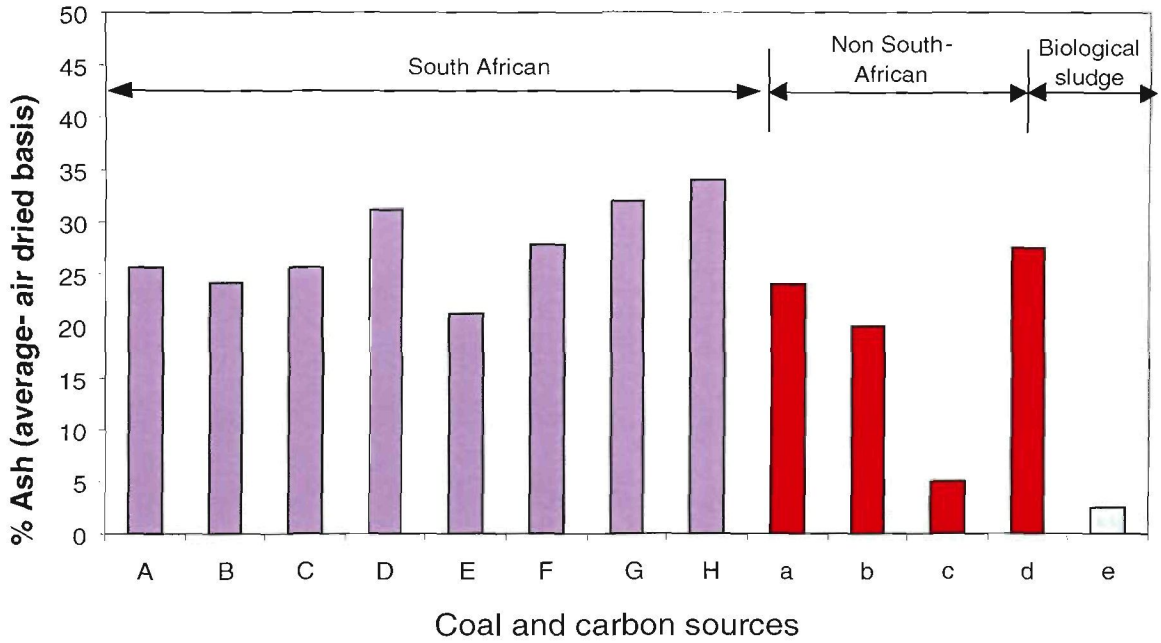

FIGURE 1.5: BAR CHART SHOWING THE VARIATION IN FEED ASH CONTENT (AIR DRIED BASIS) FOR VARIOUS LOCAL AND FOREIGN COAL SOURCES AS WELL AS FOR BIOMASS [VAN DYK, 2001b, 2002b]

The measurement of ash content is used by Sasol Mining as an operating tool to prepare blends with an ash content within the agreed limits, as well as with a relatively small variation in ash content over time. Indirectly, the blending of different coal sources according to ash content also implies that the blend is prepared with a degree of homogeneity. The budgeted ash content of the coal blend requested by gasification at Sasol Synfuels in Secunda is ±28% (air dry basis) [Keyser and Coetzer, 2000; Van Dyk and Keyser, 2005], but not optimal in terms of coal reserve availability [Van Heerden, 2005].

A compositional analysis of the ash in coal is often useful in the total description of the quality of the coal. Ash is composed of complex oxides and the ash analysis expresses this composition in terms of its oxides of Si, Al, Fe, Ti, P, Ca, Mg, Na, K, and S. The Ca and Mg contents specifically give a fair indication of the expected ash fusion behaviour. The ASTM D3682 procedure covers the analysis of the commonly determined major and minor elements in coal ash. The Sasol compositional analysis benchmark for typical SCS West blend coal is given in Table 1.5 below [Van Dyk, *et. al.*, 2001c].

TABLE 1.5: TABLE SHOWING THE ELEMENTAL ASH COMPOSITION (MASS %) FOR THE TYPICAL SCS WEST BLEND

	SiO_2	Al_2O_3	Fe_2O_3	P_2O_5	TiO_2	CaO	MgO	K_2O	Na_2O	SO_3
SCS West blend	45.5-51.2	20.9-24.7	3.6-9.3	0.6-0.8	1.2-1.4	6.6-9.1	2.1-2.9	0.6-1.1	0.5-0.9	6.1-9.5

A Ca and/or Fe rich coal source normally has a low ash fusion temperature due to the fluxing properties of the Ca and Fe minerals. Phase diagrams are used to determine the effect of ash chemistry on the potential of a fuel to slag and form clinkers. In addition to predicting melting and clinker formation, phase diagrams can be used to predict the composition of the clinkers and possibly obtain an idea of the temperature history to which the clinker was exposed [Matjie, 2005].

Thus, phase diagrams can be used to predict the temperature at which the phases will melt during heating (solidus Sh) or the temperature (liquidus Lc) at which phases will start crystallising from a molten mass during cooling. In terms of forming solid clinkers, the liquidus (Lc) temperature is an indication of when the crystals will start crystallising from the melt, initiating clinker formation [Magaginer, *et. al.*, 2001].

4.5 Ash fusion temperature

The ash fusion temperature (AFT) provides an indication as to the extent of ash agglomeration and clinkering likely to occur within the gasifier. Ash clinkering inside the gasifier can cause channel-burning, pressure drop problems and unstable gasifier operation [Nowaki, 1981; Keyser, *et. al.*, 2005].

The standard method, ISO 540, is used to demonstrate the fusion properties of laboratory prepared coal ash. The ash is heated up to 1600°C in an atmosphere that is either reducing or oxidising. The results of an AFT analysis consist of four temperatures [Carpenter, 2002], namely the initial deformation temperature (DT), softening temperature (ST), hemispherical temperature (HT) and flow temperature (FT).

There are, however, concerns that the standard AFT test is subjective [Carpenter, 2002], being based on observations rather than measurements, and that poor reproducibility is obtained. Mean deviations for the average and expert systems of

about 38°C are attainable with the AFT test [Ward, 2002; Carpenter, 2002]. The Sasol SCS benchmark for AFT can be observed in Table 1.6 below: [Govender, 2004; Van Dyk, 2002a,b].

TABLE 1.6: TABLE SHOWING THE ASH MELTING PROPERTIES (OXIDISING) FOR THE TYPICAL SCS WEST BLEND.

Sample	Initial (°C)	Hemispherical (°C)	Flow (°C)
Typical SCS West blend	1300-1390	1350-1440	1360-1470

Ideal gasifier operation is to operate at a temperature above the initial deformation temperature in order to obtain enough agglomeration to improve bed permeability, but to operate below the ash flow temperature to prevent excessive clinkering.

4.6 Mechanical Fragmentation

If a coal is mechanically unstable, it will tend to undergo fragmentation, thus changing the particle size distribution of the coal. In fixed bed gasification, fragmentation may lead to a change in the permeability of the coal bed, resulting in unstable gasifier conditions [Keyser, et. al.,2005].

Mechanical stability is determined by means of a Micum tumble test, while the Micum M10 index gives an indication of the abrasiveness of the coal. The abrasiveness index is a function of the coal rank, quality and type, as well as the PSD, where larger particles tend to fragment more than smaller particles [Breytenbach, 2006]. The typical Sasol SCS benchmark for mechanical fragmentation of the coal blend ranges between 30% and 35%. [Van Dyk, *et. al.*, 2001c].

4.7 Caking properties

Caking of coal particles can be described as the softening or plasticity property of coal, which causes particles to melt or sinter together to form larger particles when heated. Caking of coal within the gasifier can cause pressure drop fluctuations and channel-burning, resulting in unstable gasifier operation [Keyser, *et. al.,* 2005].

Certain macerals in coal, e.g. vitrinite, when of a specific rank soften and swell when they reach temperatures of approximately 400 – 600°C. Schobert [2006] points out that with regards to temperatures of the swelling of vitrinite, the characteristic

softening and re-solidification temperatures of coals vary from one coal to another; however, it seems very unlikely that any swell at 600 °C. The re-solidification temperatures on most "typical" coals are <500 °C. In extreme cases, as found in metallurgical coke ovens, the whole bed of coal fuses together to form one homogeneous mass known as coke [Slaghuis, 1993b]. Even moderately caking coals may choke the gasifier to such an extent that severe channelling may occur resulting in incomplete gasification as well as poor gas quality. Consequently, when coal quality is specified for gasification purposes, the swelling index of the coal is stipulated to be less than 1, preferably 0 [Slaghuis, 1993b; Morgan, 1991].

The caking propensity of coals for gasification purposes is characterised by means of pyrolysis. The variation in caking properties between the different coal sources currently used for gasification in Secunda and Sasolburg, as well as for non-South African coal sources tested, are given in Figure 1.6 [Van Dyk, *et. al.*, 2001c].

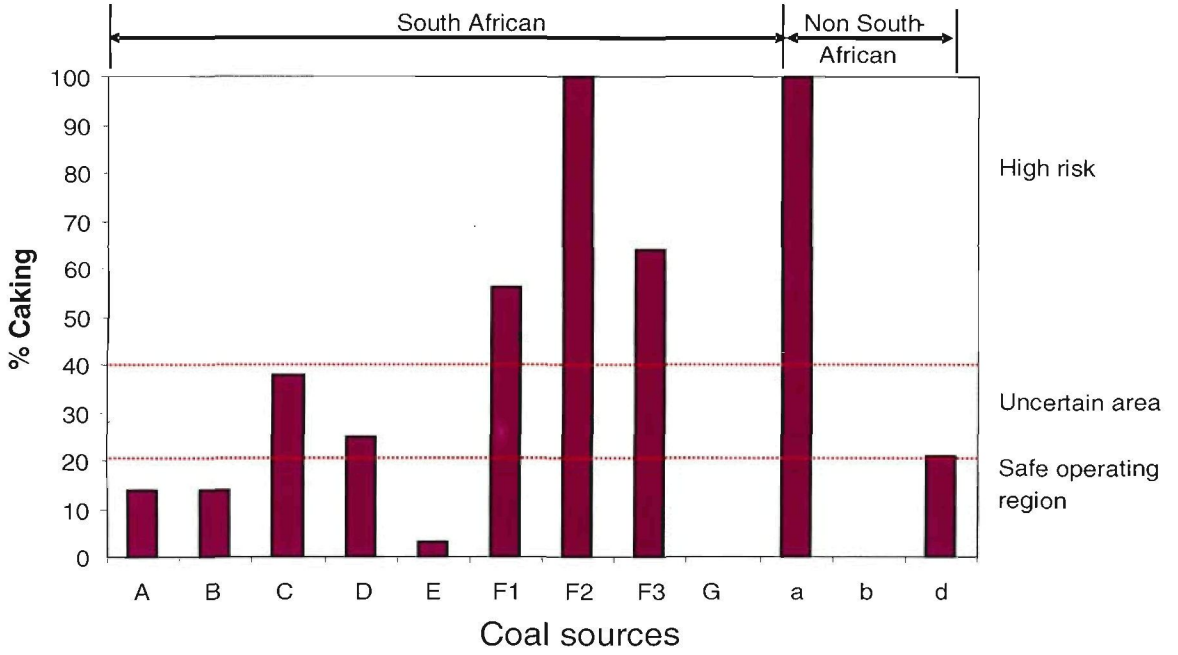

FIGURE 1.6: **BAR CHART SHOWING THE CAKING PROPENSITY AND ASSOCIATED RISK WITH RESPECT TO FIXED-BED GASIFICATION OF A NUMBER OF LOCAL AND FOREIGN COAL SOURCES**

The caking propensity and associated risk with respect to fixed-bed gasification usage (Figure 1.6) clearly indicate that coals having a caking propensity of 20% are within the safe operating region. Between 20% and 40% caking of the feed coal, the gasifyability becomes uncertain and above 40% caking propensity of the feed coal, the associated risk in fixed-bed gasification is highest.

Coal with a medium to low caking propensity shows no caking formation under atmospheric conditions, while a highly caking coal will have a much lower caking propensity under atmospheric conditions than at 26 bar. According to previous experience, coals from sources with a relatively high caking propensity have resulted in unstable gasifier operation and are therefore mixed with other coal sources having a low caking propensity, in order to obtain an acceptable blend. Normal blends used for gasification in Secunda have a caking property of between 7% and 20%, while coal blends that have been used in the Sasolburg plant have either no or very little caking formation [Slaghuis, 1993b; Morgan, 1991].

4.8 Petrographic coal and char morphology

Petrography allows for the optical consideration of the changes occurring in the carbon particles and associated minerals through the gasifier, which can be related to temperature and morphological changes [Wagner, 2004a].

Different macerals and minerals behave in relatively characteristic ways when exposed to increasing temperatures. Char-form analysis, whilst not yet an ISO standard, is a relatively common characterisation method applied on pulverized coal samples used by power utilities globally [Baily, *et. al.,* 1990]. Vitrinite-rich particles swell and form cenospheres, altering physically (becoming porous) and chemically (devolatilising). Inertinite-rich particles generally retain their physical appearance, although they alter chemically are referred to as dense chars (specifically fusinites). Particles with mixed microlithotypes either become porous in sections or do not alter physically, or can appear to react in bands, and are generally referred to as honeycomb or mixed chars [Wagner, 1998].

Gasification coal feeds differ to pulverized fuel combustion feeds by nature of the initial particle size (+6mm). Hence it is unlikely that a highly comparative char morphological characterisation can be readily applied to the gasifier dissected samples envisaged from this study. A unique particle type analysis is required to characterise the physical (and inferred chemical) changes occurring in the particles during gasification based on combustion char morphological terms and behaviours [Baily, *et. al.*, 1990].

Descriptors of the char-forms relevant to this study are given below. The descriptors are from Wagner [2004a, 2005b], and Wagner and Joubert [2005a].

Coal – microlithotype categories, including organic composition (vitrite, liptite, inertite, intermediate) and organic / inorganic associations (carbominerite).

Devolatilised coal – particles that exhibit physical changes by becoming porous and swollen, but do not show any significant change in shade of grey from parent coal. Volatile components are being driven off as the particles are exposed to increasing temperatures. The vitrinite component is likely to exhibit devolatilising behaviour more so than the other maceral types. Changes in shades of grey from parent coal to white in chars are readily observable, and can be related to increasing temperature exposure and volatile reduction.

Chars – porous chars are those chars where large pores and thin walls have developed. The pores must be relatively uniform, vitrinite being the likely precursor to this category. Chars appear white under the microscope and 99% of the time this category is isotropic. Vitrinite and other reactive maceral types are likely to contribute significantly to gas formation and tar, but are unlikely to be sustainable through the gasifier, and unlikely to contribute to the maintained high temperatures deep within the gasifier. Also referred to as cenospheres and honeycomb chars (but not really applicable here, due to the large size of the particles).

Chars – intermediate chars are those chars exhibiting a degree of porosity due to devolatilisation and degassing, but the pores are generally small or varied in size; the pore walls are thick and sections of the particle do not exhibit any physical changes (apart from a slight increase in colouring towards white). Intermediate microlithotype particles are the likely precursors for these char forms, including inertinite particles with variable reactivities (reactive semi-fusinite or inert inertodetrinite for example). These chars are generally anisotropic, showing an increasing degree of anisotropy with increasing temperature exposure. These particles are likely to contribute to gas formation as well as providing heat in the combustion zone. Also referred to as mixed chars.

Chars – dense chars are those chars which do not show any sign of alteration from the parent coal, apart from a slight increase in a shade of white. No pores are visible; cracks and fissures due to heat stress may be observed in these particles. Inert inertinite macerals, i.e. fusinites, are the likely precursors for this char form. It is likely that these chars do not contribute to gas formation, but rather play a role in maintaining the high temperatures deep within the gasifier; once ignited take longer to begin combusting than reactive vitrinite, but once ignited, burn for longer than vitrinite.

Chars – carbominerite chars are equivalent to carbominerite coal, i.e. there is an intimate relationship between the minerals and the carbon. The minerals also show signs of alteration due to temperature exposure.

Consumed char – this category reflects chars which exhibit a skeletal structure, irrespective of char morphology. The char is essentially almost combusted / gasified, the cell walls have become thin and appear brittle and a large proportion of this char type actually occurs as fragments which cannot be classified. Hence, the proportion of chars actually included in this category is low.

Stone / rock / ash – normal refers to mineral matter accounting for more than 60% of the field of view, but not exhibiting any optical signs of heat effect.

Stone / rock / ash – heat affected refers to mineral matter accounting for more than 60% of the field of view exhibiting optical signs of heat affect. Minerals transform during heating, generally melting and re-crystallizing, forming new minerals.

Now that the coal macroscopic and microscopic properties have been discussed, an understanding of the principles of sampling will be given.

5 SAMPLING

This subject has been discussed amongst others in the Coal Preparation in South Africa Handbook [2002]. "Sampling" may be defined as abstracting from a tonnage of coal (usually referred to as a "unit") a relatively small amount that may be taken as representative of the coal in the unit. Samples are normally made up of a number of "increments". An increment is the amount of coal removed from the unit by one operation or movement of the sampling device.

If coal were completely uniform, that is, if every particle in the unit had the same ash content and size distribution, then one particle would represent the entire unit, so constituting an increment. However, coal is not uniform, it is heterogeneous, i.e. it is a mixture of different sizes and qualities. Hence, the amount taken must be large enough to ensure that every particle present in the unit, has an equal chance to be present in the increment, in the same proportions as in the unit.

Figure 1.7 shows the recommended minimum width of opening of the sampling device in relation to the top size of the coal being sampled.

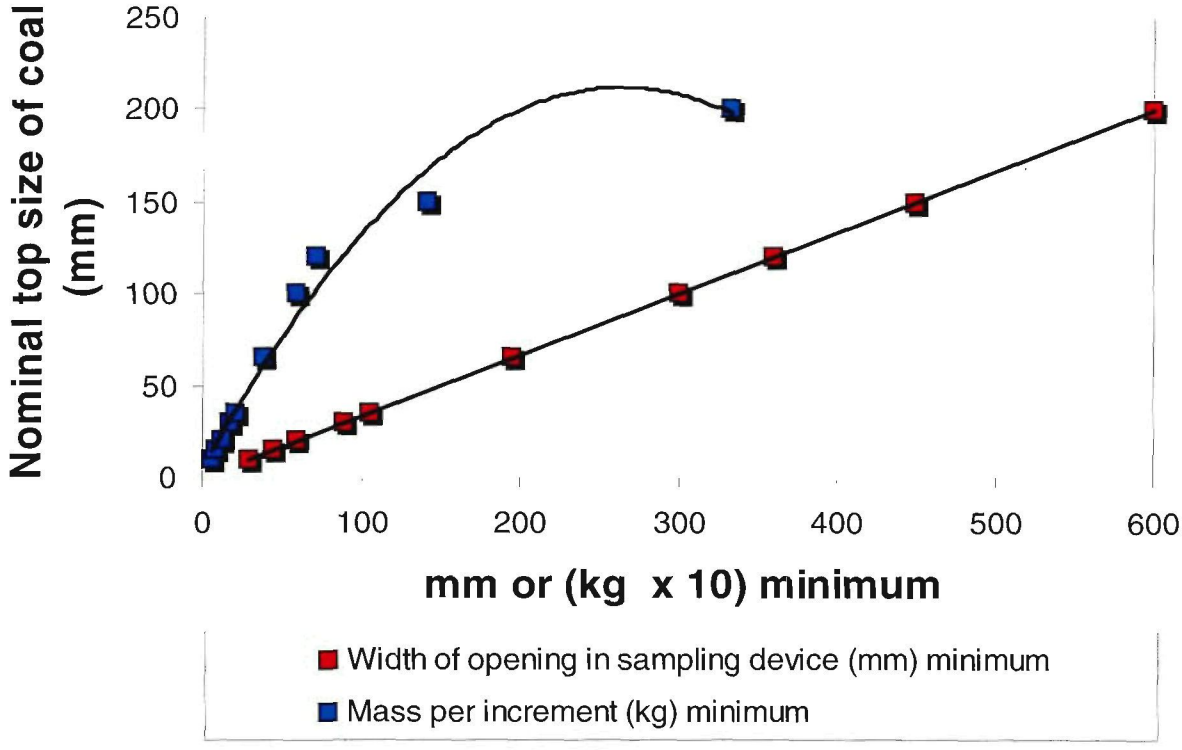

FIGURE 1.7: **GRAPH SHOWING THE RECOMMENDED MINIMUM INCREMENT SIZE AND WIDTH OF OPENING IN A SAMPLING DEVICE, REQUIRED IN RELATION TO NOMINAL TOP SIZE OF COAL WHEN SAMPLING [COAL PREPARATION IN SOUTH AFRICA HANDBOOK, 2002]**

It can readily be observed that the mass of increments required is a function of the size of the coal being sampled. The number of increments required is based on the condition of the coal, i.e. whether it is washed or unwashed. When coal is sampled, the number of increments that must be taken from conveyors or falling streams is 16 for cleaned coal or 32 for un-cleaned coal. When sampling from trucks, tubs or bucket conveyors, the number of increments increases to 24 for cleaned coal and to 48 for un-cleaned coal.

Strictly speaking, the number of increments required is not related to the tonnage of the coal being sampled. However, the number of increments is normally increased as the amount of coal being sampled, increases. The number of increments is based on 1000 tons; for larger tonnages the number of increments may be increased, though it is better to take a number of separate samples in this case. This entails considering the whole mass of coal, known as a consignment, to be made up of a number of units. Since a "truck-sampling" methodology will be applied to sub-sample the sequentially

dissected samples from the Sasol-Lurgi FBDB gasifier for the purposes of this study, a short summary of the precautions is given [Coal preparation in South Africa Handbook, 2002].

- The width of the sampling device (scoop or probe) must be at least three times the diameter of the largest size of the coal being sampled. Hence, probes can only be used for coal under about 300mm in diameter.
- The surface of trucks should be divided longitudinally into three equal strips. The same number of increments must be taken from each strip.
- When sampling by scoop, increments should be taken at the selected positions on the three longitudinal lines and holes dug at least 300mm deep in the coal. An increment should be taken from the bottom of the hole. All sizes of coal can be sampled by this method, but unfortunately only the coal fairly close to the top of the truck can be reached.

5.1 Gasifier sampling methodologies

There are two gasifier sampling methodologies referred to in the literature, i.e. turn-out and dissection [Glover, 1988, 1991; and Krishnudu, *et, al.*, 1989a,b]. A third probable gasifier sampling methodology, i.e. drill-core [Wagner, 2000] will also be discussed in this section.

5.1.1 *Turn-out (run-out) sampling methodology*

In this case, the complete gasifier contents are allowed to continuously run out through the ash-lock at the bottom of the gasifier onto the concrete plinth below. The char and ash are forced from the reactor by the action of the rotating grate. A sampling device is then periodically located into the falling stream to capture a pre-determined quantity of sample. This method of sampling assumes that the contents of the gasifier flows down the reactor in a plug-flow mode. The turn-out technique cannot show fine detail of the bed profile, but is adequate to gauge the bed height. Glover, [1988] studied the area above the ash zone, essentially being interested in the top 3.5m of the gasifier, but below the Bosman skirt. In this case, 59 x 175kg samples were taken in 2 x 8 hour shifts. This sampling methodology is essentially what was also used in the Indian pilot plant case study. [Krishnudu *et. al.*, 1989a,b].

Glover [1988] showed non-plug flow behaviour in cold model studies, concluding *"a large variation in average properties radial, but also a wide range of properties*

locally". In contrast, Madhusudhan *et al.*, [1989] showed ideal plug-flow behaviour for the solids in residence time distribution studies tested in a 1m diameter reactor.

5.1.2 Dissection (dig-out) sampling methodology

The content of the gasifier in this case is cooled sufficiently (using water or nitrogen) to allow safe access into the gasifier, once the coal-lock is removed. The char and ash samples can then be taken using a shovel. A pre-determined sampling grid scheme is used to ensure that the samples can be related back to their corresponding positions in the gasifier.

The spacing between sampling levels (in the axial direction) can be varied, but is experimentally limited to a minimum distance of approximately 30cm. Once the required number of samples from a particular level have been taken, the remaining char and ash can be removed, using pneumatic conveying. The shape of the ash-zone is mapped as sampling proceeds. Glover, [1988] sampled 12 levels containing 73 samples each, in 4 x 8 hour shifts when dissecting the #15 MK III gasifier in Sasolburg. Glover [1991] also sampled 2 MK IV gasifiers in Secunda; more detail of this work can be found in Section 6.2 of this Chapter.

5.1.3 Drill core sampling methodology

This method has been used with success in sampling submerged arc furnaces [Wagner, 2000] where bore-cores were drilled in the vertical, horizontal and angled positions [ASTM D2113, 1999; ASTM D5434, 2003]. The preferred core diameter is dependent on the application, but is typically at least 100mm. Cores of smaller diameter can also be used, provided that the diameter is at least three times the maximum size of the coarsest particle being sampled [SABS method 865, 1994]. In the case of drill core sampling of the Sasol-Lurgi FBDB gasifier contents, the drill core size should be at least 300mm in diameter. It is not known whether this option is truly viable in an un-fused, un-compacted environment, such as in a gasifier charge.

In terms of addressing the study objectives given in Section 1, the dig-out option is the preferred methodology to employ, albeit that it is more costly and time-intensive when compared to the turn-out option. Due to plant operational time constraints during a routine gasifier maintenance overall, insufficient time is allowable to naturally cool the gasifier in order to safely enter to conduct the sampling campaign. From this perspective, the turn-out option (Section 5.1.1) will be utilised in this present study.

6 REVIEW OF PREVIOUS RESEARCH DONE ON EXPERIMENTAL AND COMMERCIAL-SCALE FIXED-BED GASIFICATION REACTORS

A brief discussion on fixed-bed gasification will be given in the form of 2 case studies. The first case study reflects on the work done by Krishnudu, *et. al.,* [1989a,b] and Madhusudhan, *et. al.*, [1989]. They studied a pilot-scale reactor in India, which was quenched by cutting off the supply of oxygen and steam and samples were collected by running out the fuel bed through the ash-discharge grate. The second case study reviews the work done by Glover [1988, 1991] on commercial-scale Sasol-Lurgi FBDB gasifiers.

6.1 The pilot scale moving-bed pressure gasification plant in India

The pilot plant investigated by Krishnudu, *et. al.,* [1989a,b] and Madhusudhan, *et. al.* [1989] had a coal throughput of 850 kg/hr and was operated at pressures of up to 2.4 MPa. The main gasifier was a water-jacketed vessel having an internal diameter of 1.13m. Ash was withdrawn by means of a grate, which was rotated at different speeds. This, along with the variable rate of supply of oxygen and steam, helped to control the throughput of the gasifier. The height of the fuel bed was 3.5 m.

Sequential layer samples were collected every 250mm, starting from the bottom. These were collected by running-out the samples through the ash-lock after the gasifier had been quenched by cutting off the supply of oxygen and steam. Typical process conditions at the time of quenching are reflected in Table 1.7 for Godvari Khani-Ramagundam coal [Krishnudu, *et. al.,*1989a]. The sequential samples were analysed by means of the proximate analysis and Gray-King assays, whilst the physical properties (bulk density and true density, and screen analysis) were also determined (see Tables B1-4 in Appendix B).

Results indicated that three distinct zones existed: (1) fast devolatilisation, (2) slow devolatilisation with gasification, and (3) gasification. Also, about two-thirds of the total fuel bed height of 3.5m was occupied by slow / fast pyrolysis, the remainder was for gasification, when viewing the fixed carbon and volatile matter distribution profiles, normalised to a constant ash content (Figure 1.8). This emphasizes the importance of designing the reactor tall enough, to provide for the devolatilisation reactions to be completed.

TABLE 1.7: TABLE SHOWING THE PROCESS CONDITIONS AT THE TIME OF QUENCHING FOR THE GODVARI KHANI-RAMAGUNDAM COAL [KRISHNUDU, *et. al.*, 1989a]

Process condition	
Coal feed rate (kg/h)	850
Steam flow (kg/h)	948
Oxygen flow (M^3_n/h)	155
Blast temperature (°C)	310
Operating pressure (MPa)	2
Crude gas flow ((M^3_n/h)	1020
Gas outlet temperature (°C)	350
Gas composition (vol %)	
CO_2	33
CO	17.8
H_2	38
CH_4	9.8
O_2	0.6
N_2 (by difference)	0.8
Moisture in coal (wt % AR)	2.4
Volatile matter in coal (wt % AR)	24.9
Ash content in coal (wt % AR)	33.6
Fixed carbon in coal (wt % AR)	39.1

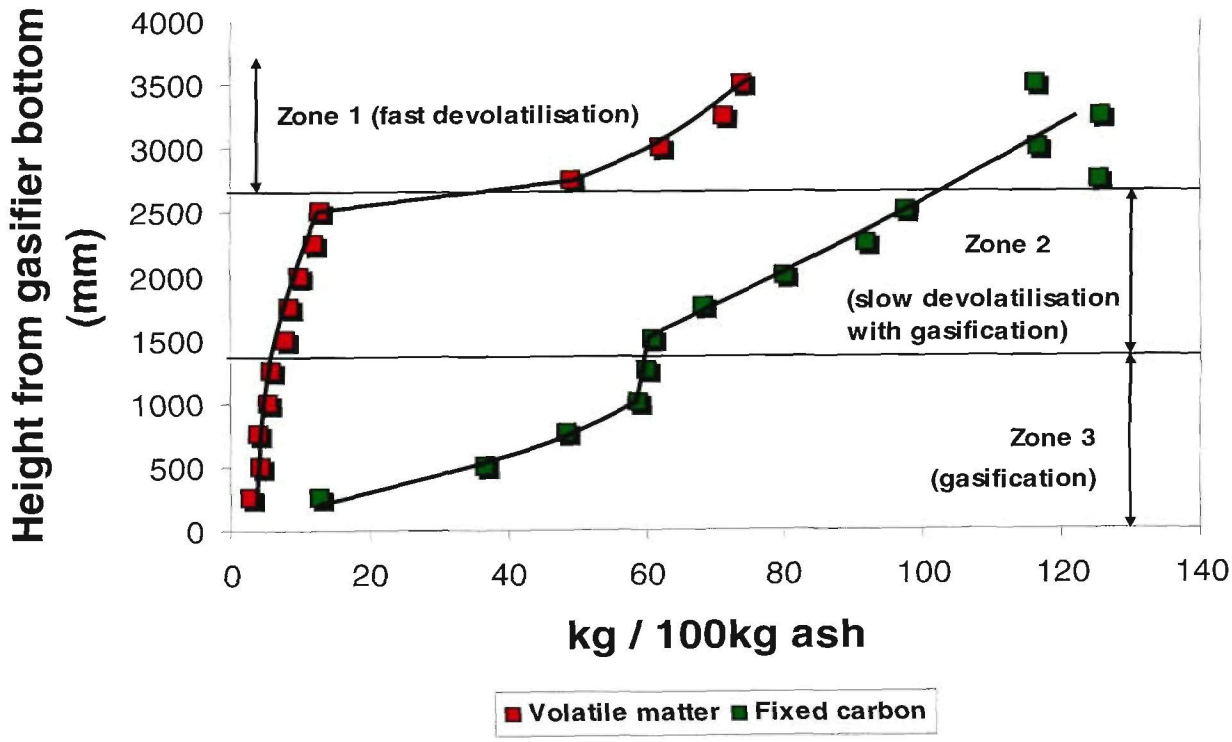

FIGURE 1.8: GRAPH SHOWING THE VOLATILE MATTER AND FIXED CARBON DISTRIBUTION PROFILES (NORMALISED TO A CONSTANT ASH CONTENT) FOR THE GODVARI KHANI-RAMAGUNDAM COAL [KRISHNUDU, *et. al.*, 1989a]

Reduction of the average particle size from 11mm (feed coal) down to 6mm (ash at the ash-grate) took place (Figure 1.9). The bulk density and true density profiles obtained are given in Figure 1.10. Based on these axial particle size and bed voidage results, a partial ash segregation model was proposed [Prasad and Reddy, 1989]. The striking feature of this model is the prediction (Figure 1.11) of an extended "hot-spot" region, which contrasts with the sharp peak usually predicted by total ash segregation and shell progressive models [Van der Walt, 1994].

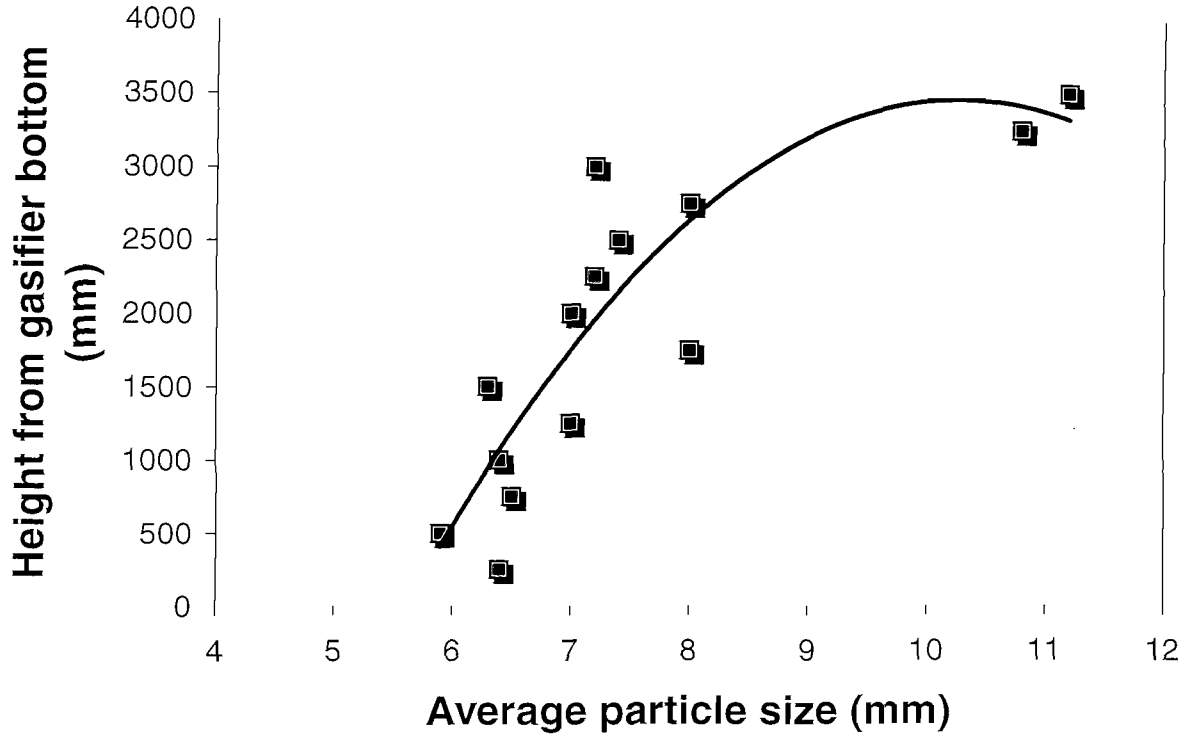

FIGURE 1.9: GRAPH SHOWING THE EFFECT OF SIZE DEGRADATION IN RELATION TO GASIFIER HEIGHT FOR THE INDIAN PILOT SCALE GASIFIER OPERATING ON GODVARI KHANI-RAMAGUNDAM COAL [KRISHNUDU, *et. al.*, 1989a]

It was further shown by Madhusudhan, *et. al.*, [1989] that this reactor behaved like a plug-flow reactor without back-mixing and that there were no stagnant layers accumulating materials of different ages. It took about 7 hours for the solids to pass through the gasifier from point of entry into the coal-lock hopper to the ash discharge point. The residence time of the gasses was about 30 seconds. Under these circumstances, no significant radial variations in the gas composition or temperature are likely; the radial profiles can thus be assumed to be uniform.

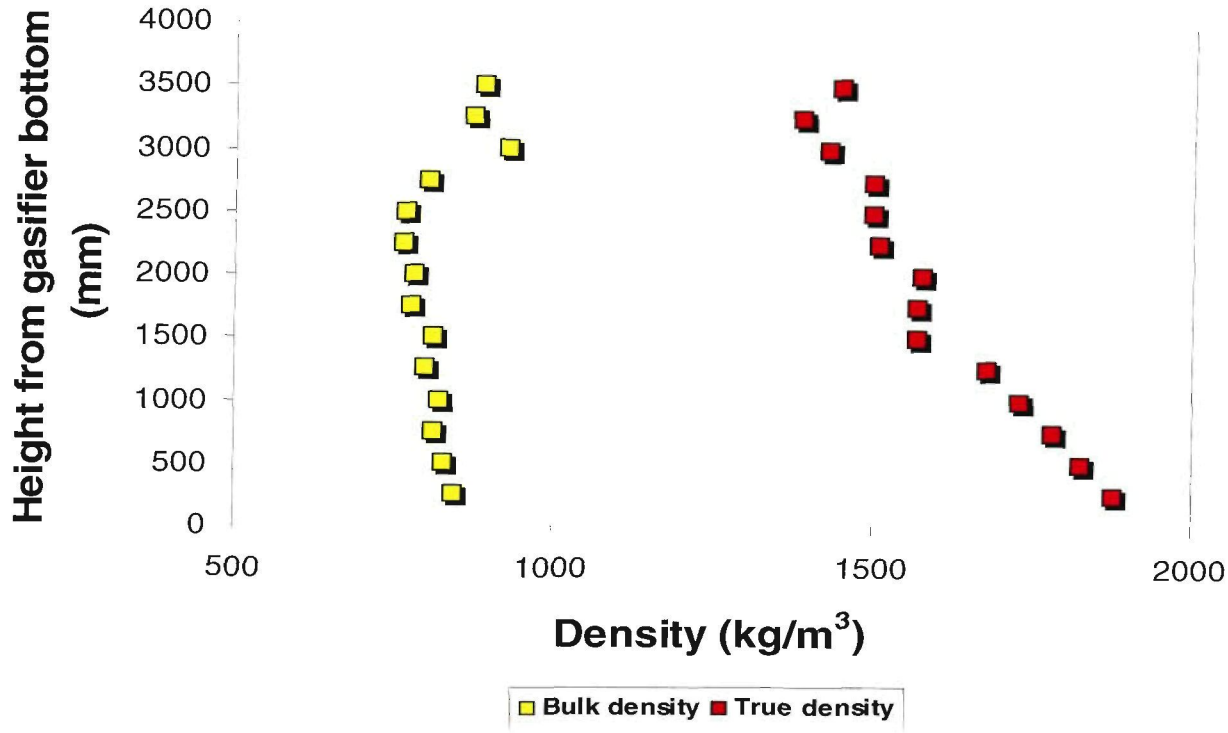

FIGURE 1.10 : FIGURE SHOWING THE BULK DENSITY AND TRUE DENSITY PROFILES RELATIVE TO SAMPLE POSITION HEIGHT FOR THE INDIAN PILOT PLANT GASIFIER OPERATING ON GODVARI KHANI-RAMAGUNDAM COAL [KRISHNUDU, *et. al.*, 1989a]

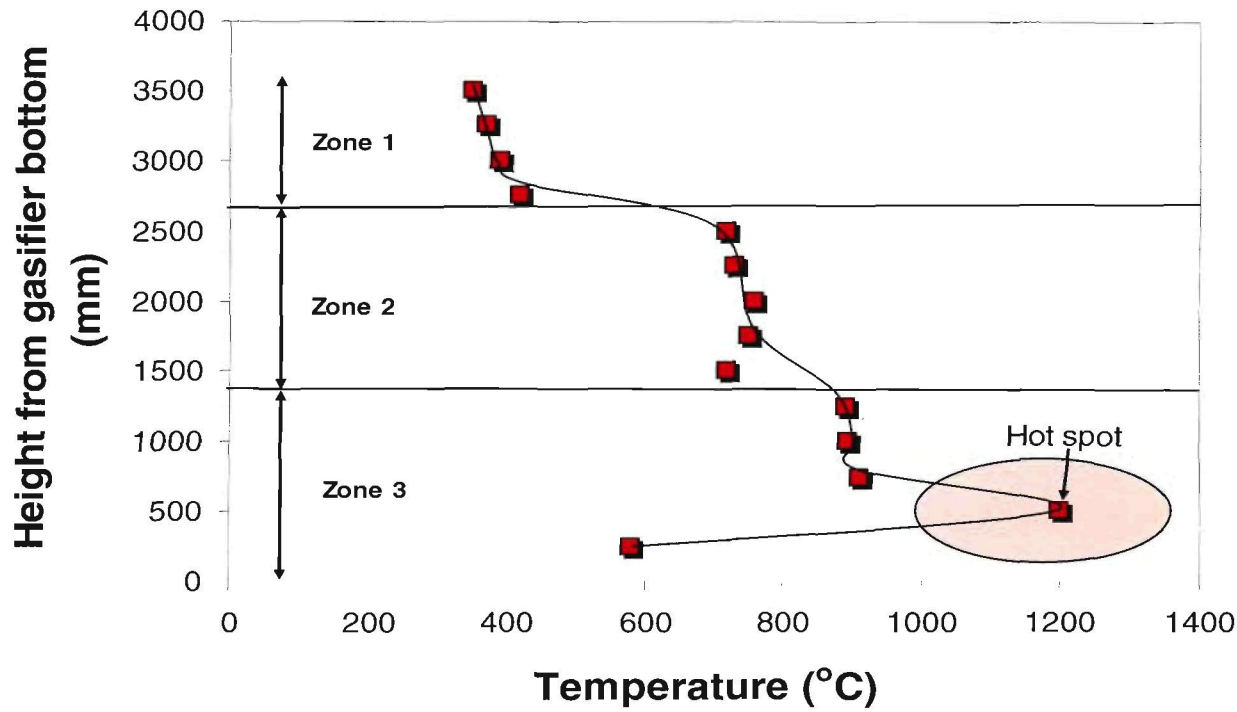

FIGURE 1.11: GRAPH SHOWING THE PREDICTED TEMPERATURE PROFILE OF THE INDIAN PILOT SCALE GASIFIER [KRISHNUDU, *et. .al.*, 1989a]

In another study [Krishnudu *et. al.*,1989b], three different high-ash Indian coals were gasified in the pilot gasifier with an oxygen–steam mixture, using different pressures for coal sized between 6mm and 25mm. Steady state conditions prevailed during sampling and the CO_2 and O_2 contents in the exit gas were controlled at 28 – 30 and 0 – 0.5 % volume respectively. The steam to oxygen ratio was adjusted so that the discharged ash was neither in the form of clinkers nor of a fine powder. Under these process conditions, the coal throughput of around 800kg/m^2.h was considerably lower than that reported for commercial plants [Handbook of Synfuels Technology, 1984].

The results from this study can thus be summarized as follows:

- Higher pressures favoured the formation of methane.
- In this pilot plant, the crude gas throughput was low (c.a. 1200 m_n^3/m^2.h) compared to the latest Sasol-Lurgi MK V gasifier having a throughput of 5000 m_n^3/m^2.h [Handbook of Synfuels Technology, 1984]. These low gas velocities might be the reason why the pilot gasifier could tolerate a higher proportion of coal fines in the feed – occasionally as high as 40% of the material was of a size less than 6mm. Normally, Sasol-Lurgi FBDB gasifiers require graded coal with a minimum allowable size of 3mm and the maximum top size of about 100 mm. Five percent of the coal, as undersized material, can be tolerated and the ratio of largest to smallest size should be 10:1 or less [Handbook of Synfuels Technology, 1984]. For high volatile matter coals, this size ratio can be more than 10, as bigger coal particles break into smaller particles and the size range becomes uniform [Van der Walt, 1994].
- About 90% of the carbon in the feed coal appeared as product gas and about 8% as tar and oil. This stresses the importance of the fixed carbon gasification step relative to the coal devolatilisation step.
- From the energy supplied to the gasifier (81.7% as coal and 17.4% as steam), 68.5% was gas, 7% was tar and oil and 20.9% as gas-liquor and jacket steam; the losses were about 2%.

6.2 Sasol-Lurgi commercial –scale fixed-bed gasification studies

Glover [1988, 1991] was involved in the sampling, analysis and interpretation of five Mark III / IV gasifier "dig-outs" between May 1986 and August 1991; two in Sasolburg (MK III) and three in Secunda. (MK IV). Water, N_2 or natural cooling were used as quench methods and samples were removed by run-out or dissection. Samples obtained ranged from 45 to over 700 per gasifier. Samples were collected in drums,

buckets or plastic bags, extra care being taken when transporting samples required for PSD analyses. The gasifier height was taken from the base of the Bosman skirt. The feed coal as well as ash, were sampled prior to shut down; and operational data was collated.

It can be observed from the findings by Glover [1988, 1991] that the fixed-bed gasifier internal characteristic profiles were predominantly measured up to the char-ash interface, not extending throughout the entire gasifier. It is therefore a major objective of this current study to quantify the entire characteristic profile deportment, thereby providing a more complete experimental data set needed for the envisaged kinetic modelling of the gasification process. The gasifier profiles that will be discussed in this section are based on an adaptation by Wagner [2004b] and include: temperature, particle size, volatile matter and carbon conversion profiles.

6.2.1 Sasolburg dissection [gasifier #15 (H_2O quenched)]

Two hundred and fifty samples were obtained from the Bosman skirt and main bed, down to the top of the ash-bed (approximately 2.5m below the Bosman skirt). The MK III gasifier extended to 5m below the Bosman skirt to the top of the ash-grate.

Ash-zone profile - samples were visually sorted into char and ash combinations and profiles of the ash-zone geometry (radially and axially) were constructed, revealing an uneven ash-bed. Ash was estimated to account for approximately 70% of the reactor volume. Wall channels or ash channels close to the jacket were evident, creeping towards the Bosman skirt. Char was common at 2.5m, whilst char-ash mixtures were determined as high as 1m into the gasifier (depth taken from below the Bosman skirt).

Carbon conversion profile - the ash content of the feed was assumed to be constant at all times (29.6%). The effects of mineral matter reactions were neglected for the purpose of the calculation used to determine char conversion (carbon burn-off) due to gasification and combustion. The fixed carbon content was 47.5% and the conversion was calculated for the char samples in the top part of the bed, as well as for the char in the ash-bed. No carbon conversion occurred within the Bosman skirt, but did start at the top of the main bed, being less advanced against the walls, at the point where the ash-zone appeared. Generally, conversion increased as the char descended through the gasifier, with approximately 20% to 30% of the char particles passing through the primary gasification / combustion zone [Glover, 1988]. Almost complete conversion (92% to 99%) occurred a short distance into the ash layer [Glover, 1991].

The percentage carbon conversion increased dramatically at the top of the ash-bed, increasing from the 60% to 70% range to 80% to 90% range in what appeared to be a few millimetres. The change was even more dramatic on the sides of the gasifier wall.

Temperature profile – Based on char optical reflectivity (reflectivity increases with increased temperature), calibration curves were constructed by heating samples in inert atmospheres at different temperatures and measuring the resultant changes in reflectivity. However, the reflectivity decreased in gasified chars, most likely due to the development of pore-structure. The temperature data obtained was limited to areas in the reactor where no appreciable gasification or combustion reactions took place. The temperature profile constructed indicated temperature ranges of between 200°C and 575°C in the Bosman skirt, while being relatively uniform (600°C) in the main bed (top section). The maximum heating rate was believed to be 100°C/minute (Figure 1.12).

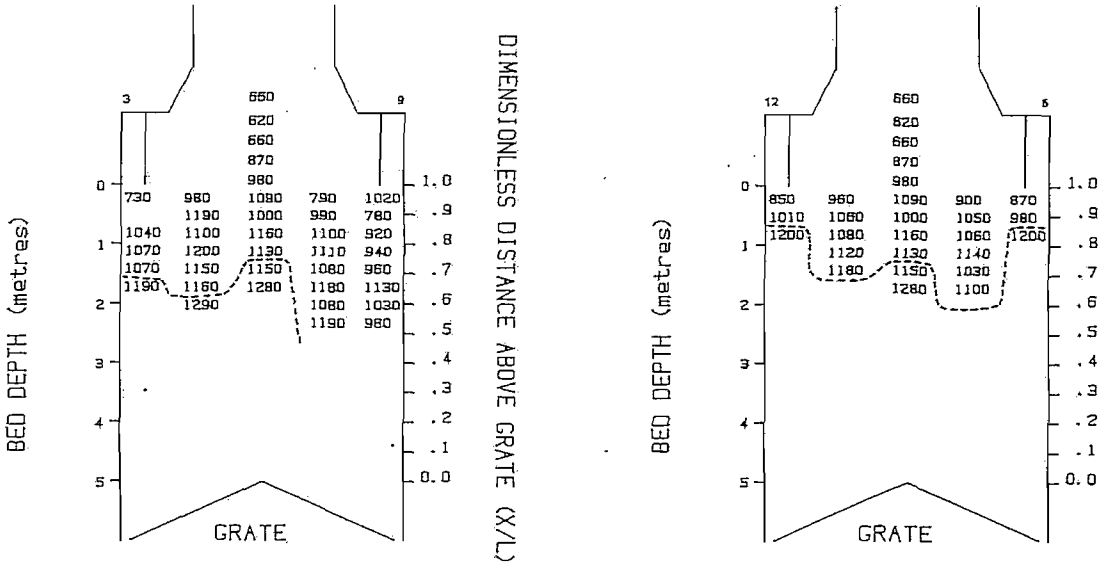

FIGURE 1.12: GRAPH SHOWING THE TEMPERATURE PROFILE IN THE SASOL ONE #15 GASIFIER. TEMPERATURES ARE INDICATED IN KELVIN. THE POSITION OF THE ASH BED IS SHOWN BY-------. (a) SECTION 3-9; (b) SECTION 12-6 [GLOVER, 1988]

An infra-red spectroscopic technique was also applied on char samples [Glover, 1991] and used to determine the temperature profile. The average bed temperatures in the top section of the main bed were around 777°C, peaking to 1026°C a short distance into the ash-zone, with a cooler zone anticipated closer to the jacket.

Volatile matter (VM) profile – VM was determined on the char samples and used to construct profiles in the Bosman skirt and the main bed region. The feed coal had a VM content of 22.86% and values of 2% to10% were reported for the char samples in the main bed. The bulk of the devolatilisation occurred within the Bosman skirt region, with no evidence of recondensation occurring [Glover, 1988].

Particle size distribution (PSD) – The PSD was not conducted, as exfoliation of the char particles due to the water quench was observed. Extensive size segregation was observed in the main bed, possibly as a result of the coal feed mechanisms. Coarser particles were observed against the jacket and in the centre of the bed, with finer particles occupying intermediate positions.

6.2.2 Sasolburg run-out [gasifier #16 – (not quenched)]

Forty-five samples from the top of the ash-grate to the top of the Bosman skirt were taken, using the run-out technique discussed in Section 5.1.1.

Ash-zone profile - Whilst lacking detail, the ash-zone profile was comparable to that obtained from gasifier # 15. Three visually distinct char particles were determined – "plastic" derived from vitrinite-rich coal, "intermediate" derived from vitrinite / intertinite coal, and "dull" derived from intertinite-rich coal.

Carbon conversion profile – The swelling char was determined to be the least reactive (i.e. more FC than other chars at the same position within the bed), while the dull char exhibited two burn-off phases, thus indicating different char types displaying different burn-off behaviours.

Temperature profile – Confirmation from the temperature profile showed that the top of the bed was located just below the Bosman skirt.

Volatile matter profile – Some speculation on sample mixing during the run-out sampling campaign existed, as the sample from the top of the bed had a lower VM content than samples from lower positions (Figure 1.13). Recondensation was observed in some Secunda gasifiers [Glover, 1991], and may be a real effect, specific to coal types. Swelling char exhibited the quickest volatile release and dull char had the greatest affinity for volatile recondensation (Figure 1.14). Volatile evolution was found to be dependent on PSD (where smaller particles released VM more readily); volatile release and temperature profiles were comparable (Figure 1.15).

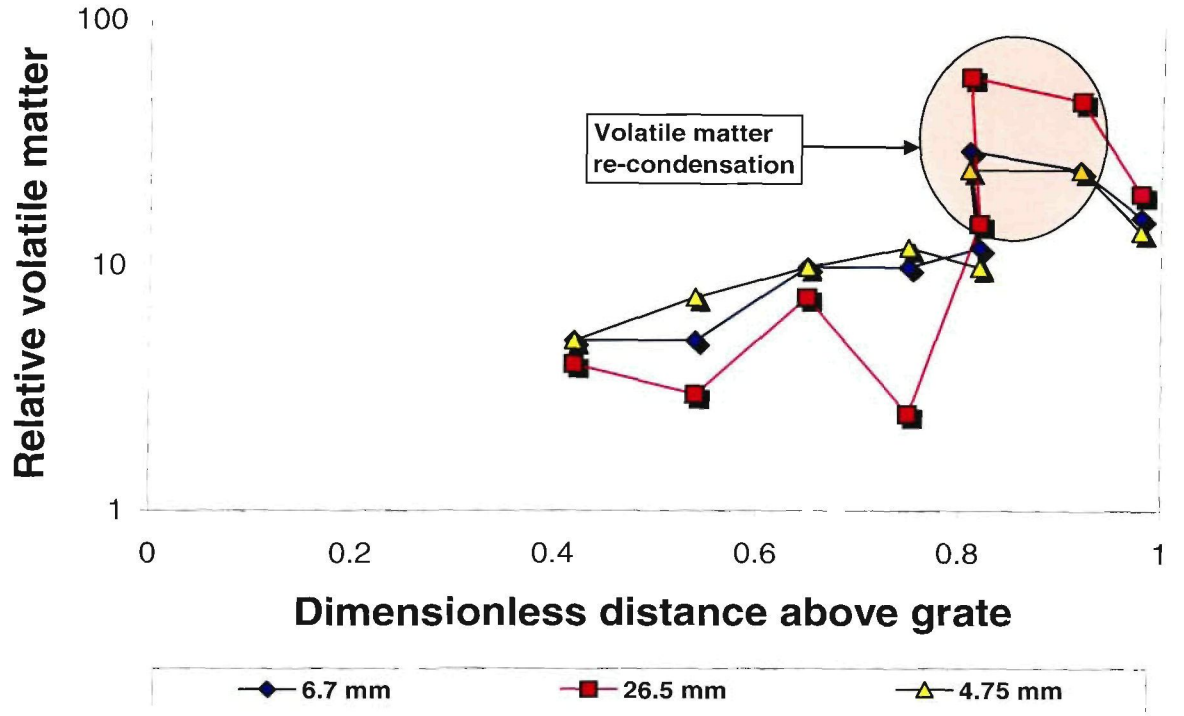

FIGURE 1.13 : GRAPH SHOWING THE VOLATILE MATTER PROFILE FOR DIFFERENT SIZED COAL IN THE SASOL ONE #16 GASIFIER. RECONDENSATION IS APPARENT TOWARDS THE TOP OF THE BED [GLOVER, 1991]

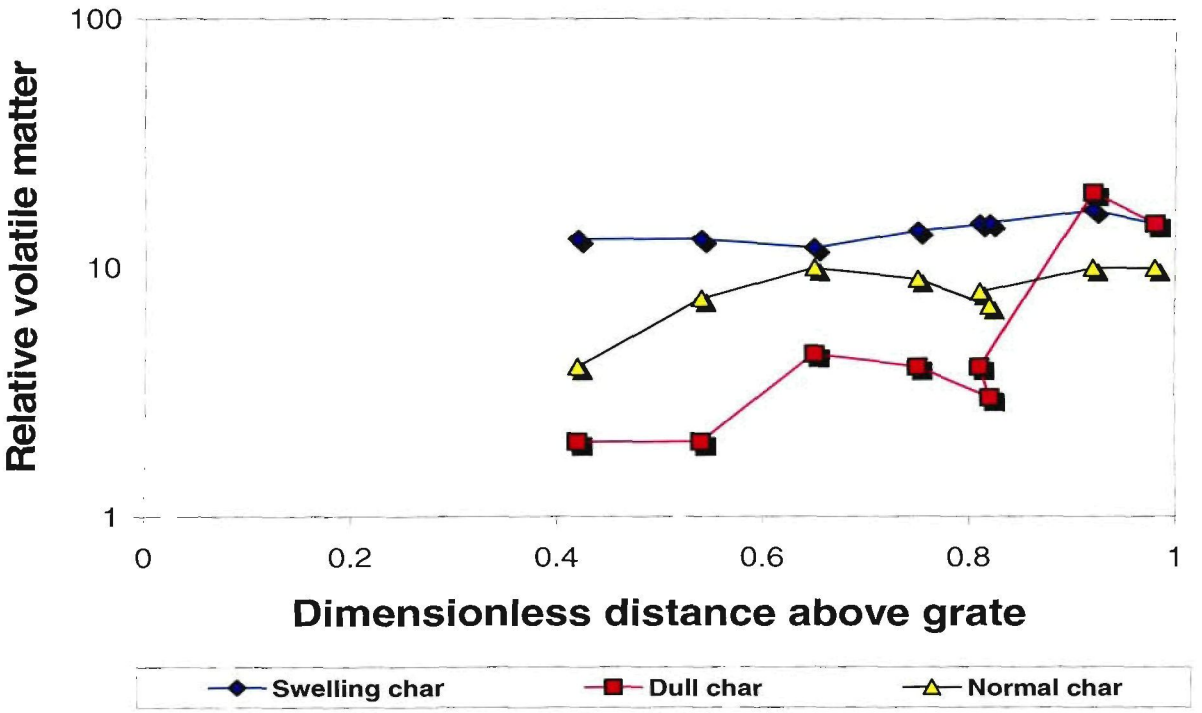

FIGURE 1.14 : GRAPH DEPICTING THE RELATIVE VOLATILE MATTER CONTENT OF THE DIFFERENT CHAR TYPES IDENTIFIED IN THE SASOL ONE #16 GASIFIER [GLOVER, 1991]

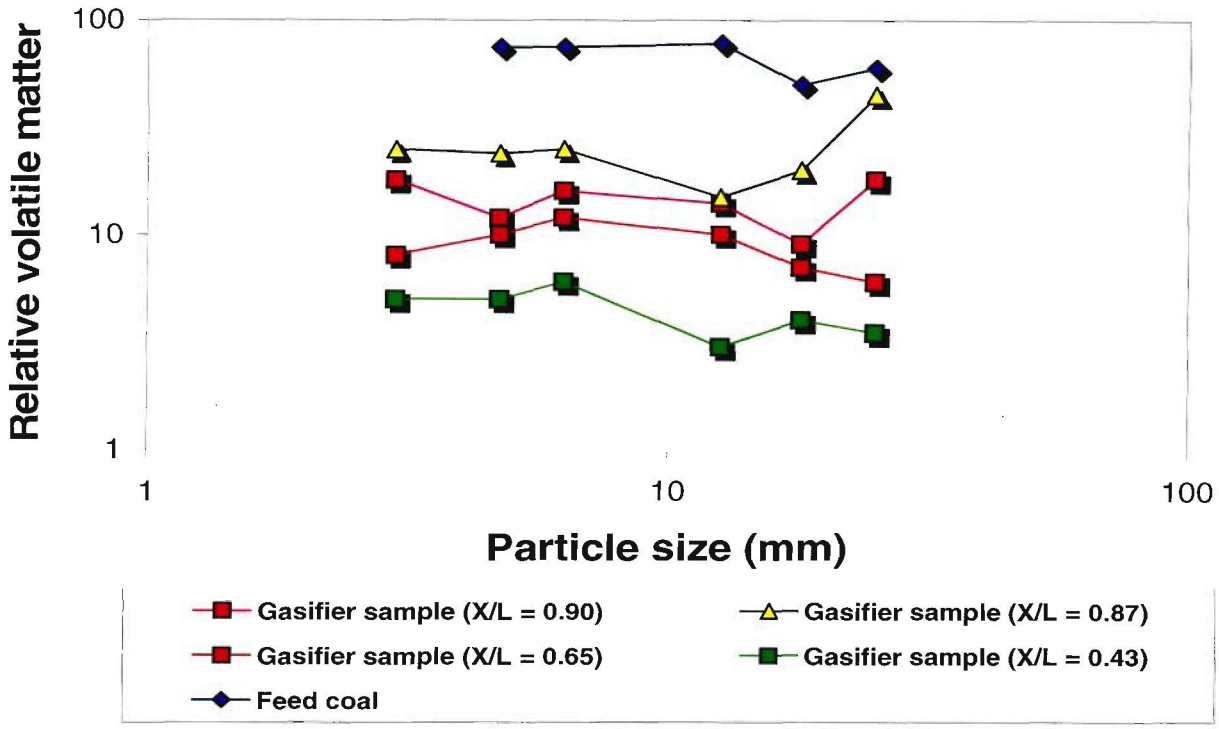

FIGURE 1.15 : GRAPH SHOWING VOLATILE MATTER CONTENT AS A FUNCTION OF PARTICLE SIZE, AT DIFFERENT BED POSITIONS IN THE SASOL ONE #16 GASIFIER [GLOVER, 1991]

PSD – The feed coal had a -6.7mm content of 4%, and a significant increase in char fines was observed in the top part of the reactor (up to 30% -6.7mm). It was found that as the bed descended towards the grate, the rate of size degradation was reduced. Sampling may have increased the proportion of fines by attrition, but these results must be treated with caution.

Ash fusion temperature (AFT) properties – AFT's conducted on the feed coal, indicated that the largest particles had higher fusion temperatures; this trend was also observed for the gasifier ash sample. XRF analysis was used to determine the acid : base oxide ratio (around 0.2, IDT 1351°C). The relationship between mineral content and ash melting temperatures is complex, with particle size having a large effect. The dull coal samples had a lower calcite content, thus higher AFT's, than the other char types; and an ash layer was observed around these particles.

Char reactivity – CO_2 reactivity was measured on the feed coal and dull and plastic chars by TGA analysis. Reactivities on larger particles (+6.7mm – 9.5mm) were also measured using a tube-furnace. The reactivity of the powdered TGA samples was significantly higher than for the larger particles and the dull char was more reactive than the plastic char in the powdered samples, but the order was reversed for the

larger samples. A possible explanation for this, is that the reactivity rate at lower temperatures is controlled by chemical reaction, rather than by mass diffusion across the particle; while at higher temperatures the opposite occurs. Dull coal had a higher ash content, which could create a higher resistance to gas diffusion [Glover, 1991].

6.2.3 Secunda dissection [gasifiers #14 (H_2O cooled) & #17 (N_2 & H_2O cooled)]

Ash-zone profile - The ash-zone profile again was found to indicate an asymmetrical ash-bed and wall channeling (20-30m radially into the bed). The mean ash-bed height was far lower, relative to the Sasolburg gasifier, caking being observed towards the top of the main bed; the samples were mechanically strong, yet brittle. Particles against the jacket walls were found not to be caked, but voids were found near the top of the gasifier (below the Bosman skirt).

Carbon conversion profile and particle size distribution – Not conducted

6.2.4 Secunda run-out [gasifier #16 (N_2 cooled for 16 hrs)]

PSD – As with the Sasolburg gasifier run-out, a significant increase in fines was observed during the descent in the Bosman skirt. However, due to the caking and the brittle nature of the char, it is likely that the fines were generated during run-out. The fines at the top of the gasifier and in the feed coal were almost equivalent, indicating little fines generation occurring within the coal-lock.

6.2.5 Specific findings and conclusions [Glover, 1988, 1991]

- The dissection, or dig-out, yielded considerably more information than the run-out technique. However, the dissection was a costly exercise, in terms of both time and number of analyses required.
- Glover considered these five investigations as first attempts; detailed photography was recommended for future dissections.
- The formation of ash wall channels was believed to be responsible for continued gasifier operational problems and the ash-bed profile in the Secunda gasifiers was found to be far lower than in the Sasolburg gasifiers.
- Uneven ash-bed profiles were found in all gasifiers; the primary cause of this could have been the radial size segregation of coal particles as they entered the gasifier.
- The position of the combustion zone was very sensitive to small changes in FC

feed rate (even by 10%), when the combustion zone was located in the middle of the reactor. The carbon feed rate was controlled by the grate-speed. Lower FC feed rate caused the position of the maximum temperature zone to move up in the gasifier, while higher FC feed rate caused this temperature zone to move down in the gasifier. This will affect gas outlet and grate temperatures, the varying of which, will have consequences. Where the combustion zone approaches the base of the gasifier, FC carryover in the ash will be high.

- Simulations by varying the ash content, but maintaining FC, did not move the combustion zone in the bed. The ash particles were assumed to have the same density and heat value as carbon and the FC content of the feed coal was considered to be a more fundamental parameter than the ash content.
- Changes in gas flow rate were shown by simulation to also affect the position of the maximum temperature zone [Glover, 1991].
- The PSD analyses were "elusive" due to quenching problems. The only PSD was conducted on the run-out tests; the effect of run-out on fines generation was unknown. Caking observed in the Secunda gasifiers [Glover, 1991] was expected to also affect the PSD determination.
- Simulations of the particle size [Glover, 1991] indicated that larger particle sizes resulted in higher combustion zones and broader temperature peaks than smaller particle sizes. Also, that fine coal and size segregation together produced mal-distribution of the gas flow.
- Particle size had an effect on certain coal properties, including reactivity and VM release. The reactivity of fine char particles was found to be higher than that of coarser particles.
- Larger particle sizes resulted in lower combustion zone temperatures, reducing the risk of ash fusion. Peak temperatures in the combustion zone increased with decreasing particle size [Glover, 1991].
- Fragmentation within the gasifier bed was not considered to be an important contributor to gasifier behaviour problems, but particle entrainment of fines was however likely.
- Petrography conducted on sized fractions may be more beneficial than run-of-mine (ROM) for predicting gasification behaviour, as larger particles tended to behave abnormally.
- Voids occurred below layers of caking and simulations by Glover [1991] indicated that bed voidage did not affect the maximum temperature zone, but could affect gas flow.
- Caking did not appear to occur close to the walls; the char particles in this

region could have acted as a "lubricant " for the caked mass. Swelling was observed in Sigma (Sasolburg coal) particles, but a caked mass did not form as was the case for the Secunda coals.

- When considering the effect of channeling on particle entrainment, Glover [1991] noted that the gas velocity would be far higher than expected where caking occurred, due to low gas permeability; caking affected fluidization in the middle of the bed. Against the walls (approximately 30cm wide as determined visually) permeability was better and due to the constriction, the gas velocity increased. This resulted in the entrainment of particles -0.5mm, which were transported out of the gasifier in the raw gas. If thermal-channeling occurred (caused by a gas cooling a hot bed) and the gas flowed towards the sides of the reactor, particles of 6mm could be entrained. The calculations may be crude, but are considered to be in the correct order of magnitude [Glover, 1988].
- Different chars appeared to react in different zones (intense gasification / combustion zone and a secondary reaction zone). A possibility existed that vitrinite-rich and intertinite-rich components in the caked mass gasified at different times and this affected the bed profile.
- It is expected that if the ratio of intertinite to vitrinite varies appreciably over a time-period equal to the transit time of char in the gasifier, operating fluctuations may result as the ash-bed will move up and down unpredictably. Dull char (intertinite-rich coal) has a higher reactivity and lower FC content, resulting in a high ash-bed in the gasifier. Swelling char (vitrinite-rich coal) was shown to have a lower reactivity and higher FC, resulting in a lower ash-bed. It was recommended that models for the gasification of single char particles include local spatial variations.
- The grate region of the gasifier, where the agents are added, could affect gas distribution, in turn affecting the processes in the upper levels of the gasifier. An experimental grate simulator was recommended in order to devise a strategy to minimize gas flow mal-distribution.
- Where thermal-channeling occurred, local steam : oxygen ratio variations could occur, possibly allowing for higher temperatures to be reached above ash-melting, giving rise to clinker formation in certain areas of the reactor.
- The localised nature of gasification reactions with respect to the overall optimisation of the gasifier must be emphasized. "Future gasification dissection experiments must have clear objectives and should preferably ...determine only specific features.... "[Glover, 1991].

CHAPTER 2
EXPERIMENTAL PROCEDURES

1 INTRODUCTION

In terms of addressing the study objectives postulated in Chapter 1, it is clear that the gasifier turn-out option (discussed in Section 5.1.1) is the only methodology that can be employed (given the gasification plant production constraints), in order to obtain clear axially-derived profiles of the Sasol-Lurgi FBDB MK IV gasifier reaction zones. A routine gasifier maintenance overall of the GG41 MK IV Sasol-Lurgi FBDB gasifier in Secunda has created an opportunity to sample the gasifier contents after water quenching.

The approach taken here was different to Glover's earlier approach [Glover, 1988], where he essentially periodically introduced a sampling device into the falling stream, whilst turning out gasifier #16 at the Sasolburg plant. In the present case, the GG41 gasifier turn-out was more controlled, whereby the increment size was kept constant ($3m^3$ sequential slices) and then sub-sampled. This approach was similar to the Indian pilot plant experience (but new-to-Sasol), where the increment size was also kept constant during the turn-out sampling campaign of the pilot-scale reactor [Krishnudu *et. al,* 1989a,b].

This Section describes the GG41 gasifier turn-out sampling methodology employed. The approach that was followed is discussed by comparing the GG41 gasifier results (characterisation profiles) to the Indian pilot plant data, as published by Krishnudu, et. al., [1989a,b], as well as to the work of Glover [1988]. The subsequent sample preparation techniques and characterisation methods used for the 32 dissected GG41 turn-out samples will also be described.

2 GG41 GASIFIER SAMPLING METHODOLOGY

A sampling plan was required for the gasifier turn-out exercise; the number of samples required being calculated according to the specifications of a statistical model. In order to determine the temperature profile, as well as the profile of the properties of interest, it was necessary to collect samples at different levels across the length of the gasifier. Samples were taken at each level according to a statistical experimental design layout. In this case, a minimum sample increment size of $3m^3$ was deemed sufficient [Coetzer, 2004].

The minimum ash-grate speed of the GG41 gasifier was controlled at 3.0 revolutions per hour, which equated to 9 tons per hour of material being discharged from the bottom of the gasifier. A MK IV gasifier typically contains c.a. 100 tons of material, thus if the grate were rotated at its slowest speed and every increment sampled every 0.5 hour, then 32 x $3m^3$ samples would be obtained in total. This implied that each sample taken represented a composite of the material in every 0.26m x 4m (height x diameter) slice of the gasifier, given that the gasifier is c.a. 9m high. This sampling campaign thus took about 17 hours to complete.

In the literature review in Chapter 1, it was stated that for a coal having a nominal top size of 65mm, that 48 X 3.9kg increments should at least be taken for the unwashed coal, using a sampling device having a width of at least 195mm in the case of truck-sampling. This implied that the sub-sampling process of each of the 32 X $3m^3$ sequential slices, yielded a mass in each case, for each sample taken, to consist of a minimum of 187kg. Two hundred litre capacity drums were thus sufficient to contain the various sequentially-taken sub-samples for characterisation purposes.

Table 2.1 shows the correlation between the GG41 gasifier turn-out sample numbers used in this study, and the corresponding gasifier height. Sample 1 was the first sample turned-out of the gasifier at the ash-grate, therefore equating to a height of 0.9m due to the volume occupied by the grate. Thereafter, each of the sample numbers corresponds to a gasifier height of 0.26m. Sample 32 was taken at the top of the gasifier and is discussed as the feed coal sample in this study.

The various zones, i.e. Bosman skirt (drying zone), pyrolysis zone, gasification (reduction) and combustion (ash-bed) zones, are colour-coded for convenience in Table 2.1, using the results obtained from this study. This will give the reader some perspective on where these zones occurred from the GG41 gasifier turn-out. The sample numbers will be used throughout in the discussion of results.

Photographic images depicting the GG41 gasifier shut-down procedure trend data obtained are given in Figures 2.1 and 2.2. The GG41 gasifier trend data shown in Figure 2.1 is for the 24-hourly flow rate measurements of steam, oxygen, high pressure boiler feed water and CO_2 before decommissioning. Figure 2.2 shows the trend data as the GG41 gasifier was brought off-line after the oxygen flow was cut.

Figures 2.3 to 2.5 show photographic images of the sampling methodology used in the GG41 gasifier turn-out campaign.

TABLE 2.1: TABLE SHOWING THE GG41 SAMPLE NUMBER RELATIONSHIP WITH THE GG41 GASIFIER HEIGHT (m)

Sample Number	Sample taken every (m)	Gasifier height cum. (m)	
32	0.26	8.96	Top of Gasifier
31	0.26	8.7	
30	0.26	8.44	
29	0.26	8.18	Drying zone
28	0.26	7.92	
27	0.26	7.66	
26	0.26	7.4	
25	0.26	7.14	
24	0.26	6.88	
23	0.26	6.62	
22	0.26	6.36	
21	0.26	6.1	Pyrolysis zone
20	0.26	5.84	
19	0.26	5.58	
18	0.26	5.32	
17	0.26	5.06	
16	0.26	4.8	
15	0.26	4.54	
14	0.26	4.28	
13	0.26	4.02	
12	0.26	3.76	
11	0.26	3.5	
10	0.26	3.24	Reduction zone
9	0.26	2.98	
8	0.26	2.72	
7	0.26	2.46	
6	0.26	2.2	
5	0.26	1.94	
4	0.26	1.68	
3	0.26	1.42	Combustion bed
2	0.26	1.16	
1	0.9	0.9	Bottom of Gasifier

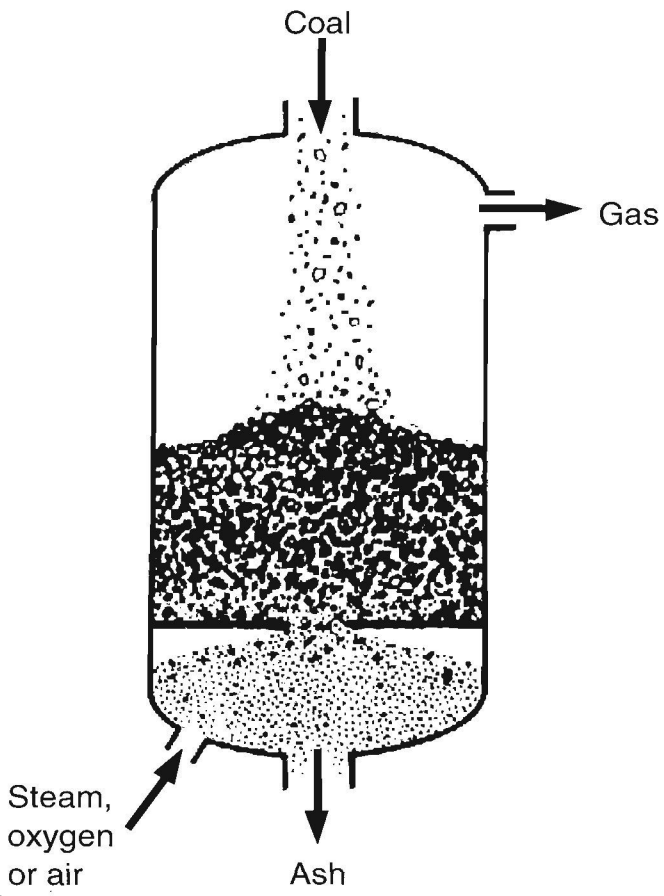

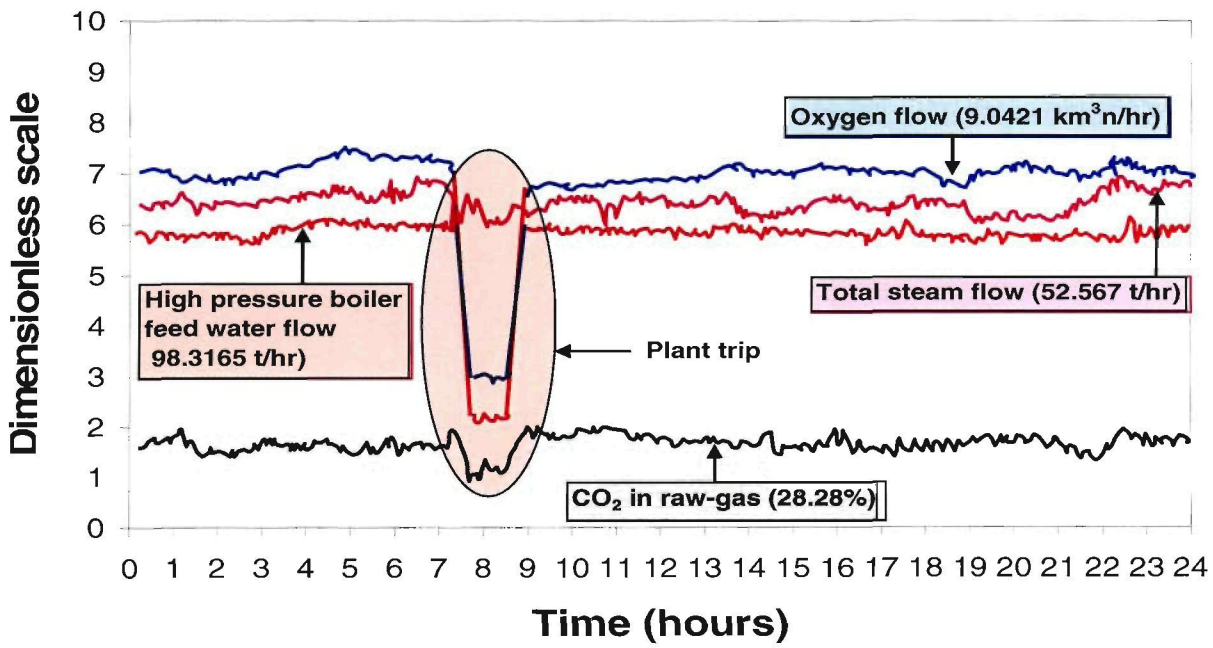

FIGURE 2.1: 24-HOURLY TREND FLOW RATE DATA FOR STEAM, OXYGEN, HIGH PRESSURE BOILER FEED WATER AND CO_2 FOR THE GG41 GASIFIER BEFORE DECOMMISSIONING

From Figure 2.1 it can be seen that the gasifier was running steadily for at least 15 hours at medium load, before being taken off-line. The oxygen flow, total steam flow, high pressure boiler feed water flow and CO_2 in raw gas flows were: 9.0 km^3n/h, 52.6 t/h, 8.3 t/h and 28.3% respectively before decommissioning.

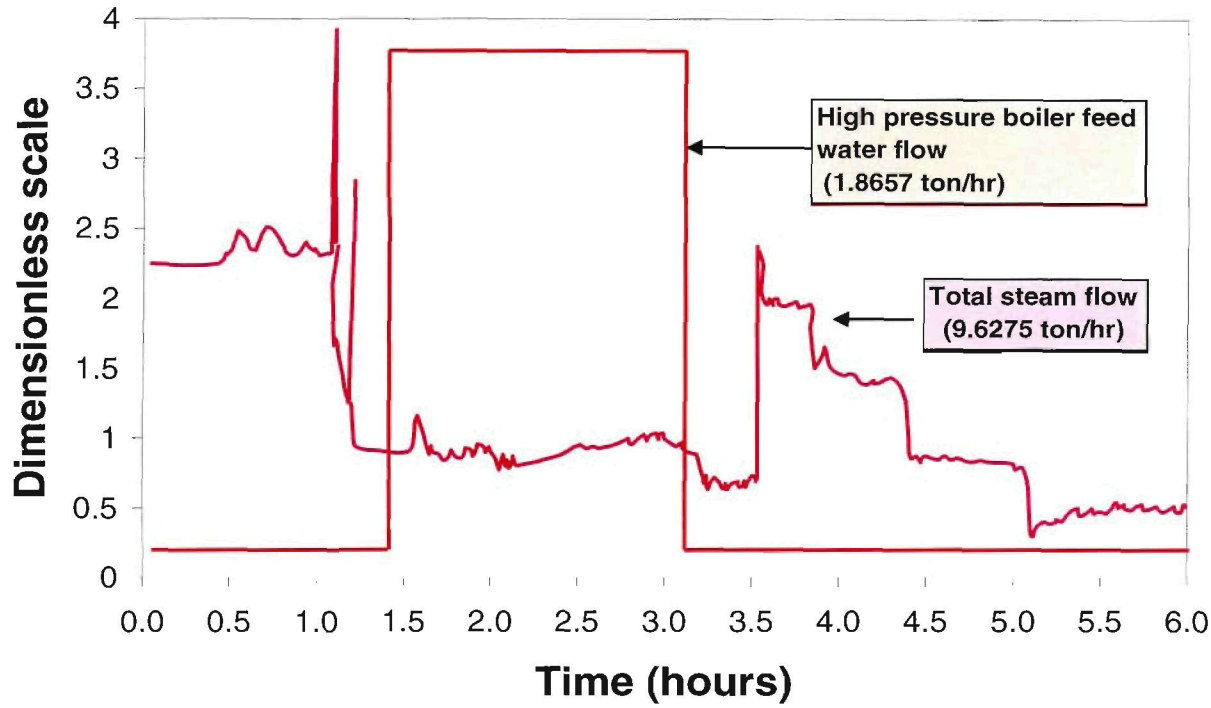

FIGURE 2.2: GG41 GASIFIER TREND DATA REFLECTING CONDITIONS USED IN THE DE-COMMISSIONING PROCESS ONCE THE OXYGEN SUPPLY WAS CUT

The trend data visible from Figure 2.2 shows that the GG41 gasifier was firstly blown with high pressure steam for a minute or two, then blown with high pressure boiler feed water for about 1½ hours, followed by further steam cooling.

After this the gasifier was drained and start-up air was blown into the depressurized gasifier for about 16 hours to further effect cooling, before sampling could commence. Figure 2.3 shows a sample increment being turned-out of the GG41 gasifier.

Figure 2.4 shows the sample increment size ($3m^3$) taken for each of the 32 samples; each of the 32 x $3m^3$ sample increments were sub-sampled as for truck-sampling into 200-litre capacity steel drums, as can be seen in Figure 2.5.

FIGURE 2.3: PHOTOGRAPH SHOWING A SAMPLE INCREMENT BEING TURNED-OUT OF THE GG41 GASIFIER

FIGURE 2.4: PHOTOGRAPH SHOWING THE FRONT-END LOADER $3m^3$ SHOVEL CONTAINING THE GG41 GASIFIER SAMPLE INCREMENT SIZE

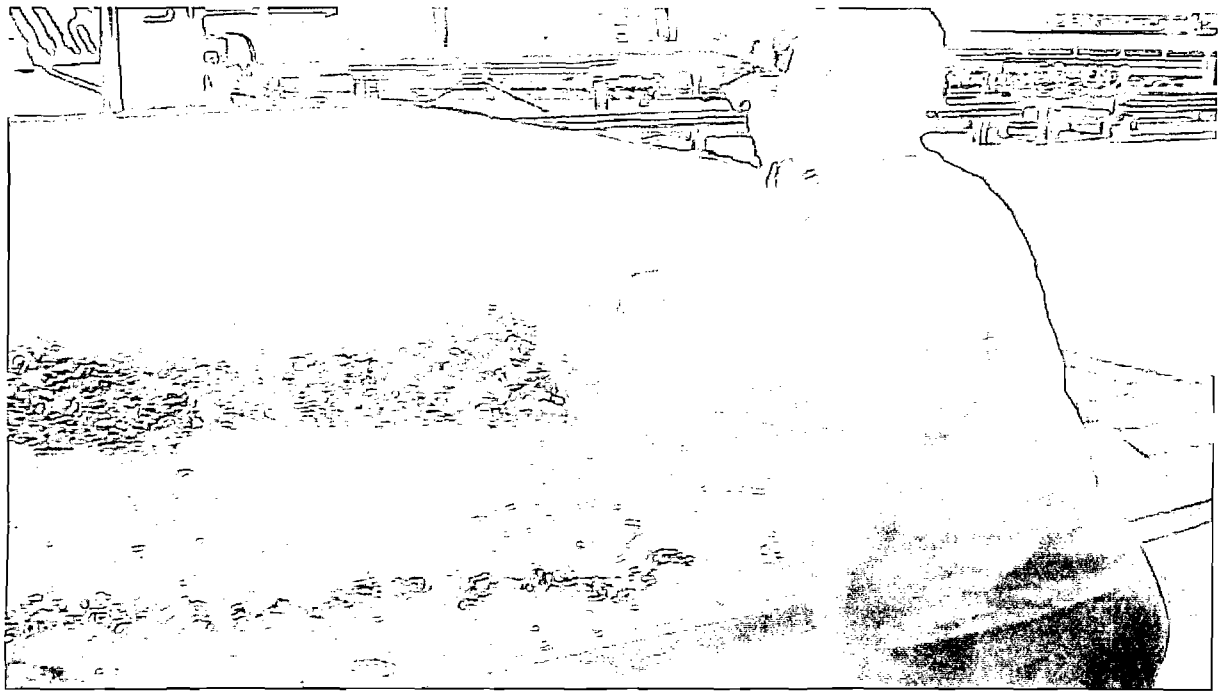

FIGURE 2.5: PHOTOGRPH SHOWING THE SUB-SAMPLING PROCEDURE OF THE GG41 GASIFIER SAMPLE INCREMENT

2.1 Process conditions at the time of quenching for the GG41 gasifier and the Indian pilot scale gasifier.

The process conditions at the time of quenching of the GG41 gasifier and the Indian pilot scale gasifier [Krishnudu, *et. al.*, 1989a] are given in Table 2.2. From Table 2.2 it can be seen that the: (1) coal : oxygen ratio, (2) coal : steam ratio; and (3) steam : oxygen ratio are reasonably comparable being: (1) 5.54 and 5.48; (2) 0.95 and 0.90; and (3) 5.8 and 6.1 for the GG41 gasifier and Indian pilot plant respectively.

Not surprisingly, similarity can also be observed in the gas compositions for the two gasifier scenarios, given in volume percent. The operating pressures differed by about 9 bar, and could slightly affect the gas composition and reaction kinetics. However, it can be concluded that it would be reasonable to assume that the data from both reactors are at least comparable, since there are no order of magnitude differences observed between the data. This comparative approach will therefore be further utilised in the context of this study.

TABLE 2.2: PROCESS CONDITIONS AT THE TIME OF QUENCHING FOR THE INDIAN PILOT PLANT AND THE COMMERCIAL-SCALE GG41 MK IV GASIFIER

PROCESS VARIABLE	INDIAN PILOT PLANT (GODVARI KHANI-RAMAGUNDAM COAL)	SASOL-LURGI GG41 (SECUNDA SCS WEST COAL BLEND)
Coal feed rate (kg/h)	850	50 000
Steam flow (kg/h)	948	52 500
Oxygen flow (M^3_n/h)	155	9 200
Blast temperature (°C)	310	344
Operating pressure (MPa)	2	2.85
Crude gas flow ((M^3_n/h)	1020	95 800
Gas outlet temperature (°C)	350	550
Gas composition (vol %)		
CO_2	33	28.3
CO	17.8	23
H_2	38	39.7
CH_4	9.8	8.8
O_2	0.6	0
N_2 (by difference)	0.8	0.2
Moisture in coal (wt %)	2.4	3.6
Volatile matter in coal (wt %)	24.9	21.8
Ash content in coal (wt %)	33.6	27.5
Fixed carbon in coal (wt %)	39.1	47.1

The feed coal proximate analysis shows that the Indian coal contained 5% more ash, 3% more volatile matter, 1% less moisture and hence 8% less fixed carbon when compared to the GG41 SCS West Secunda blend coal type on an as-received basis. Although there are differences in the coal proximate analysis characteristics for the two scenarios, it would be reasonable to assume that for the sake of comparison the ash content and moisture content be factored out when comparing fixed carbon and volatile matter behaviour.

2.2 Gasifier height factor used to compare GG41 gasifier results with the Indian pilot plant data

Not disclosed due to IP confidentiality.

From the two fixed-bed gasification case studies discussed in the literature review (Section 6, Chapter 1), it follows that the following coal-property related comparisons with the GG41 gasifier turn-out data from this new work can be made. This is shown in Table 2.4.

The reason why some coal-property related results can unfortunately not be compared with the GG41 gasifier turn-out data (Table 2.4) is due to the fact that either no information was provided or a complete set of data for comparative purposes was not available. Furthermore, new characterisation techniques, i.e char morphology, were unknown in the late 1980's and not comparable, as in the case of the different particle size ranges tested.

Glover's pioneering gasifier dissection work [Glover, 1988,1991] essentially showed detailed evidence of the complex localised behaviour occurring within the Sasol-Lurgi FBDB gasifier, i.e. variation in the radial position. Two gasifier turn-out sampling campaigns were conducted and the results would be useful for comparison with this present study. Unfortunately, the analyses were conducted on a particle size basis; results were graphically expressed in terms of a logarithmic dimensionless scale above the ash-grate versus a relative logarithmic representation of the property being studied, with no explanation being given of how the data was normalised. Therefore, only a limited number of comparisons with the work by Glover [1988,1991] can be made.

TABLE 2.4: PROPERTIES THAT WILL BE COMPARED TO THE GG41 GASIFIER DATA

Property	GG41	Indian pilot plant [Krishnudu, *et. al*, 1989a]	[Glover, 1988, 1991]
Bulk density	yes	yes	no
True density	yes	yes	no
Particle size	yes	no	no
Thermal fragmentation	yes	no	no
Mechanical fragmentation	yes	no	no
Caking propensity	yes	no	no
Ergun Index	yes	yes	no
Volatile matter	yes	yes	no
Fixed carbon	yes	yes	no
Ash	yes	yes	no
Ash fusion temperature	yes	no	no
Fischer tar	yes	no	no
Carbon conversion	yes	yes	yes
Ultimate analysis	yes	no	no
CO_2 reactivity	yes	no	no
Maceral Group	yes	no	no
Char morphology	yes	no	no
Temperature profile	yes	yes	yes

No data to compare
Incomplete set of data or illegible
Not comparable
New characterisation parameter

The properties given in Table 2.4 need to be discussed in more detail in order to provide the reader with an understanding of the necessary characterisation techniques and analytical methods utilised in this study.

3 COAL AND ASH CHARACTERISATION TECHNIQUES CONDUCTED AND UTILISED IN THIS STUDY

Figure 2.6 shows photographic images of the 32 samples taken prior to being crushed for analysis. Some insight, on the macroscopic scale, can be gathered about the particle size distribution effects that occur within the GG41 gasifier; colour changes are also evident.

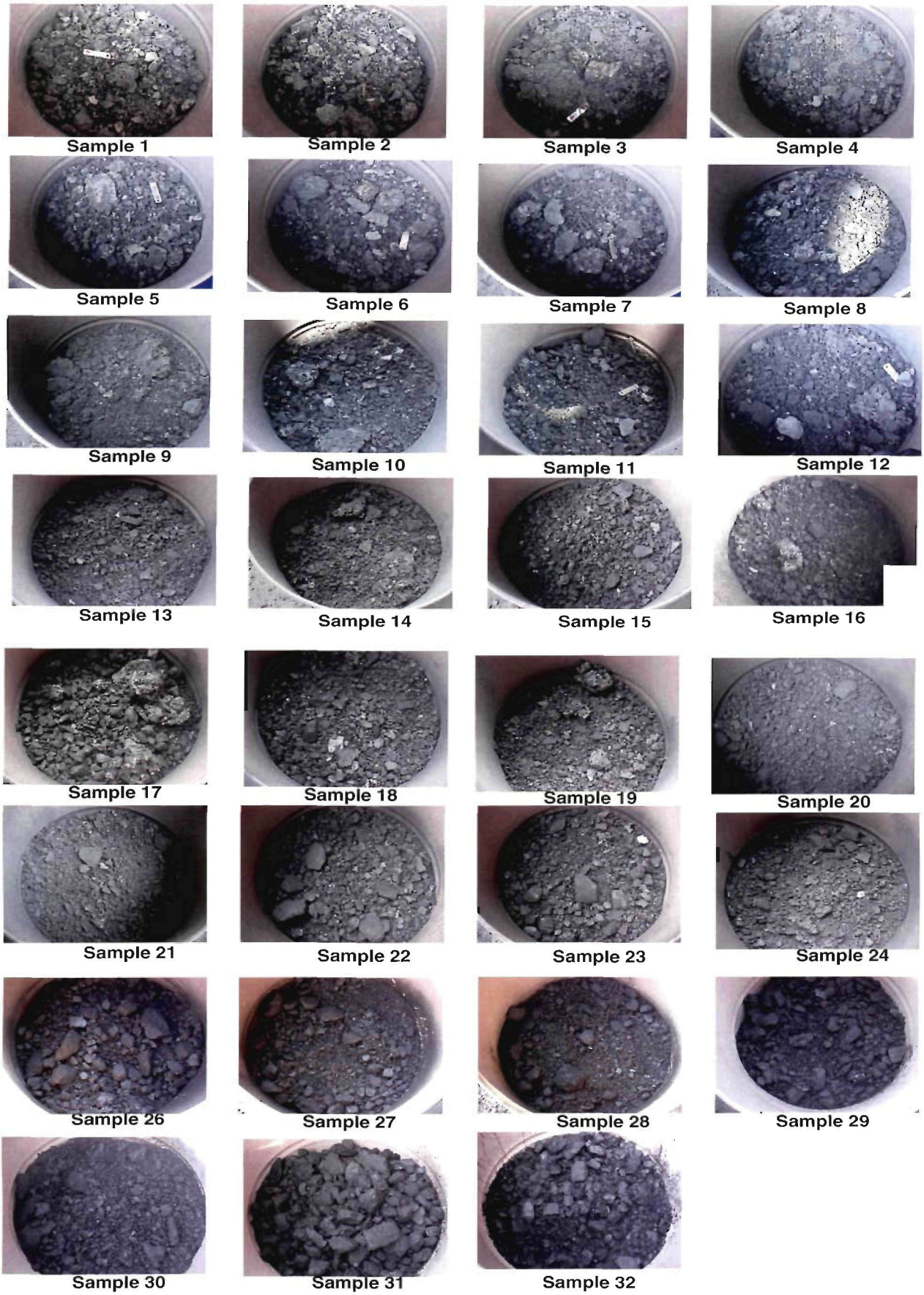

FIGURE 2.6: PHOTOGRAPHIC IMAGES SHOWING A MACROSCOPIC VIEW OF THE GG41 GASIFIER TURN-OUT SAMPLES (1 TO 32)

Each of the 32 samples was thoroughly homogenised after measuring the bulk density, riffled and split at the Coal and Mineral Technologies Laboratories (CMT) into equal quarters. Two of the representative quarters, in each case, were combined and stage-crushed to below 1mm for analytical purposes; the other two quarters were combined for particle size determination. The analytical methods used in the sample characterisation and the additional sample preparation required, will be discussed in the following section.

Since the objective of this study was not to develop analytical characterisation methodologies for the GG41 gasifier turn-out samples, but rather to use the "standard" or "unique-to-Sasol" analytical techniques, no detailed preamble will be provided. However, the reader is referred to Section 4 in Chapter 1 for a detailed review of the coal properties which impact on gasification performance, with specific emphasis on why the analysis is required, as well as some guidelines relating to the interpretation of results. From a study structure perspective, the characterisation methodologies used will be discussed in three general categories, based on the chemical, physical and petrographical properties which impact on gasification performance.

3.1 Chemical properties

Chemical properties of coal, which impact on gasification performance relate to those processes which do effect a change in chemical constitution; these in turn may lead to changes in physical properties such as the particle size distribution and surface area of the coal [Morgan, 1991].

3.1.1 Proximate analysis

The proximate analysis uses standard methods to measure the percentage of moisture (SABS 924, ISO 589), ash content (ISO 1171) and volatile matter (ISO 562). The difference between these three percentages and the mass of the original sample (100%), is referred to as the fixed carbon.

3.1.2 Fischer tar analysis

The Fischer Assay is classically measured according to SABS 1073. Another method has been developed at Sasol Technology R&D, by which the tar-producing propensity of coal can be assessed from a single trace of a TGA simulation of the proximate

analysis of coal. The in-house TGA method was used for the characterisation of the tar content of the GG41 gasifier turn-out samples [Slaghuis, 1993b].

3.1.3 Ash fusion temperature

The ash fusion temperature provides an indication as to the extent of ash agglomeration and clinkering likely to occur within the gasifier. Ash clinkering inside the gasifier can cause channel-burning, pressure drop problems and unstable gasifier operation [Keyser, *et. al.*, 2005].

The standard method, ISO 540, was used to demonstrate the fusion properties of laboratory prepared coal ash. The ash was heated to 1600°C in an oxidizing atmosphere. The results of an AFT analysis consist of four temperatures, namely: (1) initial deformation temperature (DT), (2) softening temperature (ST), (3) hemispherical temperature (HT) and (4) flow temperature (FT).

3.1.4 Ultimate analysis

Carbon, hydrogen and nitrogen are determined using the ASTM D5373 procedure, total sulphur using ASTM D4239 and the oxygen content is calculated by the difference.

3.1.5 Coal reactivity

There is no internationally accepted standard method for the determination of the reactivity of a given coal char. The method employed by the Syngas and Coal Technologies R+D Group at Sasol, measures the rate of mass loss, using a thermogravimetric analyser (TGA).

A 1g representative sample of coal was crushed to 150-300µm particle size for reactivity analysis and a 1g sample to -150µm particle size for proximate analysis. The proximate analysis was conducted and the fixed carbon content obtained was used to calculate the amount of coal needed to produce 5mg of fixed carbon (organic). The calculated mass of coal was loaded into the sample pan of the TGA and heated in an inert (nitrogen) atmosphere to 1200°C at a heating rate of 50°C/min.

The resulting char was allowed to cool to 1000°C and when the temperature had stabilised, the inert gas was replaced with carbon dioxide. The temperature was

maintained until there was complete carbon burn-off. Reactivity was then calculated at 50% carbon burn-off. The reactivities of coals from the various sources used by Sasol in Secunda vary between 2-5 h^{-1}.

3.2 Physical properties

Physical properties of coal which impact on gasification performance relate to those processes which result in a change in particle size and surface area [Morgan, 1991].

3.2.1 Bulk density

Each of the 32 coarse GG41 gasifier turn-out samples contained in the 200-litre drums were mass measured and the occupied volume was calculated when un-compacted. The density was calculated in each case, using the mass-to-volume ratio, before any splitting of the samples commenced.

3.2.2 True density

The true density of an approximately 10g sample was determined for the GG41 gasifier turn-out samples (crushed to below 1mm), using a Micromeretics Accupyc instrument. The crushed samples were dried overnight in an oven at 105°C and then cooled in a desiccator prior to being analysed in the instrument. Pressurised helium gas was used to determine the true density of the sample being analysed. The analysis was conducted in triplicate for all samples, after the instrument had been calibrated using standards of known real (true) density.

3.2.3 Particle size distribution

Each of the 32 samples' (composited) bulk fractions were wet-screened at the following screen aperture sizes: 53mm, 25mm, 12.5mm, 9.5mm, 6.3mm, 5mm, 4mm, 3.35mm, 2mm and 1mm. Eleven particle size screen fractions were obtained in total for each GG41 gasifier turn-out sample, which included the naturally fine -1mm fraction. The ASTM D4749 procedure was followed and the fractional and cumulative size distributions were calculated as needed.

3.2.4 Ergun Index

The Ergun equation was discussed in detail in Section 4.2 in Chapter 1. A standard

spreadsheet was used to calculate the index using the fractional particle size distribution masses, on the basis of the eleven size fractions discussed above.

3.2.5 Thermal fragmentation

The thermal fragmentation of coal was measured by placing a sample having a specific predetermined size distribution into a pre-heated muffle furnace at 100°C under atmospheric pressure. The coal was then heated to 700°C, and after the sample had been cooled under nitrogen and screened again, the change in size distribution was calculated. The amount of thermal fragmentation of coal was then given as a percentage decrease in Sauter diameter. The smaller the percentage decrease, the better the thermal stability.

3.2.6 Mechanical fragmentation

The mechanical stability was determined by means of a Micum tumble test. The sample was placed in a steel drum and turned at a speed of 60 revolutions per minute for 5 minutes. The sample was then sieved through the specified standard particle size fractions and the results of the tumble test were calculated using the Ergun Index, which is also known as the Sauter Mean Diameter.

3.2.7 Caking propensity

The caking propensity of the coal was determined by pyrolising a coal sample having a specific predetermined size distribution in an inert atmosphere at the typical gasifier pressure (28 bar). The sample was screened afterwards and the increase (if any) in particle size determined. This test is unique and was developed in-house by Sasol for characterising coal samples subjected to pressure and temperature conditions similar to those that prevail within the gasifier.

3.3 Petrographical properties

Petrography allows for the optical consideration of the changes occurring in the carbon particles and associated minerals through the gasifier, which can be related to temperature and morphological changes [Wagner and Joubert, 2005a].

3.3.1 Petrographic analysis

Thirty-two coal samples, crushed to -1mm, were prepared as per routine preparation for petrography following ISO standards 7404-2. A maceral group analysis as per ISO 7404-3 was conducted on sample 32, which was considered as the GG41 gasifier feed coal.

The samples were obtained and prepared to minimize contamination and 500 sampling points were determined for each sample. The particle falling directly under the cross hair was categorized, applying a 50x50 micron field of view. Large particles were classified several times, if meeting the requirements above. All particles -30 micron were not counted, due to reduced ability to accurately observe these small particles. As more than 10 categories were required and the point counter only measured up to 10 variables at a time, certain measurements were recorded separately on paper, ensuring that 500 particles were counted per block.

Reflectance analysis was conducted before, or very shortly after, the particle type analysis in order to limit the potential impact of the oil on reflectance readings. Initially every second sample was analyzed and additional samples were analyzed where significant changes in trends were determined.

3.3.2 Char morphology analysis

For all of the GG41 gasifier turn-out samples, other than the feed sample (sample 32) a char particle type analysis system was established, and the results were presented on a volume percentage basis. The particle type analysis was created specifically for these samples, with the principles based on routine microlithotype analysis (ISO standard 7404-5) and the char morphology classification schemes (Baily, *et. al.*, 1990). The assumptions and restrictions applied are listed below; each sample that was analysed has been photographed for reference purposes.

Whilst there are repeatable and reproducible standards for the routine standardised petrographic analyses, the degree of repeatability and reproducibility in the GG41 gasifier turn-out samples may be higher, due to the high proportion of fragments (particles -30 micron), and the limited number of carbon particles in the samples, occurring lower down in the gasifier. The high variability mentioned could also be due to the fact that 5 or 6 different coal sources are used as feedstock, and with petrography individual coal particles are examined.

The categories used in the char particle type analysis included: coal, devolatilised coal, porous char, intermediate char, dense char, carbominerite char, consumed char, stone / rock / ash (normal) and stone / rock / ash (heat affected). An explanation of these categories can be found in Section 4.8 in Chapter 1 of this thesis.

3.3.3 Temperature estimation using optical reflectance

The objective of analysing the turn-out samples in detail, was to work towards understanding the behaviour of the feed coal inside the gasifier, by considering the carbon conversion process and clarifying temperature profiles, applying petrographic techniques. This part of the study concerns the use of vitrinite reflectance for temperature estimation. The specific objectives were to:

(1) Prepare a range of samples from the gasifier feed (sample 32) using a temperature treatment in a standard TGA,

(2) Determine the reflectance profiles for the controlled heat-treated samples, applying standard petrographic techniques,

(3) Prepare a correlation chart of reflectance results against sample temperature, to be used as a reference for the GG41 gasifier turn-out samples,

(4) Determine the mean and maximum reflectance readings for the gasifier turn-out samples,

(5) Use the reflectance and temperature correlation to estimate the temperatures experienced by the turn-out sample,

(6) Correlate these petrographic findings to particle type analysis (char morphology).

3.3.3.1 Preparation of reflectance / temperature calibration curve

Sample 32 (feed coal at the top of the GG41 gasifier) was crushed to -1mm; eight 150µl platinum sample pans were filled with a representative portion of the -1mm prepared sample and loaded into a calibrated Mettler TGA. Each sample was initially treated in a nitrogen atmosphere at 30°C for 3 minutes to obtain equilibrium, then ramped at 50°C/min to a specific temperature. Once the designated temperature was

reached, the sample was then kept at the specific temperature in a nitrogen atmosphere for 10 minutes and subsequently cooled to room temperature. This procedure was repeated on the samples for temperatures ranging between 350°C and 1200°C, obtaining eight different samples at different temperatures. The individual samples were then mounted in resin and the blocks polished as for petrographic analysis (ISO 7404-2).

Vitrinite reflectance analysis (mean RoV %) was performed on the individual samples as per petrographic standard (ISO 7404-5) as far as possible. The results were plotted against the treatment temperatures to serve as a calibration curve.

3.3.3.2 Vitrinite reflectance on the GG41 gasifier turn-out samples

The reflectance results obtained from the GG41 gasifier turn-out samples were compared to the temperature profile calibration curve discussed in 3.3.3.1, using the formula obtained from the linear regression (calibration curve). The estimated temperatures found for the 32 x GG41 gasifier turn-out samples could then be compared to and contrasted with the Indian pilot plant data [Krishnudu, *et. al.,* 1989a,b] and with the work of Glover [1988, 1991], as well as with other petrographic determinations.

The 32 coal samples, crushed to -1mm, were prepared as per routine preparation for petrography following ISO standards (7404-2). The same coal blocks were used for both petrographic analyses, i.e. temperature estimation using optical reflectance, as well as char morphology analysis, discussed earlier in Section 3.3.2 of this chapter.

Vitrinite reflectance analyses were performed on a range of the 32 prepared gasifier turn-out samples, applying ISO standards 7404-5. Results were calculated on the following basis: (1) a mean reflectance (average temperature), (2) top 10% mean reflectance readings and (3) maximum reflectance readings (peak temperature). The top 10% reflectance reading is assumed to be an indication of the surface temperature in this case, since heat transfer through 100mm particles (as is the case in the Sasol-Lurgi gasifier) is expected to show large temperature variations across particles of this size.

Difficulties were encountered with the petrographic measurement technique on samples that were located deeper in, and particularly at the bottom of the gasifier, due to the limited amounts of carbon material available for determination of reflectance. In

addition, as a result of the physical alterations of the carbon particles, it was sometimes difficult to accurately recognize particles that had originated from vitrinite. At high temperatures, vitrinite and certain forms of inertinite may appear very similar.

4 FACT-SAGE MODELLING

The Fact-Sage thermodynamic equilibrium programme was used in the present study to identify the speciation and partitioning behaviour of the complexes formed during gasification with respect to the C, H, S, N and O elements present in the coal. The equilibrium elemental distribution profiles will be discussed in conjunction with the GG41 gasifier turn-out samples' measured ultimate analysis profiles. The objective was primarily to provide insight into the thermo-chemistry that occurs in the various gasifier reaction zones, but particularly to identify whether oxygen scavenging occurred during mineral transformation. The modelling approach that will be used here is the same as used by Van Dyk [2006], but the data obtained from the GG41 gasifier turn-out sample 32 (feed sample) will be used as model input.

The Fact-Sage package runs on a PC operating system under Microsoft Windows® and consists of a series of information, database, calculation and manipulation modules that enables one to access and manipulate pure substances and solution databases. Fact-Sage is a 32-bit application, written with a blend of Visual-Basic (45%), Delphi (20%), C++ (10%) and Fortran-90 (25%). Additional information is available at www.factsage.com.

Fact-Sage not only enables calculation and manipulation of phase diagrams, but has been established mainly in the field of complex chemical equilibrium and process simulation. For example, with Fact-Sage it is possible to access both Fact (slag, matte, salt, ceramic and aqueous) and alloy databases, import and export streams and mixtures and also import Chem-Sage data files. Another advantage of Fact-Sage is that it can take carbon-mineral reactions into account and the gas composition and atmosphere can also be varied.

The specific value for Sasol in this study, will be that these thermo-chemistry models can be used to analyze equilibrium conditions for reactions occurring between inorganic and/or organic materials. The database will thus assist in the understanding, as well as the predicting of what can and will happen with specific coal and mineral species within the gasification process.

Fact-Sage 5.3 was used for modelling work in this study. The Fact-Sage solution database contains critically evaluated thermodynamic data for SiO_2-CaO-Al_2O_3-Cu_2O-FeO-MgO-MnO-Na_2O-K_2O-TiO_2-Ti_2O_3-Fe_2O_3-ZrO_2-CrO-Cr_2O_3-NiO-B_2O_3-PbO-ZnO [Bale, *et. al.*, 2002].

The most used module for this study was Equilib, where the Gibbs energy minimization component of Fact-Sage was utilized. The concentrations of chemical species where calculated when specific elements or compounds reacted or partially reacted, in order to reach a state of chemical equilibrium.

CHAPTER 3
RESULTS AND DISCUSSION

1 INTRODUCTION

As stated, the principal aim of this study was to develop a turn-out and "new-to-Sasol" sampling methodology for the entire (GG41) commercial-scale MK IV Sasol-Lurgi fixed-bed dry bottom (FBDB) gasifier, capable of providing detailed axially-derived characterisation profiles of the internal processes occurring i.e. carbon conversion, particle size distribution and petrographic classification, including temperature profile estimation, etc. These internal characterisation profiles are expected to provide good experimental data sets that can be used to validate and advance gasification optimisation using the existing one-dimensional kinetic models at Sasol.

A graphical representation of the GG41 gasifier results obtained in this study (Figures 3.1 to 3.47) will be shown, followed by a general discussion of the results from a chemical, physical and petrographic property profile perspective; a summary will conclude this Chapter. This structure was adopted, due to the complex inter-relationship of the properties studied.

Trend lines are included in the graphs in order to guide the eye. A statistical analysis of the data, with respect to the four distinctive gasification reaction zones identified, i.e. (1) drying, (2) pyrolysis, (3) reduction and (4) combustion (ash-bed) will be incorporated throughout, in the form of a zone average value. These zones are integrated with error bars, showing the confidence intervals at a 95% confidence level. From an interpretation perspective, the reader is encouraged to note that where confidence intervals do not overlap within the zones, the change observed is statistically significant and visa-versa.

Furthermore, from the tabulated summaries (Tables 3.1 to 3.4) it should be noted that the wider the confidence interval, the less accurate the average is estimated to be for that particular zone. This could be due to significant inherent variability occurring within the zone, due to excessive chemical reaction or temperature effects for example; or it could be an indication of actual response, due to gasification characteristics within that particular zone. The estimate of the average as well as the width of the confidence interval will improve, if more experimental data is available for the zone under discussion. Further experiments on similar turn-outs will also assist in

the statistical validation of repeat tests and serve as verification for the results obtained in this base-line study.

The GG41 gasifier internal profile results will be compared to and contrasted with the Indian pilot plant data as published by Krishnudu, *et. al.* [1989a,b]. Factorisation, as previously discussed, of this data was necessary in order to compare the quarter-scale pilot plant findings to the GG41 gasifier findings. Comparison with the work conducted by Glover [1988] will also be made. Detail results relevant to the GG41 gasifier turn-out are given in Appendix A. The factorised Indian pilot plant data and Glover's detail results are given in Appendix B. The thermodynamic modelling results are presented in Appendix C.

According to the standard coal properties, i.e. proximate analysis, ultimate analysis, maceral composition, AFT, coal char CO_2 reactivity, Fischer tar content, thermal fragmentation, mechanical fragmentation, caking propensity and particle size distribution, the GG41 feed coal (sample 32) used in this study was found to be within the variation of the coal properties typically used for gasification in Secunda. The GG41 gasifier detail results given in Appendix A, show the GG41 feed coal (sample 32) property analysis in conjunction with the SCS coal blend range (before the gasification feed bunker), for comparison purposes.

RESULTS

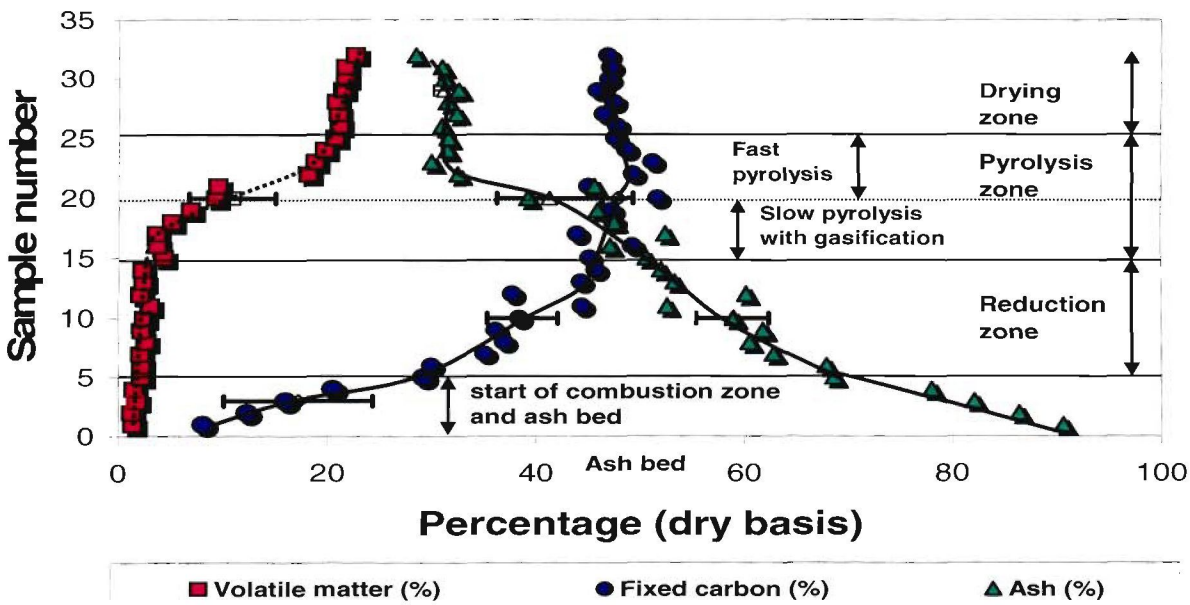

FIGURE 3.1: GRAPH DEPICTING THE PERCENTAGE VOLATILE MATTER, FIXED CARBON AND ASH DISTRIBUTION PROFILES (DRY-BASIS), HIGHLIGHTING THE GG41 GASIFIER REACTION ZONES

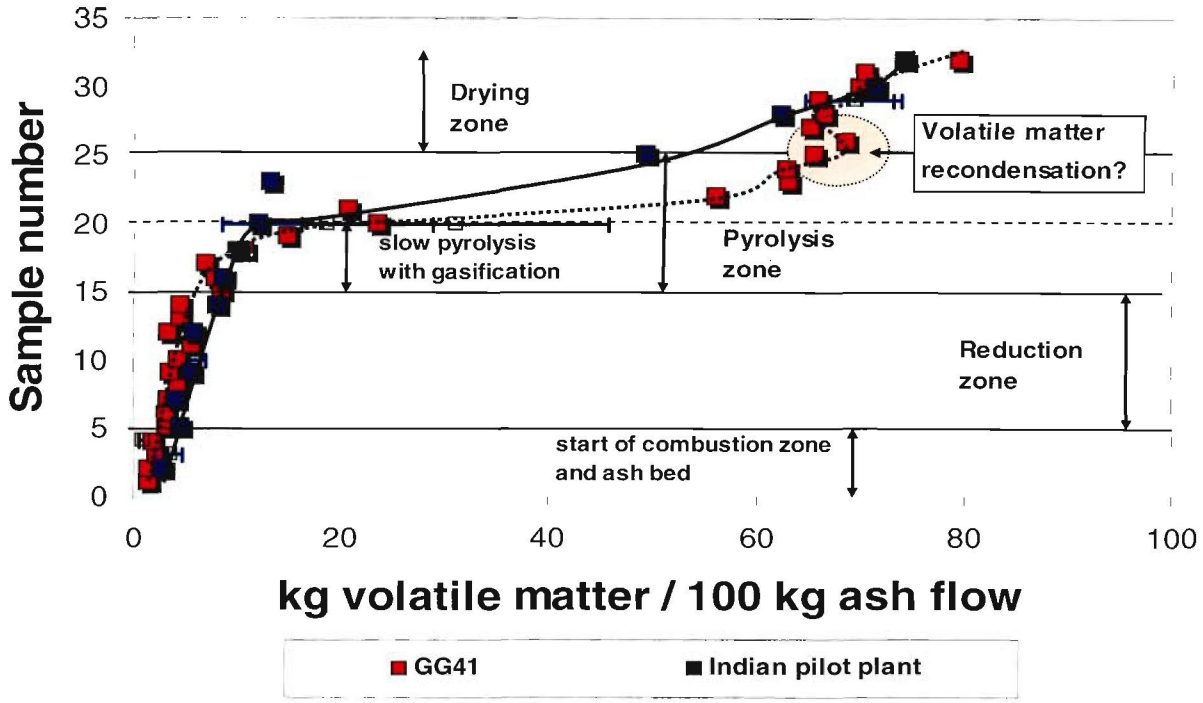

FIGURE 3.2: GRAPH SHOWING THE NORMALISED VOLATILE MATTER DISTRIBUTION AT CONSTANT ASH CONTENT FOR THE GG41 GASIFIER AS WELL AS FOR THE FACTORISED INDIAN PILOT PLANT DATA

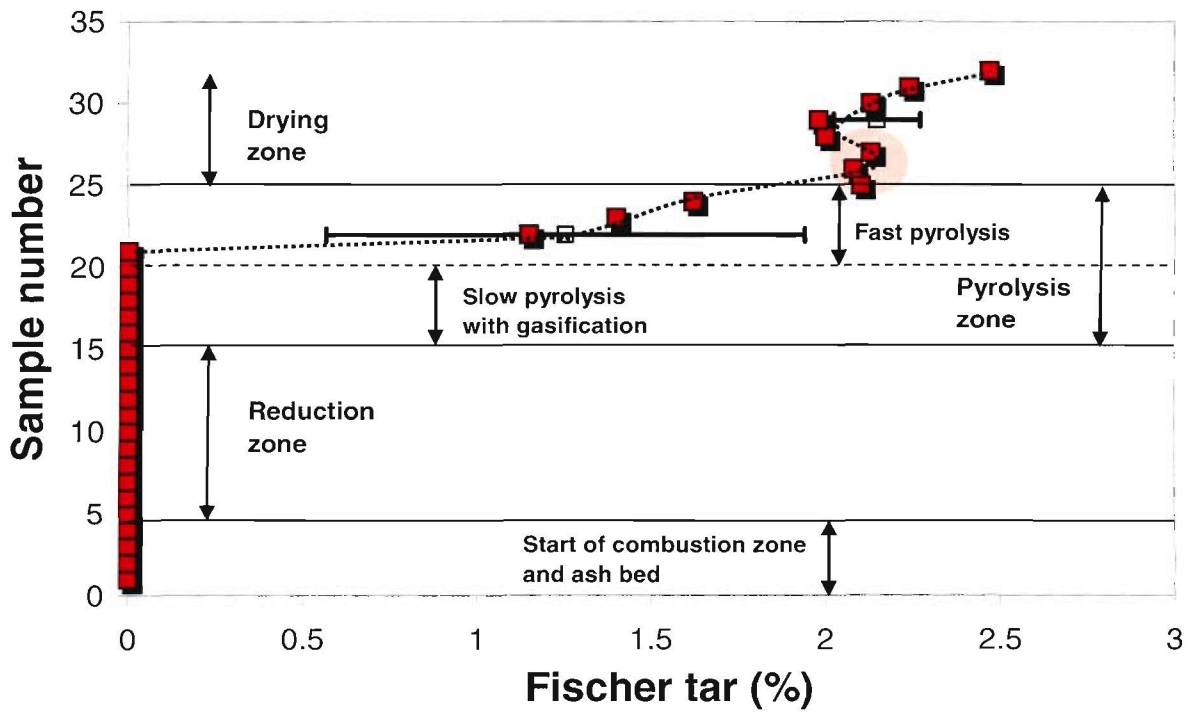

FIGURE 3.3: GRAPH DEPICTING THE RESIDUAL FISCHER TAR DISTRIBUTION PROFILE (DRY BASE) FOR THE GG41 GASIFIER, HIGHLIGHTING THE OCCURRENCE OF VOLATILE MATTER RECONDENSATION

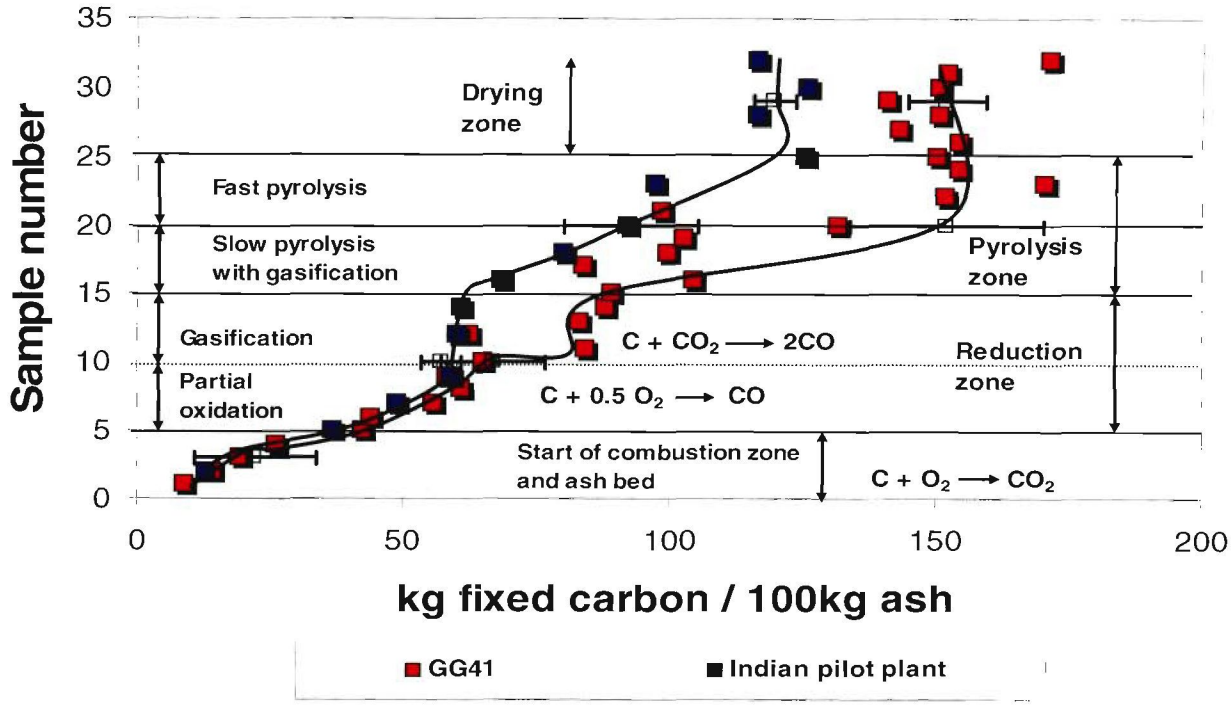

FIGURE 3.4: LINE GRAPH DEPICTING THE NORMALISED FIXED CARBON DISTRIBUTION AT CONSTANT ASH CONTENT FOR THE GG41 GASIFIER AND THE FACTORISED INDIAN PILOT PLANT DATA (DRY BASE)

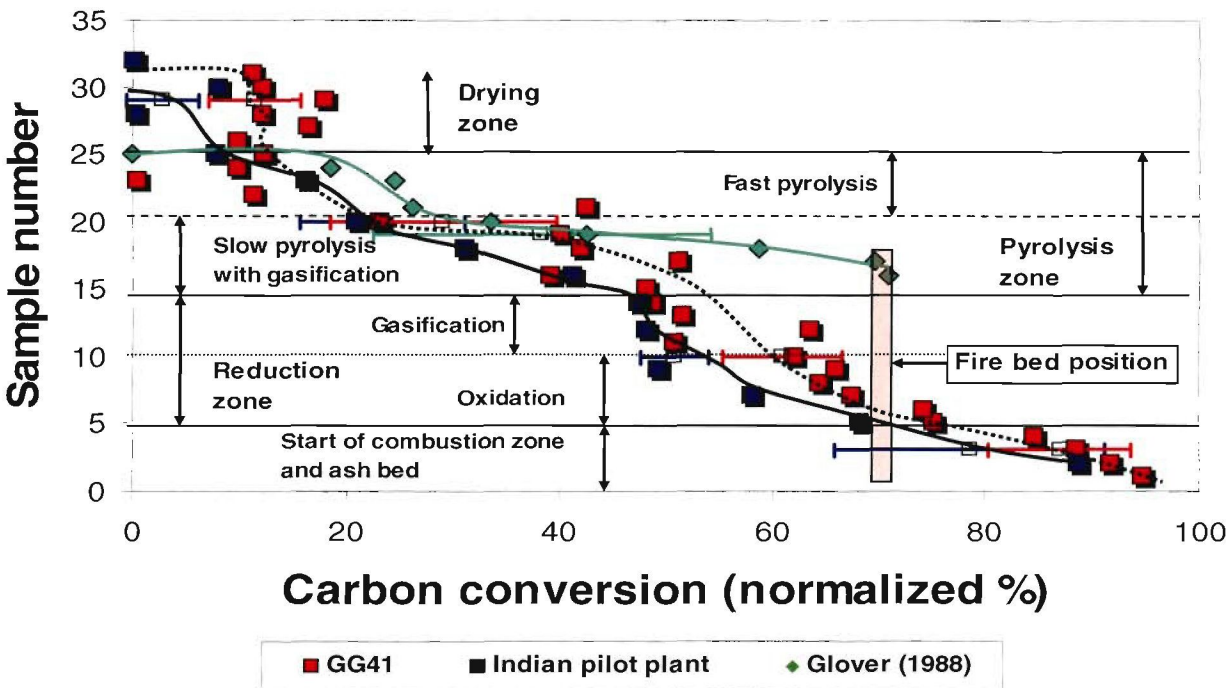

FIGURE 3.5: GRAPH SHOWING THE NORMALISED PERCENTAGE CARBON CONVERSION FOR THE GG41 GASIFIER, FACTORISED INDIAN PILOT PLANT DATA, AND THE #15 SASOLBURG MK III GASIFIER (DRY BASE)

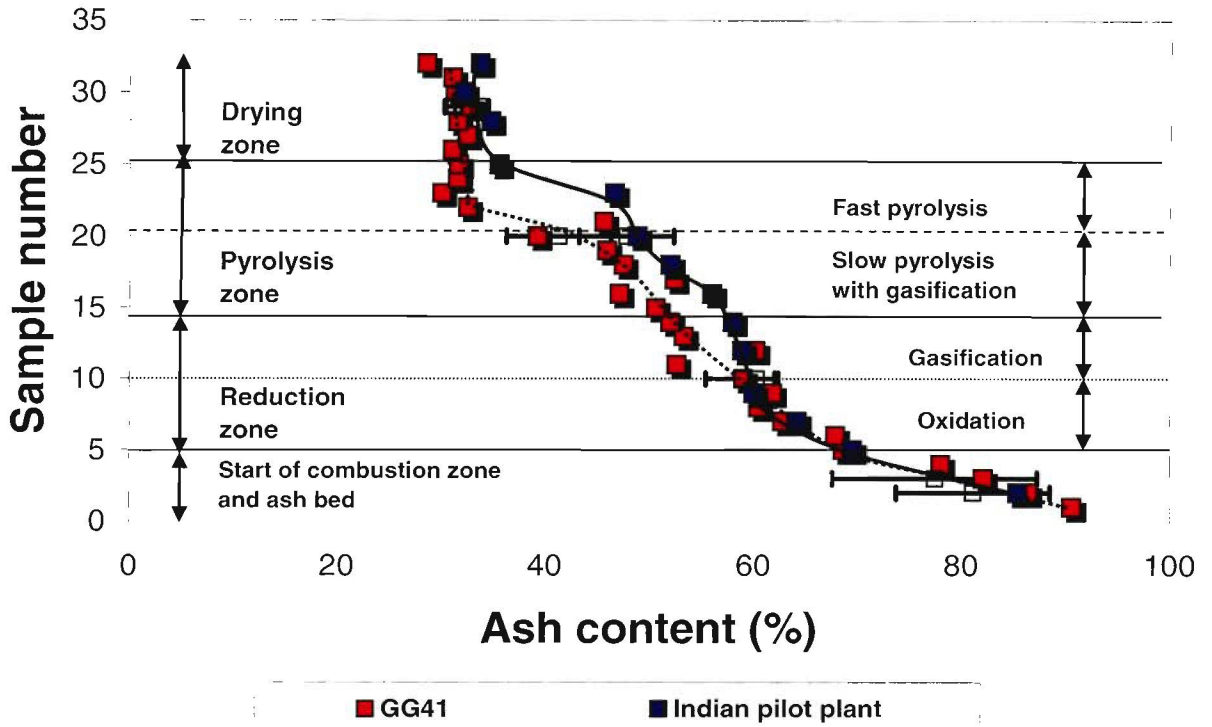

FIGURE 3.6: LINE GRAPH DEPICTING THE ASH PERCENTAGE CONTENT PROFILES FOR THE GG41 GASIFIER AND FACTORISED INDIAN PILOT PLANT DATA (DRY BASE)

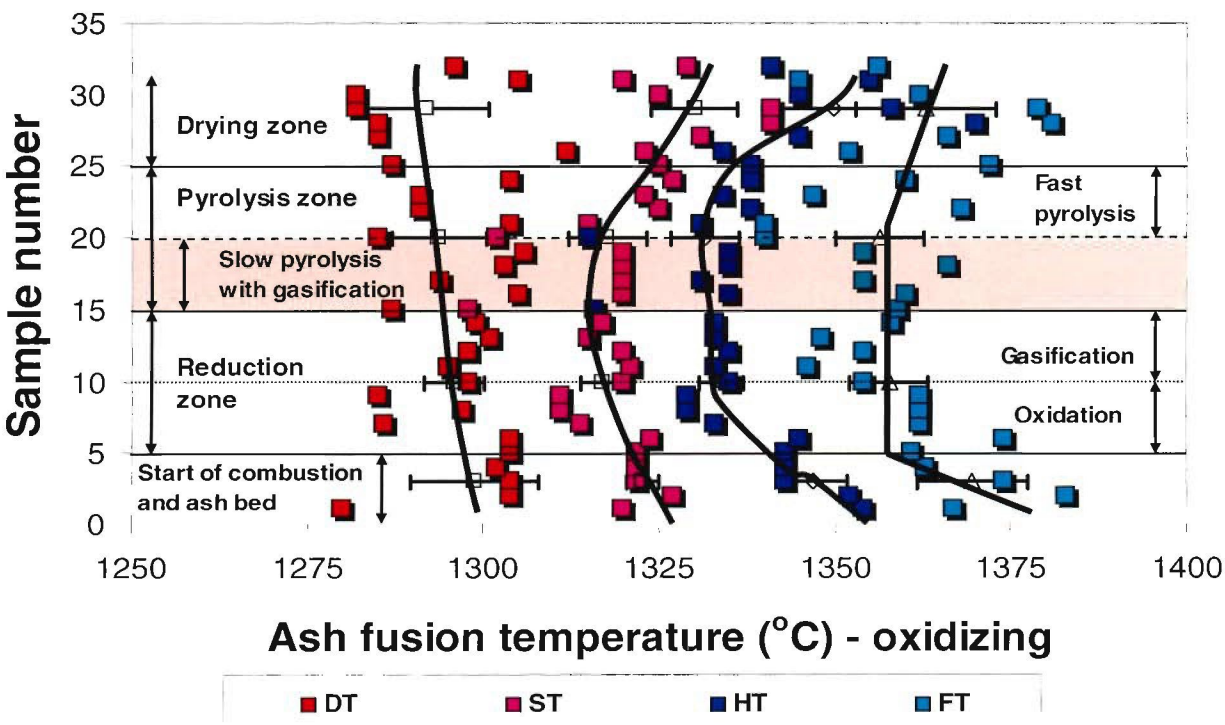

FIGURE 3.7: GRAPH SHOWING THE ASH FUSION TEMPERATURE DISTRIBUTION PROFILES OBTAINED FOR THE GG41 GASIFIER (DRY BASE)

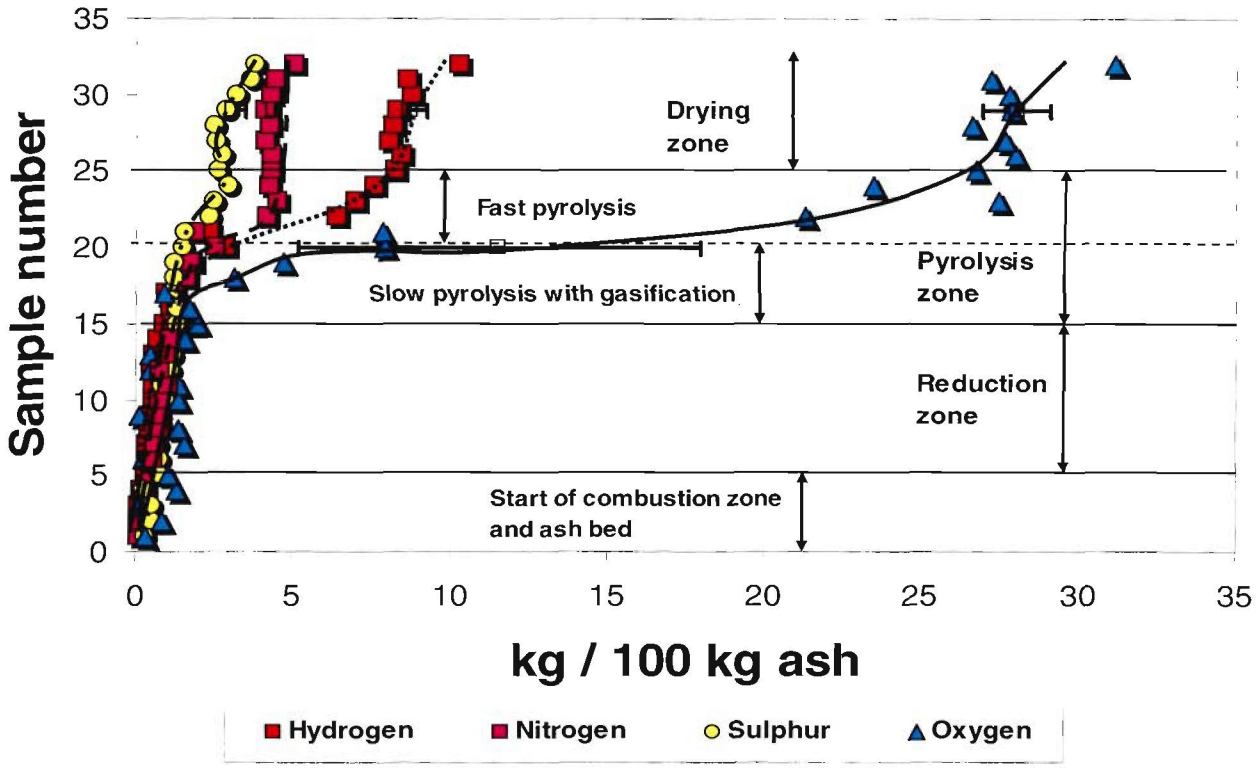

FIGURE 3.8: CHART DEPICTING THE HYDROGEN, NITROGEN, SULPHUR AND OXYGEN DISTRIBUTION PROFILES ON A NOMALISED kg / 100kg ASH BASIS FOR THE GG41 GASIFIER (DRY BASE)

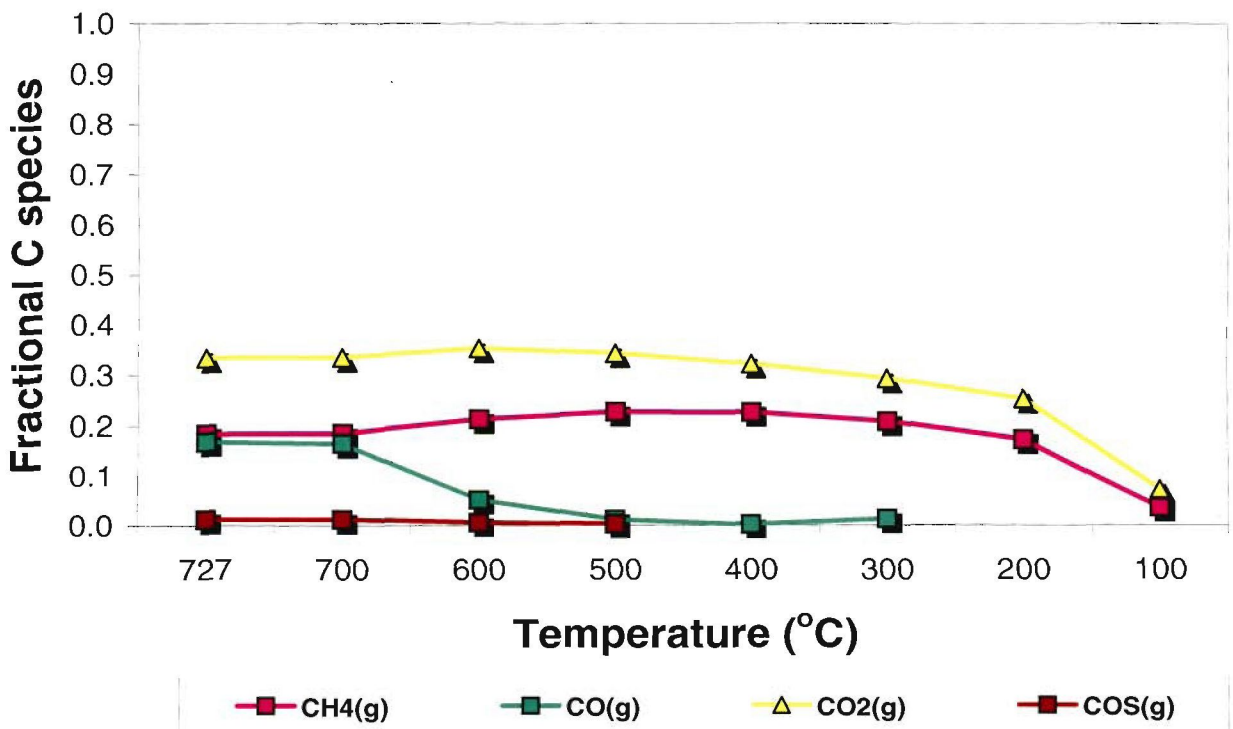

FIGURE 3.9: CHART SHOWING THE EQUILIBRIUM COMPOSITION PROFILE CALCULATED FOR CARBON IN THE DRYING AND PYROLYSIS ZONES

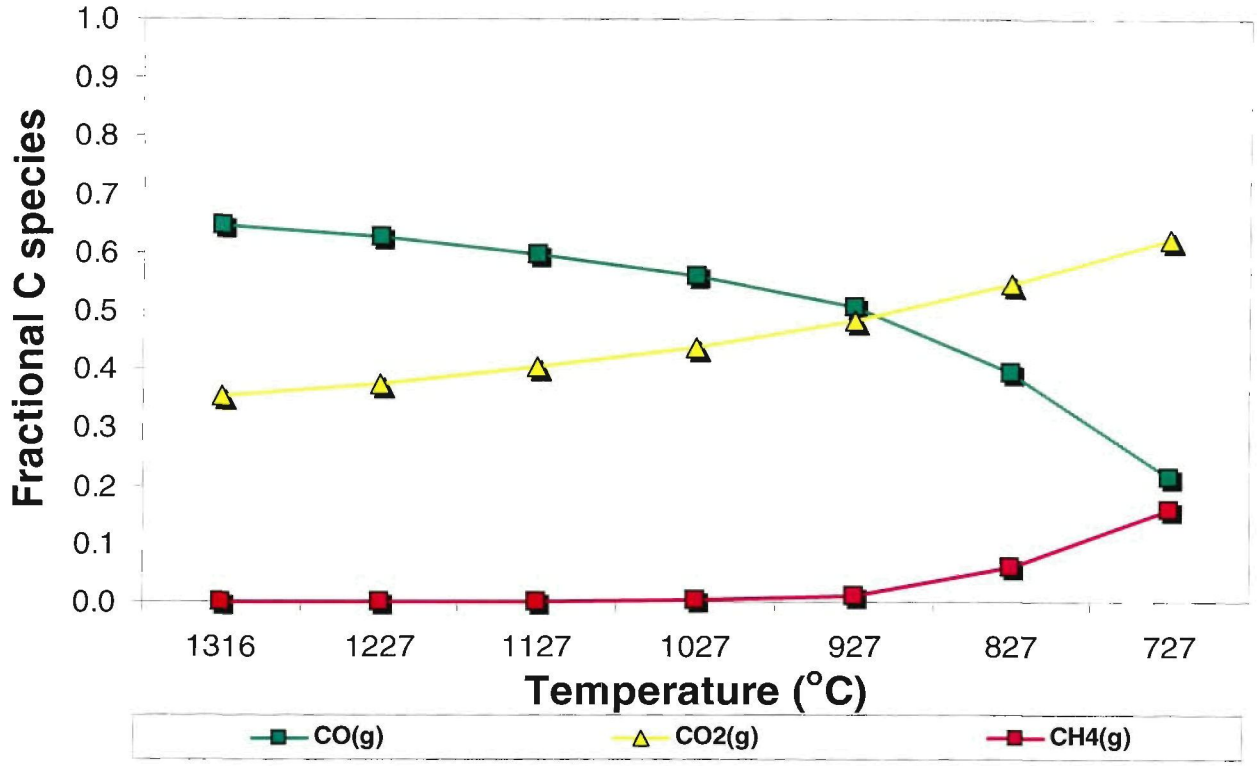

FIGURE 3.10: CHART SHOWING THE EQUILIBRIUM COMPOSITION PROFILE CALCULATED FOR CARBON IN THE REDUCTION ZONE

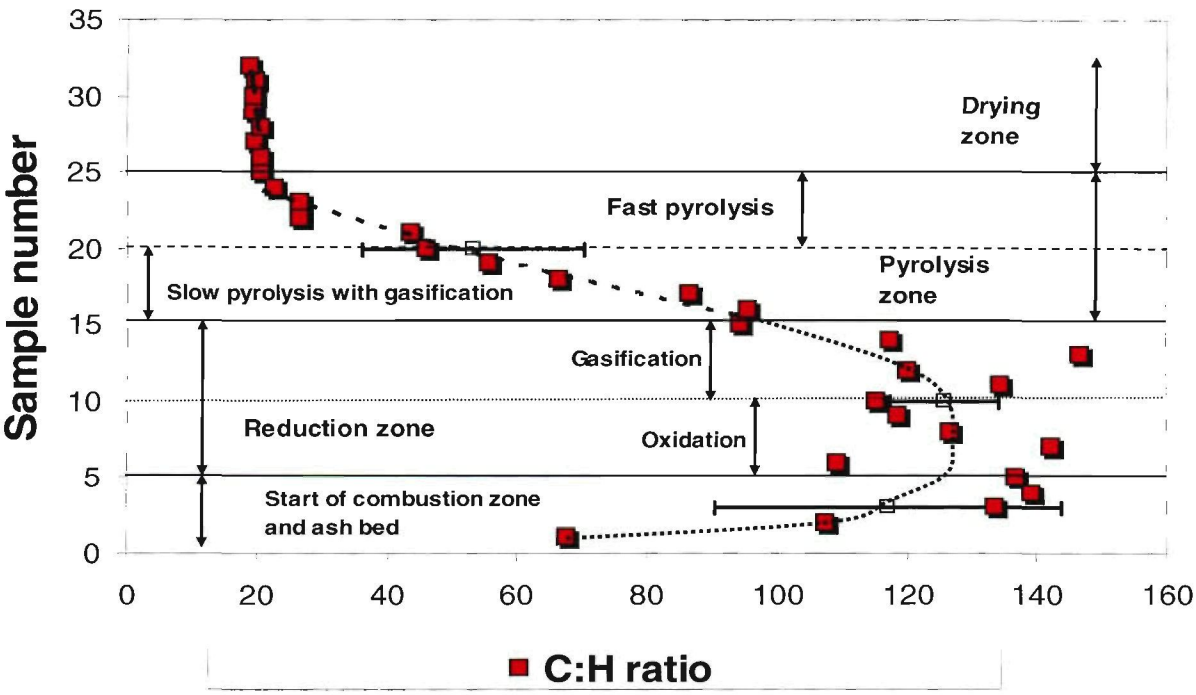

FIGURE 3.11: CHART SHOWING THE CARBON : HYDROGEN RATIO DISTRIBUTION PROFILE FOR THE GG41 GASIFIER (DRY BASE)

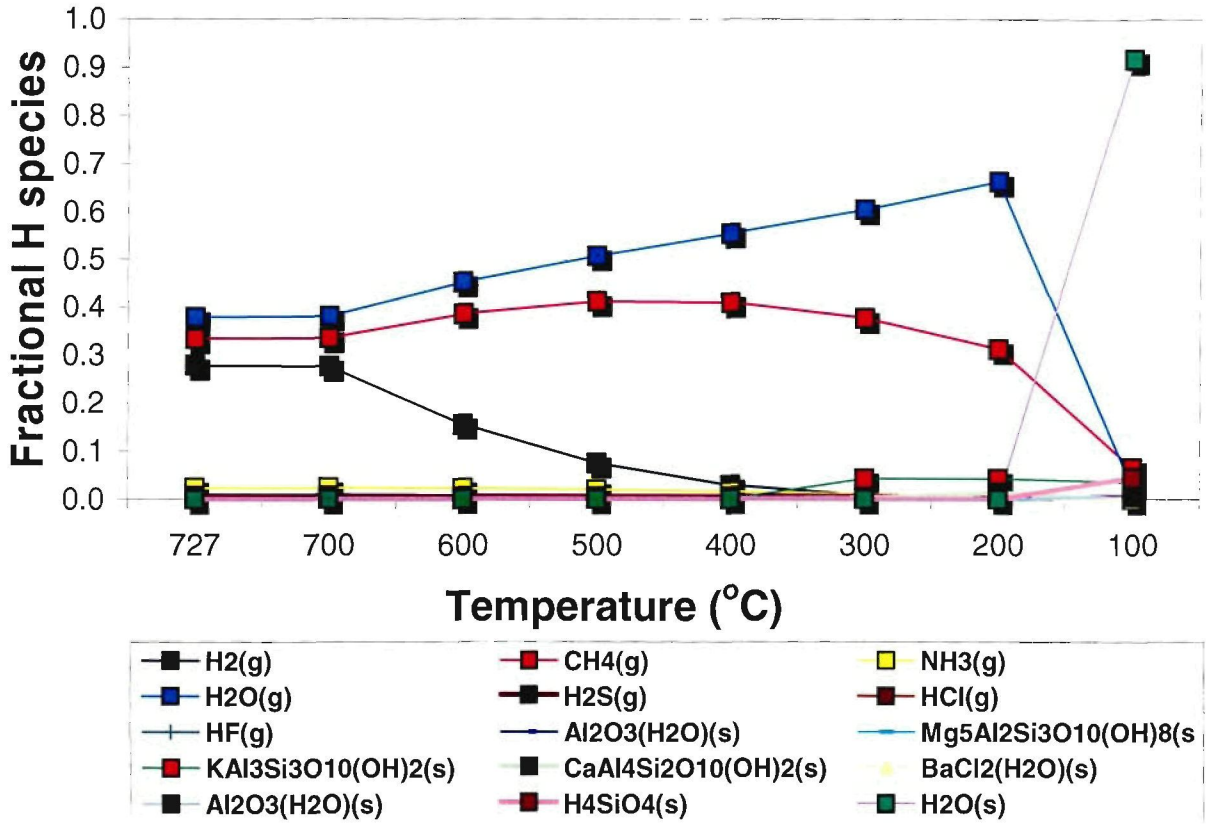

FIGURE 3.12: CHART DEPICTING THE EQUILIBRIUM COMPOSITION PROFILE CALCULATED FOR HYDROGEN IN THE DRYING AND PYROLYSIS ZONES

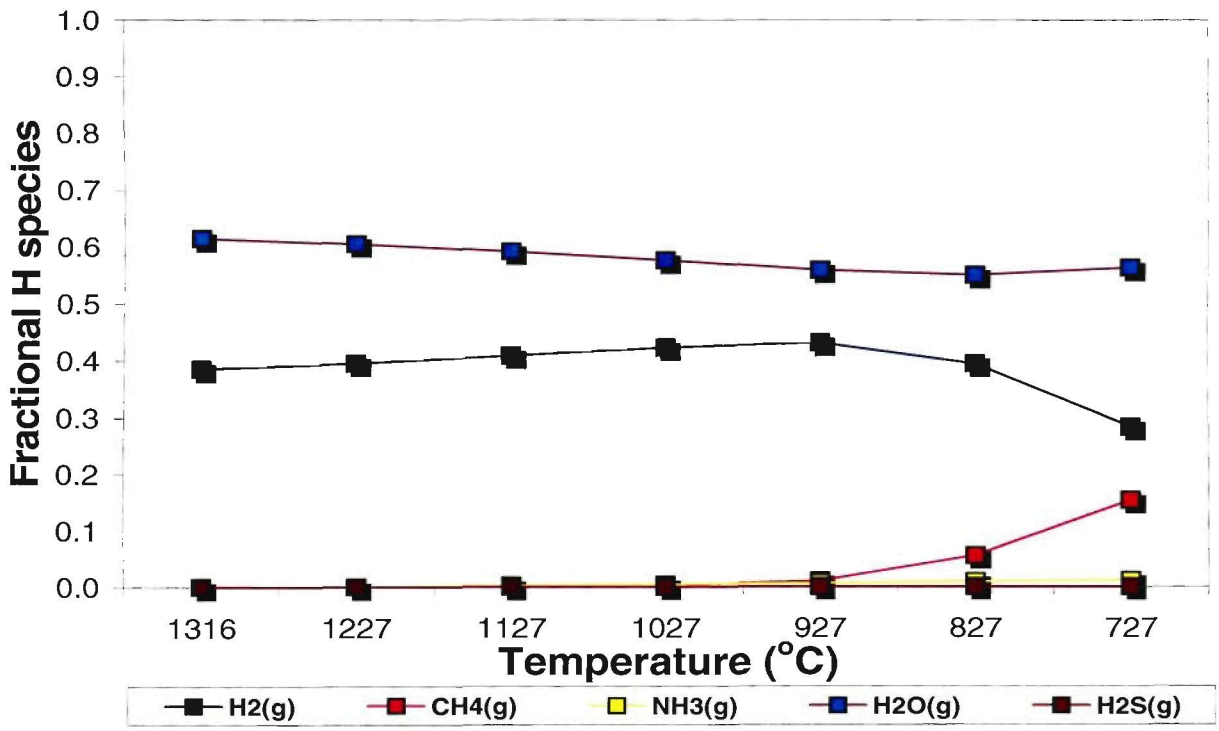

FIGURE 3.13: CHART SHOWING THE EQUILIBRIUM COMPOSITION PROFILE CALCULATED FOR HYDROGEN IN THE REDUCTION ZONE

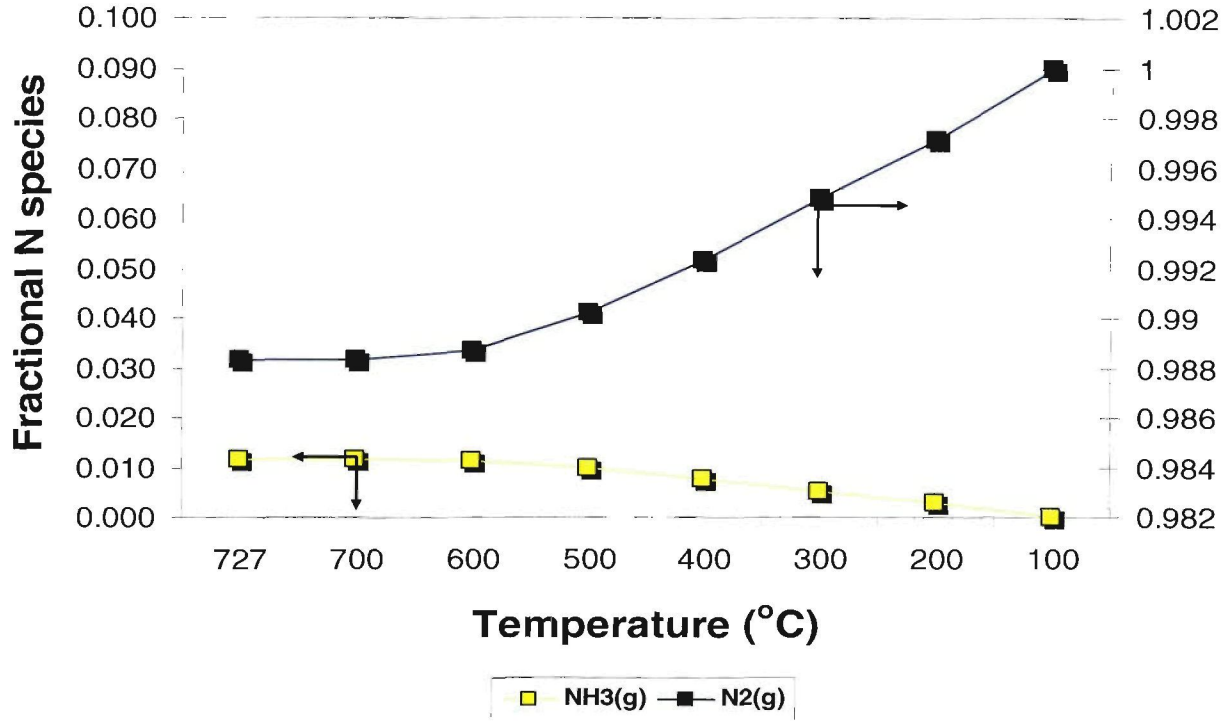

FIGURE 3.14: **CHART SHOWING THE EQUILIBRIUM COMPOSITION PROFILE CALCULATED FOR NITROGEN IN THE DRYING AND PYROLYSIS ZONES**

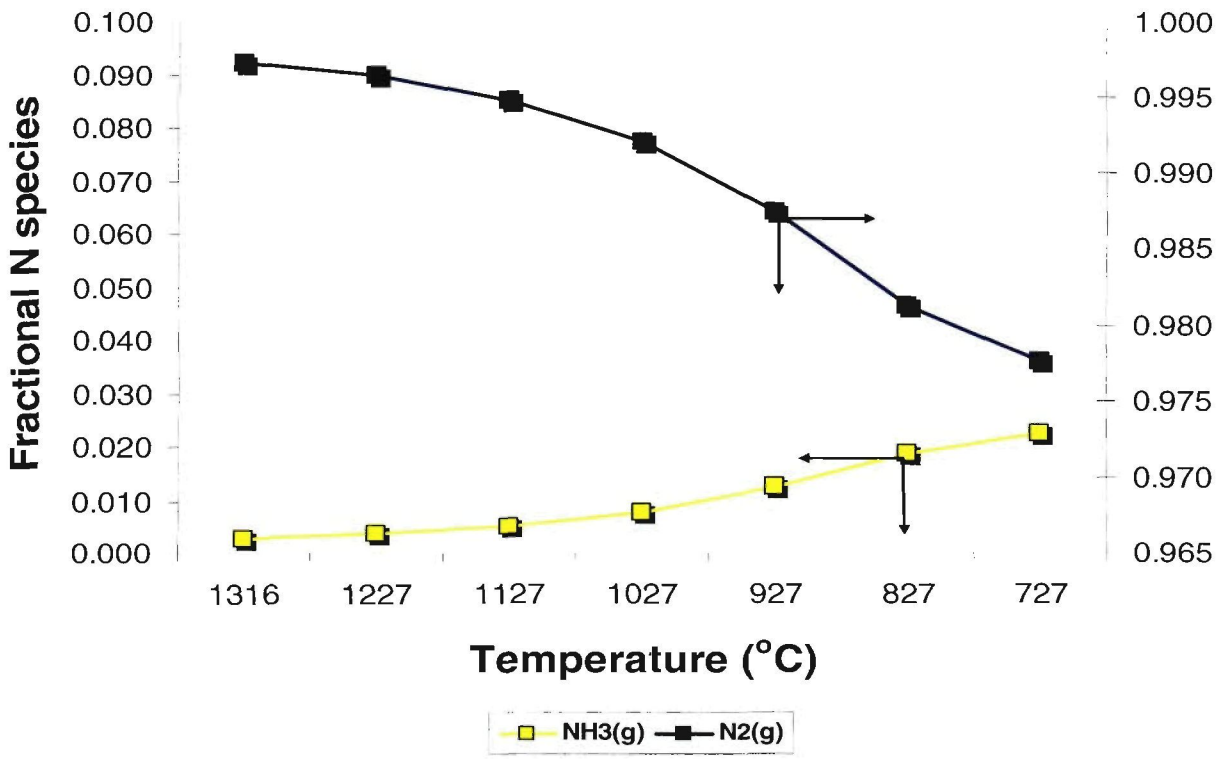

FIGURE 3.15: **CHART DEPICTING THE EQUILIBRIUM COMPOSITION PROFILE CALCULATED FOR NITROGEN IN THE REDUCTION ZONE**

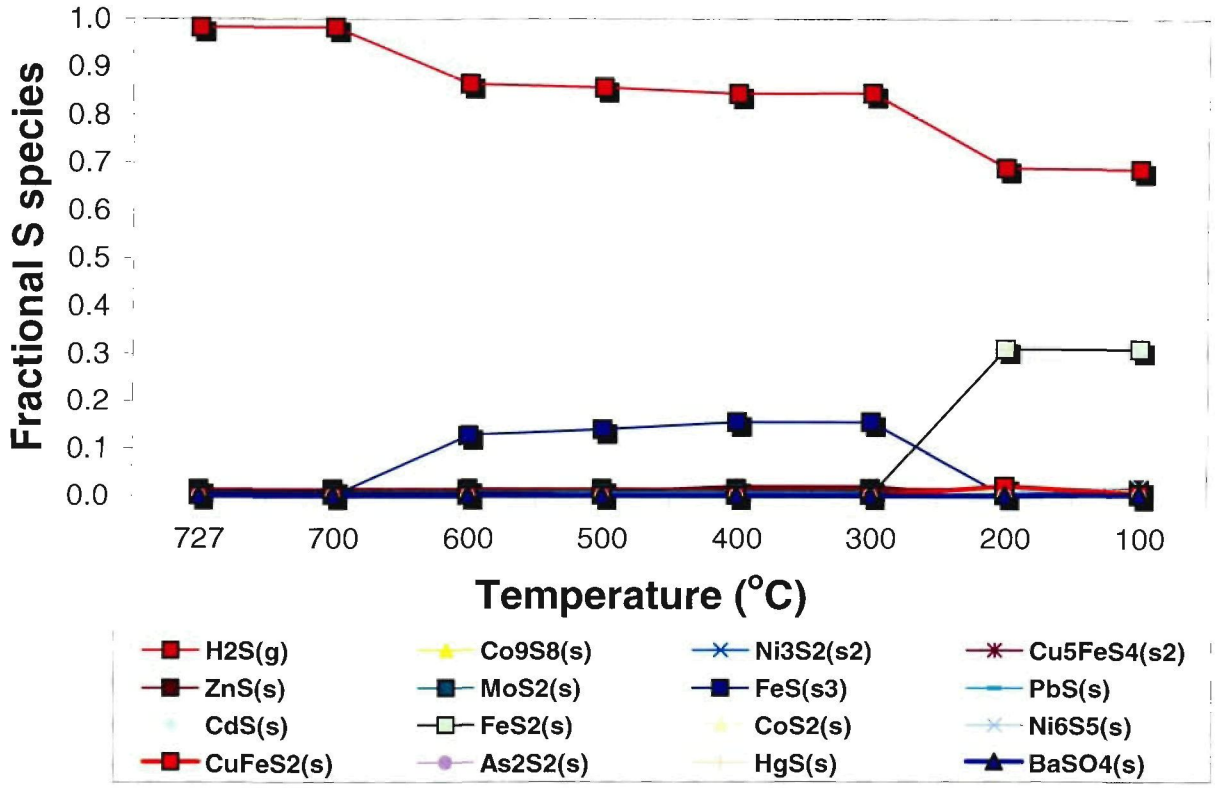

FIGURE 3.16: CHART SHOWING THE EQUILIBRIUM COMPOSITION PROFILE CALCULATED FOR SULPHUR IN THE DRYING AND PYROLYSIS ZONES

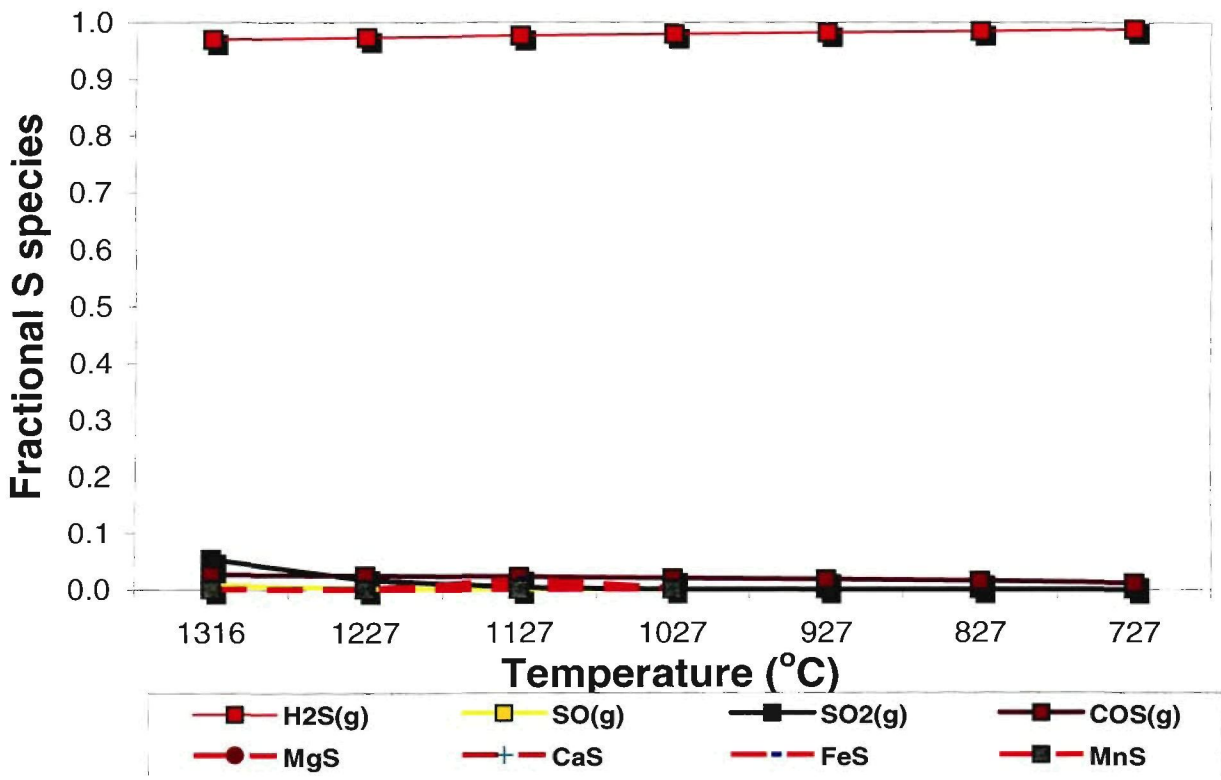

FIGURE 3.17: CHART SHOWING THE EQUILIBRIUM COMPOSITION PROFILE CALCULATED FOR SULPHUR IN THE REDUCTION ZONE

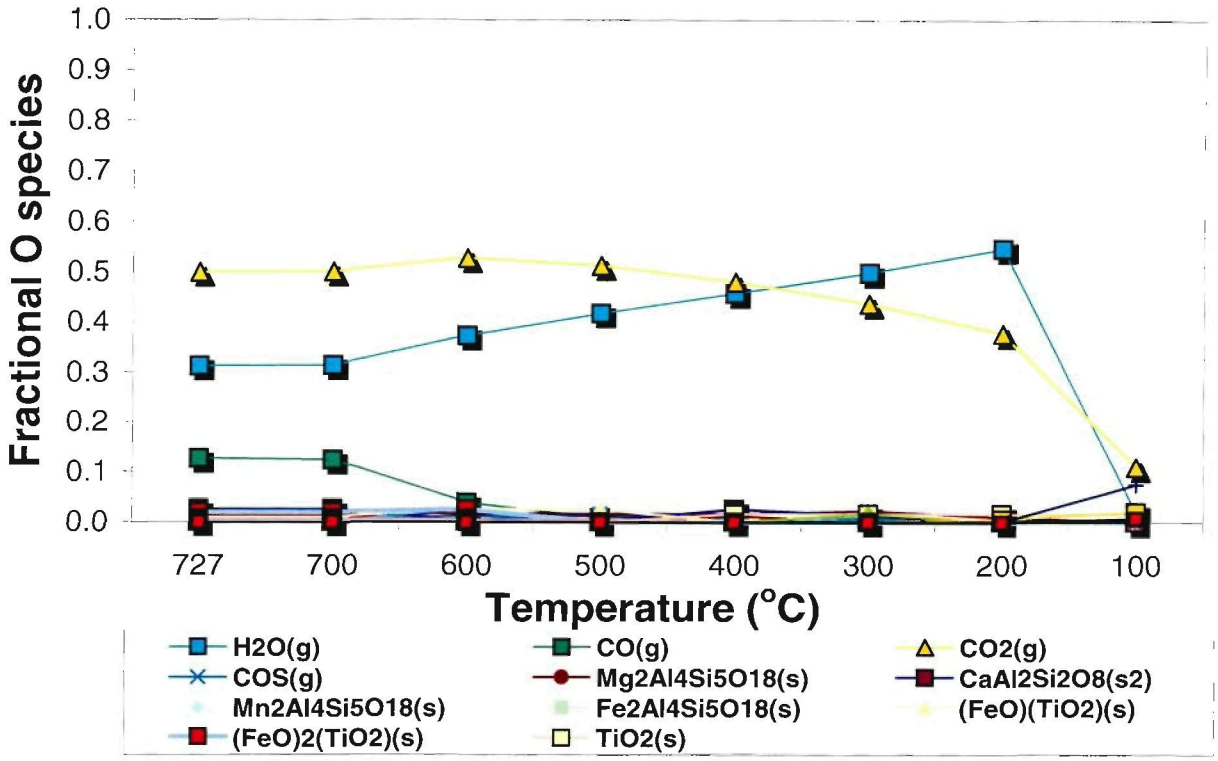

FIGURE 3.18: CHART DEPICTING THE EQUILIBRIUM COMPOSITION PROFILE CALCULATED FOR OXYGEN IN THE DRYING AND PYROLYSIS ZONES

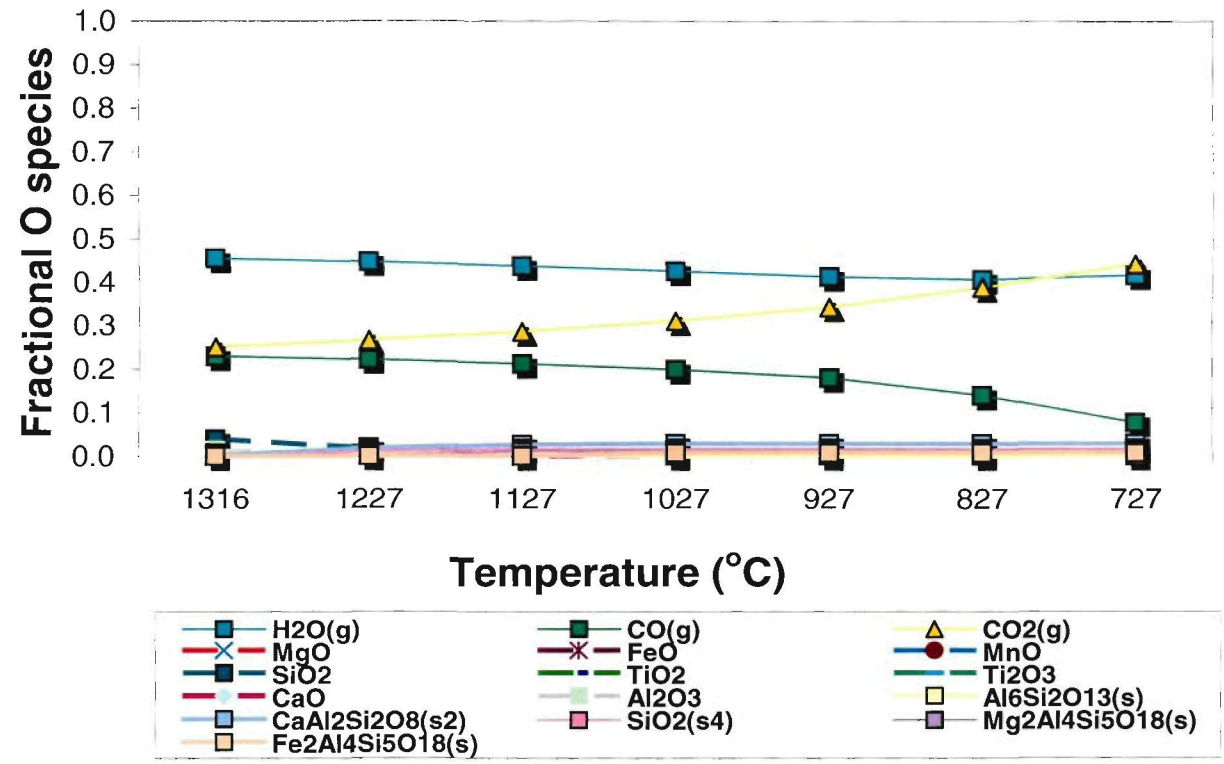

FIGURE 3.19: CHART SHOWING THE EQUILIBRIUM COMPOSITION PROFILE CALCULATED FOR OXYGEN IN THE REDUCTION ZONE

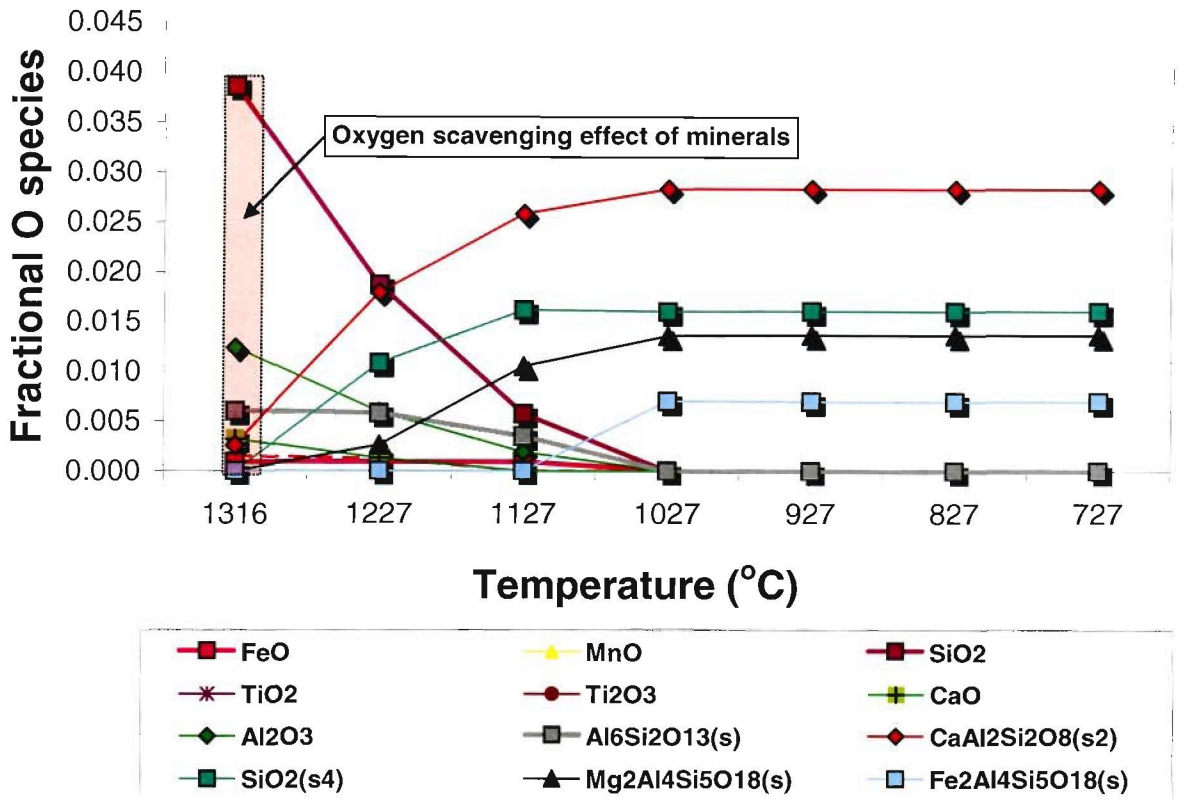

FIGURE 3.20: AN EXPANDED VIEW OF THE EQUILIBRIUM COMPOSITION PROFILE, CALCULATED FOR OXYGEN IN THE REDUCTION ZONE, HIGHLIGHTING THE OXYGEN SCAVENGING EFFECT OF MINERALS

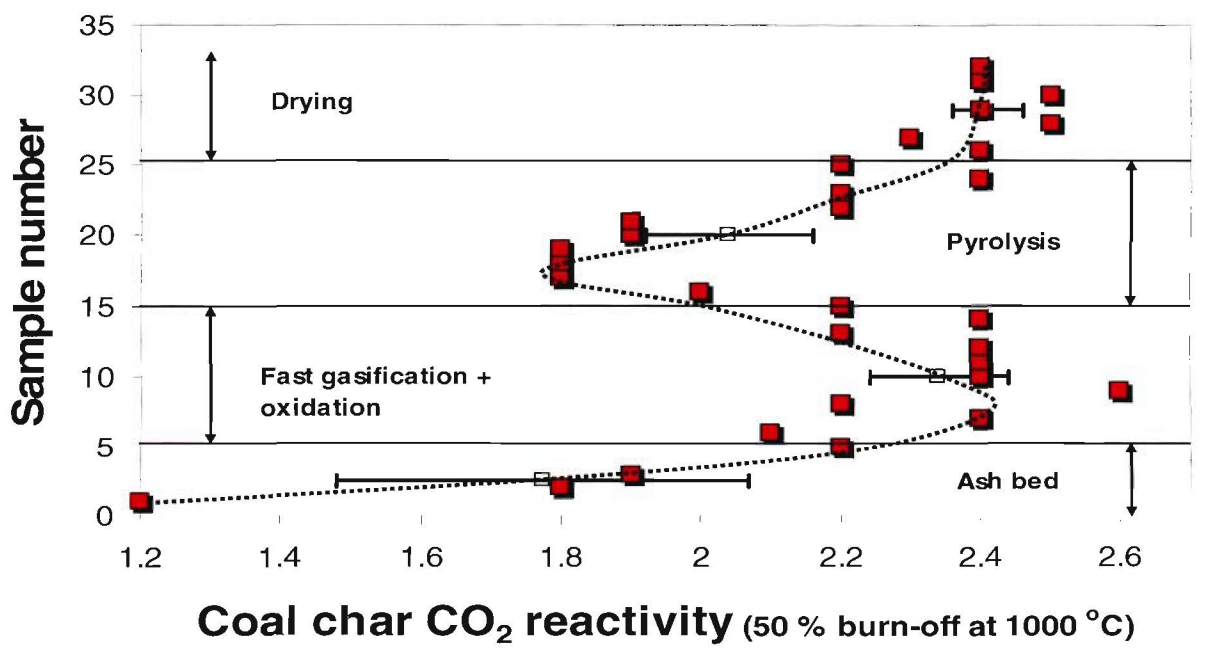

FIGURE 3.21: LINE GRAPH SHOWING THE COAL CHAR CO_2 REACTIVITY PROFILE [50% BURN-OFF AT 1000°C) FOR THE GG41 GASIFIER (h^{-1})]

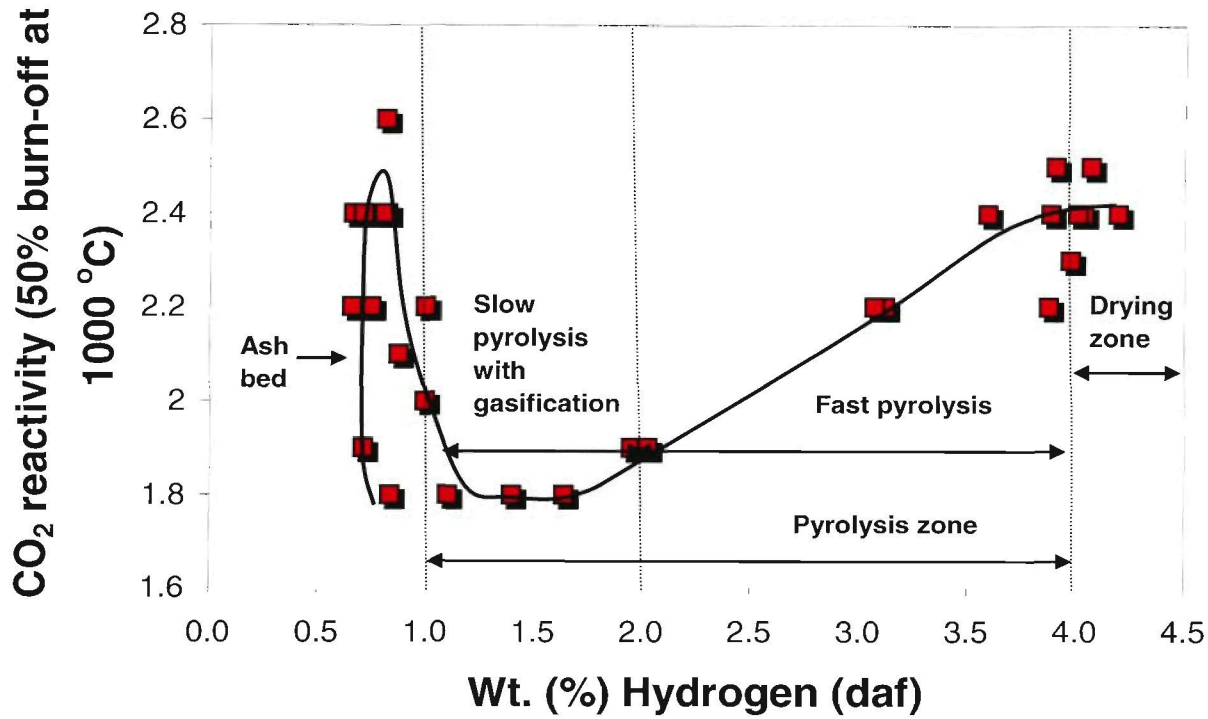

FIGURE 3.22: GRAPH SHOWING THE RELATIONSHIP BETWEEN HYDROGEN CONTENT (%daf) AND CO_2 REACTIVITY (50% BURN-OFF AT 1000 °C) FOR THE GG41 GASIFIER

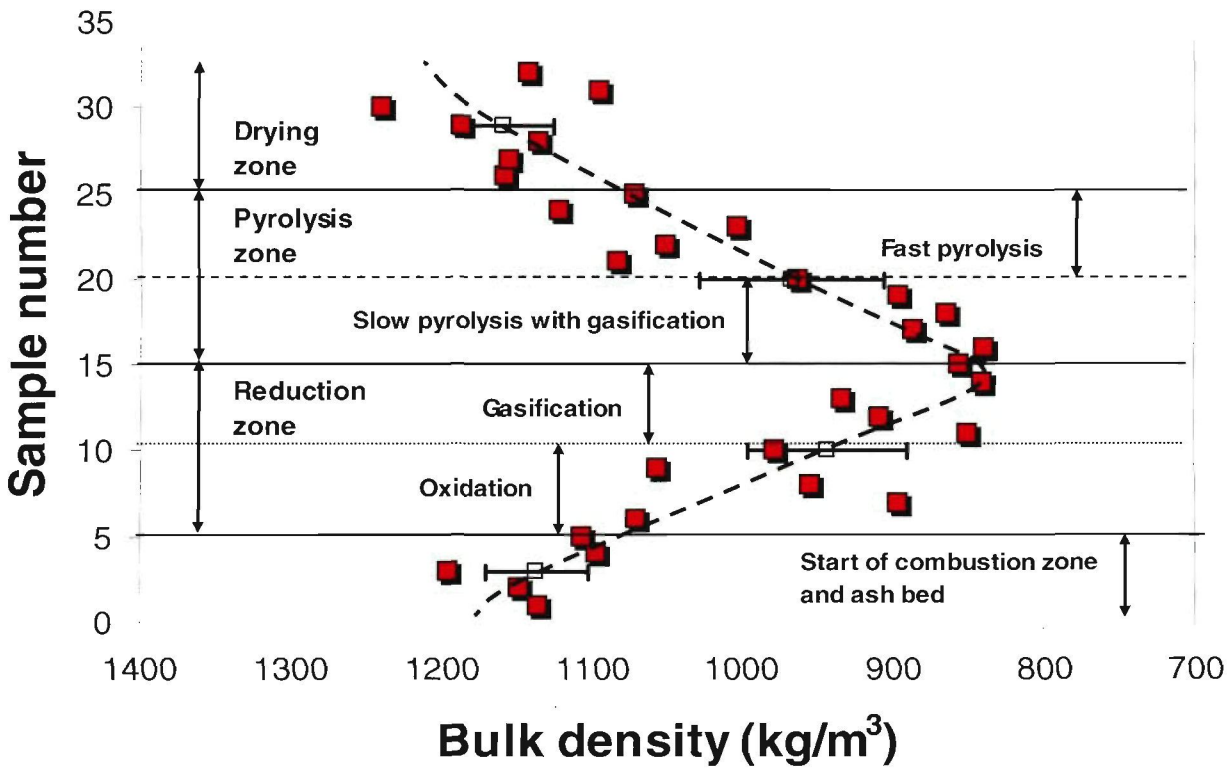

FIGURE 3.23: FIGURE DEPICTING THE BULK DENSITY PROFILE OF THE GG41 GASIFIER (AS RECEIVED BASE)

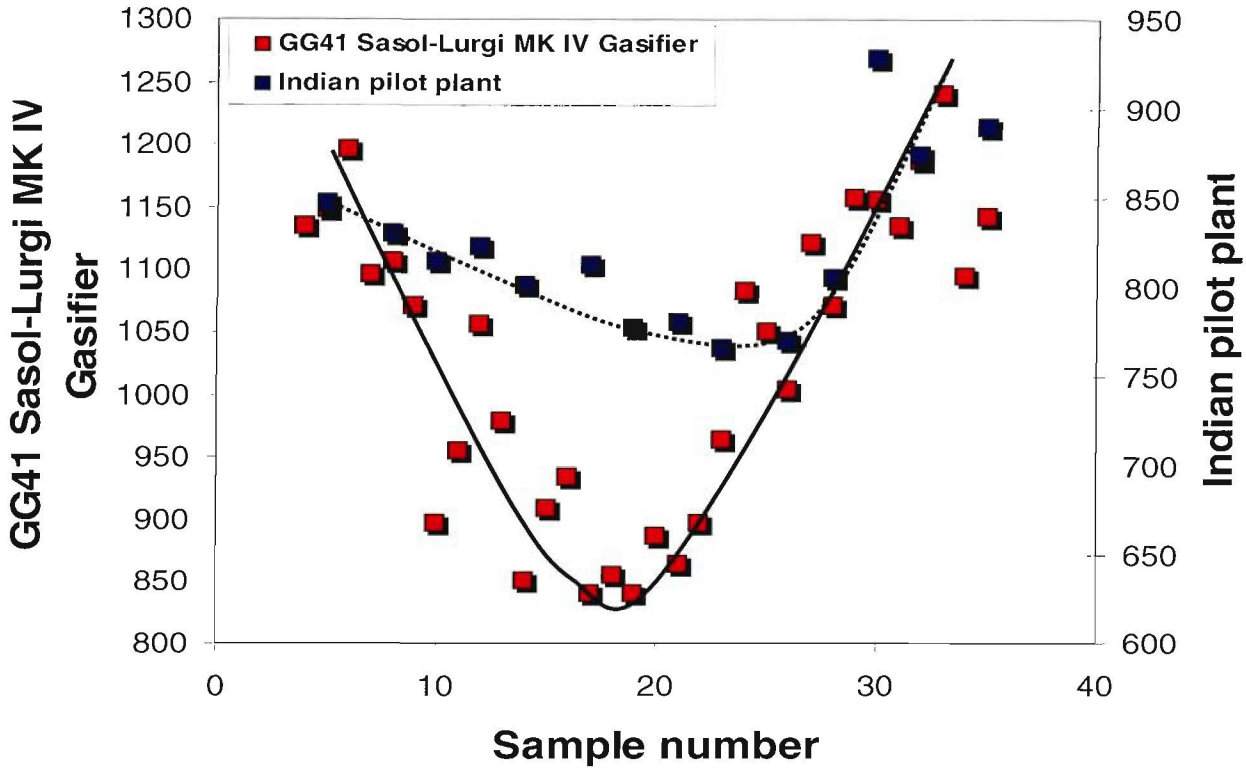

FIGURE 3.24: GRAPH SHOWING THE BULK DENSITY PROFILE COMPARISON OF THE GG41 GASIFIER DATA AND THE FACTORISED INDIAN PILOT PLANT DATA (AS RECEIVED BASE)

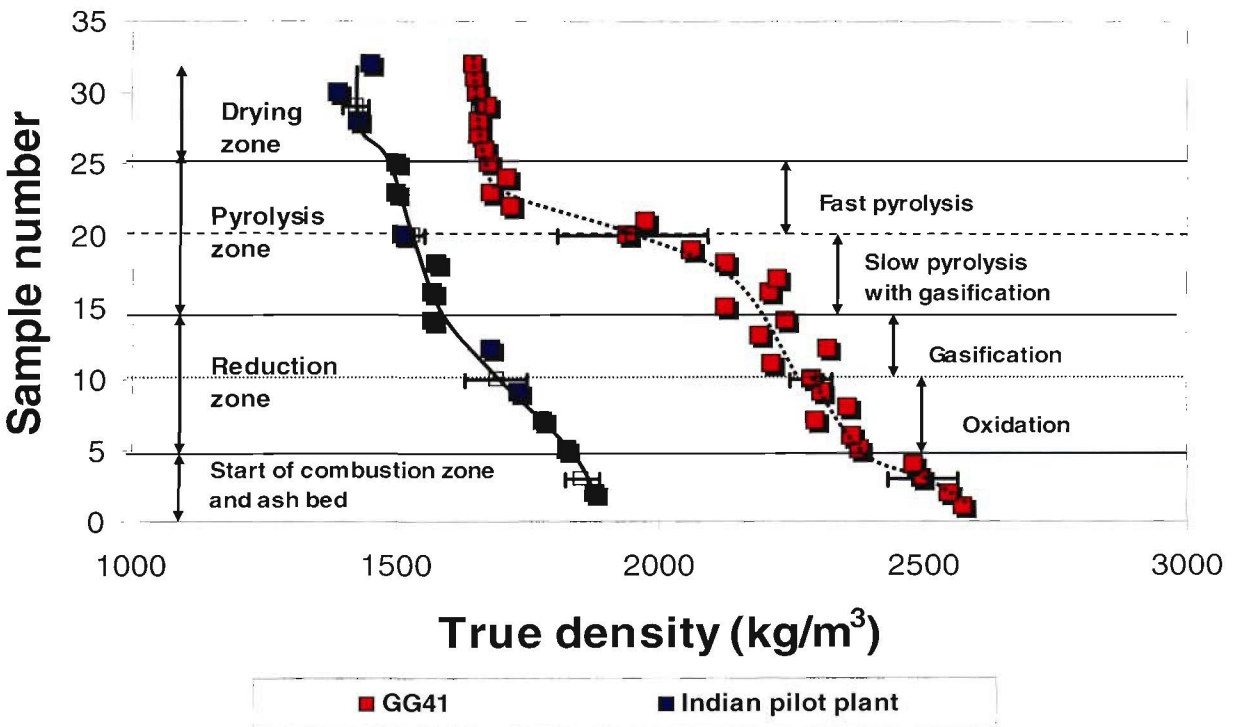

FIGURE 3.25: FIGURE DEPICTING THE TRUE DENSITY PROFILES OBTAINED FOR THE GG41 GASIFIER AND THE FACTORISED INDIAN PILOT PLANT DATA (AS RECEIVED BASE)

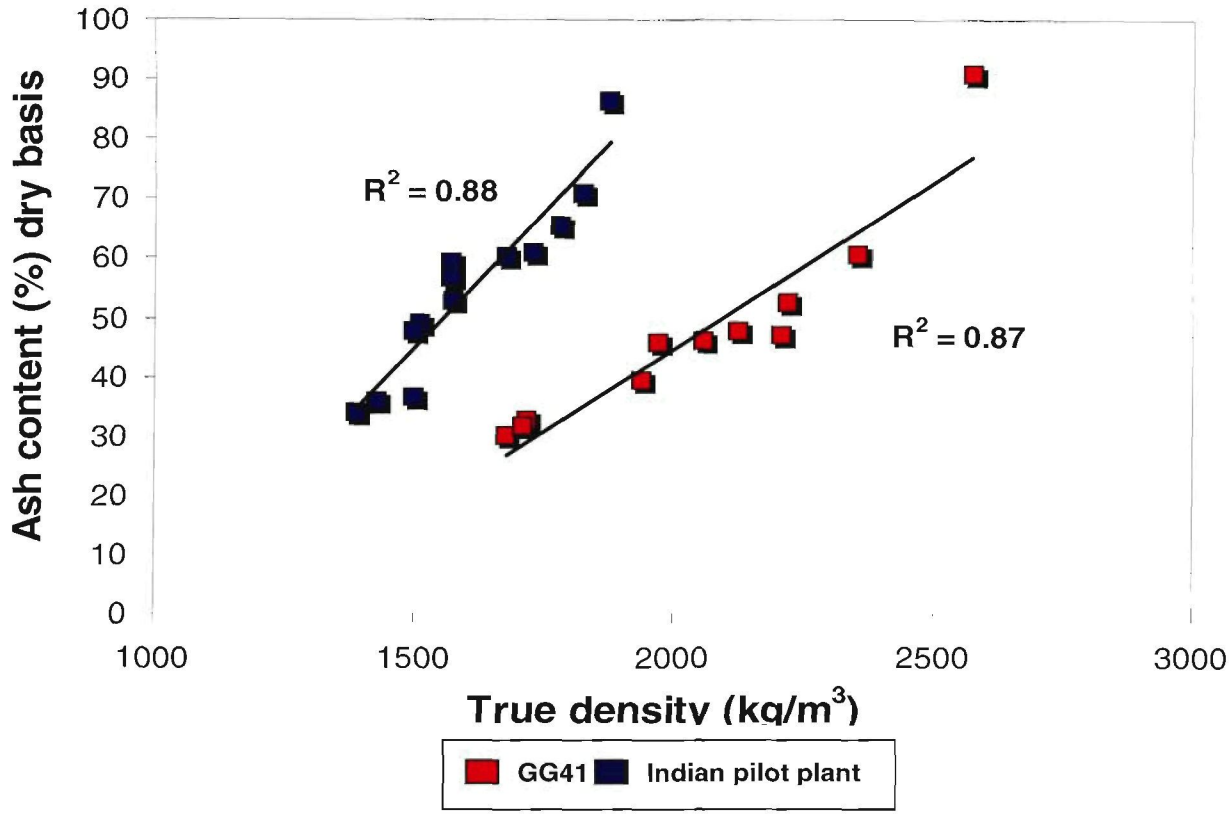

FIGURE 3.26: CHART SHOWING THE RELATIONSHIP BETWEEN ASH CONTENT (%) AND TRUE DENSITY (kg/m^3) PROFILES FOR THE GG41 GASIFIER AND THE FACTORISED INDIAN PILOT PLANT DATA (AS RECEIVED BASE)

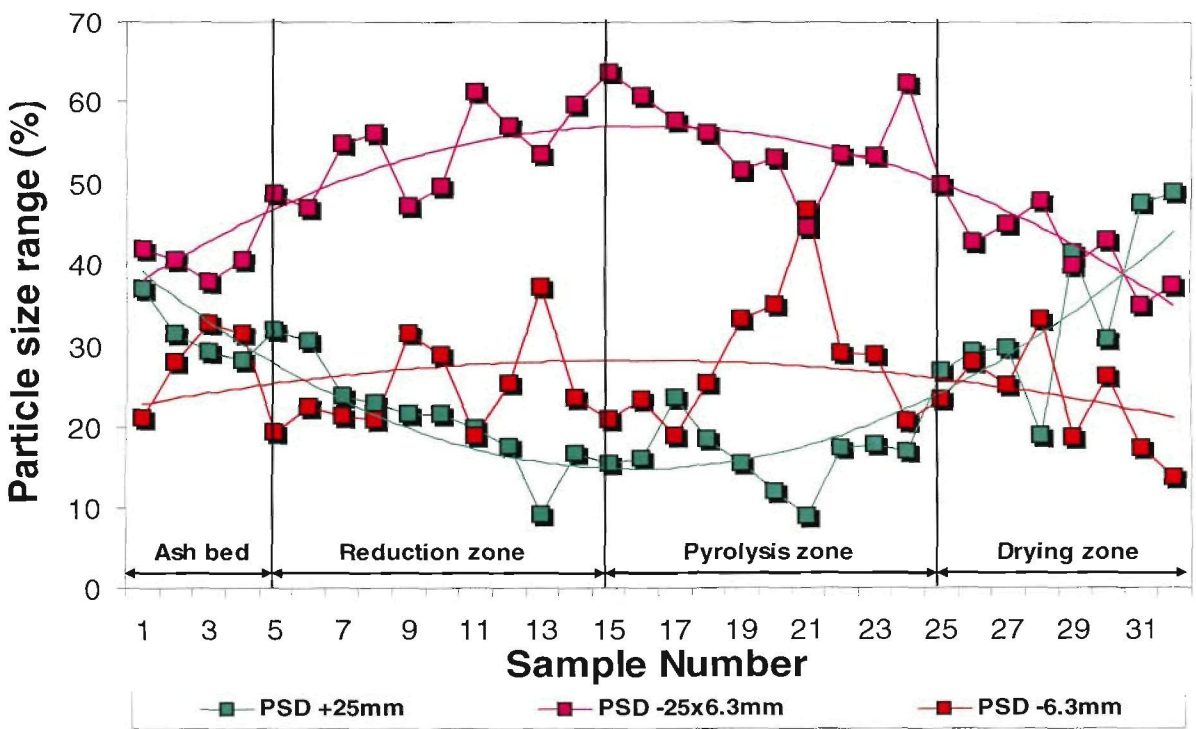

FIGURE 3.27: GRAPHIC REPRESENTATION OF THE COAL PARTICLE SIZE DISTRIBUTION TRENDS FOR THE GG41 GASIFIER (AS RECEIVED BASE)

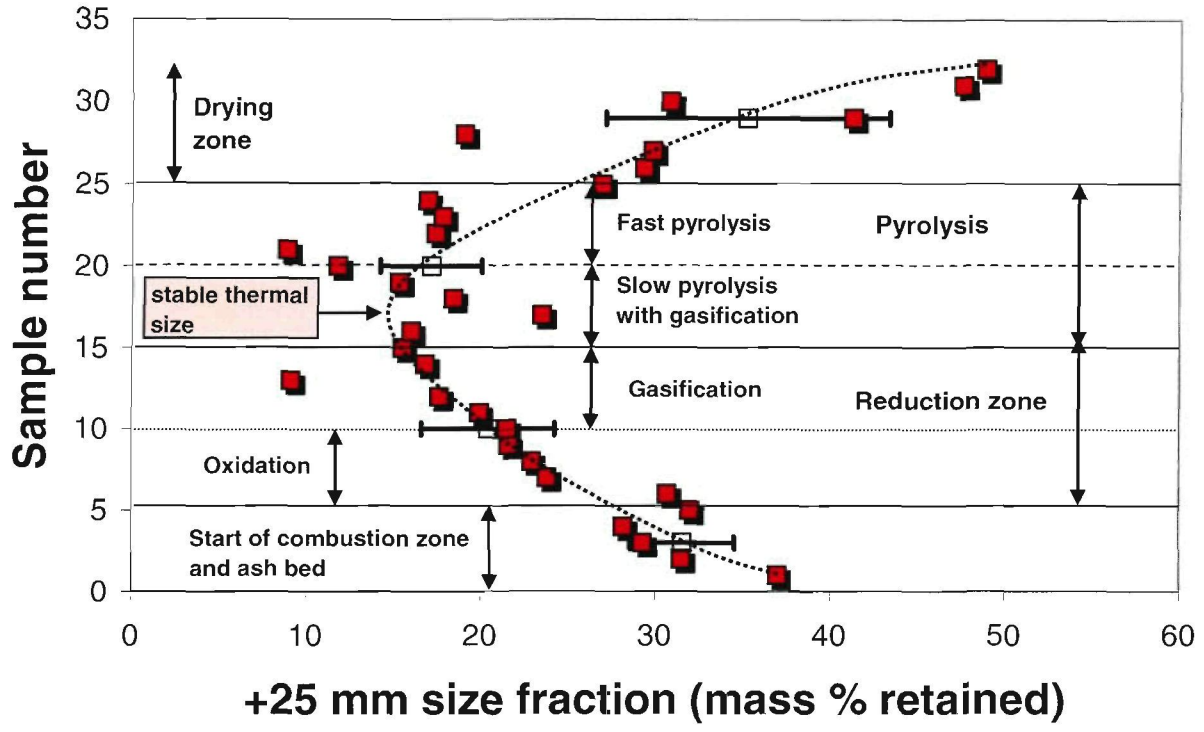

FIGURE 3.28: GRAPHICAL REPRESENTATION OF THE +25mm SIZE FRACTION DISTRIBUTION PROFILE (AS RECEIVED BASE) FOR THE GG41 GASIFIER SHOWING THE SEVERE EFFECT OF FRAGMENTATION LEADING TO GASIFIER INSTABILITY

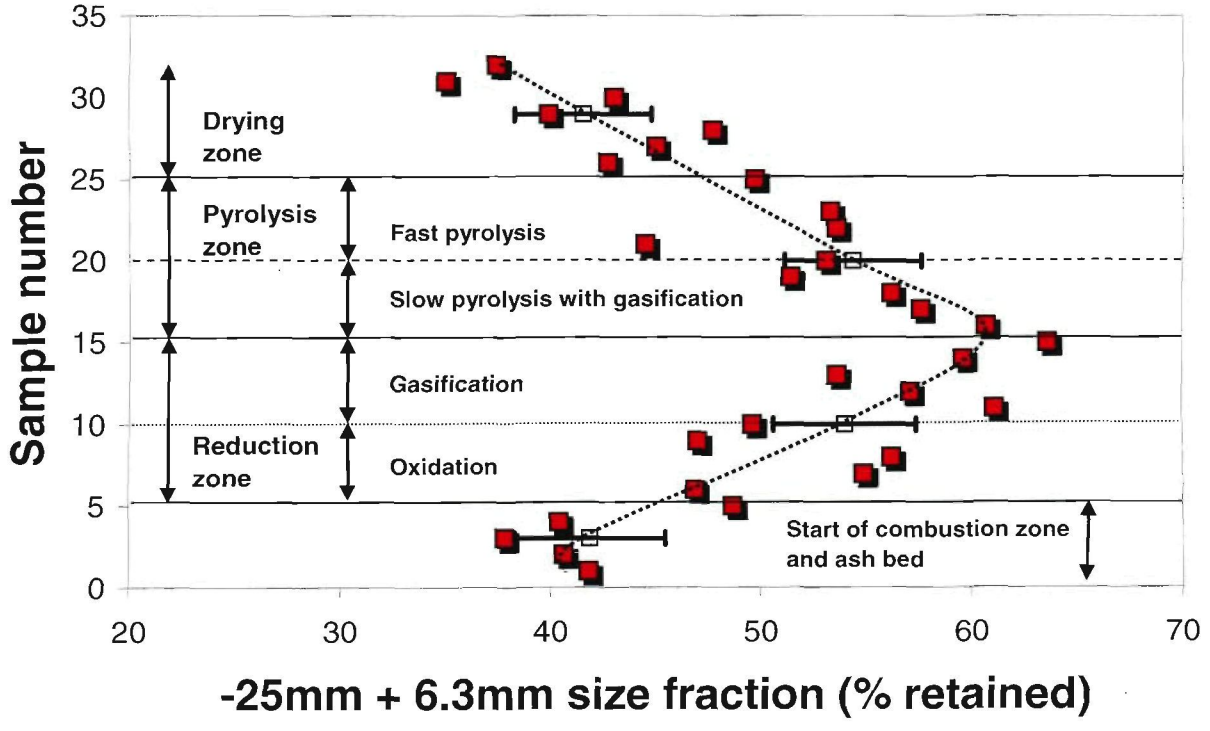

FIGURE 3.29 LINE GRAPH SHOWING THE -25mm + 6.3mm SIZE FRACTION DISTRIBUTION PROFILE OBTAINED FOR THE GG41 GASIFIER (AS RECEIVED BASE)

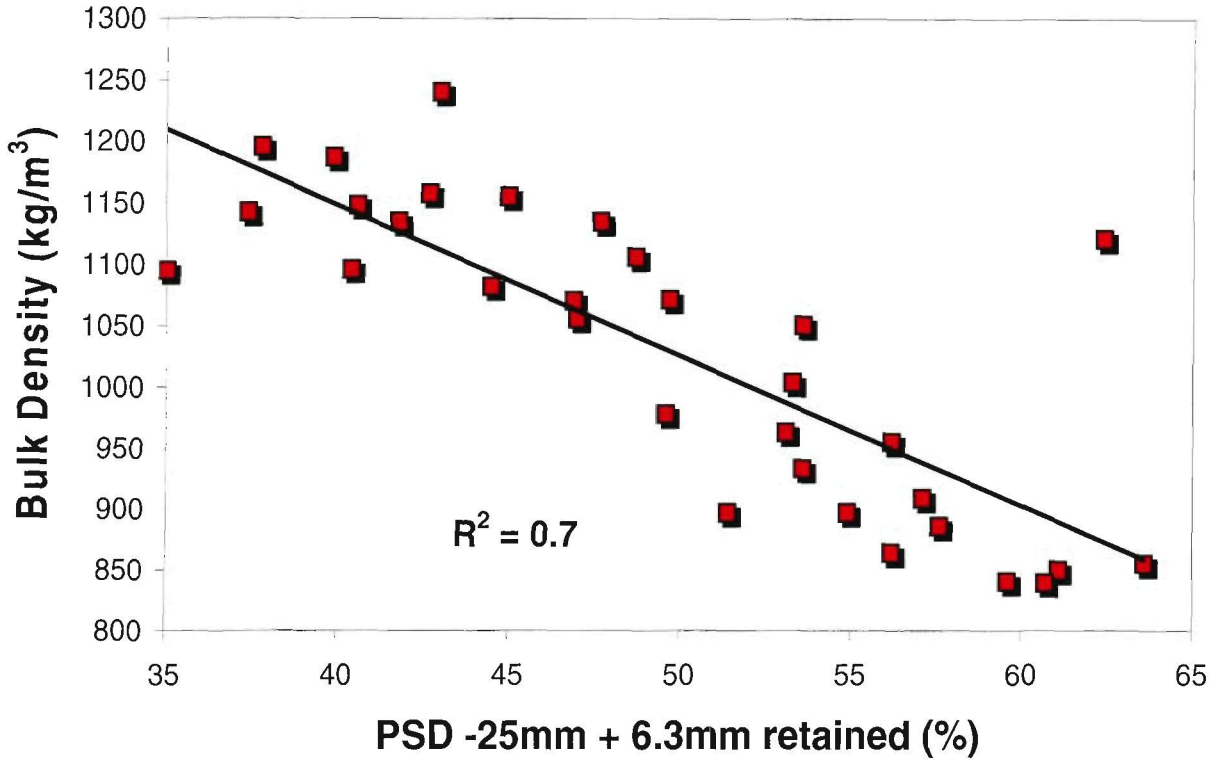

FIGURE 3.30: LINEAR PLOT SHOWING THE RELATIONSHIP BETWEEN BULK DENSITY (kg/m^3) AND PERCENTAGE -25mm +6.3mm RETAINED FRACTION OBTAINED FOR THE GG41 GASIFIER (AS RECEIVED BASE)

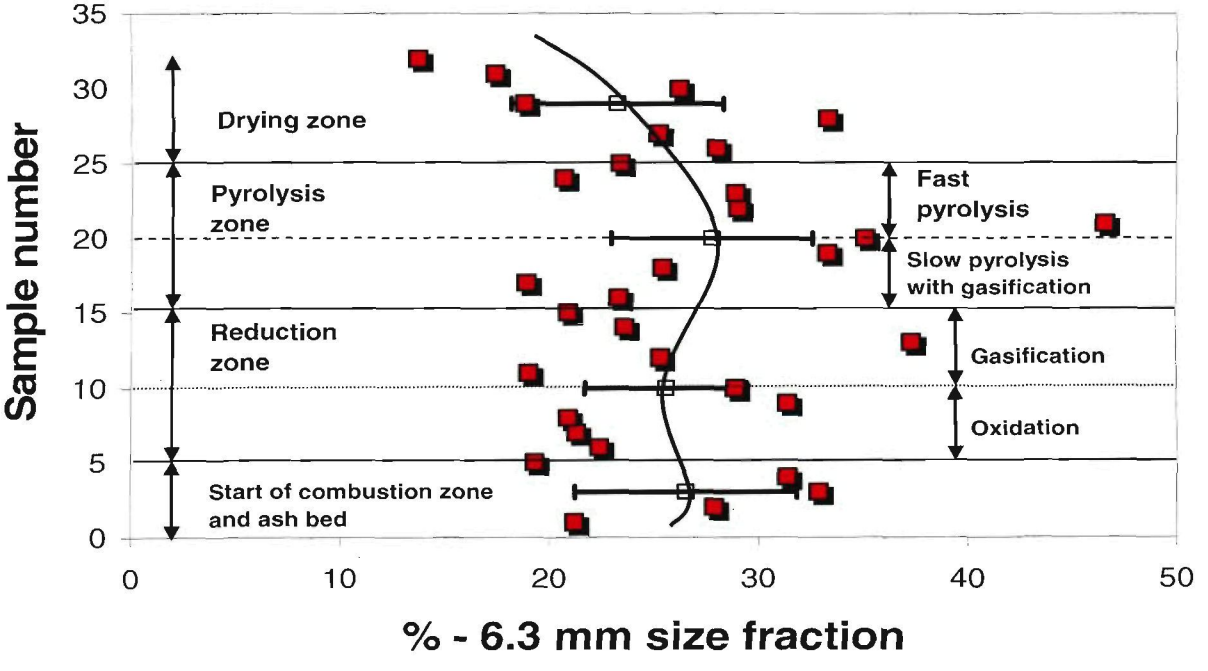

FIGURE 3.31 CHART SHOWING THE -6.3mm SIZE FRACTION DISTRIBUTION PROFILE FOR THE GG41 GASIFIER (AS RECEIVED BASE)

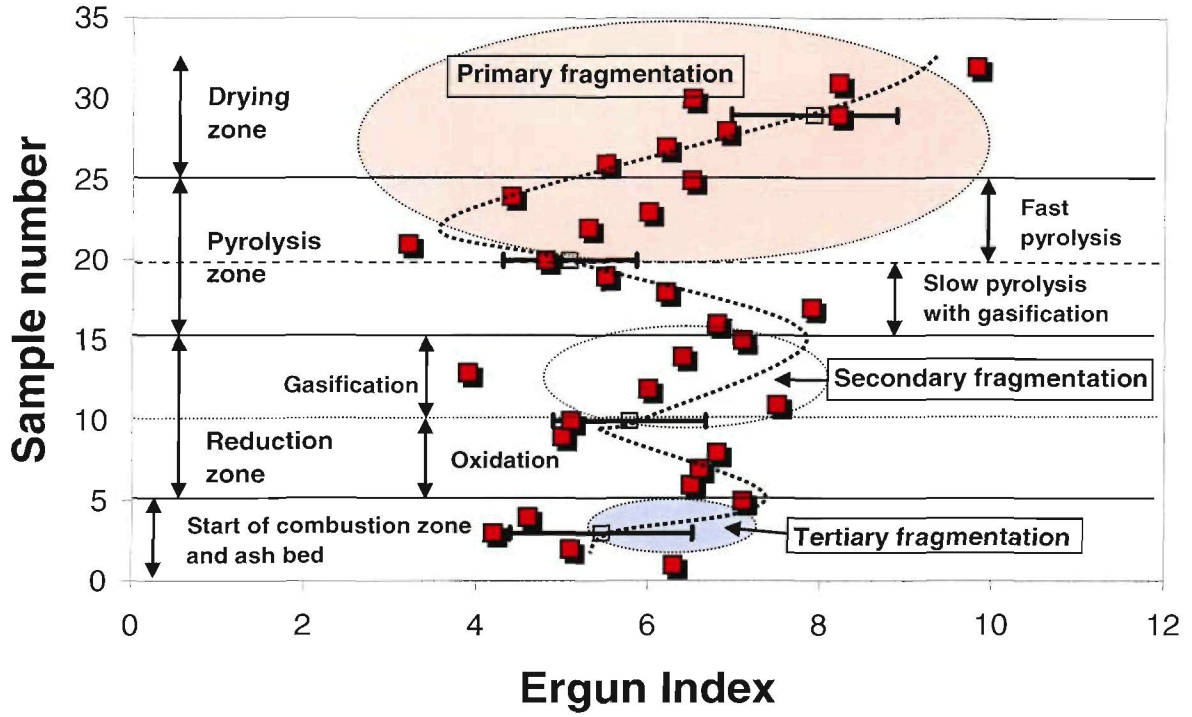

FIGURE 3.32 PLOT OF THE ERGUN INDEX PROFILE (AS RECEIVED BASE) HIGHLIGHTING THE ZONES OF PRIMARY, SECONDARY AND TERTIARY FRAGMENTATION OBTAINED FOR THE GG41 GASIFIER

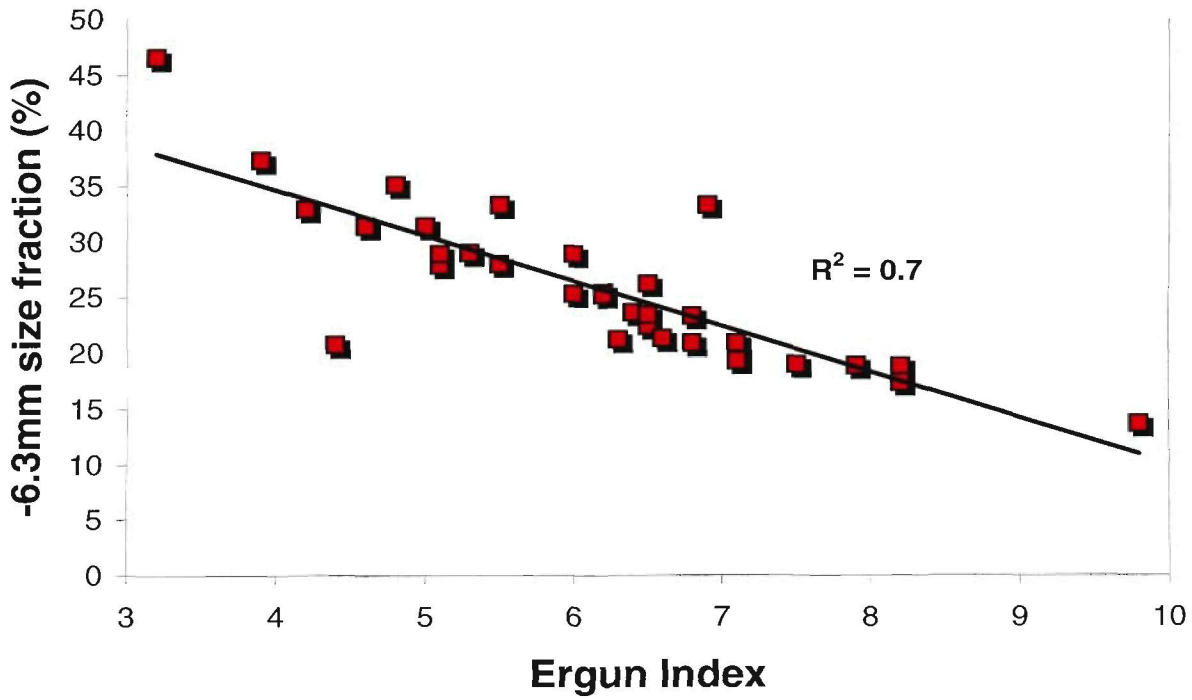

FIGURE 3.33: LINEAR PLOT SHOWING THE RELATIONSHIP BETWEEN THE ERGUN INDEX DISTRIBUTION PROFILE AND THE PERCENTAGE -6.3mm SIZE FRACTION OBTAINED FOR THE GG41 GASIFIER (AS RECEIVED BASE)

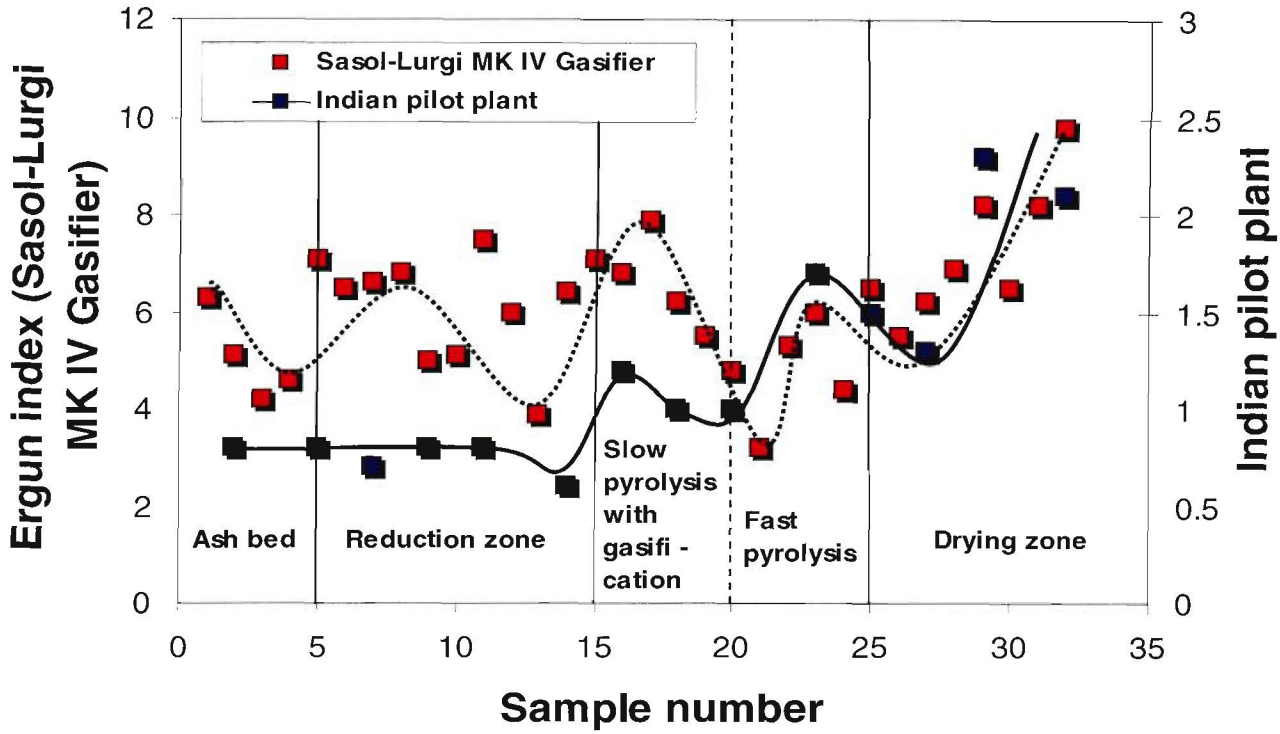

FIGURE 3.34: CHART SHOWING THE ERGUN INDEX PROFILE COMPARISON OF THE GG41 GASIFIER AND THE FACTORISED INDIAN PILOT PLANT DATA (AS RECEIVED BASE)

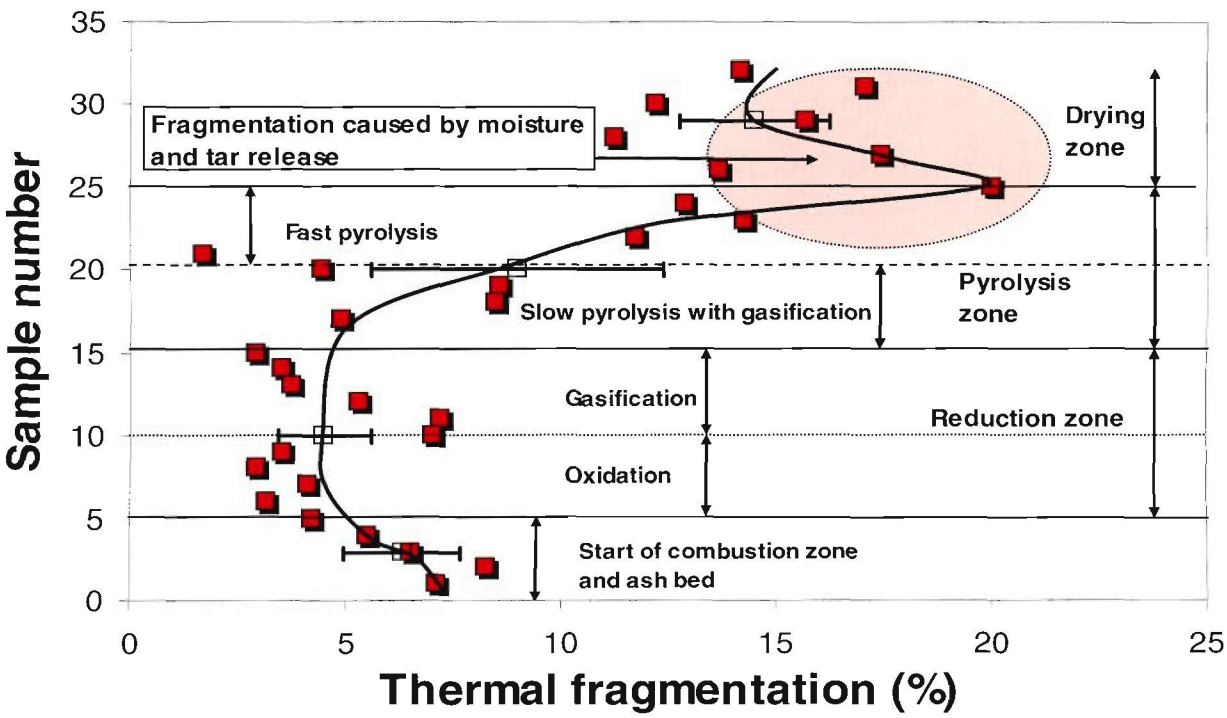

FGURE 3.35: LINE GRAPH DEPICTING THE GG41 GASIFIER THERMAL FRAGMENTATION PROFILE (AIR DRIED BASE)

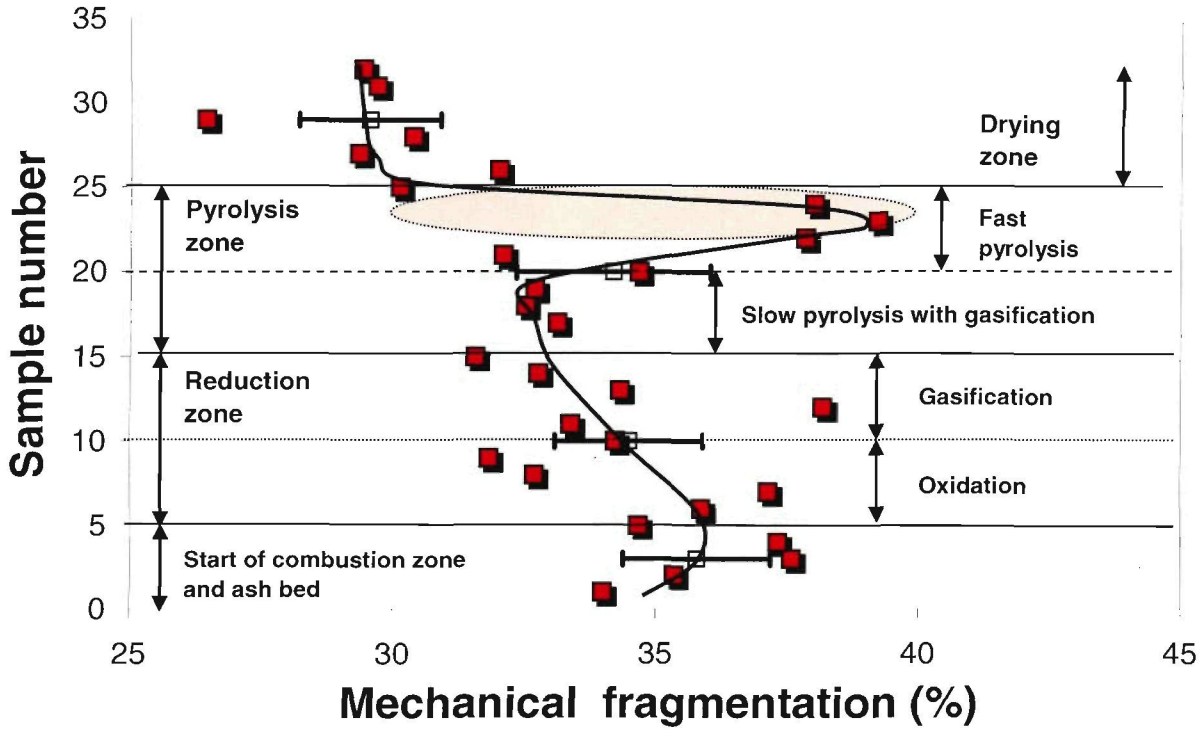

FIGURE 3.36: LINE GRAPH SHOWING THE GG41 GASIFIER PERCENTAGE MECHANICAL FRAGMENTATION PROFILE (AIR DRIED BASE)

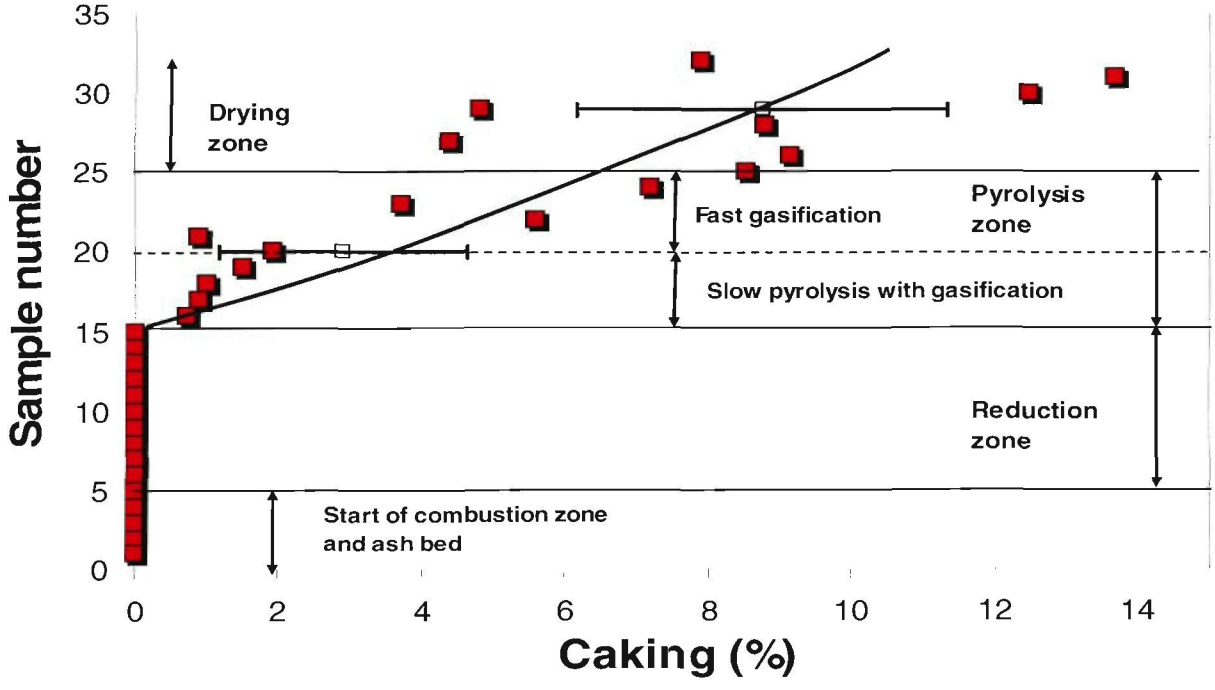

FIGURE 3.37: CHART SHOWING THE CAKING PROPENSITY PROFILE OF THE GG41 GASIFIER (AIR DRIED BASE)

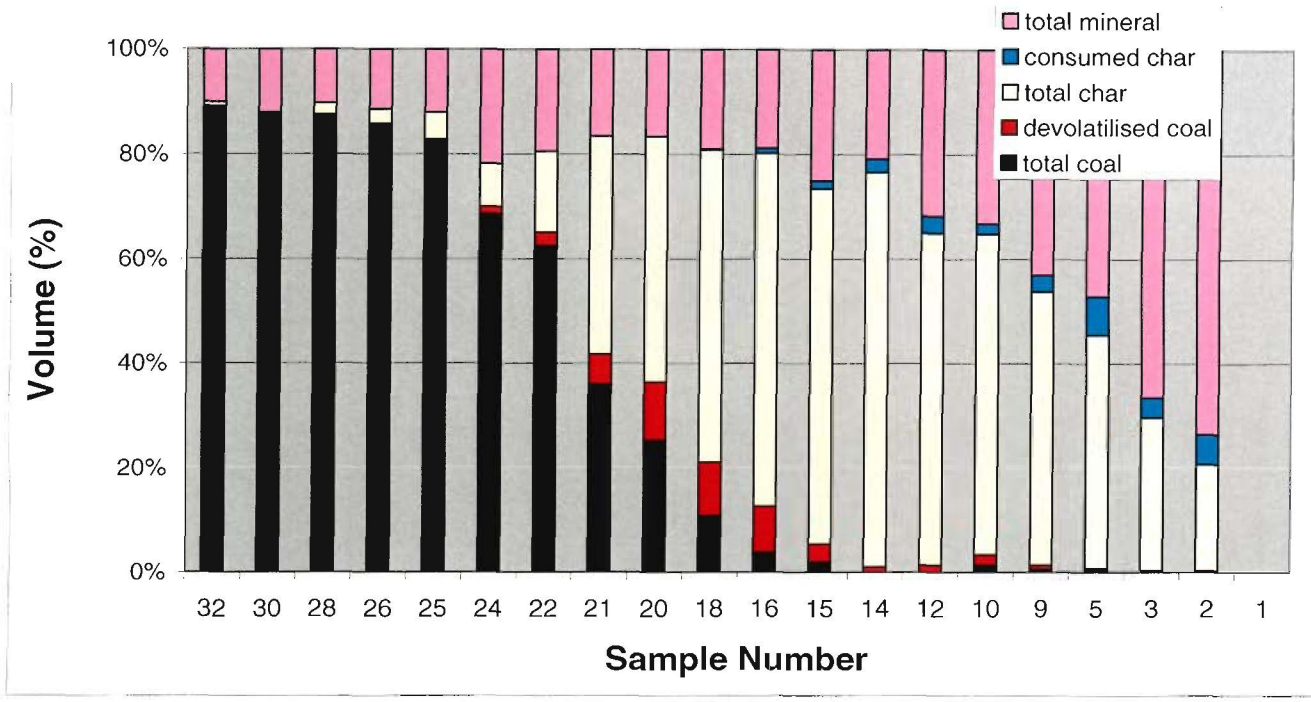

FIGURE 3.38: BAR CHART SHOWING THE CHAR MORPHOLOGY CLASSIFICATION PROFILE OF THE GG41 GASIFIER TURN-OUT SAMPLES (AS RECEIVED BASE)

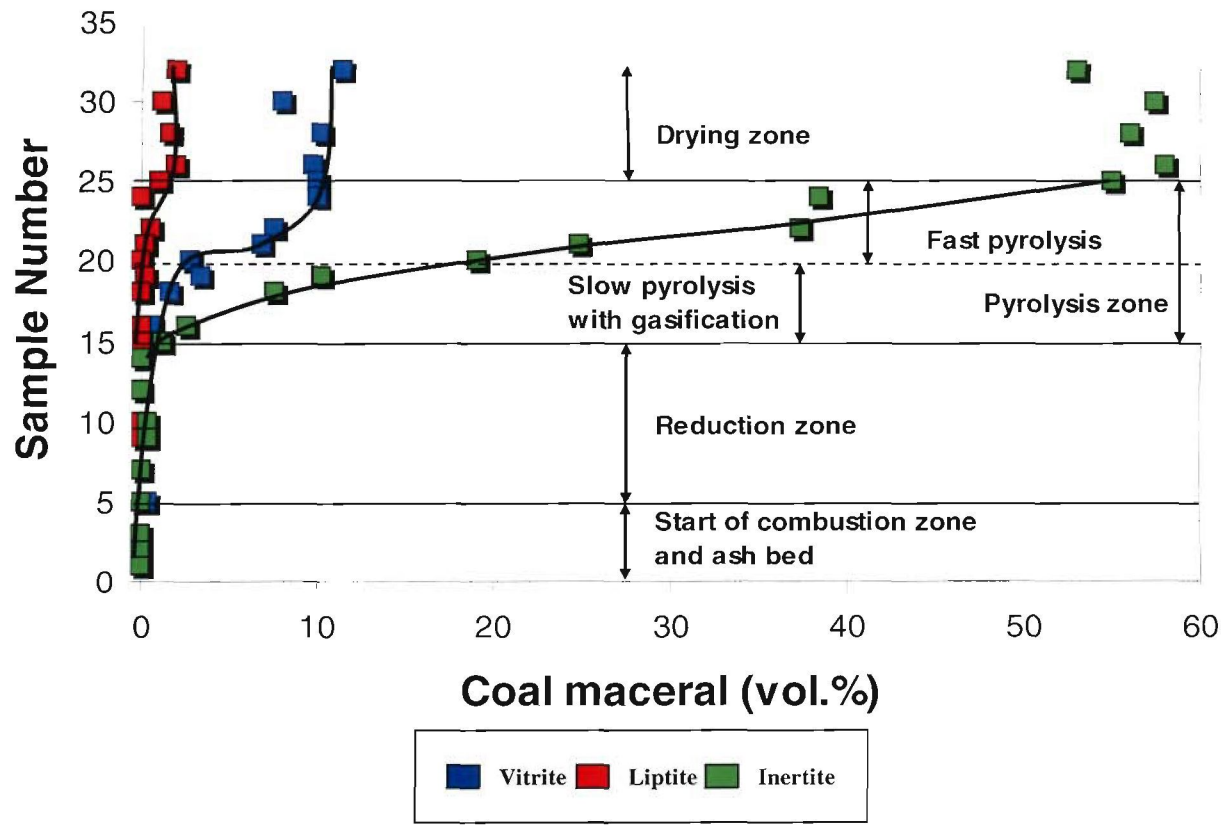

FIGURE 3.39: LINE GRAPH SHOWING THE COAL MICROLYTHOTYPE BEHAVIOUR OCCURING IN THE GG41 GASIFIER (AS RECEIVED BASE)

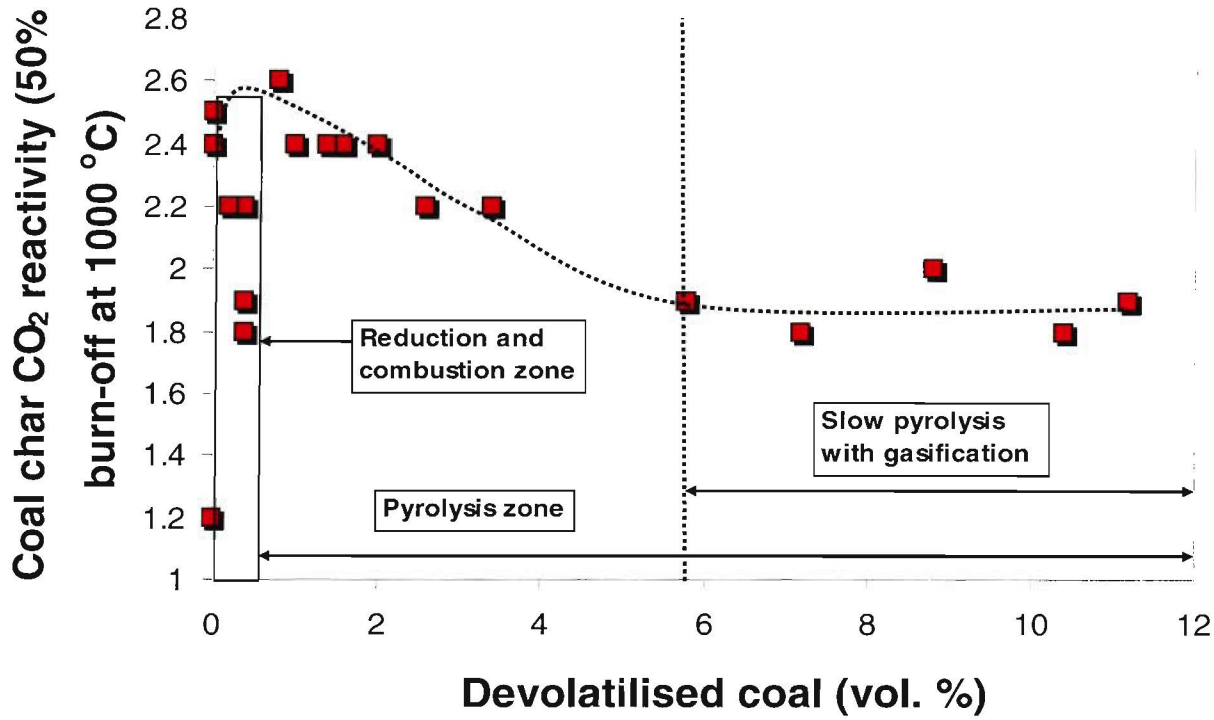

FIGURE 3.40: GRAPH SHOWING THE RELATIONSHIP BETWEEN THE GG41 GASIFIER DEVOLATILISED COAL CONTENT (vol. %) VERSUS COAL CHAR CO_2 REACTIVITY PROFILE (50% CARBON BURN-OFF AT 1000 °C)

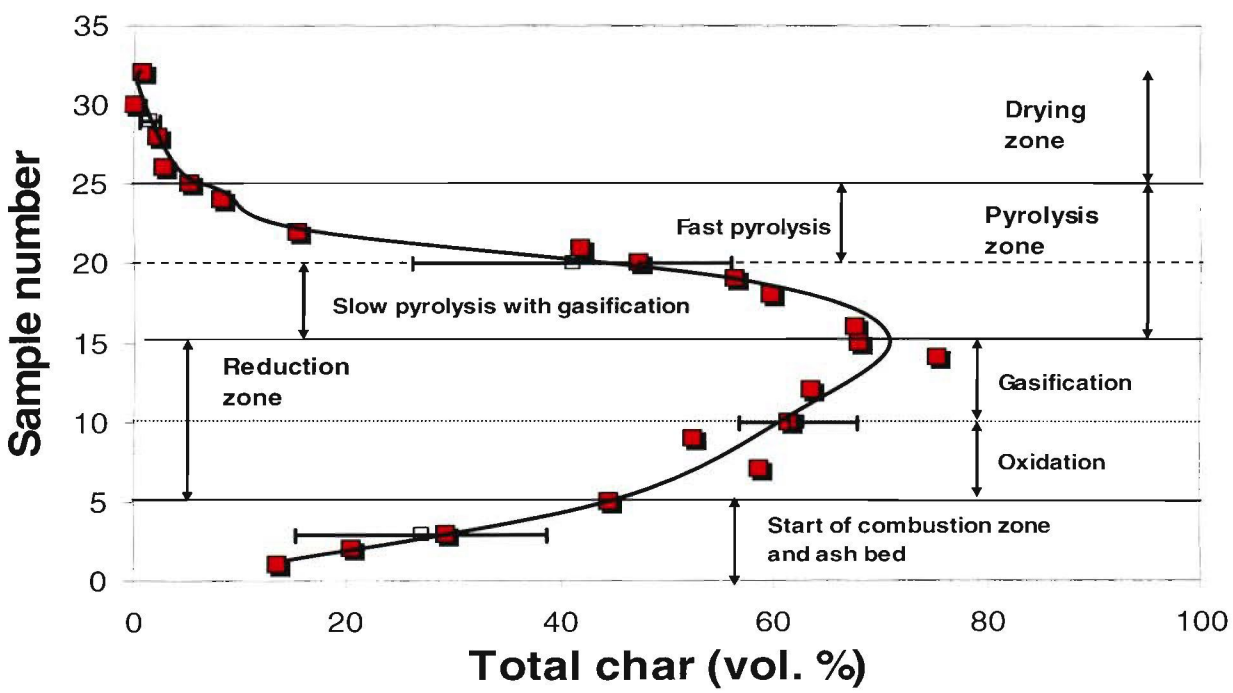

FIGURE 3.41: GRAPH SHOWING THE TOTAL CHAR (vol. %) PROFILE OBTAINED FOR THE GG41 GASIFIER (AS RECEIVED BASE)

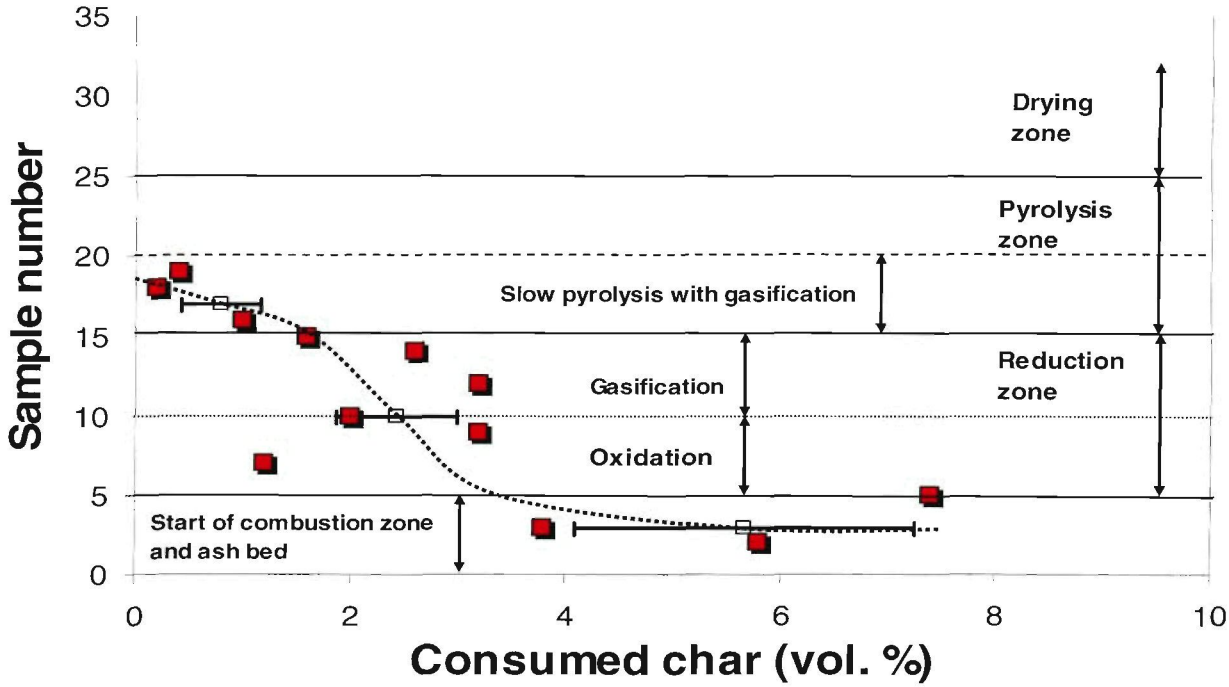

FIGURE 3.42: GRAPH SHOWING THE CONSUMED CHAR (vol. %) PROFILE OBTAINED FOR THE GG41 GASIFIER (AS RECEIVED BASE)

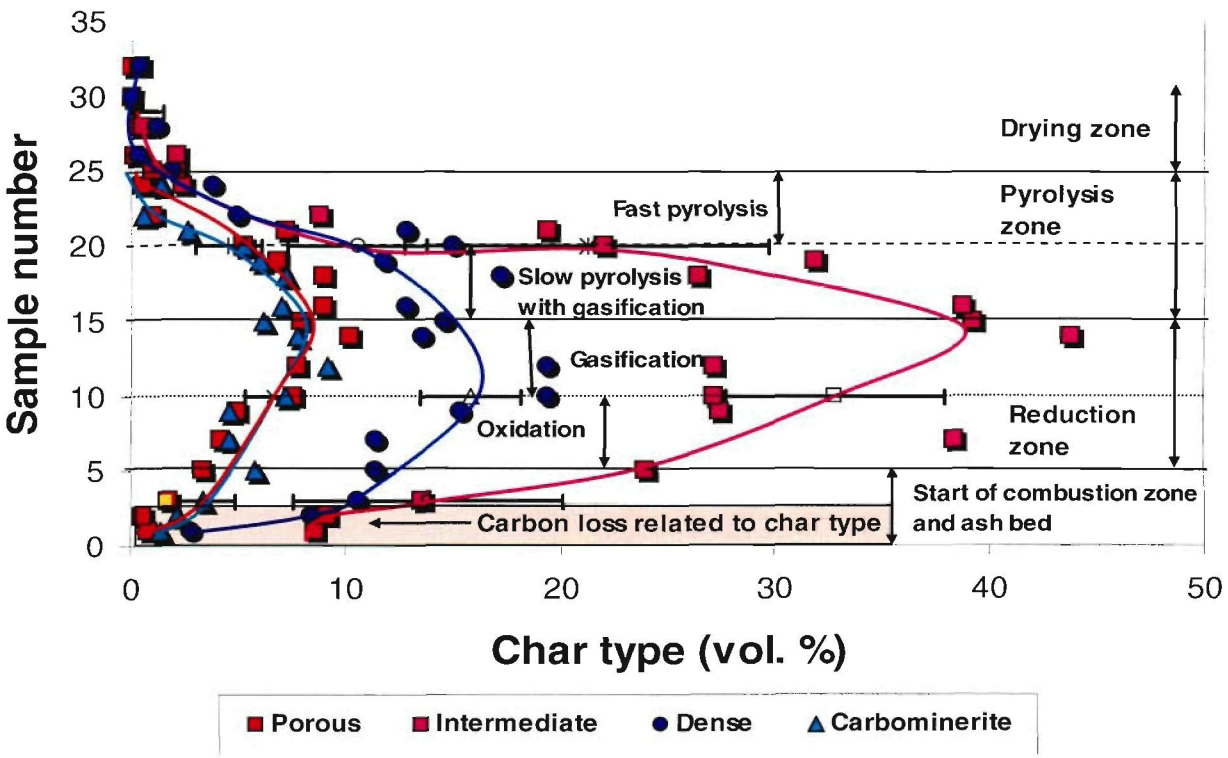

FIGURE 3.43: FIGURE SHOWING THE CHAR PARTICLE TYPE ANALYSIS (vol. %) AS A FUNCTION OF BED DEPTH FOR THE GG41 GASIFIER TURN-OUT SAMPLES (AS RECEIVED BASE)

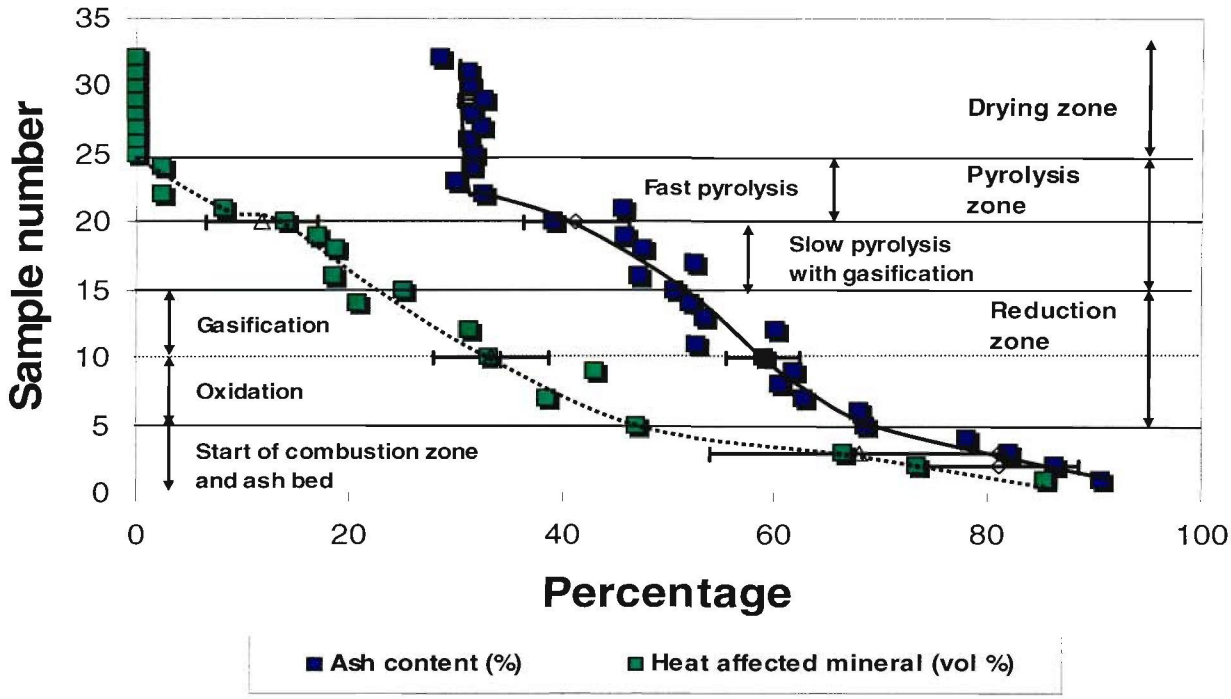

FIGURE 3.44: FIGURE DEPICTING THE HEAT-AFFECTED MINERAL (vol. %) AND ASH (%) PROFILES FOR THE GG41 GASIFIER (AS RECEIVED BASE)

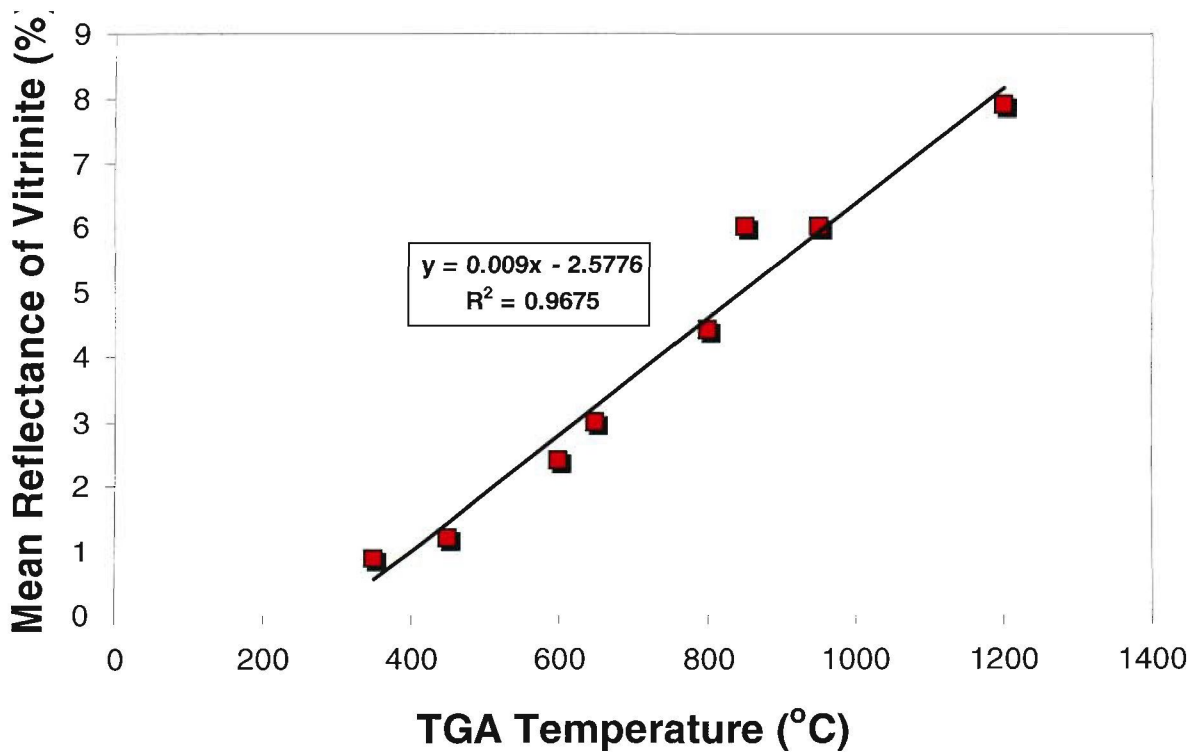

FIGURE 3.45: CHART SHOWING THE MEAN OPTICAL REFLECTANCE AND TEMPERATURE CALIBRATION CURVE FOR THE GG41 FEED COAL SAMPLE 32 (AS RECEIVED BASE)

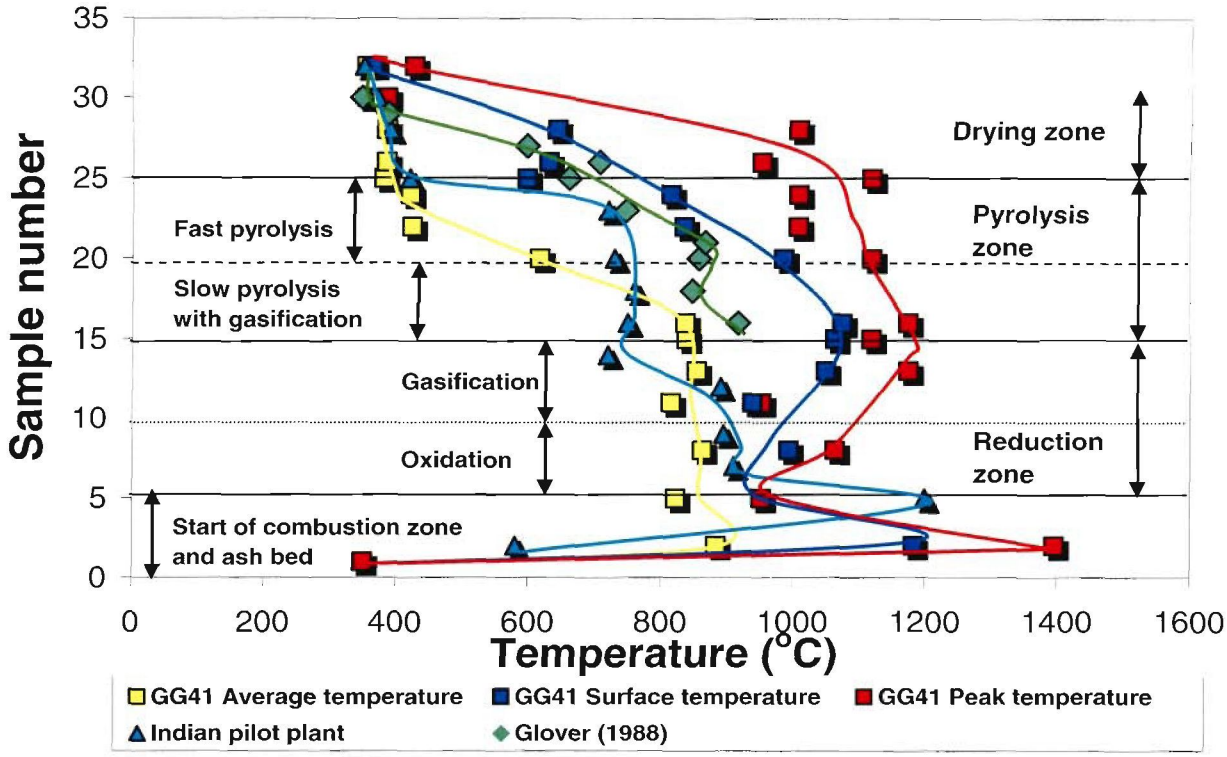

FIGURE 3.46: GRAPH DEPICTING THE SOLIDS TEMPERATURE PROFILES OBTAINED FOR THE GG41 GASIFIER SHOWING AVERAGE, SURFACE AND PEAK TEMPERATURES (°C), COMPARED TO THE FACTORISED INDIAN PILOT PLANT DATA AND THE #15 SASOLBURG MK III GASIFIER (AS RECEIVED BASE)

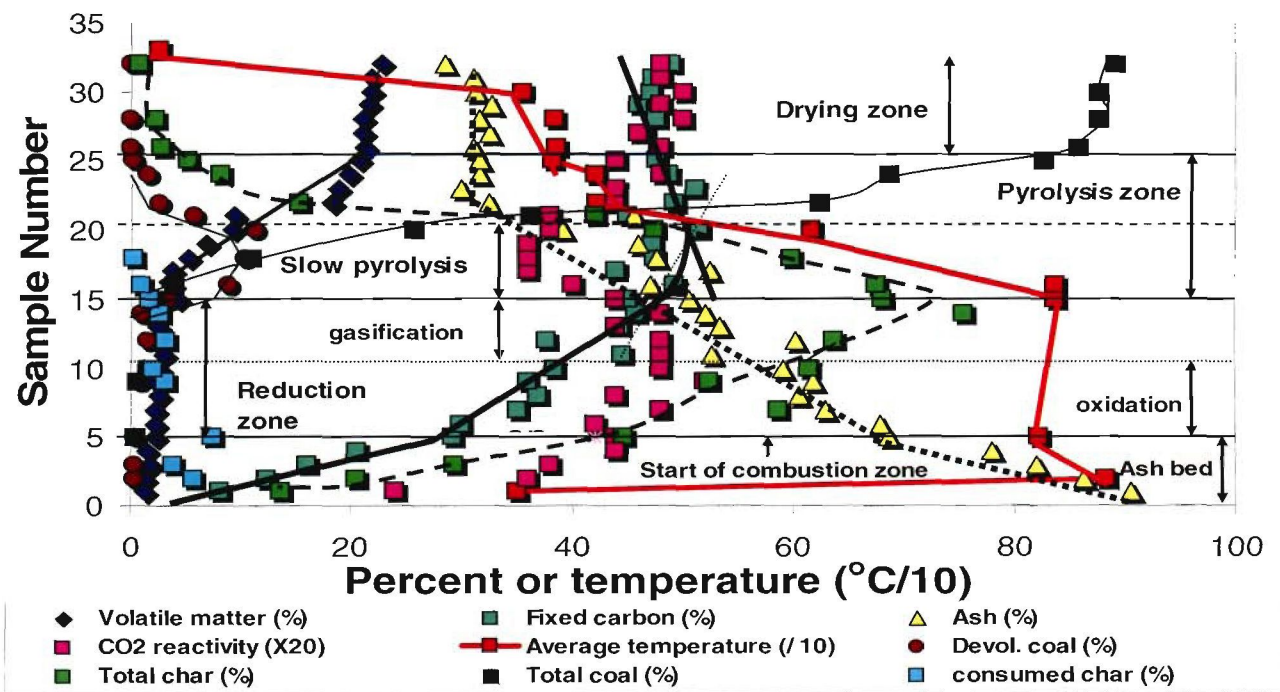

FIGURE 3.47: SCHEMATIC DIAGRAM, DEPICTING A "PAN-CAKE" MODEL OF THE SASOL-LURGI MK IV GG41 GASIFIER SHOWING REACTION ZONES WITH RESPECT TO CHEMICAL AND PETROGRAPHICAL PROPERTY PROFILES (AS RECEIVED BASE)

TABLE 3.1: TABLE SHOWING THE STATISTICAL AVERAGE CHEMICAL PROPERTY RANGE, CALCULATED FOR THE GG41 GASIFIER IN RELATION TO THE FOUR REACTION ZONES IDENTIFIED

(Green: properties are significantly different from one another; Red: properties are not significantly different)

Chemical property	Drying zone	Pyrolysis zone	Reduction zone	Combustion zone (ash-bed)
VM (%) dry	21.1 – 22.0	6.8 – 15.1	2.2 – 2.6	1.3 – 2.0
FC (%) dry	46.5 – 47.4	46.4 – 49.3	35.3 – 42.1	10.1 – 24.3
Ash (%) dry	30.2 – 32.2	36.2 – 46.3	55.4 – 62.4	73.7 – 88.5
Normalised VM (kg/100kg ash)	65.8 – 73.0	16.1 – 45.8	3.6 – 4.6	1.5 – 2.7
Fischer tar (%)	2.0 – 2.5	0.1 – 1.1	0	0
Normalised FC (kg/100kg ash)	144.7 – 159.3	103.4 – 139.9	57.2 – 76.6	10.9 – 33.8
C conversion (%)	7.2 – 15.7	18.5 – 39.8	55.4 – 66.7	80.3 – 93.7
DT (°C)	1283 – 1300	1287.0 – 1300.4	1291.7 – 1300.1	1289.6 – 1308.0
ST (°C)	1323 –1336	1312.2 – 1323.3	1314.0 – 1320.0	1320.3 – 1324.9
HT (°C)	1340 – 1358	1326.6 – 1336.3	1330.8 – 1337.0	1342.2 – 1351.8
FT (°C)	1353 – 1373	1350.1 – 1362.7	1352.2 – 1363.3	1361.7 – 1377.5
Carbon : Hydrogen ratio	19.4 – 20.3	36.2 – 70.3	117.4 – 134.1	90.4 – 143.7
Normalised C (kg/100kg ash)	163.9 – 180.7	105.9 – 152.3	57.1 – 75.6	12.3 – 33.8
Normalised H (kg/100kg ash)	8.1 – 9.3	2.0 – 5.5	0.5 – 0.6	0.1 – 0.3
Normalised N (kg/100kg ash)	4.1 – 4.6	1.8 – 3.5	0.7 – 1.0	0.2 – 0.4
Normalised S (kg/100kg ash)	2.7 – 3.5	1.4 – 2.1	0.8 – 1.1	0.3 – 0.7
Normalised O (kg/100kg ash)	27.0 – 29.1	5.2 – 17.9	0.6 – 1.4	0.3 – 1.1
CO_2 reactivity (h^{-1})	2.4 – 2.5	1.9 – 2.1	2.2 – 2.4	1.5 – 2.3

TABLE 3.2: TABLE SHOWING THE STATISTICAL AVERAGE CHEMICAL PROPERTY RANGE, CALCULATED FOR THE FACTORISED INDIAN PILOT PLANT DATA [KRISHNUDU, *et. al.*, 1989a,b] AND [GLOVER, 1988] IN RELATION TO THE FOUR REACTION ZONES IDENTIFIED

(Green: properties are significantly different from one another; Red: properties are not

Chemical property	Drying zone	Pyrolysis zone	Reduction zone	Combustion zone (ash-bed)
Indian pilot plant: Normalised VM (kg/100kg ash)	64.6 – 73.8	8.4 – 28.8	4.9 – 7.0	2.6 – 4.7
Indian pilot plant: Normalised FC (kg/100kg ash)	115.7 – 123.7	80.0 – 105.4	53.5 – 80.0	10.3 – 39.7
Indian pilot plant: Ash (%) dry	32.5 – 34.4	43.2 – 52.3	58.5 – 62.1	67.6 – 87.3
C conversion (%) [Krishnudu, et. al., 1989,a,b]	-0.6 – 6.2	15.8 – 31.2	47.6 – 54.0	65.9 – 91.2
C conversion (%)#16 I gasifier [Glover, 1988]	No data	22.5 – 54.2	No data	No data

TABLE 3.3: TABLE SHOWING THE STATISTICAL AVERAGE PHYSICAL PROPERTY RANGE, CALCULATED FOR THE GG41 GASIFIER IN RELATION TO THE FOUR REACTION ZONES IDENTIFIED

(Green: properties are significantly different from one another; Red: properties are not)

Physical property	Drying zone	Pyrolysis zone	Reduction zone	Combustion zone (ash-bed)
Bulk density (kg/m^3)	1125.5 – 1192.6	905.6 – 1028.0	890.1 – 996.4	1101.9 – 1170.9
True density (kg/m^3)	1651.7 – 1666.4	1807.7 – 2091.8	2246.2 – 2326.0	2431.7 – 2565.3
+ 25mm (%)	27.1 – 43.4	14.2 – 20.0	16.6 – 24.3	28.6 – 34.6
- 25mm + 6.3mm (%)	38.3 – 44.8	51.1 – 57.6	50.6 – 57.4	38.3 – 45.5
- 6.3mm (%)	18.2 – 28.3	23.0 – 32.3	21.7 – 29.4	21.2 – 31.9
Ergun Index	7.0 – 8.9	4.3 – 5.9	4.9 – 6.7	4.4 – 6.5
Thermal fragmentation (%)	12.7 – 16.2	5.6 – 12.4	3.4 – 5.6	5.0 – 7.7
Mechanical fragmentation (%)	27.6 – 31.3	32.4 – 36.0	33.1 – 35.9	34.2 – 37.2
Caking propensity (%)	6.2 – 11.3	1.7 – 5.5	0	0

TABLE 3.4: TABLE SHOWING THE STATISTICAL AVERAGE PETROGRAPHIC PROPERTY RANGE, CALCULATED FOR THE GG41 GASIFIER, THE FACTORISED INDIAN PILOT PLANT DATA [KRISHNUDU, *et. al.*, 1989a,b] AND [GLOVER, 1988] IN RELATION TO THE FOUR REACTION ZONES IDENTIFIED

(Green: properties are significantly different from one another; Red: properties are not)

Petrographic property	Drying zone	Pyrolysis zone	Reduction zone	Combustion zone (ash-bed)
GG41 Total char (vol %)	0.5 – 2.4	26.2 – 56.0	56.8 – 67.8	15.3 – 38.7
GG41 Consumed char (vol %)	0	0.4 – 2.1	1.9 – 3.0	4.1 – 7.2
GG41 Heated mineral (vol %)	0	6.6 – 17.1	27.9 – 38.9	54.0 – 82.1
GG41 Porous char (vol %)	0 – 0.3	3.2 – 7.4	5.4 – 8.5	0.5 – 2.8
GG41 intermediate char (vol %)	0.1 – 1.52	12.8 – 29.7	27.7 – 37.9	7.6 – 20.1
GG41 Dense char (vol %)	0.1 – 0.9	7.3 – 13.8	13.5 – 18.2	4.9 – 11.7
GG41 Carbominerite char (vol %)	0	3.0 – 6.1	5.4 – 8.0	1.5 – 4.9
GG41 Average temp. (°C)	356.2 – 382.8	461.6 – 711.4	828.0 – 860.6	429.5 – 941.9
GG41 Surface temp. (°C)	387.3 – 617.2	787.0 – 1003.7	958.1 – 1030.6	451.6 – 1205.7
GG41 Peak temp. (°C)	446.2 – 939.8	1051.1 – 1131.6	991.5 – 1136.5	439.5 – 1359.9
Indian pilot plant (temperature profile (°C)	355.2 - 384.8	590.9 - 761.1	795.2 - 912.3	505.7 - 1274.3
The #16 MK III gasifier temperature profile (°C)	382.6 - 636.4	760.4 - 871.6	No data	No data

TABLE 3.5: THE GG41 GASIFIER FEED COAL MACERAL GROUP ANALYSIS CONDUCTED ON COAL SAMPLE 32 (vol. %)

Vitrin	Liptinite	Inertinite						Total inertin.	Total Reactives	Mineral matter
		RSF	ISF	Fus/ scl	Mic	R.Int	I.Int			
20.0	2.6	14.8	33.6	1.6	0.2	3.4	6.8	42.2	18.2	17.0

RSF = reactive semi-fusinite, ISF = inert semi-fusinite, Fus/scl = fusinite & sclerotinite, Mic = micrinite R.Int = reactive inertodetrinite, I.Int = inert inertodetrinite, Total reactive macerals = vitrinite+liptinite+RSF Mmf = mineral matter free

TABLE 3.6: RELATIONSHIP BETWEEN THE GG41 REFLECTANCE OF VITRINITE (RoV %) AND CHAR MORPHOLOGY MEASUREMENTS TO DETERMINE SIGNIFICANT ZONAL LEVELS

(Colour-coding for similarity identification)

Sample ID			Particle type analysis	
GG41 zone	RoV %	Total coal	Total char	Total mineral
		(vol.%)	(vol.%)	(vol.%)
32	0.60	89.20	0.80	10.00
30	0.60	87.60	0.00	12.00
28	0.90	87.60	2.20	10.20
26	0.90	85.80	2.80	11.40
25	0.90	82.60	5.20	12.00
24	1.20	68.60	8.20	21.80
22	1.20	62.40	15.40	19.40
21		36.20	42.00	16.60
20	3.00	25.60	47.40	16.80
19		17.80	56.40	17.60
18		10.80	59.80	19.00
16	5.00	3.80	67.60	18.80
15	5.00	2.00	68.00	25.00
14		0.00	75.40	20.80
13	5.10			
12		0.00	63.60	31.80
10		1.40	61.40	33.20
9		0.60	52.40	43.00
8	5.20			
7		0.00	58.60	38.60
5	4.80	0.40	44.60	47.00
3		0.00	29.40	66.40
2	5.40	0.00	20.40	73.40
1		0.00	13.60	85.40

TABLE 3.7: RELATIONSHIP BETWEEN THE REFLECTANCE OF VITRINITE (RoV %) AND CHEMICAL PROPERTY MEASUREMENTS TO DETERMINE SIGNIFICANT ZONAL LEVELS

(Colour-coding for similarity identification)

Sample ID	RoV %	Chemical property							
GG41 zone		C (%dry)	H (%dry)	N (%dry)	S (%dry)	O (%dry)	VM (%dry)	CO_2 reactiv.	Tar (%)
32	0.60	55.76	2.94	1.44	1.09	8.87	22.70	2.40	2.50
30	0.60	53.35	2.73	1.35	1.00	8.67	21.80	2.50	2.13
28	0.90	53.20	2.59	1.34	0.78	8.39	20.90	2.50	2.00
26	0.90	53.75	2.61	1.33	0.85	8.66	21.20	2.40	2.10
25	0.90	54.34	2.62	1.36	0.82	8.46	20.80	2.20	2.10
24	1.20	54.44	2.39	1.34	0.93	7.40	19.80	2.40	1.60
22	1.20	55.58	2.08	1.37	0.76	6.91	18.20	2.20	1.10
21		47.16	1.08	0.88	0.71	3.57	9.50	1.90	0.00
20	3.00	52.66	1.14	1.01	0.59	3.10	9.30	1.90	
19		46.90	0.84	0.81	0.57	2.18	6.90	1.80	
18		47.33	0.71	0.79	0.58	1.49	5.10	1.80	
16	5.00	49.70	0.52	0.68	0.61	0.79	3.70	2.00	
15	5.00	44.39	0.47	0.61	0.65	0.98	4.30	2.20	
14		44.64	0.38	0.59	0.66	0.83	2.30	2.20	
13	5.10	44.00	0.30	0.53	0.64	0.23	2.40	2.20	
12		37.27	0.31	0.47	0.66	0.29	2.10	2.40	
10		38.11	0.33	0.48	0.58	0.80	2.50	2.40	
9		36.78	0.31	0.44	0.49	0.08	2.20	2.60	
8	5.20	36.79	0.29	0.46	0.52	0.84	2.60	2.20	
7		35.56	0.25	0.43	0.47	0.99	2.10	2.40	
5	4.80	28.78	0.21	0.36	0.54	0.71	2.20	2.20	
3		17.38	0.13	0.24	0.45	0.10	1.80	1.90	
2	5.40	12.91	0.12	0.19	0.47	0.71	1.30	1.80	
1		9.47	0.14	0.11	0.28	0.30	1.40	1.20	

TABLE 3.8: RELATIONSHIP BETWEEN THE GG41 REFLECTANCE OF VITRINITE (RoV %) AND PHYSICAL PROPERTY MEASUREMENTS TO DETERMINE SIGNIFICANT ZONAL LEVELS

(Colour-coding for similarity identification)

Sample ID	RoV %	Physical property					
GG41 zone		Bulk density	True density	PSD (%)	PSD (%)	PSD (%)	Ergun Index
		(kg/m^3)	(kg/m^3)	+25mm	-25+6.3mm	-6.3mm	
32	0.60	1143.00	1647.00	48.90	37.40	13.70	9.80
30	0.60	1240.00	1656.00	30.80	43.00	26.20	6.50
28	0.90	1135.00	1658.00	19.00	47.70	33.30	6.90
26	0.90	1158.00	1671.00	29.30	42.70	28.00	5.50
25	0.90	1071.00	1677.00	26.90	49.70	23.40	6.50
24	1.20	1122.00	1712.00	16.90	62.40	20.70	4.40
22	1.20	1051.00	1720.00	17.40	53.60	29.00	5.30
21		1082.00	1972.00	8.90	44.50	46.60	3.20
20	3.00	963.00	1939.00	11.80	53.10	35.10	4.80
19		897.00	2061.00	15.30	51.40	33.30	5.50
18		864.00	2127.00	18.40	56.20	25.40	6.20
16	5.00	840.00	2209.00	16.00	60.70	23.30	6.80
15	5.00	855.00	2126.00	15.50	63.60	20.90	7.10
14		841.00	2239.00	16.80	59.60	23.60	6.40
13	5.10	933.00	2187.00	9.10	53.60	37.30	3.90
12		909.00	2319.00	17.60	57.10	25.30	6.00
10		978.00	2289.00	21.50	49.60	28.90	5.10
9		1056.00	2309.00	21.60	47.00	31.40	5.00
8	5.20	955.00	2357.00	22.90	56.20	20.90	6.80
7		897.00	2297.00	23.80	54.90	21.30	6.60
5	4.80	1106.00	2381.00	32.00	48.70	19.30	7.10
3		1196.00	2499.00	29.30	37.80	32.90	4.20
2	5.40	1148.00	2551.00	31.50	40.60	27.90	5.10
1		1135.00	2579.00	37.00	41.80	21.20	6.30

3 CHEMICAL PROPERTY PROFILES

Chemical properties of coal which impact on gasification performance relate to those processes which do effect a change in chemical constitution, these in turn may lead to changes in physical properties such as particle size distribution and surface area of the coal [Morgan, 1991]. The turn-out samples obtained from the GG41 gasifier were characterised to understand and interpret the internal residual volatile matter, fixed carbon and ash characterisation profiles (proximate analysis results). These are firstly discussed and related to the Fischer tar, carbon conversion and ash fusion temperature profiles. The C, H, N, S and oxygen distribution profiles (ultimate analysis results) obtained are discussed in the context of thermodynamic equilibrium model predictions, using the Fact-Sage simulation package. A discussion on coal char reactivity concludes the overview.

3.1 PROXIMATE ANALYSIS RESULTS

It should once again be put into perspective that the fixed-bed gasification process is a dynamic and complex one. The "new-to-Sasol" dissection turn-out methodology employed in this study is of course an oversimplification of the dynamic radial variations continuously occurring within the reactor, but does provide the reader with a picture of the axial incrementally-averaged profiles occurring.

The volatile matter, ash and fixed carbon distribution profiles (on a dry basis) obtained from the GG41 gasifier turn-out sampling campaign are given in Table 3.1 and Figure 3.1. Corresponding chemical property data relating to the work by Krishnudu, *et. al.,* [1989a,b] and Glover [1988, 1991] is given in Table 3.2.

3.1.1 Volatile matter (VM) distribution profile

From the data shown in Table 3.1, it can be observed that the percentage VM content ranges from 21.1 – 22.0, 6.8 – 15.1, 2.2 – 2.6 and 1.3 – 2.0 in the drying, pyrolysis, reduction, and combustion (ash-bed) zones respectively. It can be concluded that the average VM content differs between the four reaction zones identified, because the confidence range values do not overlap between the zones.

From the trends shown in Figure 3.1, it appears that a very distinctive residual volatile matter distribution profile is obtained. From these results it is clear that a marginal loss of volatile matter (on a dry basis) occurs within the Bosman skirt (drying zone)

area of the GG41 gasifier, i.e. constant at c.a. 20% VM from a feed coal VM content of 23% (sample 32) which is slightly lower than the typical Sasol Coal Supply (SCS) benchmark of 24.9% minimum. This slightly lower feed coal VM content in the GG41 case, can be explained by the fact that this "coal" had been at some elevated temperature at the top of the gasifier. Although considered "feed-coal" in this case, some small difference in properties will be evident when compared to coal in the bunker, feeding the bank of gasifiers, which is only exposed to ambient temperature. The temperature profile given in Figure 3.46 shows that the GG41 gasifier solids average temperature, surface temperature, and peak temperature ranged from 356 – 383°C, 387 – 617°C, and 446 – 940°C respectively, within the drying zone of the GG41 gasifier. Descriptors of these three temperature measurements are given in Section 3.3.3.2 in Chapter 2.

A very sharp decrease in volatile matter content is observed from sample 24 (c.a. 7m above the ash lock). This decrease in volatile matter probably constitutes the start of the pyrolysis zone, which tends to change its shape once again at sample position 15 (2% VM), which is at a position c.a. 4.5m above the ash lock. This height position clearly shows the completion of the pyrolysis reaction zone (see Figure 3.1).

Below sample 15, the VM is only marginally reduced to a final value of 1%VM in sample 1 at the ash-grate. The reason for this loss in volatiles to the ash can possibly be explained by the fact that at high reaction temperatures within the combustion zone, the char pores collapse and the inorganic ash chemistry plays a strong role, resulting in glass encapsulation of the char matrix, which still contains low levels of volatile matter [Matjie, 2005].

In the work by Glover [1988] it was observed that volatile recondensation near the top of the gasifier may take place, since the volatile matter content was found to increase considerably above that of the extreme top of the bed. It was suggested that this phenomenon is probably the result of sample mixing as the char was unloaded from the gasifier. However, this increase in volatile matter at the top of the bed had also been observed by Glover [1991] in gasifier dig-outs in Secunda and would therefore appear to be a real effect specific to some coal types. Unfortunately no information regarding the Secunda coal blends were given in Glover's [1988, 1991] reports.

When recalculating the volatile matter data on a normalised constant ash content (kg VM / 100kg ash flow) for the GG41 gasifier, the recondensation phenomena is somewhat apparent (see Figure 3.2).

On this normalised basis, the volatile matter profile decreases from 79.6kg VM / 100kg ash for the GG41 feed coal (sample 32), to 66.4kg VM / 100kg ash for sample 28 (about half way into the Bosman skirt). A very slight increase in volatile matter content from 65.1kg VM / 100kg ash to 65.6kg VM / 100kg ash is observed for samples 27 to 25. Within the experimental error associated with sampling over 100 tons of material and micronizing the sub-sample for a particular analysis, as well as the analytical error typically involved, it would be prudent to ascribe that definite recondensation of volatile matter was evident when observing only the GG41 residual volatile matter profile results. Further analytical results, i.e. the residual Fischer tar content is needed to support this interesting observation and will be addressed in Figure 3.3.

The factorised Indian pilot plant data, explaining the residual volatile matter at constant ash content is also shown in Figure 3.2, where it can be observed that the data trend compares well with the commercial-scale GG41 gasifier data curve, but does not reveal any sign of VM increase in the top section of the gasifier. The volatile matter investigated in the Indian case also appears to be evolved at a slightly faster rate, when compared to the GG41 trend data up to sample 18. This is to be expected, since the particle size distribution is effectively finer for the Indian pilot plant case (top size 25mm versus 100mm for the GG41 gasifier), and chemical reactions are envisaged to be completed at a higher rate than for coarser particles, given mass and heat transfer limitations, which are typically encountered across coarse particles [Keyser, *et. al.*, 2005]. In general, a very similar and comparative volatile matter release curve is evident between these two cases, thereby validating the factorising approach with respect to comparison purposes.

Unfortunately, Glovers' results from the Sasolburg #16 MK III gasifier turn-out could not be superimposed in Figure 3.2, since the volatile matter data shown is a plot of relative volatile matter versus dimensionless distance above the ash-grate; no mention of how these calculations are done are given [Glover, 1988]. None-the-less, a qualitative comparison should suffice in terms of the further discussion on the volatile matter recondensation phenomena.

When viewing the Fischer tar residual distribution profile for the GG41 gasifier (see Figure 3.3), more information on the matter of volatile matter recondensation is observed. The Fischer tar content of the feed coal (sample 32) is shown as 2.5%. As expected, the tar content decreases with an increase in bed depth. A gradual decrease in Fischer tar content is initially observed from samples 32 to 30, further

declining to 2% tar content as the coal descends in the gasifier within the Bosman skirt area. Samples 27 to 25 then show a 0.2% increase in the Fischer tar content (8% on a feed basis), which occurs at exactly the same position as the normalised residual volatile matter content at constant ash content, indicated in Figure 3.2.

This can then be evidence that volatile matter recondensation is indeed observed in the GG41 gasifier. This finding is in agreement with Glover's earlier observations [Glover, 1988, 1991]. The coal sources and blends used in Secunda at present, have also changed quite significantly from the time that Glover did his original work, but the recondensation phenomena are still apparent and validated in the findings here.

From Figure 3.3 it is further apparent that the Fischer tar distribution decreases once more, as the coal enters the pyrolysis zone of the gasifier (sample 24), declining quite rapidly within the bed and disappearing completely at sample 21, which is roughly midway within the pyrolysis zone, at the start of the postulated "slow pyrolysis with gasification" region (Figure 3.1).

Glover [1991] also found that volatile evolution was independent of particle size. In this study, although the particle size distribution was determined for the 32 x GG41 gasifier samples, the distribution profiles characterised in this study were not conducted on a size-by-size basis, but rather as an averaged composite. No verdict relating to Glover's [1991] finding could be given in the present investigation.

3.1.2 Fixed carbon (FC) distribution profile

The fixed carbon distribution profile results (on a dry basis) obtained from the GG41 gasifier turn-out sampling campaign are given in Table 3.1 and Figure 3.1.

From the data shown in Table 3.1, it can be observed that the percentage FC content ranges from 46 – 47, 46 – 49, 35 – 42 and 10 – 24 in the drying, pyrolysis, reduction, and combustion (ash-bed) zones respectively. It can be concluded that the average percentage FC content is not significantly different between the drying and pyrolysis zones, but these zones are significantly different to the reduction and combustion zones with respect to FC behaviour. This is to be expected, since the drying and pyrolysis zones essentially prepare the char for the later reduction and combustion processes [Morgan, 1991], wherein inherent variability due to excessive chemical reaction is significantly evident.

From the trend data shown in Figure 3.1 it can be observed that the GG41 feed coal FC content (sample 32) was 49% and within the typical SCS blend range of between 44.1 and 54.6%.

It can be observed from the FC profile that a slight initial increase in FC content occurred analogous to the decrease observed in the VM curve, i.e. from 48.9% FC in the GG41 feed coal sample to 51.6% FC in sample 20 (c.a. 6m above the ash discharge grate).

The FC trend then shows a slow reversal in slope from 47.2% FC to 45.7% FC for samples 19 through to 15, where the onset of some gasification is postulated. When considering the above-mentioned observation that the pyrolysis zone is clearly depicted to range from the exit of the Bosman skirt (sample 25) up to the end of pyrolysis (sample 15), then there is a clear overlap in zones, as would be expected in a dynamic operational environment such as a commercial-scale gasifier reactor.

Reduction is postulated to occur from sample 14 (4.2 m above the ash-grate), where the CO_2 and H_2O gasification reactions are expected to occur, thereby reducing the carbon content by producing CO and H_2 etc. It can be clearly observed from the FC curve that the slope of the gasification and partial oxidation regime within the reduction zone changes significantly when compared to the two slope changes observed higher up in the gasifier, i.e. during drying and pyrolysis, as well as at the onset of slow gasification. The FC content in the reduction zone is reduced from 45.7% FC (sample 14) to 29.2% FC in sample 6 (2.2 m above the ash-grate).

Rapid fixed carbon reduction is finally observed in a fourth regime, where the onset of the combustion zone (sample 5) and ash-bed (samples 4 to 1) is evident. As oxygen and steam are added to the gasifier, counter-currently to the descending charge, the oxygen combusts the remaining char, whilst excess steam is used to control the formation of excessive slag and melting of the mineral phases present. The fixed carbon is rapidly reduced from 29% (sample 5) to 8.1% in sample 1 at the ash-grate.

The amount of fixed carbon in the ash is higher than the normal operational FC losses, but can be explained as follows: (1) although cooling occurs in the ash-lock below the grate, carbon is still reacted on. In the GG41 gasifier sampling campaign, the ash-lock was empty and used as a hopper for sampling, so the full extent of the reaction was not observed as would be the case in practice and (2) the GG41 gasifier turn-out was conducted after water quenching. In such a case, not all of the reactions

that normally would be expected to occur, would be evident. However, the value of 8.1% FC loss to the ash in the GG41 gasifier case does not differ too much from plant operational data, where 6% FC losses are generally standard [Slaghuis, 2004].

When recalculating the fixed carbon data on a normalised constant ash content (kg FC / 100kg ash flow) for the GG41 gasifier and the factorised Indian pilot plant data, the trends as shown in Figure 3.4 are obtained. Unfortunately Glover's fixed carbon profile [Glover, 1988] could not be included in this graph, since this detail information was not discernible from the report.

From the profiles shown in Figure 3.4, it can be observed that the FC trend curves begin at different levels of FC / 100 kg of ash content, i.e. 172 and 116 for the GG41 gasifier and Indian cases respectively. This difference is related to the higher ash content (34.4% on a dry basis) of the Indian coal and consequent fixed carbon content of 40.1%; compared to a GG41 gasifier feed ash content of 28.5% (dry basis) and fixed carbon content of 48.9%.

When comparing the data in the drying zone (samples 32 to 25), the normalised FC at constant ash content increases from 116 to 125 kg FC / 100kg ash flow for the Indian case, while decreasing from 172 to 151 kg FC / 100kg ash flow in the case of the GG41 gasifier. The loss of FC within the drying zone of the GG41 gasifier suggests that "hot- spots" and channel-burning caused by fluctuations in peak temperature have possibly occurred, thereby affecting the FC content in this area of the gasifier (see temperature profile in Figure 3.46).

From Figure 3.4 it can further be seen that within the pyrolysis zone (samples 25 to 15) a continuous downward trend in FC is observed for the Indian case, i.e. from 125 to 68 kg FC flow at constant ash content; whereas a more scattered FC profile is observed for the GG41 gasifier, although a general downward trend is also observed, i.e. 150 to 90 kg FC / 100kg ash flow. A change in the GG41 gasifier FC profile is evident in the "slow pyrolysis with gasification" region, i.e. from samples 20 to 15 when compared to samples 25 to 20. Within this endothermic region of the gasifier, lump coal is expected to have a definitive heat transfer gradient across the particles. The wider scatter observed in the GG41 gasifier trend data in this region, when compared to the Indian case, can possibly be ascribed to much larger heat and mass transfer effects associated with the coarser nature of the particles (<100mm) and (<25mm) for the GG41 gasifier and factorized Indian pilot plant data respectively. The temperature profile shown in Figure 3.46 clearly shows the effect of heat transfer

limitations occurring within the top half of the gasifier, where large differences in temperature are observed between the average, surface and peak temperature values.

In the reduction zone of the GG41 gasifier (samples 14 to 6), the two FC trend lines converge at sample position 10 and retain this identical FC profile downwards to the ash-grate. Cleary similar gasification / combustion, and hence carbon conversion mechanisms are evident in this region of the gasifier. However, the interesting slope of the FC curves shown from samples 14 to 10 needs some explanation.

The combustion region of the GG41 gasifier (sample 5 to 1) is oxygen-rich and the reaction $C + O_2 \rightarrow CO_2$ (ΔH = - 405.9 kJ/mol) produces the heat for the auto-thermal gasification reactions higher up in the gasifier. Partial oxidation is postulated to occur above the combustion zone, where $C + 0.5\ O_2 \rightarrow CO$ (ΔH = - 123.1 kJ/mol), for samples 6 to 9. In both cases the reactions are exothermic. However, when observing the temperature profile data given in Figure 3.46, it can be observed that a downward trend in the GG41 gasifier surface and peak temperatures occurs for samples 14 to 10, when compared to respective temperature trends higher up in the pyrolysis zone. This behaviour could thus possibly be an indication of a "heat-sink" phenomenon, where the endothermic Boudouard reaction $C + CO_2 \rightarrow 2CO$ (ΔH = 159.7 kJ/mol) occurs within the GG41 gasifier.

In the combustion zone (ash-bed), it is interesting to note that a 5% reduction in FC loss to the ash is evident for the GG41 gasifier when compared to the Indian case, i.e. 13.1% and 8.1% FC on a normalised mass basis respectively. Although there is a difference in FC losses for the two cases shown in Figure 3.4, losses to the ash occur in both cases. This observation supports the theory by Slaghuis [2004], which states that excess steam added to the bottom of the fixed-bed non-slagging gasifier for ash melting control purposes, has a "quenching" effect on the exothermic char reactions in this region. Therefore, there will always be unconsumed char in the gasifier ash.

The percentage FC conversion results for the GG41 gasifier are given in Table 3.1 and are graphically depicted together with results from the study by Glover [1988] and the factorised Indian pilot plant data [Krishnudu, *et. al.*, 1989a] in Figure 3.5.

From the data shown in Table 3.1, it can be observed that the percentage FC conversion ranged from: 7 - 16, 19 - 40, 55 - 67 and 80 - 94 in the drying, pyrolysis, reduction and combustion zones respectively; thereby indicating a constant increase in the average % FC conversion as the charge descended within the GG41 gasifier.

From Figure 3.5 it is immediately evident that some anomalies in the trend data occur, i.e. some slight overbalances (c.a. 6.2%) are obtained for the factorised Indian pilot plant data (samples 32 to 25). Also, from the GG41 gasifier conversion profile it would appear that some carbon (up to 15% FC) was consumed in the upper part of the gasifier; the likelihood of channel-burning, as discussed earlier, being a possible reason. However, if the GG41 gasifier FC results for sample 32 and 17 were ignored in the drying and pyrolysis regions due to scatter (see large error bar shown in Figure 3.4), then the FC conversion in this region would be significantly reduced and more in line with expectation. Repeatability of the sampling programme should provide more data for statistical comparison in future studies, which will then validate whether FC conversion actually occurred within the drying zone or not.

Generally however, the three trends appear quite similar in the top half (fast pyrolysis region) of the pyrolysis zone (samples 25 to 20), where approximately 30% carbon conversion has occurred. From about 40% carbon conversion onwards, the GG41 gasifier and Indian pilot plant trends deviate from the #15 Sasolburg gasifier case. This can be explained by the fact that the reactivity of the Sasolburg coals is known to be higher than for the Secunda coals, i.e. >6 hr^{-1} and from 2 to 5 hr^{-1} respectively [Van Dyk, *et. al.,* 2001c]. This implies that conversion occurs at a higher rate for coals of higher reactivity. Consequently c.a. 70% carbon conversion is observed for the Sasolburg coal at sample position 17 (5m above the GG41 gasifier ash-grate), compared to 70% carbon conversion for the GG41 gasifier and Indian case at the fire-bed position at sample 5 (2m above the ash-grate).

The carbon conversion profiles for samples 14 to 10 also appear to occur at a slower rate, when compared to the exothermic oxidation region (samples 9 to 6) and combustion region (samples 5 to 1) for both the GG41 gasifier and the Indian cases. This can then be evidence of the endothermic region of the gasifier, where solid carbon reacts with CO_2 in a "heat-sink" zone of lower carbon conversion rate, than for the exothermic zone below.

Furthermore, since these latter two coals follow similar carbon conversion profiles, it is highly likely that the Indian Godvari Khani-Ramagundam coal, being of Gondwanaland origin [Krishnudu, *et. al.,* 1989a,b] has a similar CO_2 reactivity when compared to the typical Secunda SCS blend. This will be discussed in Section 3.3 of this Chapter. Because of the higher ash fusion temperatures (AFT's) of the Sasolburg coal, the Sasolburg gasification operations controlled the gasifiers at a higher temperature than is the case for the Secunda operations, where the AFT's are lower. Because of the higher reactivity of the Sasolburg coal, in relation to the Secunda coal,

the reaction kinetics are also faster. Consequently a higher ash-bed is observed than is the case at Secunda. The higher operating temperatures at a higher ash-bed height, resulted in a higher gas yield at Sasolburg, at the expense of a lower tar yield due to cracking reactions. At Secunda, where a cooler gasifier is run and the ash-beds are expected to be lower, a higher tar yield is obtained when compared to the Sasolburg case [Glover, 1991; Van Dyk, *et. al.*, 2001c].

Glover [1991] measured the carbon conversion on a composited sample of the total particle size distribution from a dig-out of the #15 gasifier in Sasolburg. Results from this gasifier indicated that within the adiabatic core of the bed, carbon conversion reached a value of 70% at the char-ash interface (fire-bed region), and that there was almost complete conversion a short distance into the ash layer. When comparing the fixed carbon conversion profile of the GG41 gasifier in this study (Figure 3.5) to Glover's comment as to the position of the observed char-ash interface, it is apparent that the char-ash interface in the case of the GG41 gasifier should possibly be at sample position 6, a short distance away from sample position 5, where the combustion zone and ash-bed are postulated to be; this reasoning is thus in agreement with Glover's [1988] observation. For the less reactive Secunda SCS blend coal, a lower char-ash interface bed position is expected, and is indeed observed to be the case when compared to the data for the #15 gasifier in Sasolburg, where the char-ash interface occurred in the middle of the gasifier.

3.1.3 Ash distribution profile

The ash distribution profile results (on a dry basis) obtained from the GG41 gasifier turn-out sampling campaign are given in Table 3.1 and Figure 3.1.

From the data shown in Table 3.1, it is clear that the percentage ash content ranges from 30 - 32, 36 - 46, 55 - 62 and 74 - 89 in the drying, pyrolysis, reduction and combustion (ash-bed) zones respectively; the average ash content is thus significantly different between the four zones identified. The 2% variance obtained in the ash content for the drying zone, suggests that some marginal charring had occurred, which further supports the FC conversion anomaly discussed earlier, where the likelihood of "hot–spots" was given as a possible reason for the variance.

From Figure 3.1 it is apparent that in the early drying and devolatilisation processes, that the ash percentage remains reasonably constant from a feed ash content of 29% (sample 32) to 32.5% ash (sample 21). At sample position 20, a sharp slope change

is observed as slow gasification commences; carbon is converted and the ash concentration subsequently increases. This process continues fairly linearly up to sample position 5 through the rapid or "fast gasification" and oxidation zones into combustion, where a further step change in the shape is evident. The ash content increased to 68.5% in sample 5 (2m from the ash-grate); up to 91% ash was contained in sample 1 at the ash-grate itself.

The GG41 gasifier ash content data visible in Figure 3.1 is shown together with the factorised Indian pilot plant data in Figure 3.6. From Figure 3.6 it can be observed that the Indian ash content trend follows the GG41 data very closely, with convergence of the curves from about sample 10 (start of oxidation), downwards to the ash-grate. The Indian ash content data is always higher than that of the GG41 gasifier in the top part of the gasifier (up to sample 10), because of the higher ash content present in the feed coal for the Indian case.

In both experimental trends, the ash content remains relatively constant in the drying zone (Bosman skirt region of the gasifier), but a sharp increase is observed when the charge is exposed to pyrolysis conditions (up to sample 20). The trend lines show a slower ash content development in the gasification region of the gasifier (up to about sample 10) in both cases. At this convergence point, a slope change is observed for both cases. At sample position 5 both curves show a final slope change, probably highlighting the onset of combustion. Now, with an understanding of the ash content profiles, it is necessary to discuss the GG41 gasifier internal ash fusion temperature (AFT) profile obtained.

The ash fusion temperature (AFT) of a coal source gives an indication of the extent to which ash agglomeration and ash clinkering are likely to occur within the gasifier. Ash clinkering inside the gasifier can cause channel-burning, pressure drop problems and unstable gasifier operation [Van Dyk, 2006]. The results of an AFT analysis consist of four temperatures, namely: (1) initial deformation temperature DT, (2) softening temperature ST, (3) hemispherical temperature HT and (4) flow temperature FT [Slegeir, et. al.,1988]. There are, however, concerns that the standard AFT test is subjective [Carpenter, 2002], being based on observations rather than measurements, and that poor reproducibility is obtained. Despite the fact that mean deviations for the average and expert systems of about 38°C are attainable, a semi-qualitative interpretation of the GG41 gasifier AFT (oxidizing) results will be attempted. The ash fusion distribution profile results obtained from the GG41 gasifier turn-out sampling campaign are given in Table 3.1 and Figure 3.7, from which it can be observed that

the average DT (°C) does not change significantly between the four zones identified, because an almost straight line is obtained over the entire sampling range.

The ST (°C) average range shows a decrease in temperature, with a minimum in the slow pyrolysis with gasification region of the GG41 gasifier, after which it increases again to almost the same value as in the drying zone. Due to the lower ST temperatures observed in the pyrolysis and reduction zones, when compared to the drying and combustion zones, the change implies that the ash-forming minerals are exhibiting a "softening" tendency in this particular region of the GG41 gasifier.

From Table 3.1, it can also be seen that the HT (°C) average range shows the same trend as was discussed for the ST average range. Due to the lower HT temperatures observed in the pyrolysis and reduction zones, when compared to the drying and combustion zones, the change implies that the ash-forming minerals are exhibiting a "change in shape" in this particular region of the GG41 gasifier.

Finally, from the FT (°C) average range it can be observed that there is no significant difference in ash fusion flow temperature exhibited in the drying, pyrolysis and reduction zones, but that the FT is significantly different in the ash-bed when compared to the two zones above it. This finding possibly suggests that further flow / melting of the mineral species also occurs within the combustion zone of the GG41 gasifier.

From Figure 3.7 it is clear that the four AFT profiles of the GG41 gasifier range between 1280 (°C) and 1380 (°C). Within the drying zone of the gasifier (samples 32 to 25), the trends show a relatively big difference between the DT and the other three temperatures measured. However, in the pyrolysis zone a smaller difference is observed where the DT, ST and HT are within 30°C of one another. This may be an indication of the onset of "sintering and melting" of the minerals occurring in this highly reducing reactor zone within the GG41 gasifier.

In the "slow pyrolysis with gasification" region of the GG41 gasifier (samples 20 to 15), a sharp inflection is observed at sample position 20, where overlap of the ST, HT and FT data occurs. At the end of pyrolysis (sample 15), a similar characteristic downward inflection in ash fusion temperature is observed for the DT, ST and HT as was seen at sample position 20. At this point the DT and ST have a span of only 10 °C, which could point to a second wave of melting occurring in the middle of the gasifier.

From the GG41 gasifier bulk density profile, given in Figure 3.23, it can be seen that a change in the trend occurs at sample position 15 (middle of the GG41 gasifier). The reversal in bulk density observed, is argued to be due to the fact that the ash layers formed at about sample position 15, have flaked off. These ash transformed mineral layers then pack the voids between the larger char particles, subsequently increasing the bulk density towards the ash-grate (sample 1). These flakes, having a high surface area, are also expected to fuse and agglomerate, forming clinkers within the gasifier.

Ash mineral agglomeration effects also clearly play a role in the measured GG41 particle size distribution profile obtained. When observing Figure 3.29 it is clear that the bulk particle size distribution range of -25mm + 6mm content dramatically decreases downward towards the ash-grate, and the +25mm material (Figure 3.28) subsequently increases from sample position 15. This is clear evidence of the ash mineral agglomeration chemistry at work, suggesting that when trying to relate this phenomenon to the ash fusion temperature data given in Figure 3.7, that the end of the pyrolysis zone is a good indicator of the position from which slagging and agglomeration commence in the case of the GG41 gasifier.

It should be noted that it is extremely difficult to logically interpret the AFT behaviour in the reduction and combustion (ash-bed) zones of the GG41 gasifier (samples 14 to 1 in Figure 3.7), but the trends do suggest that a steady increase in AFT occurs down towards the ash-grate (sample 1). Crystallisation of molten species, i.e. anorthite, as well as the formation of alumino-silicate glass, are expected to influence the AFT measurements in the bottom part of the GG41 gasifier and could explain the increasing AFT trends observed in this region [Matjie, 2005; Van Dyk, 2006].

The GG41 temperature profile given in Figure 3.46 shows that the average, surface and peak temperatures were 650°C, 1000°C, and 1150°C respectively at sample position 20, where the first wave of sintering is postulated to occur. Pyrite (FeS_2) is transformed to FeS at 300°C (Figure 3.16) and carbonates to their respective oxides, together with the release of CO_2 within the temperature range given. At sample position 15, the GG41 gasifier solid temperature profile (Figure 3.46) indicates that the temperature range has reached a maximum of 1200°C (excluding the "hot-spot" position shown to be present in the ash-bed), resulting in a second wave of sintering / melting occurring in the middle of the GG41 gasifier.

The sulphur chemistry findings from this study are in agreement with the observations of Waanders, *et. al.*, [2003], who showed by means of Mossbauer Spectroscopy conducted on coal, char and fly ash samples obtained from the New Vaal Colliery, that at 200°C the pyrite started to change and at 400°C, 60% had been transformed to hematite, with complete transformation having occurred by 800°C. Above 1000°C, the pyrite had fused completely into the glass.

From the thermodynamic equilibrium calculations for the fractional oxygen species (Figure 3.20), it is clear that $CaAl_2Si_2O_8$ (feldspar), $Mg_2Al_4Si_5O_{18}$ (corderite) and $Fe_2Al_4Si_5O_{18}$ (ferro-corderite) melt, forming a slag phase at 1027°C, and the sum of oxygen scavenging related to mineral transformation is c.a. 7% at 1316°C. It would appear that the mineral composition is a more fundamental property than merely ash content in the gasification process, when viewed on an oxygen consumption basis.

Further fundamental understanding of the GG41 AFT profile in relation to the complex mineralogical transformation behaviour is necessary, and is being studied by Matjie [2005].

3.2 ULTIMATE ANALYSIS RESULTS

The GG41 gasifier residual carbon, hydrogen, nitrogen, sulphur and oxygen profiles are shown in Figure 3.8. Unfortunately, Glover [1988, 1991] and Krishnudu, *et. al.*, [1989a,b] did not study the ultimate analysis profiles in their earlier work, and therefore no comparisons to these findings can be made.

In order to better understand the speciation and partitioning behaviour occurring during fixed-bed gasification, Fact-Sage thermodynamic equilibrium modelling was employed, providing equilibrium compositional profiles. This data is shown mainly to provide the reader with an understanding of the main chemical reactions occurring within the GG41 gasifier. This data should not be directly compared to the elemental ultimate analysis profiles, as the effect of mineral transformation behaviour is included in the model, while volatile matter is excluded. The equilibrium profiles are depicted in Figures 3.9 to 3.20 and detailed results can be found in Appendix C.

3.2.1 GG41 Carbon distribution profile

From the data shown in Table 3.1, it can be observed that the normalised ultimate carbon content ranges from: 164 - 181, 106 - 152, 57 - 76 and 12 - 34 kg / 100kg ash

content in the drying, pyrolysis, reduction and combustion (ash-bed) zones respectively. It is clear that the average ultimate carbon content is significantly different between the four zones. This result is analogous to the FC distribution profile presented in Figure 3.4, which showed that there were also significant differences in the FC content between the four GG41 reaction zones.

It is important to note that the FC content and the ultimate carbon content approach the same normalised range within the reduction zone and the combustion zones, i.e. 57 - 77 and 11 - 34 kg / 100kg ash; for the fixed carbon profile, and 57 - 76 and 12 - 34 Kg / 100kg ash for the ultimate carbon profile respectively (Table 3.1). The carbon associated with the volatile matter in the case of the ultimate carbon is included in the analysis, therefore the difference between the two, lies only in the drying and pyrolysis zones of the GG41 gasifier. This result is expected, thus providing credibility to the sampling methodology employed in this study.

The calculated carbon equilibrium compositional profiles in the (1) drying and pyrolysis zones and (2) reduction zone of the gasifier are given in Figures 3.9 and 3.10 respectively. From the predictive carbon speciation data for the drying and pyrolysis zones, it is apparent that small quantities of methane (CH_4) and CO_2 are formed at 100°C. As the solid carbon further reacts within this zone, the CH_4 and CO_2 contents increase to c.a. 20% and 30% respectively; CO begins to form from about 500°C (18% at 727°C). Small quantities of COS (0.1%) are also formed from the transformation of pyrite and other base metal sulphides, appearing from c.a. 500°C.

Normalising the carbon species within the reduction zone (Figure 3.10), the CH_4 content is reduced from 18% at 727°C, to 1% at 927°C, disappearing completely at 1000°C. The CO_2 content is reduced from 65% at 727°C to 35% at 1316°C due to the Boudouard reaction, yielding an increase in CO. The CO content subsequently increases from 22% at 727°C to 65% at the completion of gasification.

3.2.2 GG41 Hydrogen (H) distribution profile

The normalised hydrogen distribution profile results obtained from the GG41 gasifier turn-out sampling campaign are given in Table 3.1.

From the data shown in Table 3.1, it can be observed that the normalised hydrogen content ranges from: 8 - 9, 2 - 6, 0.5 - 0.6 and 0.1 - 0.3 kg / 100kg ash in the drying, pyrolysis, reduction and combustion (ash-bed) zones respectively, showing a

decrease in the average hydrogen content with a clear difference between the four zones.

From Figure 3.8 the hydrogen content in the feed coal (sample 32) is seen to be 10.3 kg / 100kg ash. A 20% reduction occurs within the Bosman skirt area of the GG41 gasifier to a level of 8.3kg / 100kg ash at the start of the pyrolysis zone (sample 25). This reduction in hydrogen can possibly be ascribed to the loss of water as the hydrogen loss is accompanied with a 10% loss in oxygen content within this region of the gasifier (see section 3.25 below for oxygen distribution data). A sharp release of hydrogen is observed within the pyrolysis zone of the gasifier (sample 20), where 84% of the coal-bound hydrogen is volatilised from the resultant coal char. The hydrogen content further decreases to a level of 0.3kg / 100kg ash at the ash-bed position (sample 5), where after a further reduction occurs to 0.15kg / 100kg ash, relating to an overall partitioning of hydrogen to the gas phase of 99% at the ash-grate position (sample 1).

When coal is heated and volatiles are evolved, hydrogen-rich side chains are lost and the remaining char structure becomes more aromatic in nature [Morgan, 1991]. Table 3.1 shows the GG41 gasifier average range results obtained for the carbon to hydrogen ratio, and Figure 3.11 graphically depicts the trends obtained.

From the data shown in Table 3.1 (expressed on a normalised kg / 100kg ash content basis) in the drying, pyrolysis, reduction and combustion (ash-bed) zones respectively, it can be observed that the carbon to hydrogen ratio increases from 20 to reach a maximum of about 135 in the reduction zone, finally decreasing at the ash-bed region. From Figure 3.11 it can be observed that the carbon to hydrogen ratio is relatively constant within the Bosman skirt area of the gasifier, at about 20:1 carbon to hydrogen in samples 32 to 24. This ratio increases to 40:1 midway into the pyrolysis zone and the start of "slow gasification" (sample 20). At the end of pyrolysis and the start of "fast gasification" (sample 15), the carbon to hydrogen ratio is 100:1, reaching a maximum of 135:1 in the oxidation region of the reduction zone, where after it decreases drastically within the ash-bed. The aromaticity shows some scatter in the reduction and combustion zones, due to the carbon conversion reactions occurring within this highly reactive zone.

In Figure 3.5 it was shown that 70% carbon conversion occurred at the start of combustion (sample 5), where after the char was rapidly consumed a short way into the ash-bed (samples 4 to 1). This phenomenon is also apparent in Figure 3.9, where an acute reversal in the carbon to hydrogen ratio is observed as the carbon is

combusted in the zone under discussion.

The Fact-Sage calculated hydrogen equilibrium compositional profiles for the (1) drying and pyrolysis zones and (2) reduction zone of the gasifier, are given in Figures 3.12 and 3.13 respectively. From Figure 3.12 it is apparent that crystal bonded water is the most significant hydrogen-containing species present at 100°C, as well as minor quantities of H_2S and steam. Methane (31%) and steam (66%) are the major hydrogen species formed at 200°C, together with small quantities of OH released by some of the minerals.

H_2 gas is evolved from c.a. 300°C (1%), rising to 28% with an increase in temperature up to 727°C within the pyrolysis zone. At this temperature (727°C), the percentage hydrogen species distributes as: 33% methane, 38% hydrogen in the form of steam, as well as 0.64% of the hydrogen related to H_2S. From the reduction zone equilibrium profile for hydrogen (Figure 3.13), it is clear that the H_2 and steam contents remain almost constant in the temperature regime of 927°C to 1316°C, i.e. 40% and 60% respectively, once methane and ammonia are depleted.

3.2.3 GG41 Nitrogen (N) distribution profile

Table 3.1 shows the GG41 gasifier average range results obtained for nitrogen and Figure 3.8 graphically depicts the nitrogen trends obtained.

From the data shown in Table 3.1, it can be observed that the nitrogen content ranges from: 4.1 - 4.6, 1.8 - 3.5, 0.7 - 1.0 and 0.2 - 0.4 kg / 100kg ash content in the drying, pyrolysis, reduction and combustion (ash-bed) zones respectively. The average coal nitrogen content is thus significantly different among the four reaction zones within the GG41 gasifier.

The nitrogen appears to be deeply imbedded within the coal structure, as only 5% of the nitrogen is evolved within the Bosman skirt area of the GG41 gasifier (see Figure 3.8). Only from sample 20 (within the slow pyrolysis with gasification region), does the coal-bound nitrogen begin to devolatilise; at the combustion zone position (sample 5), 89% of the nitrogen has partitioned into the gas phase. The release of nitrogen, when compared to hydrogen, occurs at a slower rate, i.e. 90% and 97% at the ash-bed position for nitrogen and hydrogen respectively.

The equilibrium compositional profile for nitrogen in the drying and pyrolysis zones of the gasifier is given in Figure 3.14, which reflects the nitrogen distribution mass percentage within the temperature range of 100 °C to 727 °C. It can be seen that almost all of the nitrogen in the system speciates as N_2 in the temperature range of 100°C to 727°C, the balance is in the form of NH_3, which increases to a concentration of $1.2E^{-02}$ from about 300°C.

From Figure 3.15 it can be observed that the nitrogen speciation behaviour is very similar in the reduction zone of the reactor when compared to the drying and pyrolysis zones, except that the nitrogen contribution in the NH_3 species is reduced from 1% at 727°C to 0.3% at 1316°C; and N_2 subsequently increases to 99.7% at this peak temperature.

3.2.4 GG41 Sulphur (S) distribution profile

Table 3.1 shows the GG41 gasifier average range results obtained for the total sulphur. From the data shown in Table 3.1, it can be observed that the total sulphur content ranges from: 2.7 - 3.5, 1.4 - 2.1, 0.8 - 1.1 and 0.3 - 0.7 kg / 100kg ash content in the drying, pyrolysis, reduction and combustion (ash-bed) zones respectively, showing that the average coal sulphur content decreases from the first to the fourth reaction zones within the GG41 gasifier.

The GG41 gasifier coal sulphur partitioning behaviour is profiled in Figure 3.8 and the equilibrium speciation modelling for sulphur in the (1) drying and pyrolysis zones and (2) reduction zone is shown in Figures 3.16 and 3.17 respectively. Unfortunately the different forms of sulphur, i.e. pyritic, sulphatic, organically-bound, etc. were not quantified in this study, so no deeper insight into their devolatilisation mechanics is possible. When observing the total sulphur profile given in Figure 3.8, it is apparent that the feed coal contained 3.8kg S / 100kg ash content. Based on knowledge of the SCS coal blends used for gasification in Secunda, 50% sulphur is in the form of pyrite and the other 50% sulphur is typically organically bound [Matjie, 2005].

From Figure 3.8 it can also be seen that approximately 28% of the coal-bound sulphur is emitted within the Bosman skirt area of the GG41 gasifier. At the onset of slow pyrolysis with some gasification (sample 20), about half of the sulphur present in the feed coal had already volatilised. A steady reduction in sulphur is observed through the reduction zone and at the combustion zone (sample 5), the total sulphur content in the char is still 0.79kg / 100kg ash content, relating to an evolution of only 79%

sulphur at this stage of the gasification process. At the ash-grate (sample 1), 92% conversion of sulphur is observed.

The equilibrium compositional profile for sulphur in the drying and pyrolysis zones of the gasifier (Figure 3.16) reflects the sulphur distribution percentage within the temperature range of 100 °C to 727°C. For the purpose of the model, the suphur was assumed to be inorganically-bound in the form of pyrite at 25°C. From Figure 3.16 it can be observed that only 31% of the sulphur used in the model input is still in the form of pyrite (FeS_2) at 100°C, together with 68.7% H_2S, while the balance (0.3%) is associated with minor species related to base metal sulphides. At 300°C, pyrite is transformed to FeS (15%), whilst the amount of H_2S increases to 84.4%. At 700°C, FeS decomposes, producing even more H_2S (98%) as well as COS (1.7%). The calculated transformational behaviour of pyrite under these reducing conditions that are present within the gasifier, thus support the Mössbauer Spectroscopic findings of Waanders and Govender [2005], where iron and sulphur mineral associations in coal, as well as transformation during gasification were studied, revealing similar results, albeit at higher temperatures.

In the reduction zone (Figure 3.17), H_2S is still the dominant sulphur species (>95%), but the concentration of COS increases to 2.6% at 1316°C, and some SO and SO_2 gas are also produced at this peak temperature; as some melting of trace quantities of MgS, CaS, FeS and MnS species enter the slag, occurring at 1027°C.

3.2.5 GG41 Oxygen (O) distribution profile

Table 3.1 shows the GG41 gasifier average range results obtained for the coal-bound oxygen content. From the data shown in Table 3.1, it can be observed that the oxygen content ranges from: 27 - 29, 5 - 18, 0.6 - 1.4 and 0.3 - 1.1kg / 100kg ash content in the drying, pyrolysis, reduction and combustion (ash-bed) zones respectively. It can be concluded that the average coal oxygen content is significantly different among the drying, pyrolysis and reduction zones within the GG41 gasifier, while the coal-bound oxygen content in the reduction and combustion zones are not significantly different from one another.

Figure 3.8 also depicts the coal-bound oxygen profile for the GG41 gasifier; Figures 3.18 and 3.19 show the oxygen equilibrium speciation models for the (1) drying and pyrolysis zones, and (2) reduction zone respectively.

It can be observed from the GG41 gasifier turn-out profile (Figure 3.8) that the feed coal (sample 32) had an oxygen content of 31kg / 100kg ash content. At the start of pyrolysis (sample 25), the oxygen content is slightly reduced to 27kg / 100kg ash content, due to the loss of oxygen from the drying reaction in the upper Bosman skirt region of the gasifier. The reduction in the oxygen content of the heat- affected coal is very dramatic within the pyrolysis zone, where c.a. 90% of the coal- bound oxygen partitions into the raw gas and tar. The coal-derived oxygen is reduced to 1.9kg / 100kg ash content at the end of the pyrolysis zone (sample 15), and only minor oxygen retention is observed in sample 1 (0.3kg oxygen / 100kg ash content) at the ash-grate.

The scatter in the oxygen trend data observed in the lower half of the gasifier may be ascribed to oxy-sorption reactions occurring within the exothermic oxidation zone, resulting in mineral transformations, and will be further discussed in the Fact-Sage modelling.

The equilibrium compositional profile for oxygen in the drying and pyrolysis zones of the gasifier is given in Figure 3.18 within the temperature range of 100 °C to 727 °C. From the graph it can be observed that surface and crystal moisture dissipation are the dominant oxygen species at 100°C, together with some CO_2 evolution (11%). At a higher temperature (200°C.), water gas (55%), CO_2 (38%) and OH decomposition from K, Mg and Ca silicates, as well as from koalinite, occurs. The major percentage gas phase oxygen species present at the end of pyrolysis (727°C) are: CO_2 (50%), steam (31%), CO (13%) and the balance (6%) of the oxygen species is reflected in the mineral solid transformation processes occurring.

The model-predicted oxygen speciation behaviour in the reduction zone of the gasifier is given in Figure 3.19. From this graph it can be seen that the CO_2 concentration decreases with increasing temperature, up to 1316°C, while the CO and steam (oxygen contribution) content increases with increasing temperature. Some minerals containing oxygen, melt at 1027°C forming a slag. For normal gasifier operation excess steam is required in order to prevent excessive clinker formation [Van Dyk, *et. al.,* 2001c].

From the data given in Figure 3.20 it is clear that $CaAl_2Si_2O_8$ (feldspar), $Mg_2Al_4Si_5O_{18}$ (corderite) and $Fe_2Al_4Si_5O_{18}$ (ferro-corderite) melt, forming a slag phase between 1027 °C and 1127°C, liberating mainly iron oxide and Al_2O_3. From Mossbauer analyses, the iron oxide species was identified as hematite and the slag included an Fe-containing

glass (Waanders, *et. al.,* 2003]. The sum of oxygen scavenging, related to mineral transformation, is 7%. It would appear that the mineral composition is thus a more fundamental property in the gasification process than the ash content.

Mineralogical characterisation of the GG41 gasifier turn-out samples is expected to provide valuable insight into the slagging behaviour of the minerals present, with the possible relationship to the ash fusion temperature (AFT) profile. This phenomenon is discussed in a thesis by Matjie [2005].

3.3 GG41 GASIFIER COAL CHAR REACTIVITY RESULTS

Besides influencing the product composition and volatile matter yield, pyrolysis conditions also affect the reactivity of the gasification char that remains. The reactivity of a coal char depends on various chemical and physical properties of the char, these in turn, are influenced by the conditions under which the char was formed [Morgan, 1991]. It is known [Keyser, 2006], that if a coal is charred, cooled and exposed to air; the reactivity is negatively affected. This should be appreciated when assessing the results on coal reactivity.

Table 3.1 shows the coal char CO_2 reactivity content for the GG41 gasifier. From the data it is clear that the reactivity values range from: 2.4 - 2.5, 1.9 - 2.1, 2.2 - 2.4 and 1.5 - 2.3 (h^{-1}) in the drying, pyrolysis, reduction and combustion (ash-bed) zones respectively. Figure 3.21 shows the coal char CO_2 reactivity profile (50% burn-off at 1000°C) for the GG41 gasifier turn-out samples. From this it can be seen that a bi-modal trend in reactivity is evident, which is not clear from the data presented in Table 3.1. The initial steady decrease in reactivity observed for samples 32 to 17 is not easily explainable, since one would expect that during pyrolysis that temperatures would generally be below 1000°C. This being the case, the downward trend in coal char CO_2 reactivity could merely be an artefact of the TGA-derived reactivity, (thus not real), since samples 32 to 17 should not have seen temperatures in the GG41 gasifier higher than 1000°C. This is indeed the case when viewing the GG41 average and surface solids' temperature profile given in Figure 3.46 for this range. But, when viewing the solids' peak temperature profile data, shown in Figure 3.46, temperatures higher than 1000 °C were present within the pyrolysis zone of the gasifier. The fact that carbon conversion had already occurred in this region would also imply that "hot-spots" and channel-burning are likely to have occurred (see also Figures 3.4 and 3.5). This argument would then negate the statement that an artificial TGA-derived coal char CO_2 reactivity range was observed from sample 32 (feed sample) up to sample 17

(slow gasification region), thus providing a more plausible explanation for this observed initial decrease in reactivity.

Figure 3.21 shows that the coal char CO_2 reactivity increases from a value of 2 h^{-1} (sample 16) up to 2.4 h^{-1} (sample 10), before decreasing once more to a coal char CO_2 reactivity level of 1.2 h^{-1} at the ash-grate position (sample 1). The increase in reactivity evident for samples 16 to 10 thus clearly confirms the existence of the gasification reaction zone of the GG41 gasifier.

The decrease in coal char CO_2 reactivity observed from samples 8 to 1 can probably be related to a reduction of active surface area in the exothermic oxidation zone of the GG41 gasifier. Diffusion control limitations are then expected to dominate as the char structure realigns, but prior to this level, the gasifier is postulated to essentially be under kinetic control. Reaction kinetic studies or numerical modelling is recommended in future studies in order to test the hypothesis made since it is highly unlikely that large coal particles can be completely under kinetic control without any diffusion resistance hindering reaction. A step change in the fixed carbon distribution profile is also observed to occur at sample position 5 (see Figure 3.1), which depicts the onset of the combustion zone. The ash-bed is expected to extend from samples 1 to 4, where the char finally combusts, providing the heat for the gasification and pyrolysis reactions higher up in the gasifier.

Various other parameters have been correlated with the coal char reactivity. Fatemi-Badi, *et. al.,* [1988] found a direct correlation between coal char CO_2 reactivity and the hydrogen content of the coal during lab-scale pyrolysis experiments, where it was found that the higher the hydrogen content, the higher the reactivity.

On the other hand, Solomon, *et. al.,* [1988] used the % (daf) H content as a measure of the extent of pyrolysis, i.e. hydrogen content decreased with an increase in temperature. It was found, for a range of coal types, that there was a trend of decreasing reactivity in air with decreasing hydrogen content (increase in temperature) and most of the change occurred below 2% hydrogen, i.e. after the evolution of aliphatic hydrogen was complete. The lignite, however, increased in reactivity until between 3.5 and 4% hydrogen and then decreased in reactivity. It was concluded that the variation in reactivity with extent of pyrolysis, did not depend strongly on the char surface area measured by N_2 or CO_2. In Figure 3.22 the relationship between the GG41 gasifier hydrogen content (daf) and the coal char CO_2 reactivity is shown.

From Figure 3.22 it can be seen that the GG41 gasifier turn-out samples' coal char CO_2 reactivities were high in two regions when correlated with the dry ash-free hydrogen content, and should be explained.

Firstly, it appears that the aliphatic hydrogen evolves from the feed coal, i.e. declining from 4.2 to 2.0 weight % (daf) hydrogen content in a region of high reactivity (drying zone and fast pyrolysis region of the pyrolysis zone). A flattening of the reactivity curve is then observed below 2 weight % H up to 1 weight % H, which constitutes the "slow pyrolysis with gasification" regime. At 2 weight % H content, the tar has been released from the coal (Figure 3.3) and "slow pyrolysis with gasification" commences.

In the "slow pyrolysis with gasification" region, the heavier volatile matter fraction is still being released and the hydrogen content further decreases to 1 weight %, whilst the reactivity remains constant at c.a.1.8 (h^{-1}) until the end of pyrolysis (sample 15). At 1 weight % hydrogen, fast gasification and oxidation reactions commence in a zone of high reactivity, since the completion of pyrolysis has brought about a development of internal porosity to the resultant char [Morgan, 1991]. This results from: (1) the opening of previously closed pores, (2) creation of new pores and (3) enlargement of pre-existing and/or newly developed pores. The development of porosity during pyrolysis thus gives rise to changes in pore structural parameters such as density, specific surface area, pore size distribution, total open pore volumes, porosities and average pore diameter [Morgan, 1991].

In the combustion zone and ash-bed region (samples 5 to 1), a reduction in coal char CO_2 reactivity is observed by the sharp inflection shown on the curve in Figure 3.22. This final reduction in reactivity is possibly due to pore collapse and diffusion limitations occurring within the combustion zone of the GG41 gasifier.

It can be concluded from Figure 3.22 that the GG41 gasifier coal char CO_2 reactivity decreases with a decrease in (daf) hydrogen content up to 2 weight % hydrogen, which confirms the lab-scale results of Solomon, *et. al.*, [1988]. Thereafter, the coal char reactivity remains constant up to 1 weight % hydrogen content in the "slow pyrolysis with gasification" region, within the pyrolysis zone of the GG41 gasifier. During reduction, the coal char CO_2 reactivity was shown to increase significantly with a minimal decrease in hydrogen content, before pore collapse and diffusion limitations finally decrease the reactivity to a constant 0.75 weight % hydrogen content within the combustion zone.

4 PHYSICAL PROPERTY PROFILES

The physical properties of coal, which impact on gasification performance, relate to those processes which result in a change in particle size and surface area [Morgan, 1991]. The physical properties such as the internal particle density, particle size distribution, Ergun Index, thermal and mechanical fragmentation and caking profile results will be discussed.

Table 3.3 summarizes the respective calculated statistical average range obtained for the GG41 gasifier physical properties studied, in relation to the four reaction zones identified in this study.

4.1 DENSITY PROFILES

The GG41 gasifier coal internal bulk density and true density profile results are presented and discussed together with the data for the factorised Indian pilot plant data [Krishnudu, *et. al.*, 1989a] and subsequently compared to the GG41 profiles.

4.1.1 The bulk density profile

From the data shown in Table 3.3, it can be observed that the GG41 coal bulk density ranges from 1126 - 1193, 906 - 1028, 890 - 996, and 1102 - 1171 kg/m^3 in the drying, pyrolysis, reduction and combustion (ash-bed) zones respectively, clearly showing a significant difference between the drying and pyrolysis zones, but no significant difference between the pyrolysis and reduction zones. However, the bulk density in the combustion zone is different when compared to the two zones immediately above it, but not significantly different to the bulk density range occurring within the initial drying zone.

The coal bulk density profile obtained for the GG41 gasifier is shown in Figure 3.23. From these results it can be observed that the GG41 gasifier feed coal (sample 32) had a measured bulk density of 1150kg/m^3. As the feed coal further descends in the gasifier within the Bosman skirt (sample 29), the bulk density decreases, displaying a consistent downward trend up to sample 15 (more or less in the middle of the GG41 gasifier), where the bulk density is at its lowest, i.e. 840kg/m^3. This observed reduction in bulk density can be ascribed to the mass loss resulting from thermal decomposition reactions occurring with an increase in temperature, i.e. moisture and

volatile matter released. Primary thermal fragmentation of the coal is also expected to play a role in this particular region, since release of inherent moisture and volatiles lead to increased porosity and weakening of the mechanical integrity of the coal structure. This will be discussed in relation to measured particle size distribution changes by means of the Ergun Index.

It can furthermore be observed that a change in the trend occurs (sample 14) as the charge further descends and the bulk density is clearly reversed to 1150kg/m^3 (sample 1), which is the first sample taken at the grate, at the bottom of the gasifier. A possible explanation for the observed increase in bulk density in the reduction and combustion zones, is the inference that heat-affected lump coal carbonizes essentially, following shrinking core behaviour, where the ash minerals transform to layers on the surface of the particle with an inner carbonaceous centre [Glover, 1988]. It is envisaged that the observed reversal in bulk density, can be explained by the fact that the ash layers formed at about sample position 15, begin to flake off. These ash transformed mineral layers then pack the voids between the larger char particles and the bulk density subsequently increases. Ash mineral agglomeration effects are also expected to play a role in the measured GG41 gasifier coal char particle size distribution profile obtained and will be discussed in Section 4.2 of this Chapter.

The coal bulk density profile trends obtained for both the GG41 gasifier and the factorised Indian pilot plant data are given in Figure 3.24. From these results it can be observed that a surprisingly similar bulk density trend exists between the two sets of results, i.e. an initial decrease in bulk density, followed by a reversal in the shape of the curve as the char approaches the ash-grate, albeit that the minimum inflection points do not entirely correspond to the exact sample position.

The coal bulk density trend for the factorised Indian pilot plant data also shows that the bulk density range between highest and lowest densities is lower than for the GG41 gasifier. This can possibly be explained by the fact that the feed coal top size in the Indian pilot plant case was limited to 25mm and 22% of the coal was finer than 6.3mm; so invariably the ratio of top to bottom size will be less when compared to the GG41 gasifier where a coal, having a top size c.a. 100mm and a bottom size of 6mm, is being used. Consequently, the packing densities will be different and lower in the case of the Indian pilot plant gasifier, since less bed void-space will be available due to Sauter mean diameter differences, as given by the Ergun equation.

The encouraging bulk density comparison trend data discussed in this section of the study demonstrates once again that factorisation of the Indian pilot plant data does indeed make provision for meaningful comparison to the GG41 profiles obtained, albeit that different reactor geometries and coals were used.

4.1.2 The true density profile

From the turn-out data shown in Table 3.3, it can be observed that the GG41 coal true density ranges from 1652 - 1666, 1808 - 2092, 2246 - 2326, and 2432 - 2565 kg/m^3 in the drying, pyrolysis, reduction and combustion (ash-bed) zones respectively, showing a clear difference between the four reaction zones identified.

The true density profile for the GG41 gasifier coal is given in Figure 3.25, together with the factorised Indian pilot plant data. From Figure 3.25, it is apparent that, whereas the two feed coals have almost similar feed coal densities, i.e. 1400kg/m^3 and 1500kg/m^3 for the Indian pilot plant coal and the GG41 coal respectively, a large difference in respective final true density is observed at the ash-grate i.e. 1900kg/m^3 and 2600kg/m^3, requiring some explanation.

In the case of the factorised Indian pilot plant data, this result is rather surprising since the ash content in the first sample taken at the ash-grate was 85.4% on an air-dried basis (a.d.), compared with an ash content of 90.6% (a.d.) for the GG41 gasifier case (see Table A1 in Appendix A and Table B1 in Appendix B). The transformed ash-forming minerals are generally accepted to consist of a mixture of complex silicates and quartz, which have a density ranging between 2600kg/m^3 and 2900kg/m^3 [Lurie, 1981]. However, no mineralogical information was provided in the paper published by Krishnudu, *et. al.*, [1989a,b] regarding the Indian pilot plant study; the analytical technique used to measure the coal true density was reported as "done in the normal way", without any reference to the method used. Unfortunately, the anomaly around the final true density comparison in this current study cannot be adequately resolved.

When viewing the true density data obtained for the factorised Indian pilot study and the GG41 gasifier in relation to the four reaction zones shown in Figure 3.25, it can be observed that the true density of the coal particles only marginally increases in the drying zone of the reactor in both the Indian case and the GG41 gasifier. This is to be expected, since volatiles and moisture (Figure 3.1) are essentially being expelled in this uppermost region of the gasifier; char combustion and gasification reactions will only have an effect on the particle density lower down in the FBDB gasifier.

In the pyrolysis zone, it can be seen that the Indian coal char true density trend increases by a further 70kg/m^3, compared to the much larger increase in density of 450kg/m^3 observed in the case of the GG41 gasifier char. In both cases an increase in particulate density is expected to occur in this region of the gasifier, as mineral matter present in the coal transforms due to the increasing temperature (see also Figures 3.7 and 3.46).

In the reduction zone, the Indian factorised trend data obtained shows a further larger increase in true density of 210kg/m^3, compared to the increase of only 124kg/m^3 in the case of the GG41 gasifier. In both cases an increase in particulate density is expected to occur within this region of the gasifier, as gasification of the char results in a loss of carbon due to chemical reaction with CO_2 and steam, resulting in a lower carbon to ash mineral ratio, which impacts on the true density to further increase.

In the combustion zone (ash-bed), the Indian factorised trend data obtained shows a marginal increase in true density of only 50kg/m^3, compared to an increase in true density of 200kg/m^3 in the case of the GG41 gasifier. This lowest zone in the gasifier supports combustion, as well as cooling of the char, using excess steam to minimize clinker formation; an increase in particle density is therefore expected to occur.

Holistically, when ignoring the significant difference in final true density observed between the two cases presented, it follows from a trend perspective only, that similar reaction zone behaviour appears to be occurring in the drying, reduction, and combustion zones. However, the true density relationship between the two cases for the pyrolysis zone is different. The relationship between ash content (% dry basis) versus true density is shown in Figure 3.26 in order to gain some insight into understanding why the true density curves are nevertheless different for the GG41 gasifier turn-out data and the factorised Indian pilot plant data shown.

From the two trend curves given in Figure 3.26 it can be observed that a good linear fit is obtained. This implies that as carbon is consumed in the reaction process, the residual ash content increases in linear proportion to the former; the ash-forming minerals having a higher density than the carbonaceous fraction, thereby increasing the true density of that fraction. This does not mean that more ash is produced in the gasifier than was originally present in the feed coal, but is merely relative to a process analogous to "concentration" in coal preparation [Horsfall, 1993].

A much steeper curve, with a similar correlation coefficient is evident when comparing the factorised Indian pilot plant data to the GG41 case, possibly indicating that the slightly greater scatter in the GG41 case data is linked to the behaviour of the ash mineralogy. This suggests that the mineralogical properties are perhaps different, i.e. the biggest difference in ash content between the two cases occurs within the pyrolysis zone (Figure 3.6), at sample position 23 (20% difference in ash content). The radical ash content shift at this point in the gasifier, in the case of the GG41 data, could possibly beckon the onset of clay de-hydroxylation and CO_2 release [Matjie, 2005], leading to a rapid increase in the ash content and resultant density. If this supposition holds, then it infers that the GG41 coal possibly had a higher clay and silicate content when compared to the Indian case. Unfortunately no mineralogical data, including ash fusion temperature profile measurements, was reported by Krishnudu, *et. al.*, [1989a,b] to substantiate this observation.

4.2 PARTICLE SIZE DISTRIBUTION RESULTS

This section focuses on the internal particle size distribution behaviour in the gasification process, using the data from the GG41 gasifier turn-out, focusing on the size distribution curves obtained, as well as the use of the Ergun Index. In addition, reference is also made to other physical property behaviour, i.e. thermal fragmentation, caking and mechanical fragmentation data, in order to better understand the particle size distribution profiles.

The coal particle size distribution for the GG41 gasifier is provided in Figure 3.27 in order to give an overall snapshot of the changes occurring within the gasifier. This size distribution data should be seen together with Table 3.3 and Figures 3.28 – 3.37, in order to gain a full understanding of cause and effect, as well as of a relationship to other physical property variables.

In Glover's earlier work [1988, 1991] it was concluded that gasifier turn-out samples do not provide accurate particle size data, since the extent to which the unloading action during the run-out contributes to fragmentation is not known and results should be treated with some caution. The data from the GG41 gasifier given in Figure 3.27 shows that the feed coal (sample 32) had a -6.3mm fines content of 14% and at the ash grate (sample 1), the fines content increased to 21%, implying a 7% increase in fines production. Whether or not the GG41 gasifier water quench had exfoliated the char is unknown. Unfortunately no sample of corresponding ash for the GG41 gasifier was taken prior to the shutdown, so the effect of the quench on fines production

cannot be fully elucidated on in this work. Whilst a 7% increase in fines content may not be considered extreme, this effect must be considered in future gasifier turn-out test work.

4.2.1 The +25mm size distribution profile

Table 3.3 shows the average range results obtained for the +25mm particle size distribution. From the data shown in Table 3.3, it can be observed that the percentage +25mm particles ranged from: 27 - 43, 14 - 20, 17 – 24 and 29 - 35 in the drying, pyrolysis, reduction and combustion (ash-bed) zones respectively, indicating a significant difference between the drying and pyrolysis zones, but no clear difference between the pyrolysis and reduction zones. The +25mm distribution in the combustion zone is significantly different when compared to the two immediately prior zones, but in about the same proportion as present in the drying zone.

The percentage +25mm particle size distribution profile for the GG41 gasifier is graphically depicted in Figure 3.28. When viewing the profile, it is clear that an overall reduction (about 12%) in this size fraction occurs when comparing the feed coal sample 32 (49%) and sample 1 (37%) at the ash-grate. The graph also shows the effect of the primary fragmentation process, which causes breakage of the +25mm size fraction, occurring down to a "thermally stable" size (15% +25mm) in the "slow pyrolysis with gasification" regime. At this point c.a. 80% of the +25mm size fraction has been reduced to the finer size fractions. The significant breakage of the coarse +25mm fraction down to a "thermally stable" size, is expected to create unstable gasifier operation in the top part of the gasifier, due to pressure drop fluctuations caused by void packing. Thermal-channeling was observed in this region by Glover [1988] in a number of gasifier dig-outs; concluding that local steam : oxygen ratio variations may occur, possibly allowing for higher temperatures to be reached above the ash-melting temperature, giving rise to clinker formation in certain areas of the gasifier.

If channel-burning did occur within the drying and fast pyrolysis regions of the GG41 gasifier, then this would support the rather surprising carbon conversion anomaly observed in the drying zone (see Figure 3.5). The peak temperature profile for the GG41 gasifier (Figure 3.46) also shows that temperatures as high as 1150°C had occurred in this region of the gasifier. It would also support the AFT profile results, which showed that ash mineral softening (ST) and change of shape (HT) were also evident in this region of the gasifier. Photographs showing a macroscopic view of the

GG41 gasifier turn-out samples (Figure 2.6 in Chapter 2) shows evidence of "clinkers" present in samples 19 and 17, which would confirm the likelihood of channel-burning occurring in the upper unstable region of the gasifier.

From Figure 3.28 it can further be seen that the ash agglomeration chemistry [Matjie, 2005] tends to upgrade the particle size, thereby consistently increasing the percentage +25mm fraction below sample 15 (at the end of pyrolysis) down to the ash- grate position (sample 1).

4.2.2 The -25mm + 6.3mm size distribution profile

Table 3.3 shows the average range results obtained for the -25mm +6.3mm particle size distribution. From the data it can be seen that the percentage -25mm +6.3mm particles ranged from 38 - 45, 51 - 58, 51 - 57 and 38 - 46 in the drying, pyrolysis, reduction and combustion (ash-bed) zones respectively. Thus, the average -25mm +6.3mm size distribution is significantly different between the drying and pyrolysis zones, but there is no significant difference between the pyrolysis and reduction zones. The -25mm +6.3mm particle size distribution present in the combustion zone is clearly much smaller when compared to the two zones immediately above it; and about in the same proportion as in the drying zone.

These results are graphically represented in Figure 3.29, from which it can be observed that this size fraction changes in quantity by about 5%, when comparing the feed coal sample 32 (37%), to the ash-grate sample 1 (42%).

It should also be noted that the percentage of the -25mm +6.3mm size fraction steadily increases up to sample 15 (end of pyrolysis), i.e. from 37% (sample 32) up to 64% for sample 15. This increase in particle size is mainly due to the breakage of the +25mm fraction during primary fragmentation. A reversal in the curve occurs from sample 15 to the ash-grate (sample 1), where the agglomerating propensity of the sintered minerals results in a decrease in the -25mm +6.3mm size fraction. This size fraction is then size upgraded by the mineral agglomeration chemistry [Matjie, 2005], resulting in an increase in the +25mm content, as the charge further descends towards the ash-grate (Figure 3.28).

This is interesting, since the bulk density profile, discussed previously (Figure 3.23) shows a similar maximum occurring at sample position 15. The bulk density data obtained is graphically shown against the intermediate percentage -25mm + 6.3mm retained size

distribution data and shown in Figure 3.30. It can be observed that a linear relation is obtained between the bulk density and intermediate -25mm + 6.3mm size range content. Thus, as the amount of the -25mm + 6.3mm size fraction increases, the bulk density decreases. When viewing Figure 3.27, it is clear that the intermediate -25mm + 6.3mm size fraction forms the bulk of the coal char fraction when compared to either the +25mm size fraction or the -6.3mm size fraction. The -25mm +6.3mm fraction increases from 37% in the feed coal sample to 64% of the bulk composite at sample 15. The +25mm size fraction on the other hand decreases from an initial 50% abundance, to 15% at sample position 15. This then indicates that breakage of the +25mm fraction preferentially comminutes into the -25mm +6.3mm fraction due to chemical reaction and physical phenomena, i.e. thermal and mechanical processes occurring in the top half of the gasifier.

The -25mm +6.3mm fraction is also the dominant size fraction (40%) in the lower half of the gasifier, when compared to the coarser +25mm (35%) and finer -6.3mm (25%) size fractions. From this reasoning it then follows that the bulk density profile of the GG41 gasifier is mainly dependent on the characteristics and relative abundance of the dominant size fraction present, clearly governing the packing density distribution obtained.

4.2.3 The - 6.3mm size distribution profile

Table 3.3 shows the average range results obtained for the -6.3mm size distribution, from which it can be observed that the percentage -6.3mm ranged from: 18 - 28, 23 - 32, 22 - 29 and 21 - 32 in the drying, pyrolysis, reduction and combustion (ash-bed) zones respectively. It can be concluded that the average -6.3mm size distribution is not significantly different for any of the four reaction zones identified in the GG41 gasifier.

The percentage -6.3mm size distribution profile for the GG41 gasifier is also given in Figure 3.31. It is clear that a large amount of scatter in the data is evident. However, the trend lines show an initial limited increase in -6.3mm content as the processes of thermal and mechanical fragmentation are expected to have an effect in the primary fragmentation process up to sample position 20. Thereafter, the trend lines shows a marginal increase, as the charge further descends within the gasifier towards the ash-grate, possibly due to the ash mineral agglomerating effect. A 7% increase in the overall fine -6.3mm fraction is still evident when comparing the feed coal -6.3mm content (14%) and sample 1 (21%) at the ash-grate.

It is further necessary to relate the internal fragmentation to the Ergun Index equation, in order to gain an insight into the GG41 gasifier stability.

4.2.4 The Ergun Index (EI) profile

Table 3.3 shows the GG41 gasifier results obtained for the Ergun Index, from which it can be seen that the Ergun Index ranged from 7.0 - 8.9, 4.3 - 5.9, 4.9 - 6.7 and 4.4 - 6.5 in the drying, pyrolysis, reduction and combustion (ash-bed) zones respectively; thus the average Ergun Index distribution is only significantly different for the drying zone, with no significant differences evident between the pyrolysis, reduction and combustion zones.

The Ergun Index profile for the GG41 gasifier is given in Figure 3.32, from which it can be seen that the feed coal (sample 32) had an Ergun Index value of almost 10. This is in line with typical SCS feed coal values, which range between 7.5 and 11.6. Higher values for the Ergun Index are preferred, as this implies that there are less fines present in the feed coal when compared to the coarser size ranges present. Operating experience [Keyser, *et. al.*, 2005] has also shown that if the feed coal Ergun Index is <7.5, then gasifier stability problems are apparent.

Although there is some statistical spread in this indexed data obtained, there appears to be a clear downward trend in the Ergun Index up to sample position 20 (start of slow pyrolysis with gasification). At this point the Ergun Index has decreased to about 4, from a starting index of about 10. Higher pressure drops are experienced as the Ergun Index values decrease, which implies that the fines pack the voids between the coarser particles and create unstable gasifier operating conditions [Keyser, *et. al.*, 2005].

An increase in the Ergun Index value is observed from c.a. 4 to c.a. 7, from sample 20 to sample 15 respectively as the charge further descends in the gasifier. This can possibly be ascribed to the fact that the effect of thermal fragmentation has ceased and the mechanical strength of the char (due to sintering) has increased; less fines are thus produced in relation to the coarser sized char (see also Figures 3.35 and 3.36 which will be discussed later). The Ergun Index once more decreases to a value of 5 at sample position 10, where secondary fragmentation is postulated to occur, i.e. burn-out of carbon bridges within the gasification region of the reduction zone, leading to a weakening in the mechanical integrity of the char. The ash agglomeration characteristics then affect the Ergun Index positively and it increases to values

ranging between 5 and 7 in the oxidation region (samples 9 to 6), before a reversal in Ergun Index trend is observed in the combustion zone and ash bed-region, where tertiary fragmentation due to excess steam cooling is postulated to occur.

Figure 3.32 clearly shows that the drying zone and the upper half of the pyrolysis zone (up to sample 20) are the largest regions of instability occurring within the GG41 gasifier, which is mainly caused by breakage of the coarse +25mm size fraction, leading to pressure drop fluctuations and channel-burning. Clearly a case can be made to reduce the top size of the Sasol-Lurgi gasification operational feed coal size to the "thermally stable" size identified in this study, i.e. 15% +25mm (maximum) which is envisaged to minimize this unstable region. In so doing, other economically viable opportunities may present themselves in optimising the gasification process.

It is accepted within the gasification technical community of Sasol that the Sasol-Lurgi FBDB gasifiers operate under thermodynamically controlled conditions [Keyser, 1997]. However, if a smaller feed particle size, i.e. 25mm x 6.3mm was gasified, it may be possible to also influence the kinetics of the process. In a hypothetical scenario, it can be considered in such a case, that the heating rate for such particles would occur at a much faster rate than for particles of say 100mm x 6.3mm in size, since heat transfer limitations are minimized when reducing the size of lump coal to the gasification process. This then implies that chemical reactions occurring within the pyrolysis zone for the "thermally stable" 15% +25mm (maximum) feed coal particle size scenario would occur more rapidly than for the current scenario (100mm-6.3mm). In this event, the pyrolysis zone is expected to move up within the fixed-bed gasifier, due to faster reaction kinetics occurring within the zone, resulting in a greater gasifier volume available for gasification and combustion.

As a result of improved kinetics, the gasification load could possibly be maximized, yielding more gas per unit reactor, and could possibly also help to minimize the 5% to 7% FC carbon loss to the gasifier ash. This hypothesis should be further investigated in future fundamental studies.

The relationship between the fine -6.3mm size fraction content and the Ergun Index for the GG41 gasifier turn-out samples is given in Figure 3.33. From the relationship shown, it is evident that a reasonable linear correlation is obtained between the Ergun Index and the fine -6.3mm fraction obtained from the GG41 turn-out samples. The expected and observed overall trend is that the Ergun Index increases with a decrease in the fine -6.3mm content. This correlation is in agreement with the

literature relating to the Ergun equation [Leva, 1959], which shows that if the particle diameter of the denominator decreases, the Ergun Index increases with a subsequent decrease in pressure drop (see equation 14 in Section 4.2 in Chapter 1).

The factorised Indian pilot plant Ergun Index data is shown together with the GG41 gasifier Ergun Index data in Figure 3.34, in order to gain an understanding of how these two case studies compare. As was mentioned, the Indian pilot plant study was conducted on a coal having a top size of 25mm, whereas the GG41 gasifier had a top coal size of 100mm with 49% +25mm material. It was therefore not possible to directly compare the Indian pilot plant case to the GG41 gasifier data, since the feed particle size distributions were different. By modifying the Sauter mean diameter equation to accommodate 12 size fractions, as was the case for the Indian pilot plant, the Ergun Index could however be calculated and further factorised using the sample factor correlation given in Table 2.3 in Chapter 2. Detailed results are given in Table B3 in Appendix B.

From Figure 3.34 it can be observed that a good comparative trend relating to the Ergun Index is evident between the two case studies. The factorised Indian pilot plant trend data is fairly consistent with the GG41 gasifier profile for samples 32 to 27; thereafter, the trends deviate with the Indian pilot plant trend consecutively higher at sample position 23 than for the GG41 gasifier. This could possibly be as a result of significant caking occurring within the Indian quarter-scale gasifier and to a much lesser extent within the GG41 gasifier. Thereafter, both Ergun Index trends reach a minimum value at sample position 20, followed by an increase up to sample position 15 (end of pyrolysis). The next zone of instability occurs for both cases below sample 15, where the effect of secondary fragmentation is observed. Thereafter, the Indian case exhibits a fairly constant Ergun Index trend, which differs from the trend visible for the GG41 gasifier, where tertiary fragmentation is observed at the fire-bed interface.

In the case of the Indian pilot-scale gasifier trend, it can be observed that the Ergun Index is consecutively lower than for the GG41 gasifier below sample position 20. This observation can possibly be ascribed to the large variation in fine -6.3mm particle size distribution between the two scenarios, i.e. the ash agglomeration effect within the GG41 gasifier tends to decrease the quantity of -6.3mm material reporting at the ash-grate, whereas in the Indian case, the -6.3mm material content consistently increased to 58% -6.3mm material present in sample 1 versus 21.2% for the GG41 gasifier. This could also suggest that the ash agglomerating effects were different for

the two cases, possibly due to different mineral transformational behaviours as previously exhibited by the true density versus ash content relationship (see Figure 3.28).

4.2.5 The thermal fragmentation profile

Fragmentation is the breaking of a single particle into two or more pieces. Primary fragmentation occurs during devolatilisation, at temperatures of about 350-400°C, where it starts to de-volatilise with the production of gases, oils and tars. Secondary fragmentation occurs during combustion of the char by burn-out of carbon bridges connecting parts of the particle [Stubington and Linjewile, 1989].

Thermal fragmentation testing of the GG41 gasifier turn-out samples was conducted in order to better understand the causant process in relation to particle breakage. The measured thermal fragmentation profile of the GG41 gasifier turn-out samples is given in Table 3.3 and Figure 3.35.

From the data shown in Table 3.3, it can be seen that the thermal fragmentation percentage ranges from 12.7 – 16.2, 5.6 – 12.4, 3.4 – 5.6 and 5.0 – 7.7 in the drying, pyrolysis, reduction and combustion (ash-bed) zones respectively, indicating that the average thermal fragmentation percentage is significantly different between the drying, pyrolysis and reduction zones, but with no significant difference in the thermal fragmentation behaviour between the reduction and combustion zones of the GG41 gasifier.

From Figure 3.35 it is clear that the GG41 feed coal (sample 32) thermally fragmented (14%), which is within the required specification of the SCS blend maximum value of 25%. Although there is scatter in the data, the trend line however shows an increase in thermal fragmentation occurring in the drying zone of GG41 gasifier, where a maximum value of 20% thermal fragmentation is indicated at sample position 25 (start of pyrolysis). Thereafter, a rapidly decreasing trend in thermal fragmentation, to average levels of less than 5%, is observed in the reduction zone of the GG41 gasifier, indicating that thermal fragmentation does not have a big effect during reduction, once the carbon has been charred.

The trend line further shows a slight increase in thermal fragmentation occurring within the ash-bed, which is probably an indication of the alumino-silicate glass response to reheating in the thermal fragmentation test, but could also confirm the

tertiary fragmentation position in the GG41 gasifier, which was postulated to occur at the char-ash interface of the combustion zone (Figure 3.32).

Taking this observation into account, in relation to postulations made earlier that primary fragmentation reaches a maximum at sample 21 in the particle size distribution profiles given above, it is clear that thermal fragmentation alone is not the only process responsible for fragmentation.

In a laboratory study by Van Dyk, [2001a] it was stated that a linear correlation between total moisture and thermal fragmentation of coal was found. In this study, a linear correlation data analysis between the thermal fragmentation and total moisture content of the GG41 gasifier turn-out samples was conducted in order to assess whether the claim by Van Dyk [2001a] could be verified. The detail correlation results are given in Table A5 in Appendix A. A positive correlation was indeed found to exist between thermal fragmentation and the total moisture content for the GG41 gasifier turn-out samples, which confirms the earlier lab-scale test work of Van Dyk [2001a]. This supports the fact that moisture contributes significantly to thermal fragmentation, although it is also affected by a complex interaction of other factors.

4.2.6 The mechanical fragmentation profile

The measured mechanical fragmentation profile of the GG41 gasifier turn-out samples is given in Table 3.3 and Figure 3.36.

From the data shown in Table 3.3, it can be observed that the mechanical fragmentation percentage ranges from 27.6 – 31.3, 32.4 – 36.0, 33.1 – 35.9 and 34.2 – 37.2 in the drying, pyrolysis, reduction and combustion (ash-bed) zones respectively. From this it is clear that in the drying zone, the fragmentation value is slightly lower than in all three the remaining zones, where the mechanical fragmentation percentage was found to be similar.

From Figure 3.36 it can be observed that the feed coal (sample 32) had a measured mechanical fragmentation value of 30%, which compares favourably to the typical SCS specification range of 25% to 40%. It can further be seen that as the coal enters the gasifier, there is only a slight increase in mechanical fragmentation, as the charge descends to sample position 25 (drying zone region) of the gasifier. This implies that only minimal coal breakage, due to mechanical degradation and segregation effects is evident in the drying zone (Bosman skirt) of the GG41 gasifier.

A sharp increase in mechanical fragmentation is then observed from samples 24 up to sample 22 (10% increase), before fragmentation reverses from a 40% mechanical fragmentation value at sample 23, to a lower value of 32% at sample position 15. The increase in mechanical fragmentation in the region (samples 24 to 22), can be ascribed to the charge being exposed to rapid pyrolysis reaction conditions at the exit of the Bosman skirt, which translate into an immediate loss of volatiles and softening of the mechanical integrity of the coal. As a result, the coal is more friable and mechanically fragments up to sample position 22. The resultant reduction in mechanical fragmentation observed (samples 21 to 15) can be ascribed to the hardening and less abrasive nature of the char, which is formed at higher temperatures (Figure 3.46), as the charge descends further into the gasifier fuel bed.

Within the reduction zone (samples 15 to 10), the trend line shows a marginal increase in mechanical fragmentation occurring, when compared to the slow pyrolysis with gasification region of the GG41 gasifier. The ash mineral agglomeration effects leading to size upgrading were shown to increase the quantity of the coarse +25mm size fraction within this region of the gasifier (Figure 3.28); the observed increase in mechanical fragmentation found in this reaction zone of the GG41 gasifier could possibly be ascribed to the brittleness of the coarser size fraction as the charge descends in the gasifier. In the combustion zone, the mechanical fragmentation effect is slightly lower when compared to the reduction zone above it.

This observation, when viewed in combination with the thermal fragmentation data, shows that both thermal and mechanical fragmentation processes are responsible for primary fragmentation (Figures 3.28 and 3.32). The thermal fragmentation process is prevalent up to the start of pyrolysis at sample position 25 (Figure 3.35), thereafter showing less of an effect on particle breakage than the process of mechanical fragmentation, which reaches a maximum just above the start of the "slow pyrolysis with gasification" region, at sample position 22 (Figure 3.36). The evidence of secondary and tertiary fragmentation occurring within the GG41 gasifier was proven on the basis of the thermal fragmentation results, but in both cases the fragmentation behaviour occurring below the "slow pyrolysis with gasification" region of the GG41 gasifier, is statistically not significant.

4.2.7 The caking propensity profile

The residual caking propensity profile of the GG41 gasifier turn-out samples is given in Table 3.3 and Figure 3.37. From the data shown in Table 3.3, it can be observed

that the caking propensity percentage ranges from 6.2 – 11 and 1.7 – 5.5 in the drying and pyrolysis zones of the GG41 gasifier. No caking was identified in the samples below sample 15, since the coal had been entirely converted to char (see Table A7 in Appendix A). It can be concluded then that the average caking propensity percentage is significantly different between the drying and pyrolysis zones and both reaction zones are significantly different in caking propensity behaviour when compared to the reduction and combustion zones of the GG41 gasifier.

When comparing the caking propensity confidence intervals for the drying and pyrolysis zones (Figure 3.37), it is evident that a large statistical error exists. This can be due to significant inherent variability occurring within the zones due to excessive reaction or temperature effects for example, or it could be an indication of actual response due to gasification characteristics within that particular zone. The estimate of the average as well as the width of the confidence intervals will improve if more experimental caking propensity data points are available for the drying zone. This is recommended for future gasifier sampling campaigns.

Although Figure 3.37 shows a large amount of scatter in the caking data obtained, the trend line indicates that the caking propensity generally decreases with an increase in bed depth. It can be observed that the feed coal (sample 32) had a caking propensity of 8%, which is within the SCS benchmark range of between 7% and 27%. The residual caking propensity is lowered to less than 2% at the start of the slow pyrolysis with gasification region (sample 20) and is no longer apparent at the end of pyrolysis (sample 15).

In general, the coal blend to the GG41 gasifier had a caking propensity close to the lower limit of the SCS benchmark. At such low levels of caking one would not expect any dramatic effects in terms of caking behaviour to occur, which appears to be the case here.

5 PETROGRAPHIC PROPERTY PROFILES

Petrography allows for the optical consideration of the changes occurring in the carbon particles and associated minerals, which can be related to temperature and morphological changes through the gasifier [Wagner, 2005b].

The objective of analyzing the GG41 turn-out samples petrographically, was to enhance the understanding of the behaviour of the feed coal inside the gasifier by

considering the optical changes in the carbon and mineral components. Specific objectives were to characterise the carbon forms (coal to char) in the samples applying char morphology techniques, as well as to correlate the petrographic findings to the reflectance analytical data obtained. The maceral group analysis results for the GG41 feed coal (sample 32) will be presented, followed by a discussion of the char morphology results and finally the temperature zones within the gasifier, by utilising vitrinite reflectance, will be given. Vitrinite is the maceral used to track the changes in rank, by measuring the reflectance properties of this maceral. Vitrinite can therefore also be used to estimate temperature changes of coal particles during heating, and may therefore be used to determine temperature zones within the gasifier [Wagner, 2004a]. Table 3.4 shows the average range calculated for the petrographic properties within the four reaction zones identified in this study. The detail results are given in Table A7 in Appendix A.

5.1 GG41 GASIFIER FEED COAL MACERAL GROUP ANALYSIS RESULTS

The standard maceral group analysis results for the GG41 feed coal (sample 32) is given in Table 3.5. Petrographically, the results are typical of seam 4 Highveld coal and are within the typical SCS gasification blend range [Wagner, 2004a]. A reflectance of vitrinite (RoV) percentage value of 0.8% (4 char readings, equating to 0.8%) was determined for the GG41 feed coal.

Typically the results are reported to include total reactive macerals (vitrinite + liptinite + reactive semi-fusinite and reactive inertodetrinite) indicating the proportion of particles expected to de-volatilise and become porous and swell to varying degrees on heating. Total inertinite (inert semi-fusinite + fusinite / sclerotinite + micrinite + inert inertodetrinite) indicates the proportion of less reactive particles; fusinites particularly may pass through a heating process unaltered and hence not contribute to the process. The influence of pressure is likely to increase the reactivity of the inert particles. The role of the different macerals during utilisation is dependent on particle size, oxidizing / reducing environments, time in the system, as well as the organic and inorganic interactions between and within the particles [Wagner and Joubert, 2005a].

5.2 GG41 GASIFIER PETROGRAPHIC MORPHOLOGY RESULTS

The detailed petrographic morphology results obtained for the GG41 gasifier are graphically depicted in Figure 3.38, which shows the global changes in the carbon and mineral matter contents of the samples within the gasifier. Photographs 1 (a to f)

depict the transformation of coal to char and different char types for selected GG41 gasifier turn-out samples (Figure 3.48). Photographs 2 (a to f) show various minerals and heat-altered minerals that were observed (Figure 3.49).

From Figure 3.38 it can be seen that a decreasing proportion of total coal particles with an increase and subsequent decrease in proportion of char particles occurs. It is possible to identify reaction zones occurring within the GG41 gasifier. For example, between samples 25 and 24 (beginning of pyrolysis), there was a significant decrease in the amount of coal, largely due to a decrease in inertiite particles (Figure 3.39 to be discussed later). Prior to this point, the proportion of coal remained fairly consistent. From sample 25 (start of pyrolysis), the proportion of devolatilising coal particles shows an increase (Figure 3.38), but did not become as significant as anticipated. This could be attributed to rapid alterations occurring in the particles through the gasifier zones.

It must be noted that char development was observed within the Bosman skirt (drying zone) and pyrolysis area of the GG41 gasifier (samples 32 to 15). This confirms the observation made earlier that carbon conversion was occurring within the drying and pyrolysis zones of the GG41 gasifier (see Figures 3.4 and 3.5 from a carbon perspective and Figure 3.46 from a temperature profile perspective).

From sample 15 (end of pyrolysis zone) a very low proportion of coal particles remain, since the coal has effectively all been converted to char (Figures 3.38 and 3.39). The maximum proportion of char was determined at sample position 14, where 75% of the sample was comprised of chars, predominantly intermediate in type (see Figure 3.43 to be discussed later), after which the proportion decreases down to the base of the gasifier. The proportion of ash-forming mineral increases significantly below sample 14, as the proportion of carbon in the system decreases due to reduction and combustion.

From Figure 3.39 it can be seen from the coal particle type results that inertiite (53 vol.%) is the most abundant microlythotype in the feed coal (sample 32) when compared to vitrite (11 vol.%), and liptite (2 vol.%). Carbominerite and the intermediate coal types make up the balance. In the drying zone of the GG41 gasifier, the inertite, vitrite and liptite microlythotypes remain relatively unaltered in terms of their relative abundance in the feed coal. However, a significant change is evident in the fast pyrolysis region of the gasifier (samples 25 to 20), where a reduction of 64%, 75% and 100% occurs in inertite, vitrite and liptinite content respectively. At the end

of pyrolysis (sample 15), all the coal has essentially been converted to char.

Maceral types (vitrinite and inertinite), followed by cracks and fissures appear to play the pivotal role in the changes experienced by carbon particles when exposed to increasing temperature. From the photographs shown in Figures 3.48 and 3.49, it is evident that the vitrinite band has begun reacting (1b), whilst the inertinite shows no visible changes. The whole vitrinite band running the length of the particle showed an equal degree of porosity. Photograph (1c) of a char particle, shows a similar finding. Photograph (1e) shows a mixed char particle with a variety of pores throughout the particle; the whole particle appeared to have been exposed to the same temperature at the same time [Wagner, 2005b].

A more detailed description of the char morphology in relation to other chemical and physical properties will be discussed in Sections 5.2.1 to 5.2.4.

5.2.1 The GG41 gasifier de-volatilised coal profile

A graphical representation of the GG41 de-volatilised coal profile, together with the coal char CO_2 char reactivity burn-off trend data are shown in Figure 3.40, in order to gain some insight into this particular relationship.

The decrease in reactivity observed for samples 20 to 15 in the "slow pyrolysis with gasification region" (see also Figure 3.21) correlates to an observed increase in de-volatilised coal formation of between 6 vol.% and 12 vol.% (Figure 3.40). De-volatilised coal contains particles that exhibit physical changes by becoming porous and swollen, but do not show any significant change in shade of grey from the parent coal under optical microscopy. Volatile components are being driven off as the particles are exposed to increasing temperatures; the vitrinite component is likely to exhibit de-volatilising behaviour more so than the other maceral types. Changes in shades of grey (from parent coal to white) in chars is readily observable optically and are related to increasing temperature exposure and volatile reduction [Wagner, 2005b].

This implies that the coal char CO_2 reactivity is reduced, as the vitrinite-rich macerals de-volatilise within the slow pyrolysis with gasification region of the GG41 gasifier. At this point the primary fragmentation process is complete (Figure 3.32) and the tar-free fragmented coal (Figure 3.3), having a higher surface area, is exposed to slow pyrolysis with gasification conditions (samples 20 to 15) within the pyrolysis zone.

FIGURE 3.48: PHOTOGRAPHS (1a - f) SHOWING THE TRANSFORMATION OF COAL TO CHAR FOR THE GG41 GASIFIER TURN-OUT SAMPLES (MAGNIFICATION X500, OIL IMMERSION, REFLECTED LIGHT [WAGNER, 2005b])

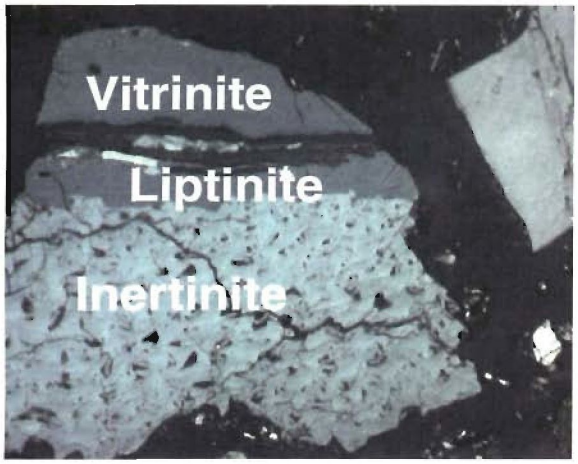

a) coal (sample 32)

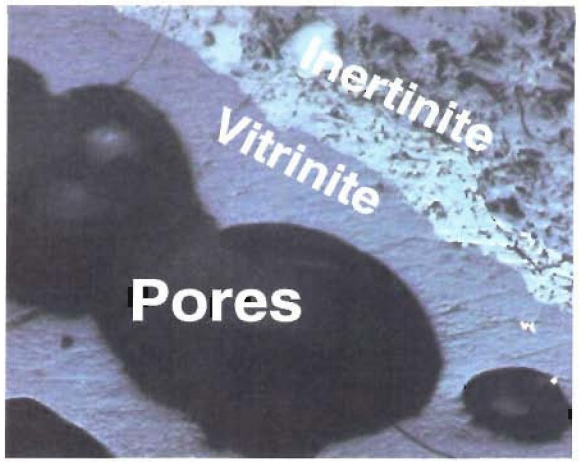

b) devolatilized coal (sample 24)

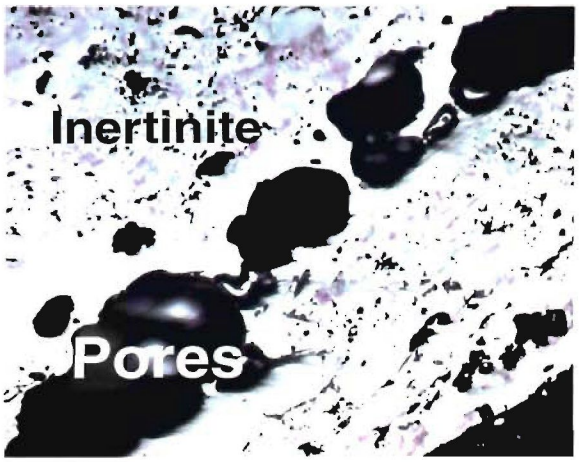

c) char particle (sample 21)

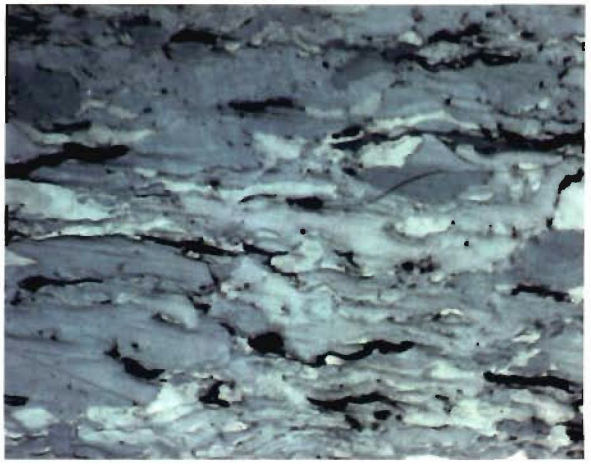

d) inertinite -rich coal particle

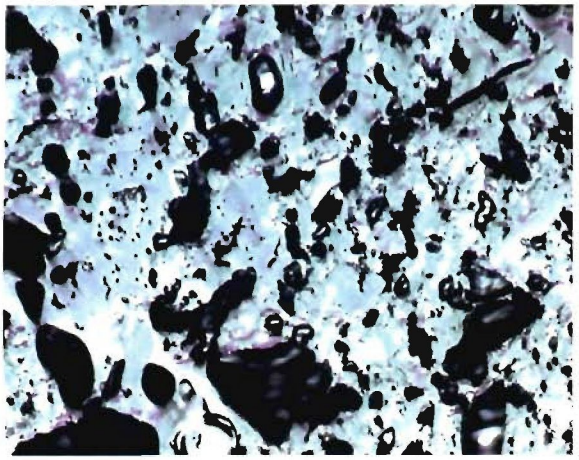

e) mixed char, originating from inertinite- rich particle

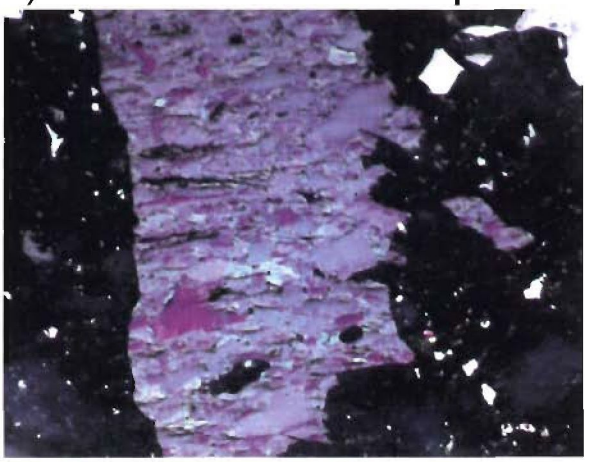

f) dense inertinite char, non-porous, x-polars

FIGURE 3.49: PHOTOGRAPHS (2a - f) SHOWING THE MINERALS OBSERVED IN THE GG41 GASIFIER TURN-OUT SAMPLES (MAGNIFICATION X500, OIL IMMERSION, REFLECTED LIGHT [WAGNER, 2005b])

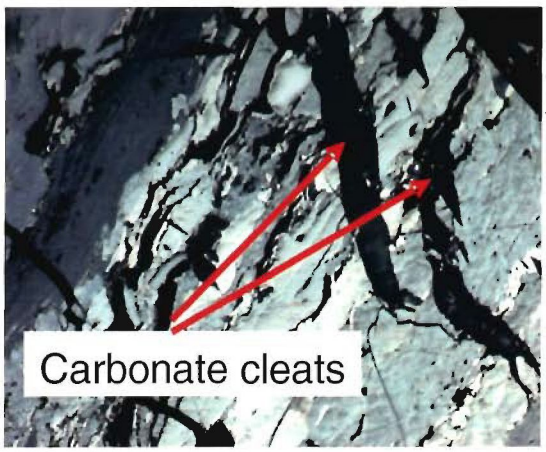

a) carbonate cleats in coal (sample 32)

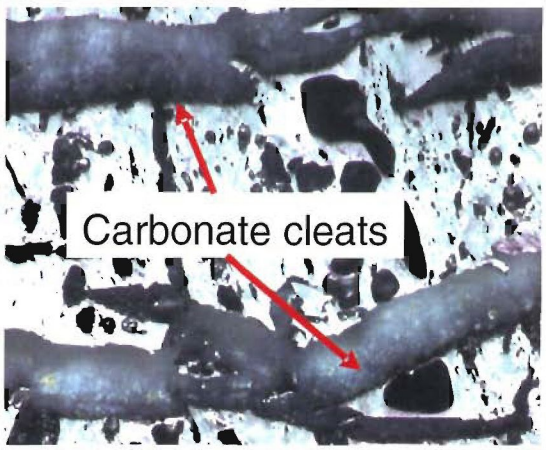

b) heat-affected carbonate cleats (sample 7)

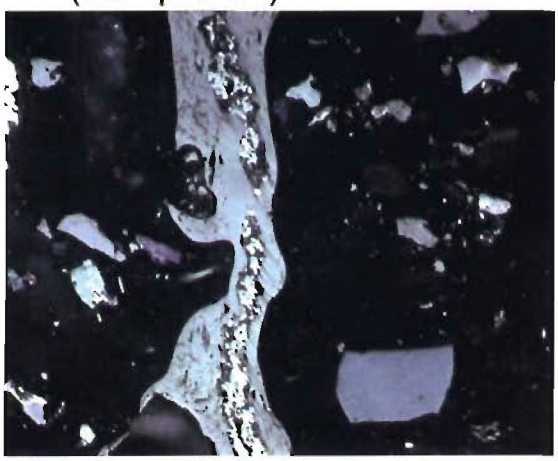

c) crystal laths (anorthite (sample 18)

d) amorphous mineral flowing (sample 9)

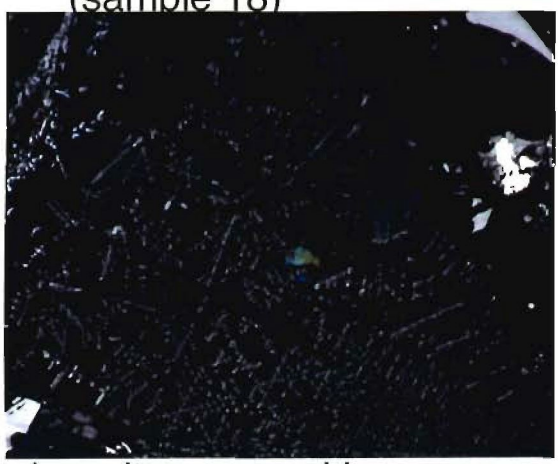

e) pyrite encased in devolatilizing coal (sample 7)

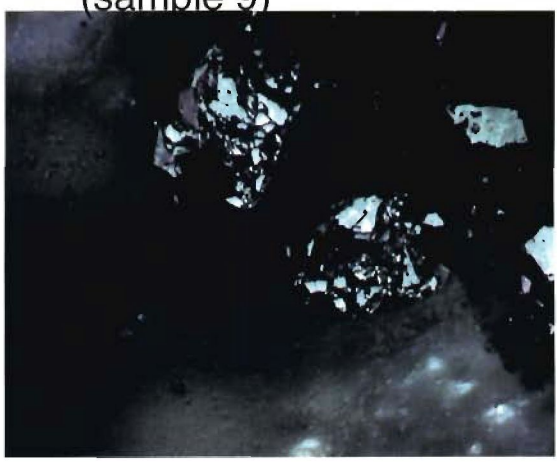

f) unusual mineral form (sample 7)

Once the de-volatilised coal percentage has decreased by about half, the internal porosity and the pore development progress as the coal char is exposed to higher temperatures (Figure 3.46); the heavier volatile fraction is further expelled. This relates to an increase in observable coal char CO_2 reactivity as the devolatilisation process diminishes after the completion of pyrolysis (see also Figure 3.21). In the reduction and combustion zones of the GG41 gasifier, the de-volatilised coal content is less than 0.5 vol. %, and the coal char CO_2 reactivity in this region diminishes with an increase in bed-depth. The aromatic character of the solid increases (Figure 3.11) due to the loss of non-aromatic side chains; the gases emitted in this regime include H_2 and CO, together with small amounts of CH_4 and CO_2.

In the "slow pyrolysis with gasification" region of the GG41 gasifier, the dry ash-free hydrogen content was shown to decrease, whilst the coal char CO_2 reactivity remained constant (Figure 3.22). The same observation is made here for the petrographically-determined devolatilised coal, which suggests that the slow gasification region can also be considered as a slow pyrolysis region, where slow devolatilisation of the heavier volatile components possibly inhibits the reactivity in this reaction zone.

5.2.2 GG41 gasifier total char profile

From the data shown in Table 3.4, it can be observed that the GG41 gasifier total char (vol.%) ranges from 0.5 – 2.4, 26.2 – 56.0, 56.8 – 67.8, and 15.3 – 38.7 in the drying, pyrolysis, reduction and combustion (ash-bed) zones respectively, thus the average "total char" percentage is significantly different between all the zones of the GG41 gasifier.

The total char formation profile for the GG41 gasifier is graphically presented in Figure 3.41, where it can be seen that c.a. 5 vol.% of the feed coal is charred within the drying zone of the GG41 gasifier. This is followed by a zone of significant char development within the pyrolysis zone of the gasifier, i.e. 48 vol.% char formation at the start of the slow pyrolysis with gasification region (sample 20) and 68 vol.% by the end of pyrolysis (sample 15), consistent with the data shown in Figure 3.38.

Within the reduction zone (samples 14 to 6), the total char content is further reduced to c.a. 45 vol.% at the start of combustion (samples 5), decreasing further to a char content of 15 vol.% at sample position 1 at the ash-grate, consistent with the data shown in Figure 3.38. Subsequently, the carbon conversion increased from 75% to

95% within the ash-bed (Figure 3.5).

5.2.3 The GG41 gasifier consumed char profile

The consumed char classification, reflects chars which exhibit a skeletal structure, irrespective of char morphology. The char is essentially almost combusted / gasified, the cell walls have become thin and appear brittle and a large proportion of this char type actually occurs as fragments which cannot be classified. Hence, the proportion of chars actually included in this category is low [Wagner, 2004a].

From the data shown in Table 3.4, it can be observed that the GG41 gasifier consumed char (vol.%) ranges from 0.4 – 2.1, 1.9 – 3.0 and 4.1 – 7.2 in the pyrolysis, reduction and combustion (ash-bed) zones respectively, with the average consumed char percentage only significantly different in the combustion zone when compared to the reduction and pyrolysis zones.

The consumed char profile is given in Figure 3.42, from which it can be seen that no consumed char remnants have formed within the upper part of the GG41 gasifier (samples 32 to 19). However, within the slow pyrolysis with gasification region, up to 1.5 vol.% of the consumed char form is evident at the end of pyrolysis. As the temperature increases within the fast gasification zone of the gasifier, the consumed char content doubles to 3 vol.% at the fire-bed position (sample 5). Char combustion reactions and excess steam cooling have a further effect on fragmentation and carbon reduction, consistent with the data shown in Figure 3.38.

5.2.4 The GG41 gasifier char type results

From the data shown in Table 3.4, it is clear that the GG41 gasifier porous char (vol.%) ranges from 0 - 0.3, 3.2 – 7.4, 5.4 – 8.5 and 0.5 – 2.8 in the drying, pyrolysis, reduction and combustion (ash-bed) zones respectively, showing a significant difference among the drying and pyrolysis zones, but with no significant difference in porous char development between the pyrolysis and reduction zones. However, both these zones are significantly different in porous char development when compared with the combustion zone.

From Table 3.4 it can also be observed that the GG41 gasifier intermediate char (vol.%) ranges from 0.1 – 1.5, 12.8 – 29.7, 27.2 – 37.9 and 7.6 – 20.1 in the drying, pyrolysis, reduction and combustion (ash-bed) zones respectively, indicating that the

average intermediate char percentage is significantly different among the various zones.

It can further be observed from Table 3.4 that the GG41 gasifier dense char (vol.%) ranges from 0.1 – 0.9, 7.3 – 13.4, 13.5 – 18.2 and 4.9 – 11.7 in the drying, pyrolysis, reduction and combustion (ash-bed) zones respectively, thus the average dense char percentage is different among the drying, pyrolysis and reduction zones, with no significant difference in dense char proportion when comparing the pyrolysis and the combustion zones.

The carbominerite char (vol.%) in the GG41 gasifier (Table 3.4) ranges from 3.0 – 6.1, 5.4 – 8.0 and 15 – 4.9 in the pyrolysis, reduction and combustion (ash-bed) zones respectively, clearly showing differences among the drying, pyrolysis and reduction zones, but there is no significant difference in carbominerite proportion between the pyrolysis and reduction zones.

Figure 3.43 is a graph of the petrographic char particle type analysis (vol. %) as a function of bed-depth. From the profiles, a clear understanding of the char type behaviour within the GG41 gasifier is obtained.

It can be observed that both the porous char and carbominerite char types follow similar burn-out profiles, i.e. commencing from sample position 20 (slow pyrolysis with gasification region) and increasing to c.a. 10 vol.% at sample position 13, where 53% carbon conversion has occurred (Figure 3.5). Both of these char forms are then combusted to near depletion at sample position 1 at the ash-grate.

The dense char type appears to form within the drying zone (0.9 vol.%), increasing steadily in the pyrolysis region to c.a. 18 vol.% at sample position 15. About 3 vol.% of this char type is still present in sample 1, thereby representing a clear indication of some carbon loss within the GG41 gasifier. As stated earlier, no pores are visible in the dense char, although cracks and fissures due to heat stress may be observed in these particles. Inert inertinite macerals, such as fusinites, are the likely precursors for this char form. It is likely that these chars do not contribute to gas formation, but rather play a role in maintaining the high temperatures within the gasifier. Once ignited, inert inertinites take longer to begin combusting than reactive vitrinite, but once ignited, remain longer than vitrinite.

It is worth noting that the gasification reactivity of the dense char type appears to occur at a slower rate that for the other three char types studied, i.e. the carbominerite, intermediate and porous char types all reach their respective maximum in char development by about sample 15 (end of pyrolysis), before the char is consumed in the gasification (reduction) and combustion zones of the GG41 gasifier. However, the dense char development continues until about sample 10 (1.5m lower down than for the other char types) before consumption of the dense char is visible.

Glover's earlier observation stating that dull char could possess the greatest affinity for volatile matter recondensation [Glover, 1988] could not be validated in this study when observing samples 27 to 25 (area where volatile recondensation was observed) in the drying zone of the GG41 gasifier (Figure 3.2). From Figure 3.43 it can be observed that the intermediate char type is the most abundant char form within the drying zone of the gasifier, i.e. 2 vol.%, but some dull char (0.9 vol.%) and porous char (0.3 vol.%) is also evident. Further work in this regard is necessary with future gasifier turn-out studies, where hand picking of the different char forms from this part of the gasifier can help with the understanding of char recondensation.

The intermediate char type profile shows that it is by far the most abundant form of char type within the GG41 gasifier. In the Bosman skirt area of the gasifier, this char type is already present. At sample position 20 (start of slow gasification), the intermediate char type is already 22 vol.%, increasing further to 44 vol.% at sample position 14. At the char-ash interface (sample 5), the intermediate char type is reduced to 24 vol.%, reducing further to a final concentration of 8.6 vol.% in sample 1 at the ash-grate. As for the dense char type carbon loss discussed above, the loss of carbon is even more significant with respect to the intermediate char.

Intermediate chars are those chars exhibiting a degree of porosity due to devolatilisation and degassing, but the pores are generally small or varied in size, the pore walls thick and sections of the particle do not exhibit any physical changes (apart from a slight increase in whiteness). Intermediate microlithotype particles, or inertinite particles with variable reactivities (reactive semi-fusinite, or inert inertodetrinite for example) are the likely precursors for these char forms. These chars are generally anisotropic, showing an increasing degree of anisotropy with increasing temperature exposure. These particles are likely to contribute to gas formation as well as to provide heat in the combustion zone; also referred to as mixed chars [Wagner, 2004a].

5.2.5 *The GG41 gasifier heat- affected mineral profile*

From the data shown in Table 3.4, it can be observed that the GG41 gasifier heat-affected mineral (vol.%) ranges from 6.6 – 17.1, 27.9 – 38.9 and 54.0 – 82.1 in the pyrolysis, reduction and combustion zones respectively, thus differences among these three reaction zones of the GG41 gasifier are evident.

The heat-affected mineral profile for the GG41 gasifier is graphically depicted together with the GG41 gasifier ash content trend data in Figure 3.44. From the figure it can be seen that the heat-affected minerals are only observed to appear below the Bosman skirt (drying zone) area of the gasifier.

A steady increase in heat-affected mineral development is seen within the slow and fast gasification regimes up to the ash-bed, i.e. from 15 vol.% (sample 20) to 47 vol.% (sample 5). Significant mineral changes are observed within the highly exothermic combustion zone, where 85 vol.% heat-affected minerals occur at the ash-grate. In general, a similar trend is visible when comparing the heat-affected mineral distribution profile and the GG41 gasifier ash content profile.

From the GG41 gasifier AFT profile, given in Figure 3.7, it was shown that mineral sintering was postulated to begin commencing at sample position 20 and a very narrow band in heat-affected mineral development (Figure 3.44) is shown from this point to the end of pyrolysis (sample 15). At the end of pyrolysis and the start of fast gasification (sample 15), mineral melting was postulated to occur from the AFT data and a significant change in heat-affected mineral content can be observed from the graph given in Figure 3.44. Van Dyk [2006] has conducted an in-depth study of mineral-matter transformation occurring during Sasol-Lurgi FBDB gasification and Fact-Sage modelling should be considered to better understand the mineral transformation behaviour with respect to the petrographically-derived heat-affected minerals. An understanding of the mechanisms responsible for slagging and sintering during mineral transformation will also provide insight into the relationship between the heat-affected minerals and the AFT [Matjie, 2005].

5.3 *TEMPERATURE PROFILE RESULTS*

In this section, a discussion of the results obtained from the use of vitrinite reflectance for temperature estimation will be conducted. By comparing the vitrinite reflectance values from the GG41 gasifier turn-out samples to a standard temperature profile

determined from the GG41 feed sample 32 (heated to known temperatures in a TGA); the mean, surface and peak temperatures could be determined for each turn-out sample. It is believed that this petrographic exercise, i.e. char morphology characterisation and temperature estimation is a first of its kind within Sasol and possibly globally. It is anticipated to provide a significant insight into the behaviour of the carbon particles during gasification, on its own and in conjunction with the other analyses performed.

The solid particulate temperature profile of the GG41 gasifier will be discussed together with the earlier findings by Krishnudu, *et. al.* [1989a] and Glover [1988], given in Figure 3.46. Detailed vitrinite reflectance analysis results and estimated temperatures for the GG41 turn-out samples are given in Tables A8 and A9 in Appendix A. Table 3.4 provides the statistical range calculated for the GG41 gasifier average, surface and peak temperature profiles obtained with respect to the four reaction zones identified.

5.3.1 The GG41 gasifier temperature profile results

The temperature calibration curve for the GG41 feed sample 32 is given in Figure 3.45. It can be observed that an excellent linear correlation was obtained for the calibration. This result shows that the reflectance of vitrinite (RoV) changes in a linear fashion with respect to temperature; therefore this calibration curve can be used to infer temperatures from the RoV measurements of the GG41 gasifier turn-out samples 2 to 32.

The RoV for sample 1 was not measured, due to difficulties with the determination owing to a lack of "carbon" present in the sample. It was therefore assumed in this case that sample 1 had experienced a temperature of 350°C, since this is the temperature at which the ash is discharged from the ash-lock. The "true" solids temperature at sample position 1 is, however, possibly higher than 350°C in reality, since some cooling is expected to occur within the ash-lock, below the ash-grate.

From the data shown in Table 3.4, it can be seen that the GG41 gasifier average temperature ranged from 356 – 383, 462 – 711, 828 – 861 and 439 - 942 °C in the drying, pyrolysis, reduction and combustion (ash-bed) zones respectively, indicating a significant difference between the drying, pyrolysis and reduction zones of the GG41 gasifier. The average temperature in the combustion zone reflected the largest temperature range of the zones identified in the GG41 gasifier, but intermediate in

range when compared to the other zones.

From Table 3.4 it can also be observed that the GG41 gasifier surface temperature ranged from 387 – 617, 787 – 1004, 958 – 1031 and 452 - 1206 °C in the drying, pyrolysis, reduction and combustion (ash-bed) zones respectively. It can be concluded that the average surface temperature is significantly different between the drying and pyrolysis zones, but there is no significant difference in surface temperature between the pyrolysis and reduction zones. Due to the cooling effect (estimated temperature of 350°C for sample 1); a wide surface temperature range of 452 – 1206 °C is evident in the combustion zone, statistically not significantly different to the other three GG41 gasifier reaction zones.

It can further be observed from Table 3.4 that the GG41 gasifier peak temperature ranged from 446 – 940, 1051 – 1132, 992 – 1137 and 440 – 1360 °C in the drying, pyrolysis, reduction and combustion (ash-bed) zones respectively. The average peak temperature is significantly different between the drying and pyrolysis zones, but there is no significant difference in peak temperature between the pyrolysis and reduction zones. Due to the cooling effect (estimated temperature of 350°C for sample 1), a wide surface temperature range of 440 – 1360 °C is evident for the combustion zone, statistically not significantly different to the other three GG41 gasifier reaction zones.

Figure 3.46 shows that the GG41 turn-out samples 32 and 30 had a similar average estimated temperature of 354°C within the drying zone of the gasifier. From sample 28, a change in the estimated average sample solids temperature to a maximum (peak) of 1008°C occurred, which correlates with the first significant amount of char reported in the particle type analyses (see Figure 3.43).

At the start of "slow pyrolysis with gasification" (sample 20), another marked increase in estimated temperature is displayed, i.e. average temperature of 617°C, surface temperature of 986°C and a maximum peak temperature of 1119°C. This finding correlates with results reported on the particle type analyses (Figure 3.43) and total char results (Figure 3.41), where a significant increase of char particles were observed (from 15 vol. % in sample 22, to 47 vol. % in sample 20).

A third noticeable change in reflectance was determined at sample position 16 (end of pyrolysis and start of reduction). The mean RoV changed from 3 RoV % (sample 18) to 5 RoV % (sample 16), correlating to an estimated average temperature ranging from 617°C to 837°C respectively. From sample 16 to the base of the gasifier, the

mean reflectance value remained at around 5 RoV %, indicating this to be the maximum mean reflectance determinable. The maximum reflectance reading and the maximum estimated temperature obtained were thus determined at sample position 16.

It has to be taken into account that the degree of confidence when using vitrinite reflectance for solids' temperature estimation decreases towards the bottom of the gasifier as the vitrinite particles are consumed. By sample 16, less than 1% coal vitrite type particles (Figure 3.38) and 9% porous chars remain (Figure 3.43) for reflectance analysis. At this midpoint level in the gasifier, the estimated average temperature is 837°C, surface temperature is 1075°C and maximum temperature is 1175°C.

As expected, the GG41 gasifier surface temperature trend is always higher than the average temperature, which is an indication of heat transfer limitations occurring within coarse particles. When comparing the GG41 gasifier peak temperature profile to the average and surface temperature trends, it is evident that significant temperature variations occur within the axially-derived sample layers in the gasifier, particularly in the top half of the GG41 gasifier, where endothermic conditions exist. This difference in temperature range (average, surface and peak temperature) appears to become less in the reduction zone as the char is further gasified, even less still in the oxidation zone, where exothermic conditions prevail. Within the combustion zone and ash-bed (samples 5 to 1), an interesting peak is noticeable in the surface and peak temperature trends, which requires some discussion.

Gasification agent (oxygen and steam) are added counter-currently to the descending charge (within the ash-bed) and the heat transfer between solid and gas rapidly increases the gas temperature in order to drive the reduction and pyrolysis reactions higher up in the gasifier. Reactions in this zone are highly exothermic and the rate of oxidation and combustion of the highly aromatic char proceeds rapidly. The agent distributor is attached to the slowly-rotating ash-grate which extends 0.9m from the base of the gasifier (sample 1) and the agent nozzles extend a short distance above the grate (into sample position 2). The possibility of uneven gas distribution and poor ash-bed mixing, leading to channeling and localised steam / oxygen variations, may possibly explain the high localised temperature extreme observed at sample position 2. At this point, the peak temperature is well above the ash fusion temperature, which gives rise to clinker formation.

This observation confirms the postulation made by Glover [1991], from which he considered oxygen enrichment as the likely cause of channel-burning.

5.3.2 The temperature profiles of the Indian pilot plant [Krishnudu, et. al., 1989a] and work conducted by Glover [1988] on the #15 Sasolburg gasifier

From Table 3.4 the factorised Indian pilot plant profile data obtained shows the temperature range from 355 – 385, 591 – 761, 795 – 912, and 506 – 1274 °C occurring in the drying, pyrolysis, reduction and combustion (ash-bed) zones respectively. In the Indian case, the average temperature is thus significantly different between the drying, pyrolysis and reduction zones when related to the GG41 gasifier zonal positions. The temperature in the combustion zone is significantly different from the drying zone, but not significantly different to the other two reaction zones above it.

The factorised Indian pilot plant temperature profile data obtained (Figure 3.46) shows remarkable similarity to the GG41 gasifier average temperature trend, with the exception of the high temperature peak observed in the ash-bed (sample position 4.5). This is interesting and warrants further discussion, since a different analytical technique was applied to obtain the temperature profile of the Indian coal.

According to van der Walt [1994], Gray-King assays were done on the Indian sequential samples (temperatures ranged from 400°C to 900°C), and a correlation between the volatile matter content in the char fractions and the temperature of this low-temperature carbonisation was established. The correlation was given as:

$$\log VM = 12.823 - 4.308 \log T \quad (17)$$

$$\log VM = 5.689 - 1.613 \log T \quad (18)$$

Where VM is the dry, ash-free volatile matter content in the char; T is the temperature in °C for -212 micron coal (equation 17); and for 25-100mm coal lumps, (equation 18).

Extrapolating outside of the temperature range (> 900°C) casts some doubt on the predicted highest temperature peak value of 1200°C occurring within the ash-bed for the Indian case. This observation is therefore in agreement with Johnson and Thomas [1987], who stated that the use of residual volatiles yield as a temperature indicator for the char samples is questionable. However, the fact that this temperature peak also occurs in the ash-bed region analogous to the GG41 gasifier case, where optical

reflectance was correlated with controlled feed coal temperature in the range 350°C to 1200°C (Figure 3.45), does offer some respite for the predictive method used by Krishnudu, *et. al.* [1989a].

The factorisation approach used for the Indian pilot plant data, assumed a simple constant factor related to sample height and no correction was made for the ash-grate height when scaling-up. This implies that the factorised Indian pilot plant data temperature spike observed at sample position 4.5, probably occurs lower down in the gasifier, analogous to the hot-spot region shown for the GG41 gasifier at sample position 2.

One could argue that both predictive temperature techniques are incorrect, since the GG41 gasifier peak temperature of 1400°C (sample 2) is also outside the calibration range, but the GG41 gasifier surface temperature at sample 2 is below 1200°C and also has this characteristic spike profile, which seems to suggest that the increased temperature observed in this region is correct and the peak temperature result of 1400°C should be treated with some caution. The distribution of oxygen and steam (agent) within the ash-bed appears to be a common effect for both the GG41 gasifier and the Indian cases. Further investigation, in order to fully understand the implications for Sasol-Lurgi FBDB gasification is advised.

Glover [1988] used an infra-red spectroscopic technique on the recovered char particles to estimate the solids temperature profile. The average bed temperatures were found not to vary significantly in the top part of the main bed (being in the order of 777°C) and some evidence was found that the gasifier jacket water acted to cool the boundary layer. Without the interfering effects of the ash-channelling, the bed could be described as an adiabatic core with a cooler boundary layer. The temperatures in the vicinity of the char-ash interface were approximately 877°C, peaking to 1027°C.

The Sasolburg #15 gasifier dissection results (after Glover [1988]), were averaged from the temperature profile data provided in Figure 1.12 (b) in Chapter 1, and are also given in Figure 3.46 for comparison to the GG41 gasifier and factorised Indian pilot plant data temperature profiles. It can be observed from the trends in Figure 3.46 that the #15 gasifier was operating at a higher average temperature when compared to the other two cases. This is not an unexpected result since the ash fusion temperatures of the Sasolburg coal are known to be higher than is the case at Secunda. The gasifiers are purposely operated at higher temperatures (below ash-

melting) resulting in the use of less excess steam and a resultant positive impact on the H : CO ratio. [Van Dyk, 2006].

In Table 3.4, it can also be observed from the #15 Sasolburg gasifier data [Glover, 1988], that the average temperature significantly differed between the drying and pyrolysis zones, i.e. 383 – 636 and 760 - 872 °C respectively. No data was supplied for the gasification and combustion zones.

Now that an explanation of the temperature profiles has been given, It is necessary to assess whether the reflectance data used for the GG41 gasifier turn-out (correlated with temperature) can be used to identify zonal regions in the Sasol-Lurgi FBDB MK IV gasifier, using the petrographic, chemical and physical property data that has previously been presented.

5.3.3 The GG41 gasifier temperature correlation with petrograhic char morphology

Table 3.6 shows a comparison of the petrographically-determined char morphology particle type distribution results, together with the GG41 gasifier RoV % measurements, to determine significant zonal levels occurring within the gasifier with respect to temperature. The table is colour-coded to identify regions of similarity for the reflectance data obtained and also applied to some of the char morphology data for comparative purposes. The four GG41 gasifier zones, i.e. drying (samples 32 to 26), pyrolysis (samples 25 to 15), reduction (samples 14 to 6) and combustion (samples 5 to 1) are also included for reference purposes.

The reflectance data obtained indicates five distinct temperature zones, i.e. 0.6, 0.9, 1.2, 3.0 and 5.0 RoV %. From level 16, the mean reflectance value becomes consistent, implying maximum temperatures at this point. As increased reflectance in a carbon particle is non-reversible, the particle will always reflect the maximum reflectance attained; this cannot be linked to the temperature in the surrounding environment. With the addition of steam at the bottom of the gasifier, the surrounding environment will have a lower temperature than at the middle of the gasifier.

From the particle type analysis results shown in Table 3.6, the total coal and total char values also correspond to some extent with the zones identified. There is a slight mismatch in space between the zones defined by reflectance and the zones defined

by the carbon particles; possibly indicating that as a particle is exposed to heat, the reflectance alters as the particle takes up the heat, followed by physical alterations. Chemical alterations are possibly occurring at the same time as the two petrographically observable changes in the particles.

From these results, it appears as if the reflectance technique is more able to determine early alterations in the coal particles exposed to increasing heat in the gasifier environment. This finding is not uncommon and is in line with observations regarding weathering and oxidation in coal, as reflectance analysis is a highly sensitive technique [Wagner 1998]. The total mineral (vol.%) trend correlates well with the four GG41 reactor zones shown, but a poorer correlation is evident for the complex carbon behaviour.

5.3.4 The GG41 gasifier temperature correlation with chemical properties

Table 3.7 shows a comparison of the GG41 gasifier chemical property distribution results together with the RoV % measurements, in order to determine significant zonal levels occurring within the gasifier with respect to temperature. The table is colour-coded to identify regions of similarity for the reflectance data obtained and also applied to the chemical property data for comparative purposes. The four GG41 gasifier zones, i.e. drying (samples 32 to 26), pyrolysis (samples 25 to 15), reduction (samples 14 to 6) and combustion (samples 5 to 1) are also included for reference purposes.

From this data obtained it appears that the volatile matter (% dry) distribution closely follows the reflectance (temperature) trend, which implies that coarse coal volatile diffusion is not a limiting factor in the top part of the gasifier (within the pyrolysis zone), where the average temperatures range is between 400°C and 900°C (Figure 3.46). Subsequently, the Fischer tar distribution profile is also closely related to the reflectance data (Figure 3.3).

Since the reflectance (temperature) relationship exists together with the volatile matter and tar distribution data, it is not surprising that Krishnudu, *et. al.*, [1989a,b] used the residual volatile matter correlation with respect to carbonisation temperature of the sequential Indian pilot plant samples in order to predict the solid temperature profile within the pilot-scale reactor. The final volatile yield is therefore dependent on the final pyrolysis temperature.

In general, the C, H, S, N and O data (% dry basis) also indicate five different zones occurring within the gasifier (Table 3.7). A slight lag is once more observed between the reflectance (temperature) zones and these chemical properties as the particles take up heat. The onset of slow pyrolysis (sample 20), relates to a common zonal change for C, H and N, whereas the S and O species are more reactive than the aforementioned higher up in the pyrolysis zone. The oxygen distribution data tends to correlate reasonably well with the reflectance (temperature) zone positions, particularly with respect to the highest temperature zone, commencing at sample 16 (end of pyrolysis). No correlation between coal char CO_2 reactivity and reflectance (temperature) is evident. The complexity of the gasification process with respect to chemical property behaviour is clearly exhibited in Table 3.7.

5.3.5 The GG41 gasifier temperature correlation with physical characteristics

Table 3.8 shows a comparison of the GG41 gasifier physical property distribution results together with the RoV % measurements, to determine significant zonal levels occurring within the gasifier with respect to temperature. The table is once again colour-coded to identify regions of similarity for the reflectance data and also applied to the physical property data for comparative purposes. The four GG41 gasifier zones, i.e. drying (samples 32 to 26), pyrolysis (samples 25 to 15), reduction (samples 14 to 6) and combustion (samples 5 to 1) are also included for reference purposes.

The physical property data given in Table 3.8 shows no clear delayed correlation effect with vitrinite reflectance, except in the case of the true density profile. The GG41 gasifier true density profile appears to be clearly driven by the temperature gradient within the gasifier.

The bulk density trend data correlation with reflectance is interesting in that a delayed effect is observed up to the end of the pyrolysis zone (sample 14). Thereafter, a reversal in the bulk density curve is observable as fast gasification and oxidation reactions occur towards the base of the reactor.

The reflectance data obtained cannot exhibit the cooling effect which occurs in the bottom half of the gasifier, yet it is known that a reversal in the temperature profile will occur in this region as excess steam is added at the base of the reactor (Figure 3.46). The reversal in the bulk density zonal trend data reflected in Table 3.8 (samples 15 to 1) could be speculated to possibly be indicative of the "real" temperature profile

distribution occurring within the gasifier as a function of the particle size distribution alteration and subsequent packing density changes obtained. This packing density has been shown to be related to the amount of intermediate -25mm +6.3mm particles present (Figure 3.30).

The particle size data shown in Table 3.8 does not generally correlate with the five zonal reflectance (temperature) regions in terms of clear distinctive progressive temperature gradients, but can at least be fitted into five zonal regions indicative of step changes occurring. A correlation between the -6.3mm size distribution profile and the Ergun Index is observed from Table 3.8 and Figure 3.33, showing regions of high pressure drop and resultant gasifier instability occurring within the GG41 gasifier (Figure 3.32).

In conclusion, Tables 3.6 to 3.8 clearly show the complex averaged axial inter-relationship response between the chemical, physical and petrographic properties with respect to temperature in the fixed-bed gasification process.

6 THE GG41 GASIFIER "PAN-CAKE" MODEL

Finally, a "pan-cake" model showing the axial distribution profiles of most of the parameters investigated, together with the average temperature profile is given for the GG41 gasifier in Figure 3.47. The work of Glover [1988] refers to a W-shape profile (at least in the radial direction) which is very different from a pan-cake model and can be referenced in Figure 1.12 in Chapter1.

From Figure 3.47 a clear visual indication of the positions of the drying, pyrolysis, reduction and combustion (ash-bed) zones within the GG41 MK IV gasifier are noticeable.

Within the Bosman skirt region of the GG41 gasifier (samples 32 to 26), temperatures of up to 400°C are evident, resulting in some preliminary charring of the coal and minor recondensation of tar occurring. Water is driven off and the thermal fragmentation mechanism weakens the coal's structural mechanical integrity, resulting in breakage of the coarse +25mm and -25mm +6.3mm particles.

An excellent positional correlation between the petrographically-derived de-volatilised coal type, in relation to the pyrolysis zone, as indicated by the volatile matter distribution profile is apparent (samples 25 to 15). In this region, the coal char CO_2

reactivity is suppressed initially as volatiles are expelled and tars released. However, midway within the pyrolysis zone a slow gasification zone is apparent, wherein endothermic reactions dominate, thus increasing the char reactivity; the fixed carbon shows a subsequent mild step change (samples 20 to 15).

The total coal petrographic profile shows clearly that all the coal has essentially been converted to char by the end of pyrolysis. Within this zone, the average temperature increases to 850°C, thus preparing the resultant char for the gasification reactions that occur lower down in the reactor, as can be observed from the total char profile, which reaches a maximum at sample 14. Just before the onset of slow pyrolysis (sample 21), the thermal and mechanical fragmentation mechanisms conclude the primary fragmentation process, resulting in breakage and shattering of coal / char. The ash content increases from 28% to 50% within the pyrolysis zone and "hot- spots" caused by channel-burning lead to high localised peak temperatures, resulting in some melting of the ash-forming minerals. The pyrolysis zone occupies half of the reactor space available within the GG41 MK IV gasifier, when including the Bosman skirt (drying zone) region.

Reduction occurs at the end of pyrolysis (samples 14 to 10), where the coal char CO_2 reactivity is observed to reach a maximum at the onset of partial oxidation (sample 10). The char is now rapidly consumed as shown by the reversal in the total char profile and steep slope change in the fixed carbon trend. The mechanical integrity of the highly aromatic char is weakened due to a further temperature increase, resulting in secondary fragmentation breakage of particles (samples 14 to 10). Further melting of the ash-forming minerals act as a "glue" and agglomerate particles together, thereby increasing the amount of the coarse +25mm fraction. The char pores collapse at the fire-bed, with a resultant reduction in coal char CO_2 reactivity and diffusion control takes over from the up-to-then kinetically controlled regime.

Within the combustion zone and ash-bed (samples 5 to 1), the remaining char / carbon is essentially combusted and excess steam is added to minimize clinker formation. The steam and oxygen agents added through nozzles just above the ash-grate (sample position 2), result in localised oxygen-enrichment causing a resultant high peak temperature, above the ash fusion.

The resultant ash contains 9% fixed carbon; the carbon loss can be attributed to incomplete combustion of the intermediate char type (possibly related to reactive semi-fusinite and inert interodetrinite microlythotypes present in the feed coal) and to

a lesser extent to the dense char, but not to other char types identified, i.e. porous char and carbominerite char.

Oxygen scavenging, which occurs during mineral transformation, is observed to consume expensive gaseous oxygen forming species such as $Mg_2Al_4Si_5O_{18}$ (corderite) and $Fe_2Al_4Si_5O_{18}$ (ferro-corderite) that melt, forming an anorthite slag phase at 1027°C, and the sum of oxygen scavenging related to mineral transformation of c.a.7% oxygen.

The results presented in this thesis are of great significance for the understanding of the critical processes occurring within a commercial-scale Sasol-Lurgi MK IV FBDB gasifier. Clear zonal profiles and interpretation of the internal petrographical, chemical and physical property behaviour in relation to these zones have been attained through the course of this investigation.

Profile evaluation on a factorised basis with a quarter-scale Lurgi gasifier operating on Indian coal, has provided an excellent basis for comparison. The good agreement obtained thus substantiates credibility of the current findings with respect to repeatability. This also has implications regarding scale-ability to smaller gasifier sizes, should the need arise to conduct small scale gasification experiments that can be scaled-up to a commercial-sized 4m diameter reactor.

The findings of this study also indicate where optimisation opportunities exist for the MK IV gasifier, i.e. char type responsible for carbon-loss, oxygen scavenging effect of minerals, volatile matter recondensation in the cooler zone of the gasifier, localised oxygen sparging causing hot-spots just above the ash-grate, and most importantly, reduction of the top size of the feed coal to a "thermally stable" size resulting in a more stable gasifier operation with possible process efficiency benefits.

CONCLUSIONS AND RECOMMENDATIONS

Gasification behaviour is particle dependent, whilst gasifier (reactor) behaviour is an averaging process of individual responses of each particle [Glover, 1991]. It was hypothesized, that if it were possible to extract and analyse particles from different reaction zones within a gasifier, it may be likely to enhance the understanding of the contribution that these particles make towards gasification. This better understanding of the particle-type compositional responses could act as an enabler to further manipulate gasifier performance.

The primary focus of this study was to evaluate the proposed sequential (axial) sampling "turn-out" methodology of the entire Sasol-Lurgi FBDB MK IV gasifier, in order to present samples that accurately describe operational aspects occurring in the reaction zones within the reactor. Characterisation of the chemical, physical and petrographical properties of the sample increments were expected to deliver distinct profiles of the drying, pyrolysis, reduction and combustion (ash-bed) zones, which could be used to advance the kinetic modeling capability of the process. In order to interpret the coal property transformational behaviour occurring within the commercial-scale gasifier, the following analyses were undertaken:

- Proximate and ultimate analysis
- Coal char CO_2 reactivity analysis
- Ash-melting characteristics
- Density characteristics
- Particle size distribution
- Thermal and mechanical fragmentation
- Caking propensity
- Char morphology
- Temperature profile using optical reflectance

Secondary objectives included:

- Obtaining a better understanding of the loss of carbon to the discarded ash,
- Ascertaining whether oxygen scavenging during mineral transformation occurs during gasification, and
- Developing an understanding of the zones of instability occurring within the gasifier.

CONCLUSIONS

According to the standard coal properties, i.e. proximate analysis, ultimate analysis, maceral composition, AFT, coal char CO_2 reactivity, Fischer tar content, thermal fragmentation, mechanical fragmentation, caking propensity and particle size distribution, the GG41 feed coal used in this study was found to be within the variation of the coal typically used for gasification, therefore representative of and comparable to the coal currently used for gasification purposes at Secunda.

The new-to-Sasol "controlled" GG41 gasifier turn-out and sampling methodology employed, provided good residual internal profile results, clearly showing the complexity and interdependency of the coal properties studied with respect to transformational behaviour during gasification. By keeping the turn-out sample increment size constant whilst maintaining a constant ash-grate discharge speed to simulate plug-flow conditions (minimise vortex-swirl), 32 fractional "slices" of the entire gasifier contents could be successfully extracted.

The incremental truck-sampling methodology used, was also found to produce reasonable sub-samples; subsequent size reduction and preparation for analytical purposes required that in some cases the sub-sample slices be further reduced. Considering that about 100 tons of the GG41 gasifier solid material content had to be sampled and the sub-samples analysed, it is plausible when observing the "pan-cake" model derived for the GG41 gasifier, that minimal scatter in the data trends were evident.

The GG41 gasifier reaction zones, i.e. drying, pyrolysis, reduction and combustion (ash-bed) zones, have been successfully elucidated using the chemical property analysis profiles studied, i.e. proximate, ultimate and coal char CO_2 reactivity distributions. Although the axial sampling methodology employed, provided an over-simplification of the complex localised radial coal property transformational behaviour, the averaging effect obtained provides a clear "snapshot" in time of the reaction zones present, being the first ever representation of the zonal profiles occurring within the Sasol-Lurgi MK IV reactor.

The GG41 gasifier drying zone was found to be prevalent within the Bosman skirt feeder region in the uppermost (1.5m) part of the fixed-bed gasifier. Volatile matter recondensation and some evidence of particle size segregation were observed as the charge descended, denoted by the increase in -6.3 mm content and decrease in

+25mm content within this zone. These findings are in agreement with the work conducted by Glover [1988, 1991], who also observed these phenomena to occur within this region.

The pyrolysis zone was found to be the largest reaction zone (2.86m) situated below the drying zone within the GG41 gasifier, followed by the reduction zone (2.34m), and combustion (ash-bed) zone (1.94m including the volume occupied by the ash-grate). Whilst the boundaries of the pyrolysis zone were very clearly defined by the residual volatile matter distribution profile, distinctive regional overlap with a "slow pyrolysis with gasification" region was observed in the bottom half of the pyrolysis zone, above which a "rapid devolatilisation" region existed. This finding is in agreement with the work of Krishnudu, *et. al.*, [1989a,b], who also reported a "slow pyrolysis with gasification zone" occurring within the quarter-scale Lurgi 1.13m diameter fixed-bed reactor, although the relative factorised positions of this zone were found to differ slightly in the two respective cases.

The reduction zone was found to also exhibit an overlap in zonal fronts, i.e. a gasification region occurred below the pyrolysis zone and co-existed in equal proportions, with an oxidation frontal region occurring above the combustion zone. The combustion zone was found to be very shallow (0.26m), below which the ash-bed region existed. These findings clearly suggest that text book pictures showing axially depicted reaction zones occurring within the fixed-bed gasifier, i.e. drying, pyrolysis, gasification and combustion, inadequately describe the "real" situation; in practise, overlap of reaction regions within zones indeed also transpires.

The GG41 gasifier profile comparison, conducted on a factorised basis with a quarter-scale Lurgi gasifier operating on Indian coal [Krishnudu, *et. al.,* 1989a,b], provided an excellent basis; the good agreement obtained, thus substantiates credibility of the current findings with respect to repeatability. This also has implications regarding scale-ability to smaller gasifier sizes, should the need arise to conduct small scale gasification experiments that can be scaled-up to a commercial-sized 4m diameter reactor.

From the unique GG41 gasifier **petrographic** char morphology results obtained, it has been found that the maceral type (vitrinite, and inertinite), followed by cracks and fissures occurring within the particle, appears to play a pivotal role in the changes experienced by carbon particles when exposed to increasing temperature. Whole vitrinite particles and vitrinite bands within particles devolatilised first, followed at

higher temperatures by reactive inertinite types. The porous chars remained predominantly isotropic and the mixed and dense chars showed varying degrees of anisotropy, which is related to the aromaticity of the carbon. At the end of pyrolysis (middle of the GG41 MK IV gasifier) all the coal was found to be essentially converted to char, but chars continued to increase as the charge further descended within the gasifier, becoming consumed in the oxidation / combustion zone.

The GG41 gasifier char type results further showed that both the porous and carbominerite char types follow similar burn-out profiles, i.e. commencing from the "slow pyrolysis with gasification" region within the pyrolysis zone, increasing to c.a. 10 vol. % within the reduction zone, where 53% carbon conversion occurred. Both of these char forms were then combusted to near depletion at the ash-grate, therefore not contributing to the carbon loss in the ash discharge. The dense char and intermediate char types, on the other hand, are clearly responsible for the few percent carbon loss that is consistently obtained at the Secunda gasification operations.

Glover [1988] concluded that dull char could possess the greatest affinity for volatile matter recondensation, but could not be validated in this study in the area where volatile recondensation was observed within the drying zone of the GG41 gasifier. Intermediate char was found to be the most abundant char form within the drying zone of the gasifier, but some dull and porous char was also evident.

The GG41 gasifier particle type analysis, based on the total coal and total char values, indicated five different temperature zones within the gasifier when related to the optical reflectance (temperature profile). A slight lag time between the zones defined by reflectance and the zones defined by the carbon particles was evident, basically inferring that as a particle is exposed to heat, the reflectance alters as the particle "absorbs" the heat, followed by physical and chemical alterations. It appears as if the reflectance technique is more able to determine early alterations in the coal particles exposed to increasing heat in the environment. This finding is not uncommon and is in line with observations regarding weathering and oxidation in coal [Wagner 1998].

It is believed that this combined petrographic exercise (temperature estimation using optical reflectance and char morphology classification) is the first of its kind within Sasol and possibly globally; it was shown to provide a significant insight into the behaviour of the carbon particles during gasification, on their own and in conjunction with the other analyses performed.

The GG41 gasifier chemical property profiles (proximate, ultimate and coal char CO_2 reactivity) studied, were found to be extremely useful in elucidating on the reaction zones present within the Sasol-Lurgi MK IV gasifier. A greater level of detail understanding of the volatile matter and fixed carbon behaviour was obtained after normalisation.

From a proximate analysis perspective, the GG41 gasifier profiles obtained, compared favourably to the factorised Indian pilot plant data, essentially vindicating the simplistic factorisation (scaling) approach applied, albeit that different coals and fixed-bed reactor geometries were being compared.

Normalised carbon conversion results showed that similar conversions were evident for both the GG41 gasifier and the Indian pilot plant cases, suggesting that coal reactivities were probably similar, i.e. 2 - $5h^{-1}$. The #15 gasifier carbon conversion profile [Glover, 1988] was found to be different to the foremost and can be explained by the fact that the reactivity of the Sasolburg coal is known to be higher (6 - $10h^{-1}$) than for Secunda Highveld coals, also resulting in a much higher fire-bed position (midway in the gasifier). The char-ash interface (fire-bed) position in the case of the GG41 gasifier, was postulated to commence 2m from the base of the ash-grate, where c.a. 70% carbon conversion had been obtained. This finding is in agreement with Glover [1988, 1991], who concluded from his "dig-out" studies, that the char-ash interface was always typically found when a carbon conversion value of 60% to 70% had been attained.

The GG41 gasifier AFT profile showed a decrease in the softening temperature (ST) and the hemispherical temperature (HT) at the onset of the "slow pyrolysis with gasification" region, probably signaling that some preliminary sintering had already occurred in this region of the gasifier. The end of the pyrolysis zone was found to be a good indicator of where mineral melting and slagging occurred within the GG41 gasifier. An increase in the coarse +25mm size fraction content was observed from the onset of the reduction zone to the base of the GG41 reactor, clearly showing the size-upgrading effect of the ash mineral dissolution chemistry, resulting in an increase in particle size and clinker formation in the bottom half of the GG41 gasifier.

The GG41 gasifier ultimate analysis profiles provided good insight into understanding the development of aromaticity of the char, expressed by the carbon : hydrogen ratio. Equilibrium compositional profiles calculated for C, H, N, S and O provided good discernment regarding the speciation and partitioning behaviour occurring within the

fixed bed-reactor. Fact-Sage thermodynamic equilibrium modeling of the Sasol-Lurgi FBDB gasifier related to the ultimate analysis results, was found to be useful in identifying an oxygen scavenging effect created by the mineral transformation behaviour occurring during reduction. It was found that large oxygen-containing species such as $Mg_2Al_4Si_5O_{18}$ (corderite) and $Fe_2Al_4Si_5O_{18}$ (ferro-corderite) form within the reduction zone. Oxygen is the most expensive input cost to the gasification process and 2% of the gasification input oxygen was found, in this study, to be consumed in the mineral transformation (non-slag) phase. It would appear that it is more a function of mineral composition than merely ash content that is significant in the gasification process, when viewed on an oxygen consumption basis.

The GG41 gasifier coal char CO_2 reactivity profile clearly revealed the position of the fire-bed in the reactor, as shown by the deflection in the curve at this point. It is summised that the reduction in reactivity observed below the fire-bed position can possibly be related to diffusion control limitations, where the pore structure collapses with a resultant reduction in active surface area. A kinetically controlled regime is postulated to dominate in the upper 7m of the reactor. The coal char CO_2 reactivity was also correlated with the dry-ash-free hydrogen content, confirming the lab-scale results of Fatemi-Badi, *et. al.*, [1988] and Solomon, *et. al.,* [1988] in that the commercial-scale observation also showed a deflectance around 2% hydrogen content. Thereafter, the coal char reactivity remained constant up to 1% hydrogen content in the "slow pyrolysis with gasification" region within the pyrolysis zone of the GG41 gasifier. During reduction, the coal char CO_2 reactivity was shown to increase significantly with a minimal decrease in hydrogen content, before pore collapse and diffusion limitations finally decreased the char reactivity at a constant hydrogen content within the combustion zone.

The GG41 ***physical property*** profiles (bulk density, true density, particle size distribution, thermal and mechanical fragmentation, as well as caking propensity) studied, also provided significant insight into the complex heterogeneous nature of the coal transformation processes occurring within the fixed-bed reactor. In the case of the bulk density profile, a shrinking core and flaking mechanism was proposed to explain the increase in density occurring in the bottom half of the gasifier. This profile was also found to be in agreement with the factorised Indian pilot plant bulk density data [Krishnudu, *et. al.,* 1989a,b].

The true density profiles obtained for the GG41 gasifier turn-out and the factorised Indian pilot plant data were found to be in some disagreement, particularly in the

pyrolysis and reduction zones of the reactor. A plausible explanation cannot be given, but mineralogical differences between the two coals studied and density measurement techniques used, are expected to be responsible for this anomaly.

The GG41 gasifier +25mm size fraction distribution profile was found to clearly show the fragmentation effects occurring within the reactor. Primary fragmentation was found to cause breakage of the +25mm size fraction down to a "stable thermal" size (15% +25mm) in the "slow pyrolysis with gasification" region of the pyrolysis zone. At this point c.a. 80% of the +25mm size fraction had been reduced to the finer size fractions. The significant breakage of the coarse +25mm fraction down to a "stable thermal" size is expected to create unstable gasifier conditions in the top part of the gasifier, due to pressure drop fluctuations caused by void packing. Thermal-channelling was observed in this region by Glover [1988] in a number of gasifier dig-out's; concluding that local steam to oxygen ratio variations may occur, possibly allowing for higher temperatures to be reached above ash-melting, giving rise to clinker formation in certain areas of the gasifier. The reduction of the top size of the Secunda feed coal to a "stable thermal" size prior to gasification should be further explored.

A good correlation was obtained for the relationship between bulk density versus the -25mm + 6.3mm size fraction content, indicating that the bed-packing density is highly dependent on the relative abundance of this intermediate size fraction. The -6.3mm size fraction content was statistically found to not be significantly different between the four GG41 reaction zones identified, implying that breakage of the coarser +6.3mm sizes occurred continuously, and could possibly be related to breakage caused by the ash grate when sampling.

The Ergun Index was successfully used to profile the fragmentation zones identified and to show areas within the gasifier where pressure drop and resultant instability occurs. This is a first-ever identification of this phenomenon occurring within a fixed-bed gasifier and is expected to lead to significant optimisation challenges to ensure better stability. A correlation of the relationship between Ergun Index and the -6.3mm size fraction was found to be in agreement with the literature relating to the Ergun equation [Leva, 1959], which shows that if the Sauter diameter of the denominator, i.e. -6.3mm fraction content increases then the pressure drop also increases. The GG41 gasifier Ergun Index profile compared very favourably with the factorised Indian pilot plant case, albeit that the top size used in the Indian case was 25mm versus 100mm for the GG41 gasifier.

A qualitative understanding of the primary fragmentation mechanism was also obtained in this study from the commercial-scale GG41 gasifier samples. A positive linear correlation was indeed found to exist between thermal fragmentation and total moisture content, which confirms the earlier lab-scale work of Van Dyk [2001a]. The thermal fragmentation process was found to be prevalent up to the start of the pyrolysis zone (i.e. within the drying zone), thereafter showing less of an effect on particle breakage than the process of mechanical fragmentation. Due to the low level of caking present in the GG41 gasifier coal feed sample, no dramatic effects in terms of caking behaviour could be elucidated on from this study.

The average temperature profile measurements of the solid particles, revealed the temperature range occurring within the pyrolysis zone of the GG41 gasifier. The average (mean) temperature ranged from c.a. 400^{o}C up to 850^{o}C within this region, which is in agreement with literature-cited temperature ranges typically reported for pyrolysis [Slaghuis, 1989]. In this highly endothermic region of the gasifier, the particle surface temperature and peak temperature showed visible evidence of heat transfer limitations occurring through lump coal when compared to the mean particle temperature (variations by as much as 700^{o}C), providing some evidence of the complex radial and localised behaviour occurring within the averaged axial sample slices. In the oxidizing and combustion regimes, exothermic conditions prevail and heat transfer differences across the particles are minimized.

The GG41 gasifier solids average temperature profile was also found to be in reasonable agreement with the factorised work of Krishudu, *et. al.,*[1989a.b], albeit that two different coal types and temperature profile estimation methods were utilized. A characteristic spike, indicative of an increase in temperature, was found in the sample taken directly above the ash-grate in the case of the GG41 gasifier, seeming to indicate that agent distribution through the nozzles positioned just above the grate is not uniform, resulting in localised oxygen concentration increases with subsequent "hot-spots" and channel-burning occurring. This finding is also observed from the Indian pilot plant case study, suggesting that this is a design issue that is possibly common to the Lurgi fixed-bed gasifier.

It is concluded that the primary and secondary objectives of this study were successfully accomplished and that a "pan-cake" model showing the coal property transformational behaviour occurring within the GG41 FBDB MK IV reactor, with respect to the reaction zones present, has been successfully attained. The findings of this study also clearly indicate where optimisation opportunities exist for the MK IV

gasifier, i.e. char type responsible for carbon-loss, oxygen scavenging effect of minerals, volatile matter recondensation in the cooler zone of the gasifier, localised oxygen sparging causing hot-spots just above the ash-grate, and reduction of the top size of the feed coal to a "thermally stable" size, could result in a more stable gasifier operation with possible process efficiency benefits.

RECOMMENDATIONS

The experimental data obtained from this study should be used as input for the Sasol Technology (1-dimensional) kinetic models in order to validate / improve their predictive capability. Modelling of the petrographic char morphology and tar distribution profile, together with the commonly-used "ash and fixed carbon" properties will provide significant insight into the pyrolysis zone behaviour. Plant control philosophy optimisation should form the key output of the kinetic process modelling.

Repeatability of the "new-to-Sasol" GG41 gasifier sampling methodology in further turn-out study campaigns should be conducted using the standard Bosman skirt and standard ash-grate internal mechanical configuration in order to statistically evaluate the repeatability between tests and gasifiers running at medium load conditions. Thereafter, turn-out studies on gasifiers having other internal mechanical configurations, i.e. rubble finger (fitted on the ash-grate to improve ash-bed mixing), as well as "Unifeeder" designs (thought to minimize segregation effects in the drying zone) should be studied and compared.

Further gasifier sampling campaigns should ensure that ash samples are taken from the ash-lock prior to water quenching, so that the extent of char exfoliation and mechanical fragmentation caused by the rotating ash-grate during sampling on the fine -6.3mm size fraction can be better understood. The carbon conversion phenomenon that was found to occur within the drying zone should also be verified, since this result is unexpected and could be because of channel-burning due to lump coal segregation effects, or it could merely be as a result of the top of the bed "turning-over" on itself during sampling.

Further turn-out studies should also include hand picking of the different char forms from samples taken in the lower part of the Bosman skirt region of the gasifier, in order to help with the understanding of the char recondensation phenomenon with particular emphasis on the dense and intermediate char types.

The relationship between the bulk density profile and the -25mm +6.3mm size fraction of the MK IV gasifier should be confirmed in future turn-out studies, since this was found to be mainly dependent on the characteristics and relative abundance of the dominant size fraction present, which then clearly governed the packing density distribution obtained.

A detailed petrographic and reactivity characterisation study of the Sasol Coal Supply (SCS) coal sources should be undertaken in order to ascertain the reactivity, concentrations and partitioning behaviour of the intermediate microlithotype particles, which are the likely precursors for the dense and intermediate char forms, i.e. inertinite particles with variable reactivities, eg. reactive semi-fusinite, or inert inertodetrinite. Once characterised petrographically, the study should ascertain whether it is possible to optimise blending of the various coal sources based on a new petrographic parameter in order to minimize the presence of some of these lower reactive char precursors prior to gasification, in order to minimize the 5% to 7% carbon loss in the Sasol-Lurgi FBDB gasifier.

The use of reflectance of vitrinite (RoV) as a proxy for temperature could potentially give incorrect temperature readings of particles that were subjected to chemical reaction. Different calibrations for particles that have been allowed to react away to say 10, 20, 50, 80% carbon conversion in a TGA apparatus should be conducted and the calibration curve results compared with an inertly heated environment case.

A detailed mineralogical investigation of the GG41 gasifier turn-out samples should be conducted in order to provide more clarity on the qualitative observations made regarding AFT reported in this study. The trace, minor and major element distribution profiles from the GG41 gasifier should be characterised in order to also assist in validating the Fact-Sage thermodynamic equilibrium model predictions of the fixed-bed gasifier.

Further work should investigate the possibility of suppressing oxygen scavenging during mineral transformation, thereby providing a fundamental understanding of how the capturing of oxygen by mineral matter can be minimized.

The reduction of the Secunda gasifier feed coal top size to a stable "thermal size" of (15% +25mm x 6.3mm) should be tested on the GG09 test gasifier and subsequently "turned-out" to exhibit the reaction zone positions and the likelihood of kinetic and stability benefits. As a result of the expected improved kinetics, gasification load

could possibly be maximized yielding more gas per unit reactor, possibly helping to also minimize the 5% to 7% carbon loss in the discharge ash. This hypothesis should be further investigated in future fundamental studies.

Correlation effects between thermal fragmentation, mechanical fragmentation, Ergun Index, moisture content, caking propensity and particle breakage should be further studied. Actual fragmentation behaviour is represented by the observed changes in PSD from sampling position to sample position within the gasifier. Predicted fragmentation is derived from thermal / mechanical tests (done outside of the gasifier). Predicted behaviour must then be compared with actual behaviour.

A discreet element model (DEM) of the drying and pyrolysis zones of the GG41 gasifier should be built using a typical "bunker fill design". The particle size data from this study should be used as input for the model and should include the effect of thermal breakage and chemical reaction. Once the base-case model is set up, it is envisaged that the effect of different feed particle sizes on particle breakage under temperature conditions could be modelled. This should also visually show the effect of particle size segregation on the zone-bed shape and the impact on gasifier stability.

Reaction kinetic studies or numerical modeling work should be conducted in order to ascertain kinetic and diffusion control regions within the gasifier in order to support the GG41 gasifier CO_2 coal char reactivity measurements. It is highly unlikely that large coal particles can be completely under kinetic control without any diffusion resistance hindering reaction.

Sasol-Lurgi should re-assess the design of the oxygen nozzle distributors positioned on the ash-grate after a gasifier with a rubble finger has been turned-out and characterised. It is possible that the rubble finger assists in homogenizing the ash-bed, thereby better distributing the agent than in the case of a standard ash-grate.

The GG09 test gasifier reports (1999 – 2006) should be "data-mined" and re-examined in the context of these new findings of the internal coal property transformational behaviour impacting on gasifier performance, so that a more thorough understanding of the previous test gasifier results, and thereby greater value from this earlier relevant work, can thus be obtained. The GG41 feed coal data (sample 32) should also be used as input for the statistical model developed by Coetzer [2005], in order to validate the prediction of gasifier performance as a function of coal properties and process variables.

It is likely that the possibilities presented in this thesis will ultimately have a major impact on the profitability of many existing and new Sasol-Lurgi gasification plants. The results of this thesis represent a contribution towards a better understanding of these key phenomena.

APPENDIX A: GG41 GASIFIER DETAIL RESULTS

TABLE A1: THE GG41 GASIFIER PROXIMATE ANALYSIS RESULTS REPORTED ON AN AS RECEIVED (%) BASIS, AS WELL AS DRY (%)

Sample number	Moisture as received (%)	Volatile Matter as received (%)	Fixed Carbon as received (%)	Ash as received (%)	Volatile Matter dry basis (%)	Fixed Carbon dry basis (%)	Ash dry basis (%)
1	0	1.4	8.1	90.6	1.4	8.1	90.6
2	0.1	1.3	12.3	86.3	1.3	12.3	86.4
3	0.2	1.8	16.0	82.0	1.8	16.0	82.1
4	0.2	1.5	20.5	77.8	1.5	20.5	78.0
5	0.4	2.2	29.1	68.3	2.2	29.2	68.6
6	0.6	2.2	29.8	67.4	2.2	29.9	67.9
7	0.8	2.1	34.8	62.3	2.1	35.0	62.8
8	0.8	2.6	36.6	60.0	2.6	36.9	60.5
9	0.7	2.2	35.8	61.3	2.2	36.1	61.8
10	0.6	2.5	38.2	58.7	2.5	38.4	59.0
11	1.2	2.9	43.9	52.0	3.0	44.4	52.6
12	0.6	2.1	37.5	59.9	2.1	37.7	60.2
13	1.5	2.4	43.6	52.5	2.4	44.3	53.3
14	0.6	2.3	45.4	51.7	2.3	45.7	52.0
15	1.2	4.3	44.5	50.0	4.3	45.1	50.6
16	1.4	3.7	48.5	46.5	3.7	49.2	47.1
17	1.1	3.6	43.4	51.9	3.6	43.9	52.4
18	1.2	5.0	46.8	47.0	5.1	47.4	47.5
19	1.2	6.8	46.6	45.4	6.9	47.2	45.9
20	1.2	9.1	50.9	38.7	9.3	51.6	39.2
21	1.7	9.3	44.2	44.8	9.5	45.0	45.6
22	2.4	17.8	48.2	31.7	18.2	49.3	32.5
23	2.6	18.4	49.8	29.2	18.9	51.2	30.0
24	2.9	19.2	47.3	30.6	19.8	48.7	31.5
25	3.0	20.1	46.2	30.7	20.8	47.6	31.6
26	3.4	20.5	46.2	29.9	21.2	47.8	31.0
27	3.4	20.4	44.9	31.3	21.1	46.5	32.4
28	3.4	20.2	45.9	30.5	20.9	47.5	31.5
29	3.7	20.7	44.2	31.4	21.5	45.9	32.6
30	3.8	21.0	45.2	30.0	21.8	47.0	31.2
31	3.8	21.0	45.4	29.8	21.8	47.2	31.0
32	**3.6**	**21.8**	**47.1**	**27.5**	**22.7**	**48.9**	**28.5**
SCS BLEND (before feed bunker)	**3.5 – 5.5**	**21.4 – 25.7**	**42.6 – 51.6**	**22.2 – 30.5**	**24.9 – 27.2**	**44.1 – 54.6**	**23.0 – 32.3**

TABLE A2: THE GG41 GASIFIER NORMALISED VOLATILE MATTER, NORMALISED FIXED CARBON, CARBON CONVERSION AND ASH FUSION TEMPERATURE RESULTS

Sample number	Normalised Volatile matter (kg / 100kg ash) #	Normalised fixed carbon (kg / 100kg ash) #	Carbon conversion (%) **	AFT (DT) (°C)	AFT (ST) (°C)	AFT (HT) (°C)	AFT (FT) (°C)
1	1.52	8.91	94.8	1280	1320	1354	1367
2	1.49	14.26	91.7	1304	1327	1352	1383
3	2.22	19.51	88.6	1304	1322	1343	1374
4	1.92	26.30	84.7	1302	1322	1343	1363
5	3.16	42.63	75.2	1304	1322	1343	1361
6	3.25	44.11	74.3	1304	1324	1346	1374
7	3.42	55.75	67.5	1286	1314	1333	1362
8	4.34	60.96	64.5	1297	1311	1329	1362
9	3.52	58.39	66.0	1285	1311	1329	1362
10	4.27	65.09	62.1	1298	1320	1335	1354
11	5.63	84.32	50.9	1295	1321	1333	1348
12	3.45	62.58	63.5	1298	1320	1335	1354
13	4.55	83.07	51.6	1301	1315	1333	1348
14	4.45	87.80	48.8	1299	1317	1333	1358
15	8.55	89.04	48.1	1287	1298	1316	1359
16	7.87	104.44	39.1	1305	1320	1335	1360
17	6.91	83.76	51.2	1294	1320	1331	1354
18	10.74	99.67	41.9	1303	1320	1335	1366
19	14.97	102.71	40.1	1306	1320	1335	1354
20	23.62	131.58	23.3	1285	1302	1315	1340
21	20.73	98.66	42.5	1304	1315	1331	1340
22	56.03	151.98	0.1	1291	1326	1338	1368
23	63.04	170.84	0.4	1291	1323	1334	1347
24	62.84	154.64	9.9	1304	1327	1338	1360
25	65.60	150.52	12.3	1287	1326	1338	1372
26	68.50	154.58	9.9	1312	1323	1334	1352
27	65.14	143.39	16.4	1285	1331	1345	1366
28	66.42	150.72	12.2	1285	1341	1370	1381
29	65.99	140.89	17.9	1282	1341	1358	1379
30	69.87	150.70	12.2	1282	1325	1345	1362
31	70.45	152.35	11.2	1305	1320	1335	1345
32	**79.55**	**171.48**	**0.1**	**1295**	**1329**	**1341**	**1356**
SCS BLEND (before feed bunker)	-	-	**97.8 (test 28 GG9)**	**1300 - 1390**	-	**1350 - 1450**	**1350 - 1470**

\# Normalised volatile matter = [100 / fractional ash (dry)] * fractional VM (dry).

\# Normalised fixed carbon = [100 / fractional ash (dry)] * fractional FC (dry).

** Carbon conversion = $[(FC_{in} - FC_{out}) / FC_{in}] * 100$

= 48.9 – [feed ash (dry) / fractional ash (dry) * fractional FC (dry)] / 48.9

TABLE A3: THE GG41 GASIFIER ULTIMATE ANALYSIS, FISCHER TAR AND COAL CHAR CO_2 REACTIVITY RESULTS

Sample number	C (% daf)	H (% daf)	N (% daf)	S (% daf)	O (by diff.) (% daf)	Fischer Tar (%)	CO_2 Reactivity (50% burn-off at 1000 °C) (hr^{-1})
1	91.9	1.4	1.1	2.7	2.9	0	1.2
2	89.7	0.8	1.3	3.3	4.9	0	1.8
3	95.0	0.7	1.3	2.5	0.5	0	1.9
4	92.8	0.7	1.2	0.8	4.4	0	2.2
5	94.1	0.7	1.2	1.8	2.3	0	2.2
6	95.7	0.9	1.2	1.7	0.5	0	2.1
7	94.3	0.7	1.1	1.2	2.6	0	2.4
8	94.6	0.7	1.2	1.3	2.2	0	2.2
9	96.5	0.8	1.2	1.3	0.2	0	2.6
10	94.6	0.8	1.2	1.4	2.0	0	2.4
11	95.5	0.7	1.2	1.0	1.6	0	2.4
12	95.6	0.8	1.2	1.7	0.7	0	2.4
13	96.3	0.7	1.2	1.4	0.5	0	2.2
14	94.8	0.8	1.3	1.4	1.8	0	2.4
15	94.2	1.0	1.3	1.4	2.1	0	2.2
16	95.0	1.0	1.3	1.2	1.5	0	2.0
17	95.2	1.1	1.4	1.3	1.0	0	1.8
18	93.0	1.4	1.6	1.1	2.9	0	1.8
19	91.4	1.6	1.6	1.1	4.2	0	1.8
20	90.0	1.9	1.7	1.0	5.3	0	1.9
21	88.3	2.0	1.6	1.3	6.7	0	1.9
22	83.3	3.1	2.1	1.1	10.4	1.15	2.2
23	81.8	3.1	2.0	1.1	12.0	1.41	2.2
24	81.9	3.6	2.0	1.4	11.1	1.62	2.4
25	80.4	3.9	2.0	1.2	12.5	2.10	2.2
26	80.0	3.9	2.0	1.3	12.9	2.08	2.4
27	79.2	4.0	2.0	1.3	13.6	2.13	2.3
28	80.2	3.9	2.0	1.2	12.7	2.00	2.5
29	79.1	4.0	2.0	1.4	13.5	1.98	2.4
30	79.5	4.1	2.0	1.5	12.9	2.13	2.5
31	79.7	4.0	2.1	1.7	12.6	2.24	2.4
32	**79.5**	**4.2**	**2.1**	**1.6**	**12.7**	**2.47**	**2.4**
SCS BLEND (before feed bunker)	**72 - 89**	**3.1 – 5.2**	**1.7 – 2.5**	**1.1 – 2.2**	**10.2 – 16.4**	**2.5 – 3.5**	**2 - 5**

TABLE A4: THE GG41 GASIFIER BULK DENSITY, TRUE DENSITY, ERGUN INDEX, THERMAL FRAGMENTATION, MECHANICAL FRAGMENTATION AND CAKING PROPENSITY RESULTS

Sample number	Bulk density (kg/m^3)	True density (kg/m^3)	Ergun Index	Thermal fragmentation (%)	Mechanical fragmentation (%)	Caking propensity (%)
1	1135	2579	6.3	7.12	33.99	0.00
2	1148	2551	5.1	8.24	35.36	0.00
3	1196	2499	4.2	6.52	37.59	0.00
4	1096	2484	4.6	5.49	37.33	0.00
5	1106	2381	7.1	4.20	34.67	0.00
6	1070	2363	6.5	3.17	35.82	0.00
7	897	2297	6.6	4.12	37.15	0.00
8	955	2357	6.8	2.90	32.70	0.00
9	1056	2309	5.0	3.52	31.84	0.00
10	978	2289	5.1	7.03	34.24	0.00
11	850	2213	7.5	7.21	33.39	0.00
12	909	2319	6.0	5.32	38.19	0.00
13	933	2189	3.9	3.77	34.33	0.00
14	841	2239	6.4	3.52	32.78	0.00
15	855	2126	7.1	2.92	31.58	0.00
16	840	2209	6.8	5.00	32.00	0.72
17	886	2223	7.9	4.89	33.13	0.90
18	864	2127	6.2	8.49	32.53	1.00
19	897	2061	5.5	8.58	32.70	1.48
20	963	1939	4.8	4.46	34.68	1.93
21	1082	1972	3.2	1.72	32.10	0.90
22	1051	1720	5.3	11.76	37.85	5.61
23	1004	1682	6.0	14.25	39.23	3.71
24	1122	1712	4.4	12.88	38.02	7.18
25	1071	1677	6.5	20.00	30.13	8.54
26	1158	1671	5.5	13.65	32.02	9.16
27	1155	1660	6.2	17.43	29.36	4.40
28	1135	1658	6.9	11.25	30.39	8.80
29	1187	1673	8.2	15.71	26.44	4.82
30	1240	1656	6.5	12.19	28.00	12.47
31	1095	1650	8.2	17.08	29.70	13.69
32	**1143**	**1647**	**9.8**	**14.16**	**29.44**	**7.89**
SCS BLEND (before feed bunker)	**-**	**-**	**11.6**	**15 - 25**	**30 - 35**	**7 - 27**

TABLE A5: LINEAR CORRELATION DATA ANALYSIS RESULTS (ANALYSIS TOOLPACK PACKAGE) FOR GG41 GASIFIER VARIABLES: AVERAGE TEMPERATURE, ERGUN INDEX, THERMAL FRAGMENTATION, MECHANICAL FRAGMENTATION, CAKING AND MOISTURE

	Temp ave.	Ergun Index	Thermal frag.	Mech. frag.	Caking	Moisture
Temp ave.	1					
Ergun Index	-0.83312012	1				
Thermal fra.	-0.83053277	0.68921296	1			
Mech. frag.	0.43491974	-0.55522488	-0.27087314	1		
Caking	-0.74547086	0.57216975	0.55994953	-0.41086789	1	
Moisture	-0.95607567	0.83532803	0.74708761	-0.60420052	0.77168666	1

TABLE A6: THE GG41 GASIFIER FRACTIONAL PARTICLE SIZE DISTRIBUTION RESULTS REPORTED ON A PERCENTAGE RETAINED BASIS

Sample number	Screen Size 53 mm	Screen Size 25 mm	Screen Size 12.5 mm	Screen Size 9.5 mm	Screen Size 6.3 mm	Screen Size 5 mm	Screen Size 4 mm	Screen Size 3.35 mm	Screen Size 2 mm	Screen Size 1 mm	Screen Size -1 mm
1											
2	9.2	22.3	19.5	11.3	9.8	5.6	1.9	3.3	5.6	5.0	6.6
3	12.5	16.8	17.0	10.8	10.0	5.9	2.4	2.7	5.9	6.3	9.7
4	14.4	13.8	17.6	11.2	11.6	7.4	1.9	2.9	6.2	4.9	8.2
5	14.4	17.6	24.5	12.8	11.4	6.0	1.8	1.8	3.4	2.4	4.0
6	17.3	13.4	21.7	13.9	11.3	7.0	1.4	2.5	4.4	2.8	4.3
7	13.7	10.1	25.5	16.1	13.3	7.8	1.0	2.1	3.8	2.5	4.2
8	9.4	13.5	28.0	15.9	12.3	7.8	1.0	2.2	3.6	2.3	4.0
9	11.0	10.6	19.2	14.0	13.8	10.3	1.5	3.2	5.8	4.0	6.6
10	12.3	9.2	23.3	13.6	12.7	9.1	1.4	2.6	5.1	3.9	6.8
11	5.9	14.0	30.0	17.4	13.7	8.1	1.2	2.0	2.9	1.7	3.0
12	9.0	8.6	25.6	17.2	14.3	10.0	1.9	2.3	3.9	2.7	4.7
13	2.8	6.3	21.3	16.4	15.9	10.0	3.2	4.1	4.9	4.7	10.3
14	6.8	10.0	28.9	16.2	14.5	7.0	3.5	3.0	3.9	2.4	3.9
15	3.9	11.6	32.7	17.0	13.9	9.0	1.6	2.1	3.1	2.0	3.1
16	6.5	9.5	27.7	17.7	15.3	9.6	2.3	2.5	3.7	2.1	3.1
17	13.7	9.8	28.0	16.4	13.2	7.2	2.2	2.2	3.1	1.7	2.5
18	7.8	10.6	27.8	17.5	10.9	8.7	2.5	2.7	4.4	2.9	4.2
19	5.9	9.4	22.5	14.2	14.7	9.6	3.3	7.2	5.7	3.3	4.1
20	3.2	8.6	22.8	14.5	15.8	10.5	3.8	4.3	6.3	4.0	6.1
21	1.6	7.3	18.9	11.8	13.8	11.7	2.9	4.5	7.7	6.3	13.5
22	3.9	13.5	27.0	12.9	13.7	9.1	2.4	3.3	5.1	3.3	6.0
23	4.2	13.6	26.0	12.4	14.9	9.3	3.8	3.9	5.3	2.8	3.7
24	4.2	12.7	21.3	10.4	13.8	10.8	3.1	4.2	7.0	4.8	7.8
25	5.8	21.1	27.6	10.3	11.8	6.8	3.0	2.8	4.0	2.4	4.3
26	6.5	22.8	22.3	8.8	11.6	8.6	2.3	3.0	4.7	3.1	6.2
27	7.7	22.1	23.4	9.4	12.2	7.6	2.6	3.3	4.2	2.7	4.7
28	3.7	15.3	21.4	10.7	15.6	16.2	1.4	4.2	7.4	3.9	0.2
29	12.5	28.8	21.0	7.8	11.1	7.5	1.5	2.1	2.9	1.6	3.1
30	9.1	21.7	20.8	8.4	13.8	9.8	2.1	3.1	4.7	2.4	4.1
31	14.4	33.2	21.0	5.0	9.0	5.8	1.4	1.9	2.9	2.0	3.6
32	**16.2**	**32.7**	**23.1**	**6.2**	**8.1**	**4.6**	**1.2**	**1.6**	**2.3**	**1.2**	**2.7**
SCS BLEND (test 28 GG09, before feed bunker)	**17.6**	**28.8**	**25.0**	**8.9**	**10.3**	**4.1**	**1.9**	**0.7**	**0.9**	**0.5**	**1.3**

TABLE A7: GASIFIER GG41 TURN-OUT INVESTIGATION – PETROGRAPHIC RESULTS

GASIFIER GG41 TURN OUT INVESTIGATION - PETROGRAPHIC RESULTS

Mar-05

TABLE 1: MACERAL GROUP ANALYSES (% by vol.)

SAMPLE		VITRINITE	LIPTINITE	INERTINITE						TOTAL		Mineral Matter	TOTAL	RANK INDICATOR	
				R.SF	I.SF	FUS	MIC	R.INT	I.INT	I.INERT	R.INERT	(if counted)	REACTIVES	MEAN RANDOM %RoV	Category
541	32	20.0	2.6	14.8	33.6	1.6	0.2	3.4	6.8	42.2	18.2	17.0	40.8	0.61	Med. C

LIPTINITE = exinite (old terminology) | R.SF=reactive semi-fusinite | I.SF = inert semi-fusinite | FUS = fusinite | MIC = micrinite | R.INT = reactive inertodetrinite | I.INT = inert inertodetrinite

TOTAL I.INERT = total inert inertinite | TOTAL R.INERT = total reactive inertinite | TOTAL REACTIVES=vitrinite+liptinite+R.SF+R.INT

Table 2: Particle type analysis (% vol.)

Sample		COAL						DEVO	CHAR					consume	STONE / ROCK / ASH			
lab no	ID	Vitrite	Liptite	inertite	intermed	carbomine	TOTAL	COAL	Porous	intermed	dense	cbmn	TOTAL	char	normal	heat affected	TOTAL	comments
541	32	11.4	2.0	53.0	10.0	12.8	89.2	0.0	0.0	0.4	0.4		0.8		10.0		10.0	v. high RoV chars - smallish, contaminants
540	31						0.0	0.0									0.0	
539	30	8.0	1.2	57.4	10.8	10.6	87.6	0.0	0.0	0.0	0.0				12.0		12.0	rare stress cracks in vit mono particles
538	28						0.0	0.0									0.0	
537	28	10.2	1.6	56.0	8.0	11.8	87.6	0.0	0.4	0.6	1.2		2.2		10.2		10.2	larger particles of char - contaminants. No crackign observed
536	27						0.0	0.0									0.0	
535	26	9.8	2.0	58.0	8.0	8.0	85.8	0.0	0.2	2.2	0.4		2.8		11.4		11.4	large char particles, no devol coal - contaminants
534	25	10.0	1.0	55.0	8.4	8.2	82.6	0.2	1.0	2.2	2.0		5.2		12.0		12.0	more devol particles seen (3 or so)
533	24	10.0	0.0	38.4	9.6	10.4	68.6	1.4	0.6	2.4	3.8	1.4	8.2		19.4	2.4	21.8	fine fissures in inertinties. Heated ash and cbmn
532	23						0.0										0.0	
531	22	7.6	0.6	37.4	8.2	8.6	62.4	2.6	1.0	8.8	5.0	0.6	15.4		17.0	2.4	19.4	heat affected pyrites, carbs unaltered
530	21	6.8	0.2	24.8	2.8	1.6	36.2	5.8	7.2	19.4	12.8	2.6	42.0		8.4	8.2	16.6	
529	20	2.8	0.0	19.0	2.2	1.6	25.6	11.2	5.2	22.0	15.0	5.2	47.4		2.8	14.0	16.8	mineral crystals; fissured inerts inc reflectance
528	19						0.0										0.0	
527	18	1.6	0.0	7.6	1.2	0.4	10.8	10.4	9.0	26.4	17.2	7.2	59.8	0.2	0.2	18.8	19.0	shift in all reflects; consumed chars?
526	17						0.0										0.0	
525	16	0.6	0.0	2.6	0.2	0.4	3.8	8.8	9.0	38.8	12.8	7.0	67.6	1.0	0.2	18.6	18.8	v.red paticles with lamda plate 1. relared to degree o aromaticity?
524	15	0.2	0.0	1.2	0.4	0.2	2.0	3.4	8.0	39.2	14.8	6.2	68.0	1.6	0.0	25.0	25.0	2nd altered pyrite. Spores in a coal particle
523	14	0.0	0.0	0.0	0.0	0.0	0.0	1.0	10.2	43.8	13.6	7.8	75.4	2.6	0.0	20.8	20.8	small coal frags; rare devol coal.
522	13						0.0										0.0	
521	12	0.0	0.0	0.0	0.0	0.0	0.0	1.4	7.8	27.2	19.4	9.2	63.6	3.2	0.6	31.2	31.8	green tinge to certain particles. Some solids are remnant porous frags. No coal observed
520	11						0.0										0.0	
519	10	0.0	0.0	0.4	1.0	0.0	1.4	2.0	7.6	27.2	19.4	7.2	61.4	2.0	0.0	33.2	33.2	coal particles observed
518	9	0.2	0.0	0.4	0.0	0.0	0.6	0.8	5.0	27.4	15.4	4.6	52.4	3.2	0.0	43.0	43.0	pyrite droplets & other min flows encompasing fines. Lots diff mins - heat change?
517	8						0.0										0.0	
516	7						0.0										0.0	
515	6						0.0										0.0	
514	5	0.4	0.0	0.0	0.0	0.0	0.4	0.4	3.4	24.0	11.4	5.8	44.6	7.4	0.0	47.0	47.0	
513	4						0.0										0.0	
512	3	0.0	0.0	0.0	0.0	0.0	0.0	0.4	1.8	13.6	10.6	3.4	29.4	3.8	0.0	66.4	66.4	
511	2	0.0	0.0	0.0	0.0	0.0	0.0	0.4	0.6	9.2	8.4	2.2	20.4	5.8	0.0	73.4	73.4	lots frags & chars; red intensity rel faint
510	1						0.0										0.0	

Single particle analysis under x-hairs 50x50m view
red labda filter in
>30mm particles ignored
rock/stone<60% in f.o.v
intermed <5% mixed macerals in f.i.v in a single particle

TABLE A8: VITRINITE REFLECTANCE ANALYSIS ON TGA TREATED GG41 GASIFIER -1mm #32 (FEED SAMPLE) FOR TEMPERATURE CALIBRATION

Sample °C	RoV Average	Standard Deviation.
350	0.9	0.36
450	1.2	0.23
600	2.4	0.18
650	3.0	0.38
800	4.4	0.42
850	6.0	0.79
950	6.0	0.63
1200	7.9	1.22

TABLE A9: VITRINITE REFLECTANCE ANALYSIS ON THE GG41 GASIFIER TURN-OUT SAMPLES SHOWING AVERAGE, SURFACE AND PEAK TEMPERATURE RESULTS

Sample number	RoV % Mean	Temperature Average (°C)	RoV % Maximum	Temperature Peak (°C)	RoV % Top 10% average	Temperature Surface (°C)
2	5.4	884	8.5	1396	8.1	1183
5	4.8	823	6.0	953	6.0	953
8	5.2	863	7.0	1064	6.4	994
11	4.8	816	6.0	953	5.9	939
13	5.1	854	8.0	1175	6.9	1050
15	5.0	839	7.5	1119	7.0	1064
16	5.0	837	8.0	1175	7.1	1075
20	3.0	617	7.5	1119	6.3	986
22	1.2	424	6.5	1008	4.9	835
24	1.2	421	6.5	1008	4.8	815
25	0.9	381	7.5	1119	2.8	597
26	0.9	385	6.0	953	3.1	630
28	0.9	385	6.5	1008	3.2	643
30	0.6	354	0.9	385	0.8	372
32	0.6	354	1.3	426	0.7	364

APPENDIX B FACTORISED INDIAN PILOT PLANT RESULTS [KRISHNUDU, et. al., 1989a] AND GLOVER [1988] DETAIL RESULTS

Not disclosed due to IP confidentiality.

TABLE B5: CARBON CONVERSION AND SOLIDS TEMPERATURE RESULTS AFTER GLOVER [1988] FOR THE #15 MK III GASIFIER IN SASOLBURG

Height below Bosman skirt (m)	Sample number correlation with GG41	Carbon conversion (%)	Sample number correlation with GG41	Temperature profile of solids (°C)
2.4	15.5	71.0	32	387
2.1	17	69.6	30.5	347
1.8	18	58.8	29	387
1.5	19	42.6	27.5	597
1.2	20	33.6	26	707
0.9	20.5	26.2	24.5	661
0.6	22.5	24.6	23	747
0.1	24.5	18.6	21.5	867
0	25	0	20	857
			18.5	847
			16	917

APPENDIX C: FACT-SAGE MODELLING RESULTS

Drying and devolatilisation zone

The 1st zone modelled was the drying and devolatilisation zone. The coal (organic and inorganic components) were added with a specific mass flow as reactants. Each element, reactant or species was added separately. A summary of the elements added as the total coal stream is given in Table C1.

TABLE C1: SUMMARY OF INPUT REACTANTS INTO FACT-SAGE DEVOLATILISATION ZONE

Element	Mass flow (kg/hr)
H_2O	2550
C	25557
H	1329
N	713
S	681
O	4154
Pyrite	526
Quartz	2631
Microline	250
Muscovite / Illite	381
Kaolonite	6913
Anatase	39
Ankerite	-
Siderite	-
Calcite	881
Dolomite	1328
Apatite*	65
Gypsum	144
Tar and oils**	2858
TOTAL	51000

* Not included in model due to FactSage software limitations.

** Not included in model.

The gas flow from the reduction zone was added as reactants which reacted with coal (Table C2). The temperature range according to the ASPEN model for this zone was from ambient conditions, when the coal enters the gasifier, to 727°C at the end of the pyrolysis zone.

TABLE C2: GAS FLOW FROM REDUCTION ZONE

Gas(kg/hr)	Reduction zone outlet gas into pyrolysis and drying zone
H_2O	27 159
O_2	0
C	0
H_2	1 961
CH_4	6 417
CO	15 761
CO_2	42 742
N_2	142
T(°C)	690

Schematically it implies that the up-flowing gas from the reduction zone reacted with the down-flowing coal and mineral matter in the gasifier (Figure C1).

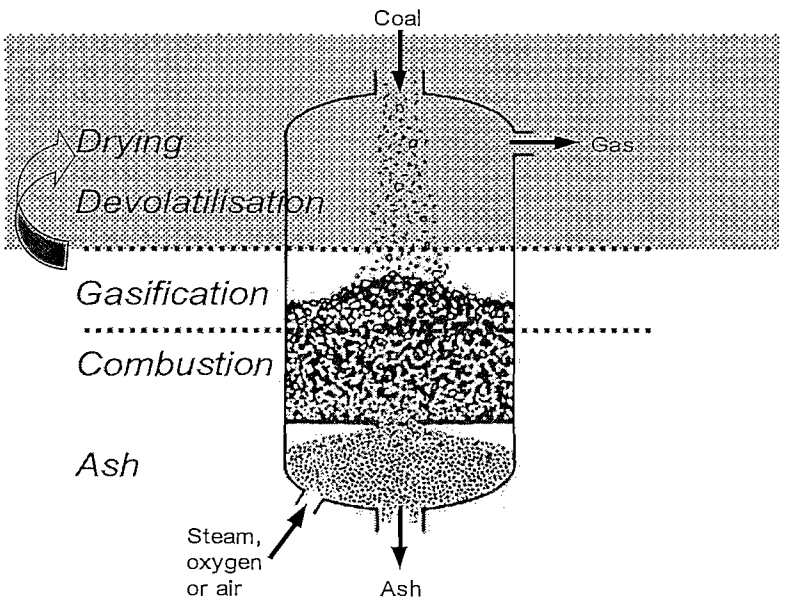

FIGURE C1: DRYING AND PYROLISYS ZONE

Reduction zone

A similar approach and procedure as for the drying and devolatilisation zones was followed in order to model the reduction and combustion zones respectively. The differences in the models were mainly in the temperature ranges and reactants used as input. The results with regards to the mineral-matter from the drying and devolatilisation zones as per the Fact-Sage model were used as input for the Fact-Sage reduction zone model.

The temperature range for the reduction zone was specified as 727°C, when the coal enters the zone (stream 2) and reacts with the up-flowing gas from the combustion zone (stream 1) at a temperature of 1316°C.

Combustion zone

A similar approach and procedure as for the drying and devolatilisation and reduction zones was followed in order to model the combustion zone. The differences in the models were mainly in the temperature ranges and reactants used as input. The results with regard to the mineral-matter from the gasification zone as per the Fact-Sage model were used as input for the Fact-Sage combustion zone model.

The temperature range for the gasification zone was specified as 1200°C, when the coal and minerals enter the zone (stream 2) and react with the up-flowing agent into the gasifier (stream 1) having a temperature of 344°C.

The modelling approach followed here was according to Van Dyk [2006]. Further detail can be found in this thesis.

C2: FACT-SAGE MODELLING RESULTS

TABLE C3: CARBON SPECIATION WITHIN THE DRYING AND PYROLYSIS ZONES

Carbon (Pyrolysis Zone)	Temperature (°C)							
Carbon Species	727	700	600	500	400	300	200	100
CH4(g)	1.8E-01	1.9E-01	2.1E-01	2.3E-01	2.3E-01	2.1E-01	1.7E-01	3.6E-02
CO(g)	1.7E-01	1.7E-01	5.2E-02	1.2E-02	1.7E-03	1.4E-02	0.0E+00	0.0E+00
CO2(g)	3.3E-01	3.4E-01	3.5E-01	3.4E-01	3.2E-01	2.9E-01	2.5E-01	7.4E-02
COS(g)	1.2E-02	1.2E-02	6.0E-03	2.9E-03	0.0E+00	0.0E+00	0.0E+00	0.0E+00
C(s)	3.1E-01	3.1E-01	3.8E-01	4.2E-01	4.5E-01	5.0E-01	5.7E-01	9.2E-01

TABLE C4: CARBON SPECIATION WITHIN THE REDUCTION ZONE.

Carbon (Reduction Zone)	Temperature (°C)						
Carbon species	1316	1227	1127	1027	927	827	727
CO(g)	6.5E-01	6.3E-01	6.0E-01	5.6E-01	5.1E-01	3.9E-01	2.2E-01
CO2(g)	3.5E-01	3.7E-01	4.0E-01	4.4E-01	4.8E-01	5.5E-01	6.2E-01
CH4(g)	0.0E+00	1.04E-04	4.1E-04	2.0E-03	1.1E-02	5.9E-02	1.6E-01

TABLE C5: HYDROGEN SPECIATION WITHIN THE DRYING AND PYROLYSIS ZONES

Hydrogen (Pyrolysis Zone)	Temperature (°C)							
Hydrogen Species	727	700	600	500	400	300	200	100
H2(g)	2.8E-01	2.8E-01	1.6E-01	7.5E-02	2.9E-02	8.2E-03	1.4E-03	1.8E-04
CH4(g)	3.3E-01	3.4E-01	3.9E-01	4.1E-01	4.1E-01	3.8E-01	3.1E-01	6.6E-02
NH3(g)	2.3E-02	2.3E-02	2.3E-02	2.0E-02	1.5E-02	1.1E-02	5.9E-03	5.5E-05
H2O(g)	3.8E-01	3.8E-01	4.5E-01	5.1E-01	5.6E-01	6.1E-01	6.6E-01	2.5E-02
H2S(g)	6.4E-03	6.4E-03	5.7E-03	5.6E-03	5.5E-03	5.5E-03	4.5E-03	4.5E-03
HCl(g)	0.0E+00	0.0E+00	3.5E-03	3.5E-03	2.0E-03	2.0E-03	1.7E-03	9.0E-10
HF(g)	0.0E+00	0.0E+00	0.0E+00	0.0E+00	0.0E+00	3.1E-04	6.3E-06	1.6E-08
Al2O3(H2O)(s)	0.0E+00	0.0E+00	0.0E+00	0.0E+00	0.0E+00	0.0E+00	1.8E-03	0.0E+00
Mg5Al2Si3O10(OH)8(s	0.0E+00	0.0E+00	0.0E+00	0.0E+00	0.0E+00	1.3E-03	1.3E-03	0.0E+00
KAl3Si3O10(OH)2(s)	0.0E+00	0.0E+00	0.0E+00	0.0E+00	0.0E+00	4.3E-02	4.3E-02	3.6E-02
CaAl4Si2O10(OH)2(s)	0.0E+00	0.0E+00	0.0E+00	0.0E+00	0.0E+00	1.8E-03	1.4E-02	0.0E+00
BaCl2(H2O)(s)	0.0E+00	0.0E+00	0.0E+00	0.0E+00	0.0E+00	0.0E+00	1.5E-03	0.0E+00
Al2O3(H2O)(s)	0.0E+00	0.0E+00	0.0E+00	0.0E+00	0.0E+00	0.0E+00	0.0E+00	6.1E-03
H4SiO4(s)	0.0E+00	0.0E+00	0.0E+00	0.0E+00	0.0E+00	0.0E+00	0.0E+00	4.5E-02
H2O(s)	0.0E+00	0.0E+00	0.0E+00	0.0E+00	0.0E+00	0.0E+00	0.0E+00	9.2E-01

TABLE C6: HYROGEN SPECIATION WITHIN THE REDUCTION ZONE

Hydrogen (Reduction Zone)	Temperature (°C)						
Hydrogen Species	1316	1227	1127	1027	927	827	727
H2(g)	3.9E-01	4.0E-01	4.1E-01	4.2E-01	4.3E-01	3.9E-01	2.8E-01
H(g)	3.4E-04	1.3E-04	3.5E-05	8.2E-06	1.5E-06	1.8E-07	1.3E-08
CH4(g)	0.0E+00	1.0E-02	4.0E-02	1.9E-03	1.1E-02	5.6E-02	1.5E-01
NH3(g)	0.0E+00	0.0E+00	2.8E-03	4.3E-03	6.8E-03	1.0E-02	1.2E-02
H2O(g)	6.1E-01	6.0E-01	5.9E-01	5.7E-01	5.6E-01	5.5E-01	5.6E-01
H2S(g)	0.0E+00	0.0E+00	3.4E-04	3.4E-04	3.4E-04	3.4E-04	3.4E-04

TABLE C7: NITROGEN SPECIATION WITHIN THE DRYING AND PYROLYSIS ZONES

Nitrogen (Pyrolysis Zone)	Temperature (°C)							
Nitrogen Species	727	700	600	500	400	300	200	100
N2(g)	9.9E-01	9.9E-01	9.9E-01	9.9E-01	9.9E-01	9.9E-01	1.0E+00	1.0E+00
NH3(g)	1.2E-02	1.2E-02	1.1E-02	9.8E-03	7.7E-03	5.2E-03	3.0E-03	0.0E+00

TABLE C8: NITROGEN SPECIATION WITHIN THE REDUCTION ZONE

Nitrogen (Reduction Zone)	Temperature (°C)						
Nitrogen Species	1316	1227	1127	1027	927	827	727
N2(g)	1.0E+00	1.0E+00	9.9E-01	9.9E-01	9.9E-01	9.8E-01	9.8E-01
NH3(g)	2.7E-03	3.6E-03	5.2E-03	7.9E-03	1.3E-02	1.9E-02	2.2E-02

TABLE C9: SULPHUR SPECIATION WITHIN THE DRYING AND PYROLYSIS ZONE

S (Pyrolysis Zone)	Temperature (°C)							
Sulphur Species	727	700	600	500	400	300	200	100
H2S(g)	9.8E-01	9.8E-01	8.6E-01	8.6E-01	8.4E-01	8.4E-01	6.9E-01	6.9E-01
COS(g)	1.7E-02	1.7E-02	8.3E-03	4.0E-03	1.6E-03	4.9E-02	7.8E-03	0.0E+00
Co9S8(s)	5.5E-03	5.5E-03	5.5E-03	5.5E-03	5.5E-03	5.5E-03	0.0E+00	0.0E+00
Ni3S2(s2)	7.0E-03	7.0E-03	7.0E-03	6.2E-03	7.8E-03	7.8E-03	0.0E+00	0.0E+00
Cu5FeS4(s2)	6.9E-03	6.9E-03	5.9E-03	8.3E-03	2.1E-02	2.1E-02	0.0E+00	0.0E+00
ZnS(s)	1.4E-02	1.4E-02	1.5E-02	1.5E-02	1.5E-02	1.5E-02	1.5E-02	1.5E-02
MoS2(s)	9.2E-03	9.2E-03	9.2E-03	9.2E-03	9.2E-03	9.2E-03	9.2E-03	9.2E-03
FeS(s3)	0.0E+00	0.0E+00	1.3E-01	1.4E-01	1.5E-01	1.5E-01	0.0E+00	0.0E+00
PbS(s)	0.0E+00	0.0E+00	1.3E-03	4.4E-03	4.5E-03	4.5E-03	4.2E-03	3.9E-03
CdS(s)	0.0E+00	0.0E+00	0.0E+00	0.0E+00	3.9E-04	3.9E-04	3.9E-04	3.9E-04
FeS2(s)	0.0E+00	0.0E+00	0.0E+00	0.0E+00	0.0E+00	0.0E+00	3.1E-01	3.1E-01
CoS2(s)	0.0E+00	0.0E+00	0.0E+00	0.0E+00	0.0E+00	0.0E+00	1.2E-02	1.2E-02
Ni6S5(s)	0.0E+00	0.0E+00	0.0E+00	0.0E+00	0.0E+00	0.0E+00	8.7E-03	2.1E-02
CuFeS2(s)	0.0E+00	0.0E+00	0.0E+00	0.0E+00	0.0E+00	0.0E+00	2.1E-02	5.2E-03
As2S2(s)	0.0E+00	0.0E+00	0.0E+00	0.0E+00	0.0E+00	0.0E+00	1.2E-03	1.8E-03
HgS(s)	0.0E+00	0.0E+00	0.0E+00	0.0E+00	0.0E+00	0.0E+00	0.0E+00	3.8E-05
BaSO4(s)	0.0E+00	0.0E+00	0.0E+00	0.0E+00	0.0E+00	0.0E+00	0.0E+00	2.3E-03

TABLE C10: SULPHUR SPECIATION WITHIN THE REDUCTION ZONE

S (Reduction zone)	Temperature (°C)						
Sulphur Species	1316	1227	1127	1027	927	827	727
HS(g)	3.3E-03	1.6E-03	6.0E-02	2.0E-02	5.5E-03	1.3E-03	2.4E-04
H2S(g)	9.7E-01	9.7E-01	9.8E-01	9.8E-01	9.8E-01	9.9E-01	9.9E-01
SO(g)	7.9E-03	2.1E-03	3.8E-04	5.5E-05	5.9E-06	5.3E-07	4.6E-08
SO2(g)	5.4E-02	1.7E-02	4.0E-03	7.6E-04	1.2E-04	1.8E-05	4.1E-06
COS(g)	2.6E-02	2.5E-02	2.2E-02	2.0E-02	1.8E-02	1.5E-02	1.1E-02
MgS	4.2E-04	1.3E-03	6.6E-03	7.4E-04	0.0E+00	0.0E+00	0.0E+00
CaS	8.8E-04	1.4E-03	6.1E-03	4.6E-04	0.0E+00	0.0E+00	0.0E+00
FeS	2.5E-04	1.0E-03	1.8E-02	2.7E-03	0.0E+00	0.0E+00	0.0E+00
MnS	1.6E-06	6.4E-06	1.1E-04	4.9E-04	0.0E+00	0.0E+00	0.0E+00

TABLE C11: OXYGEN SPECIATION WITHIN THE DRYING AND PYROLYSIS ZONES

Oxygen (Pyrolysis Zone)	Temperature (°C)							
Oxygen Species	727	700	600	500	400	300	200	100
H2O(g)	3.1E-01	3.1E-01	3.7E-01	4.2E-01	4.6E-01	5.0E-01	5.5E-01	2.1E-02
CO(g)	1.3E-01	1.2E-01	3.9E-02	8.7E-03	1.3E-03	1.0E-02	2.8E-04	2.5E-07
CO2(g)	5.0E-01	5.0E-01	5.3E-01	5.1E-01	4.8E-01	4.4E-01	3.8E-01	1.1E-01
COS(g)	0.0E+00	0.0E+00	4.5E-03	1.5E-02	5.8E-03	2.6E-04	0.0E+00	0.0E+00
SiO2(s2)	1.5E-02	1.5E-02	1.7E-02	1.7E-02	1.6E-02	2.3E-02	9.9E-03	0.0E+00
Mg2Al4Si5O18(s)	1.2E-02	1.2E-02	3.4E-03	3.5E-03	1.2E-02	0.0E+00	0.0E+00	0.0E+00
KAlSi2O6(s2)	2.1E-03	2.1E-03	1.2E-02	1.2E-02	2.8E-03	0.0E+00	0.0E+00	0.0E+00
CaAl2Si2O8(s2)	2.6E-02	2.6E-02	2.1E-03	2.1E-03	2.6E-02	1.4E-02	0.0E+00	0.0E+00
V2O3(s)	2.7E-04	2.7E-04	2.6E-02	2.6E-02	2.7E-04	1.7E-02	3.0E-04	3.0E-04
Mn2Al4Si5O18(s)	4.8E-03	4.8E-03	2.7E-04	2.7E-04	4.8E-03	4.8E-03	0.0E+00	0.0E+00
Fe2Al4Si5O18(s)	6.3E-03	6.3E-03	4.8E-03	4.8E-03	0.0E+00	0.0E+00	0.0E+00	0.0E+00
(FeO)(TiO2)(s)	1.0E-02	1.0E-02	2.7E-02	2.5E-02	0.0E+00	0.0E+00	0.0E+00	0.0E+00
(FeO)2(TiO2)(s)	2.0E-02	2.0E-02	2.5E-02	2.6E-04	0.0E+00	0.0E+00	0.0E+00	0.0E+00
FeCr2O4(s)	2.6E-04	2.6E-04	2.6E-04	6.2E-03	2.6E-04	2.6E-04	2.6E-04	0.0E+00
(BaO)(SiO2)2(s)	6.2E-03	6.2E-03	6.2E-03	0.0E+00	0.0E+00	0.0E+00	0.0E+00	0.0E+00
TiO2(s)	0.0E+00	0.0E+00	0.0E+00	0.0E+00	1.7E-02	1.7E-02	1.7E-02	1.7E-02
Mg5Al2Si3O10(OH)8(s	0.0E+00	0.0E+00	0.0E+00	0.0E+00	0.0E+00	5.0E-03	5.0E-03	0.0E+00
KAl3Si3O10(OH)2(s)	0.0E+00	0.0E+00	0.0E+00	0.0E+00	0.0E+00	4.2E-03	4.2E-03	0.0E+00
CaAl4Si2O10(OH)2(s)	0.0E+00	0.0E+00	0.0E+00	0.0E+00	0.0E+00	1.8E-02	0.0E+00	0.0E+00
Al2O3(H2O)(s)	0.0E+00	0.0E+00	0.0E+00	0.0E+00	0.0E+00	0.0E+00	5.9E-03	2.0E-02
(CaO)2(Al2O3)2(SiO2	0.0E+00	0.0E+00	0.0E+00	0.0E+00	0.0E+00	0.0E+00	5.0E-02	0.0E+00
Mn3Al2Si3O12(s)	0.0E+00	0.0E+00	0.0E+00	0.0E+00	0.0E+00	0.0E+00	2.1E-03	0.0E+00
BaCl2(H2O)(s)	0.0E+00	0.0E+00	0.0E+00	0.0E+00	0.0E+00	0.0E+00	1.2E-03	0.0E+00
H2O(s)	0.0E+00	0.0E+00	0.0E+00	0.0E+00	0.0E+00	0.0E+00	0.0E+00	7.6E-01
H4SiO4(s)	0.0E+00	0.0E+00	0.0E+00	0.0E+00	0.0E+00	0.0E+00	0.0E+00	7.5E-02
KAl3Si3O10(OH)2(s)	0.0E+00	0.0E+00	0.0E+00	0.0E+00	0.0E+00	0.0E+00	0.0E+00	3.6E-03
CaCO3(s2)	0.0E+00	0.0E+00	0.0E+00	0.0E+00	0.0E+00	0.0E+00	0.0E+00	5.5E-03
CaMg(CO3)2(s)	0.0E+00	0.0E+00	0.0E+00	0.0E+00	0.0E+00	0.0E+00	0.0E+00	8.2E-03

TABLE C12: OXYGEN SPECIATION WITHIN THE REDUCTION ZONE

Oxygen (Reduction Zone)	Temperature (°C)						
Oxygen Species	1316	1227	1127	1027	927	827	727
O	1.3E+03	1.2E+03	1.1E+03	1.0E+03	9.3E+02	8.3E+02	7.3E+02
H2O(g)	4.5E-01	4.5E-01	4.4E-01	4.3E-01	4.1E-01	4.1E-01	4.2E-01
CO(g)	2.3E-01	2.2E-01	2.1E-01	2.0E-01	1.8E-01	1.4E-01	7.7E-02
CO2(g)	2.5E-01	2.7E-01	2.9E-01	3.1E-01	3.4E-01	3.9E-01	4.4E-01
MgO	1.5E-03	1.2E-03	3.5E-02	8.9E-04	0.0E+00	0.0E+00	0.0E+00
FeO	9.2E-04	9.2E-04	9.2E-04	3.2E-05	0.0E+00	0.0E+00	0.0E+00
MnO	5.9E-04	5.9E-04	5.9E-04	5.9E-04	0.0E+00	0.0E+00	0.0E+00
SiO2	3.9E-02	1.9E-02	5.8E-03	1.4E-02	0.0E+00	0.0E+00	0.0E+00
TiO2	1.8E-02	1.8E-02	1.8E-02	1.2E-03	0.0E+00	0.0E+00	0.0E+00
Ti2O3	6.3E-05	7.5E-05	8.8E-05	6.0E-06	0.0E+00	0.0E+00	0.0E+00
CaO	3.2E-03	1.3E-03	3.2E-02	5.5E-04	0.0E+00	0.0E+00	0.0E+00
Al2O3	1.2E-02	5.9E-03	1.9E-03	4.6E-03	0.0E+00	0.0E+00	0.0E+00
Al6Si2O13(s)	6.0E-03	5.8E-03	3.5E-03	0.0E+00	0.0E+00	0.0E+00	0.0E+00
CaAl2Si2O8(s2)	2.6E-03	1.8E-02	2.6E-02	2.8E-02	2.8E-02	2.8E-02	2.8E-02
SiO2(s4)	0.0E+00	1.1E-02	1.6E-02	1.6E-02	1.6E-02	1.6E-02	1.6E-02
Mg2Al4Si5O18(s)	0.0E+00	2.6E-03	1.1E-02	1.4E-02	1.4E-02	1.4E-02	1.4E-02
Fe2Al4Si5O18(s)	0.0E+00	0.0E+00	0.0E+00	7.0E-03	7.0E-03	7.0E-03	7.0E-03

REFERENCES

ALPERN, B., Nahuys, J. and Martinez, L., *Mineral Matter in Ashy and Non-washable coals – Its Influence on Chemical Properties*, ***Symposium on Gondwana Coals, Lisbon – proceedings and papers***, 1984, 70, (2), pp. 299-317.

ASTM method D 2113-99, *Standard Practice for Rock Core Drilling, and Sampling of Rock for Site Investigation,* 1999.

ASTM D 3682-01, *Standard test Method for Major and Minor elements in Combustion Residues, from Coal Utilization Processes,* ***ASTM International***, 2002, pp. 1-7.

ASTM method D 5434-03, *Standard Guide for Field Logging of Subsurface Explorations of Soil and Rock*, 2003

BAILY J.G, Tate A., Diesel C.F.K. and Wall T.F., A char morphology system with applications to coal combustion, ***Fuel*** vol. 69, 1990, pp. 225-234.

BALE, C.W., Chartrand, P., Degterov, S.A., Eriksson, G., Hack, K., Manfoud, R. B., Melancon, J., Pelton, A.D. and Peterson, S., *FactSage Thermochemical Software and Databases, GTT-Technologies, Germany*, Calphad, 2002, 26, pp.189-228. www.factsage.com.

BENNETT, C.O., and Myers, J.E., "*Momentum, Heat, and Mass Transfer*", McGraw-Hill, Inc. 1982.

BERKOWITZ, N., *"An Introduction to Coal Technology", Academic Press,* 1979, pp. 201-203

BLAZEK, C.F., Baker, N.R., and Tison, R.R., *High-Btu Coal Gasification Processes,* ***ANL/CES/TE 79-2,*** Institute of Gas Technology for the Argonne National Laboratory, January 1979.

BORREGO, A.G., Alvorez, D. and Menendez, R., *Effects of Inertinite content in Coal on Char Structure and Combustion*, ***Energy and Fuels*** *vol 43,* 1997, pp 702-761.

BOTES F.G; The *Development of a Heterogeneous One-Dimensional Gasifier Model,* ***Sasol Technology Internal Report,*** September 1996.

BREYTENBACH, L., *"Coal Drop Shatter test data Interpretation"*, ***Sasol Technology R+D Internal Memorandum***, June 2006, pp. 1-9.

BROWN, D.J., ***Coal Flotation.*** (In Fuerstenau, D.W., Red Froth Flotation 50th Anniversary Volume), New York: ***AIMME,*** 1962, pp. 518-538.

BRYERS R.W. and Taylor T.E.; An *Examination of the Relation between Ash Chemistry and Ash Fusion Temperature in various Coal Size and Gravity Fractions using Polynomial Regression Analysis.* ***Journal of Engineering for Power,*** *Vol. 98*, 1976, pp. 528-539.

CARPENTER, A.M., *Coal Quality Assessment – the Validity of Empirical Tests*, ***IEA Clean Coal Centre,*** 2002, pp. 1-100.

COETZER, R., *Personal Communication,* October, 2004.

COETZER, R., *Report on Alternative Statistical Models for the Prediction of Gasifier Performance as a Function of Coal Properties and Process Variables (Models Developed on Data from Tests 14 to 31 on the Test Gasifier)*, ***Sasol Technology Bulletin / Research Report***, December 2005, pp. 1-45.

DAKIC, D., Van de Honing, G.,and Valk, M., *Fragmentation and Swelling of various coals during Devolatilization in a Fluidised Bed,* ***Fuel, Vol. 68***, 1989, pp. 911-916.

DEER, W.A., Howie, R.A. and Zussman, J., *An introduction to the Rock Forming Minerals*, ***Longmans,*** 1966.

DENN M.M, Wei J, Yu W.C and Cwiklinski R; *Detailed Simulation of a Moving-Bed Gasifier,* ***Final Report EPRI-AP-2576***, *Electric Power Research Institute, Palo Alto, CA*, September 1982.

England T; (Ed) ***Coal Preparation in South Africa Handbook***, SACPS, Fourth English Edition, 2002, p.p 23-60.

FALCON R.M.S; *Coal in South Africa – Part III: Summary and Proposals – the Fundamental Approach to the Characterisation and Rationalisation of South Africa's Coal, Minerals Sci. Eng., Vol.10, No.2,* April 1978, pp. 130-153.

FALCON R.M.S; *The Petrograhic Components of Coal, R Falcon Research Laboratory (Pty.) Ltd., Johannesburg, S.A.*, 1981.

FALCON C.M. and Falcon R.M.S; *The Application of Coal Petrography to Certain Beneficiation Technologies on South African Coal, The Geological Society of Southern Africa*, Johannesburg, 1983.

FALCON, R.M.S. and Snyman, C.P., *An Introduction to Coal Petrography: Atlas of Petrographic Constituents in the Bituminous Coals of Southern Africa*, Published by the Geological Society of South Africa,1986.

FALCON L.M., and Falcon R.M.S.; *The Petrographic Composition of Southern African coals in relation to Friability, Hardness, and Abrasive Indices.* ***Journal of the South African Institute of Mining and Metallurgy,*** *Vol. 87, No. 10*,1987, pp. 323-336.

Financial Mail, *"Sasol 50th Birthday Special Edition",* September 2000, pp 10-11.

FATEMI-BADI, M., Scaroni, A.W. and Jenkins, R.G., *Chraracterization of Chars produced during Pyrolysis of a Sub-bituminous Coal,* ***Proc. Ann. Int. Pittsburgh Coal Conference.,*** 1988, pp. 742 – 757.

GIVEN, P.H., Peover, M.E., and Wyss, W.F., "*Chemical Properties of Coal Macerals: Introductory Survey and some Properties of Exinites*, ***Fuel,*** 39, 1960, pp.323-340.

GLOVER G; *An Experimental study of the Physical and Chemical Processes occurring within a Lurgi Mark IV Coal Gasifier with a view to Determining an Optimization Path.* ***Part 1: Rationale and preliminary observations, Sasol Technology R+D internal report***, 1988.

GLOVER G; *An Experimental study of the Physical and Chemical Processes occurring within a Lurgi Mark IV coal gasifier with a view to Determining an Optimization Path.* ***Part 2: The Sasol One Gasifiers, Sasol Tehnology R+D internal report***, 1991.

GLOVER G, Van der Walt T.J., Glasser D, Prinsloo N.M and Hildebrandt D; *DRIFT Spectroscopy and Optimal Reflectance of Heat-Treated Coal from a Quenched Gasifier,* ***Fuel, Vol. 74,*** 1995, pp. 1216-1219.

GOVENDER A; *Suitability of Sulcis, Sardinia coal for Gasification purposes,* ***Sasol Technology R+D Internal Research Report,*** January 2004.

GRAINGER, L. and Gibson, J., *Coal Utilization: Technology, Economics and Policy*, Graham and Trotman, 1981, pp. 1-30.

MEYERS, R.A.,(Ed) ***Handbook of Synfuels Technology***, Mc Graw-Hill, New York, NY, 1980, pp.139 – 140.

HARTMAN, H.F., Belk, J.P., and Reagan, D.E., *Low-Btu Coal Gasification Processes, Vol 1. Summary, Screening and Comparisons,* ***ORNL/TM-13/V1***, Oak Ridge National Laboratory for the U.S. Department of Energy, November 1978.

HEBDEN, D., Edge, R.F. and Foley, K. W. Investigations with a Small Pressure Gasifier. Part 1 – The Study of Reactions occurring in the Fuel Bed, ***Trans. Int. Gas. Eng. 104***, (*Gas Council Research Communication GC14),* 1954-55, pp. 305-344.

HEBDEN, D and Stroud, H.J.F., *"Coal Gasification Processes*, in ***Chemistry of Coal Utilisation, Second Supplementary Vol.***, Elliot, M.A. (Ed.), Wiley-Interscience, 1981, pp. 665-784.

HORSFALL D.W; (Ed), *Coal Preparation and Usage – Coal Processing for Management, Vol. 3, Coal Publications (Pty.) Ltd.*, 1993.

HOWARD, J.B., Peters, W.A. and Seiro, M.A., *Coal Devolatilization information for Reactor Modelling – Assessment of Data and Apparatus Availability with Recommendations for Research*, ***Department of Chemical Engineering***, Cambridge, Massachusetts, 1981.

JAEGER M, and Mayer; The *Noell Conversion Process – a Gasification Process for the Pollutant-free disposal of Sewage Sludge and the Recovery of Energy and Materials,* ***Water Science and Technology, Vol 4, No 8***, pp 37-44, 2000.

JOHNSON, C.A. and Thomas, K.M, Fundementals of Coal Gasification, ***Fuel* 66**, 1987, pp 17-25.

KEYSER, M.J., *"Gasification Modelling: A Perspective View"*, ***Sasol Technology R+D Internal Memorandum,*** November, 1997.

KEYSER M.J and Coetzer R; *Findings on the Statistical Evaluation of Tests 3 to 12 on the Test Gasifier with a Uniflo Grate,* ***Sasol Technology R+D Internal Research Report***,

October 1999.

KEYSER M J and Coetzer R; *Findings on the Statistical Evaluation of Tests 24 to 31 with SCS West blended Feedstock on the Test Gasifier,* ***Sasol Technology R+D Internal Research Report,*** June 2000.

KEYSER, M.J., Conradie, M., Coertzen, M., and Van Dyk, J.C., "*Effect of Coal Particle Size Distribution on Packed Bed Pressure Drop and Gas Flow Distribution",* ***Fuel, 85,*** *2006,* pp. 1439-1445.

KEYSER, M.J., Personal communication, July 2006.

KRISHNUDU, T., Madhusudhan, B., Narayan Reddy, S, Seshagiri Rao, K. and Vaidyeswaran, R; *Moving Bed Pressure Gasification of some Indian Coals;* ***Fuel Processing Technology 23***, pp. 233-256, 1989 (a).

KRISHNUDU, T., Madhusudhan, B., Reddy, S.N, Sastry, V.S.R., Seshagiri Rao, K. and Vaidyeswaran, R. *Studies in a Moving-Bed Pressure Gasifier : Prediction of Reaction Zones and Temperature Profile* ***Ind. Eng. Chem. Res.*** 1989 (b), ***28***, pp. 438-444.

LEVA, M., *"Fluidization",* McGraw-Hill Book Company, Inc., 1959.

LURIE J (Ed.), South African Geology for Mining, Metallurgical, Hydrological and Civil Engineering, McGraw-Hill Book Comp., Johannesburg, 3RD Rev.Ed. 1981, pp. 10-18.

MADHUSUDHAN, B., Narayan Reddy, S, Krishnudu T, Mallikarjunan, M.M, Anjaneyulu, T.S.R., Khaleel Akmal, M.A., Seshagiri Rao, K. and Vaidyeswaran, R; *Residence Time Distribution Studies on the Flow of solids in a Moving Bed Pressure Gasifier,* ***Indian Chem. Eng. Vol XXXI No. 4*** (October – December 1989).

MAGAGINER N., Van Alphen C., Inkson M.B. and Misplon B.J; *Characterising fuels for Biomass – Coal fired Co-generation, Proceedings of 75th Annual Congress of the S.A.* Sugar Technologists Association, South Africa, 2001.

MATJIE, R.H; *Factors influencing the Sintering and Slagging Behaviors of Coal Mineral matter and Formation of Anorthite during the Sasol-Lurgi fixed bed Coal Gasification Process,* ***PhD Study Proposal,*** *University of Pretoria*, 2005.

MORGAN, P.M., *An Experimental and Modelling Study of Coal Pyrolysis in a Lurgi Gasifier*, ***MSc Thesis***, University of the Witwatersrand, 1991.

NOWACKII P., *Coal Gasification Processes*, ***Energy Technology review*** No.70, pp. 77-137, 1981.

PINHEIRO, H.J., (Ed) ***Bulletin 113***, *"A Techno-Economic and Historical Review of the South African Coal Industry in the 19th and 20th Centuries*,; 2000, pp 11-12.

PRASAD, K.B.S., and Reddy, S.N.; *A Realistic Model of a Moving Bed Coal Gasifier;* ***Recent Adv. Chem. Eng., Proc. Int. Conf.*** (Eds. D.N. Saraf and D. Kunzru) Tata Mc Graw-Hill Publ. : New Delhi, India, pp 303 – 9, 1989.

RADULOVIC, P.T., and Smoot, D.L., ***AIChE J.***, 1992, ***38***, 681-693.

SABS method 865: 1994, *The Drilling, Preparation, and Testing for Compressive Strength of Cores taken from Hardened Concrete*, Rev. 1, pp. 2-11, 1994.

SANDERS D, Coal Characterisation in Marketing - *an Elementary Approach, Workshop on Coal Characterisation - for Existing & Emerging Technologies, CRC for Black Coal Utilisation, Newcastle, Australia,* 1996.

Sasol Annual Report, 2003, pp. 23. www.sasol.com

SASOL-LURGI Technology Company (Pty) Ltd., ***Company Profile and Reference List,*** November 2005.

SCHILLING, H.D., Bonn, B. and Krauss, U., *Coal Gasification – Existing Processes and New Developments,* Graham & Trotman Publ. 1979.

SCHOBERT, H, Personal communication, July 2006.

SHADLE L.J, and Swanson M.L; Coal *Gasification in a Transport Reactor,* ***Ind. Eng. Chem. Res,*** *2001, 40(13),* pp 2782-2792.

SLAGHUIS, J.H., *Volatile material in Coal and the role of Inherent Mineral Matter*, 1989, (***Dip. Tech***. UNISA).

SLAGHUIS, J.H., *Coal Gasification, A Study guide for the National Diploma in Fuel Technology*, ***Coal Processing III, Part A***, 1993 (a), pp. 1-81.

SLAGHUIS J.H; Coal Gasification: *A Study Guide for the National Diploma in Fuel Technology,* ***Coal Processing III, Part B.*** Sasolburg: Sasol Technology R&D, 1993 (b).

SLAGHUIS H; *Recovery and Utilisation of Char from Gasification Ash, Stage-Gate B Research Document,* ***Sasol Technology R&D Internal Report,*** (Aug 2004).

SLEGEIR, W.A., Singletary, J.H. and Kohut, J.F., *Application of a Microcomputor to the Determination of coal ash Fusibility Characteristics*, ***Journal of Coal Quality,*** 1988, 7 (2), pp. 48-54.

SMITH W.H, Roux H.J. and Steyn J.G.D; *The Classification of Coal Macerals and their Relation to certain Chemical and Physical Parameters of Coal, Publication of the Geological Society of Southern Africa*, 7, pp 111-115, 1983.

SNYMAN, C.P., Van Vuuren, M.C.J., and Barnard, J.M., "*Chemical and Physical Characteristics of South African Coals and a suggested Classification System,* ***Coal 8306, Isbn No. 07998 2799 8***, January 1984.

SOLOMON P.R., Serio, M.A., Hamblen, D.G., Markham, J.R., Best, P.E., abd Bassilakis, *Chemical and Physical Development of Char Particles during Devolatilisation.,* ***Final Report, Contract No. DE-AC21-85MC22050, Advanced Fuel Research Inc.,*** East Hartford, Connecticut, May 1988.

STACH, E., Mackowsky, M.T.H., Teichmuller, M., Taylor, G.H., Chandra, D. and Teichmuller, R., ***Stach's Textbook of Coal Petrology,*** *Third revised and enlarged edition,* Berlin Gebruder Borntraeger, 1982.

STOPES, M.C., *"On the Four Visible Ingredients in Banded Bituminous Coals"*, ***Proc. R. Soc. Lond., series B, 90***, 1919, pp. 470-487.

STUBINGTON, J.F.,and Linjewile, T.M., *"The Effects of Fragmentation on Devolatilisation of Large Coal Particles,* ***Fuel, Vol. 68***, 1989, pp. 155-160.

TSAI S.C; *Fundamentals of Coal Beneficiation and Utilisation, Coal Science and Technology 2,* ***Elsevier,*** 1982.

VAN ALPHEN C; *CCSEM Characterisation of Secunda GA9 Feedstock and Gasification Ash.* ***Contractual Report***, (2003), pp. 1-24.

VAN DE VENTER E; *"Secunda Coal-to-Syngas Technology Area" –* ***Sasol-Lurgi Technology Strategy Document,*** *September 2004.*

VAN DER WALT, T.J., *An Experimental and Modeling study of Moving-bed coal Gasifiers,* ***PhD Thesis in Engineering***, University of the Witwatersrand, 1994.

VAN DER WALT, T.J., *Personal Communication,* January 2005.

VAN DYK J.C; *Development of an Alternative Laboratory Method to determine Thermal Fragmentation of coal sources during Pyrolysis in the Gasification Process.* ***Fuel*** 80, pp. 245-249, 2001 (a).

VAN DYK J.C; *Characterisation of Pellets manufactured from Biological sludge by Seghers in Toronto, Canada,* ***Sasol Technology R+D Internal Report,*** September 2001 (b).

VAN DYK, J.C., Keyser, M.J., and van Zyl, J.W., *Suitability of Feedstocks for the Sasol-Lurgi Fixed Bed Dry Bottom Gasification Process*, ***GTC Conference***, San Francisco, USA, October 2001 (c).

VAN DYK J.C; *Results from Test Gasifier Runs obtained with Split Feed Particle Size Distributions (35x4mm and 35x70mm Fractions*), ***Sasol Technology R+D Internal Report,*** July 2002 (a).

VAN DYK J.C; *Co-Gasification of Wood with Coal – Findings and Conclusions of a Full Scale Test,* ***Sasol Technology R+D Internal Report,*** August 2002 (b).

VAN DYK, J.C. and Keyser, M.J., *Characterization of Inorganic material in Secunda coal and the Effect of Washing on Coal Properties*, ***SAIMM***, Journal of the South African Institute of Mining and Metallurgy, ***Volume 105, No. 1***, January 2005, pp. 1-6.

VAN DYK J.C, *Manipulation of Gasification Coal Feed in order to Increase the Ash Fusion Temperature of the coal to Operate the Gasifiers at Higher Temperatures,* ***PhD Thesis in Prep.****, University of the North West*, 2006.

VAN HEERDEN, J.H.P., *Sasol Technology Coal and Syngas Technology Strategy Report,* ***Sasol Internal Report***, 2005.

WAANDERS, F.B., Vinken, E., Mans, A, and Mulaba-Bafubiandi, A.F., *Iron Minerals in Coal, Weathered Coal, and Coal Ash – SEM and Mossbauer Results,* ***Hyperfine Interactions, 148/149; 2003,*** Kluwer Academic Publishers, pp. 21-29.

WAANDERS, F.B., and Govender, A., *Mineral Associations in Coal and their Transformation during Gasification,* ***ICAME 2005***, Montpellier, France, Sept. 2005, Accepted for publication : Hyperfine Interactions.

WAGNER N.J.; *The Effect of Weathering on Stored discard coals and the Impact on Combustion,* ***PHD thesis***, University of the Witwatersrand, South Africa, 1998.

WAGNER N.J; *Samancor / Sasol Ferrochrome Furnace Digout* ***Interim Report, Furnace Excavation,*** 2000. ***(Confidential).***

WAGNER N.J; *The Determination of Different Carbon Forms from a Mined Gasifier Ash sample,* ***Sasol Technology R&D Internal Memorandum***, 2004(a).

WAGNER, N.J; *Consideration of Reports by dr. G. Glover on 5 Gasifier Investigations (1986-1988),* ***Sasol Technology R+D Internal Memorandum***, April 2004(b).

WAGNER, N.J., and Joubert, J., *Enhanced Understanding of the Carbon Conversion Process during Gasification as Determined Petrographically,* ***In proc. FFF Indaba***, 2005(a).

WAGNER, N.J., *Petrographic Results on Gasifier 41 Turn-out Samples;* ***Sasol Technology R+D Internal Memorandum,*** April 2005(b).

WARD C.R; *Analysis and Significance of Mineral matter in Coal Seams,* ***International Journal of Coal Geology***, 2002, 50, pp. 135-168.

YOON, H., Wei, J, and Denn, M.M; A *model for Moving-Bed Coal Gasification Reactors,* ***AIChE J., 24***, pp. 885-903, 1978.